

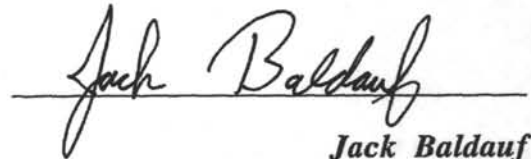
# SCIENCE PROSPECTUS

## FY95 PROGRAM

Prepared from Original Proposals and Working Group Reports



*Philip D. Rabinowitz*  
Director  
ODP/TAMU



*Jack Baldauf*  
Manager  
Science Operations  
ODP/TAMU



*Timothy J.G. Francis*  
Deputy Director  
ODP/TAMU

Compiled by:  
Shaune Lafferty Webb  
Staff Researcher, Science Operations ODP  
and  
Jack Baldauf  
Manager, Science Operations ODP

JANUARY 1994

## TABLE OF CONTENTS

<b>Introduction</b> .....	1
ODP Cruise Participant Application Form	
ODP Sample Request Form	
<b>Location Map</b> .....	9
Legs 157 - 165	
<b>Operations Schedule</b> .....	10
Legs 157 - 165	
<b>Leg 157 Prospectus</b> .....	13
Gran Canaria and the Madeira Abyssal Plain	
<b>Leg 158 Prospectus</b> .....	63
TAG Hydrothermal Mound	
<b>Leg 159 Prospectus</b> .....	85
Return to Hole 735B	
<b>Leg 160 Prospectus</b> .....	113
Eastern Equatorial Atlantic Transform	
<b>Leg 161 Prospectus</b> .....	149
Mediterranean I	
<b>Leg 162 Prospectus</b> .....	203
Mediterranean II	
<b>Leg 163 Prospectus</b> .....	247
North Atlantic Arctic Gateways II	
<b>Leg 164 Prospectus</b> .....	283
Gas Hydrates	
<b>Leg 165 Prospectus</b> .....	315
Diamond Coring System: A Brief Engineering and Operations Prospectus	

---

# INTRODUCTION

---

This FY95 Science Prospectus presents the scheduled scientific operations for ODP Legs 157 through 165. These legs represent scientific cruises commencing July 1994 and continuing through February 1996.

The purpose of this document is to provide the reader with a brief overview of the scientific operations for each cruise as summarized from the initial JOIDES proposals or JOIDES Working Group results. All information included herein is correct at the time of writing but may be subject to future changes.

Also enclosed with this document is information on how individuals can become involved with any of the above scientific programs. For additional information, please contact the Manager of Science Operations at the following address:

Dr. Jack Baldauf  
Manager of Science Operations  
Ocean Drilling Program  
Texas A&M University Research Park  
1000 Discovery Drive  
College Station, TX 77845-9547  
U.S.A.

Tel: (409) 845-9297  
Fax: (409) 845-0876  
E-mail: [baldauf@nelson.tamu.edu](mailto:baldauf@nelson.tamu.edu)

***Ocean Drilling Program Cruise Participant Application Form***

**Name** (first, middle, last) \_\_\_\_\_

**Institution** (including address) \_\_\_\_\_

**Telephone** (work) \_\_\_\_\_ (home) \_\_\_\_\_ **Telex/Cable** \_\_\_\_\_ **Fax** \_\_\_\_\_

**Permanent Institution Address** (if different from above) \_\_\_\_\_

**Bitnet or Internet Address** \_\_\_\_\_

**Present Position** \_\_\_\_\_ **Country of Citizenship** \_\_\_\_\_

**Place of Birth** \_\_\_\_\_ **Date of Birth** \_\_\_\_\_ **Sex** \_\_\_\_\_

**Passport No.** \_\_\_\_\_ **Place Issued** \_\_\_\_\_ **Date Issued** \_\_\_\_\_ **Exp. Date** \_\_\_\_\_

**Geographic Region(s), Scientific Problem(s) of Interest** (Leg number(s) if known) \_\_\_\_\_

**Date(s) Available** \_\_\_\_\_

**Reason(s) for Interest** (if necessary, expand in letter) \_\_\_\_\_

**Expertise** (petrologist, sedimentologist, etc.) \_\_\_\_\_

**Education** (highest degree and date; see note below) \_\_\_\_\_

**Experience** (attach curriculum vitae) \_\_\_\_\_

**Selected Publications You Have Written Relevant to Requested Cruise** \_\_\_\_\_

**Personal and/or Scientific References** (name and address) \_\_\_\_\_

**Previous DSDP/ODP Involvement and Nature of Involvement** (i.e. cruise participant, shore-based participant, contributor, reviewer, etc.) \_\_\_\_\_

Note: Graduate student applications should include a letter from their primary advisors, documenting the student's scientific experience and detailing how participation on the cruise would fit into their graduate degree programs.

Staffing decisions are made in consultation with the co-chief scientists and take into account nominations from partner countries; final responsibility for staffing rests with ODP at TAMU. Please return this form to: **Manager of Science Operations**

Applicants from JOIDES partner countries should send a **copy** of their applications to their respective national ODP offices.

**Ocean Drilling Program**  
**Texas A&M University Research Park**  
**1000 Discovery Drive**  
**College Station, TX 77845-9547**  
**Fax: (409)845-0876**

## *Responsibilities of Shipboard Scientists*

Shipboard scientists collect, analyze and compile data conforming to ODP standards and format. They assist the co-chief scientists in producing shipboard scientific reports by recording data on standard ODP computerized and paper forms and writing a description of their disciplines' results for each site chapter of the *Initial Reports of the Proceedings of the Ocean Drilling Program*.

Scientists aid the curatorial technician by taking samples for themselves and others for later shore-based study. A team of highly trained marine technicians, some specializing in particular equipment areas, assist the shipboard scientists by maintaining the flow of core samples through the laboratories and helping with analyses.

At the end of the cruise, all shipboard scientists are requested to complete cruise evaluations. These evaluations guide ODP in upgrading laboratory equipment and procedures and in improving life on board ship.

Shipboard scientists are primarily on board to pursue their own scientific interests. After the cruise, they are responsible for analyzing their samples and reporting the results, which are included in the ODP database and published in the cruise volumes. Following is a brief description of the shipboard responsibilities of the scientific staff.

### **Sedimentologists**

provide accurate visual and written descriptions of the cored sediments and interpret the depositional and diagenetic history or other related sedimentological processes. They work as a team, designating a lead sedimentologist for each site and exchanging specific responsibilities from site to site. Sedimentologists' responsibilities include:

- written and graphic core descriptions on ODP data forms, including the sedimentologic portion of core description sheets (barrel sheets)
- smear-slide preparation and petrographic analysis of smear slides and thin sections
- selection of samples for shipboard analyses of XRD, XRF, carbonate percentage and thin sections

The **paleontologists'** chief responsibility is to assign an age to the core-catcher samples as soon as possible after cores are recovered. They may need to examine additional samples to provide as complete a biostratigraphic characterization of the cored section as possible within the time available, including recognition of boundaries and hiatuses.

A reference library with texts, journals and reprints is available to help shipboard paleontologists identify fossil groups that do not fall within their areas of expertise.

### **Petrologists**

classify thin sections and hand specimens and provide the written and graphic descriptions of all igneous and metamorphic rocks recovered on the cruise. Petrologists should be experienced in one or more of the following aspects of the petrology of oceanic rocks: chemical petrology, volcanology, mineralogy and petrography.

#### **Paleomagnetists**

conduct or supervise all paleomagnetic measurements including the reduction of paleomagnetic data to intensities and direction of magnetization.

Paleomagnetists work with other shipboard scientists and the drilling crew to ensure that core material is not magnetically damaged by heating or exposure to strong magnetic fields and that core sections are not inverted.

**Structural geologists** record structural features of the core and their relationships to other igneous, metamorphic, or sedimentary features. In addition, they integrate and constrain their observations with borehole logging, core magnetic, and microstructural (petrographic) data to produce local and regional tectonic interpretation. Structural geologists may choose to record their observations using customized versions of ODP Visual Core Description (VCD) forms, independent structural VCD forms, or spread-sheets.

### **Physical properties specialists**

select cores to determine velocities, shear strength, thermal conductivity and index properties (water content, porosity and bulk density). They also ensure that data are collected in a manner consistent with ODP format. The physical properties specialists and the sedimentologists select samples for carbonate analyses.

**Organic chemists** monitor cores for gas and oil (hydrocarbon accumulations) and organic compounds. They advise when hydrocarbons in cores may constitute a safety or pollution hazard.

**Inorganic geochemists** are primarily responsible for conducting interstitial water, X-ray diffraction (XRD) and X-ray fluorescence (XRF) analyses. ODP chemists and marine technicians assist in these analyses.

**Logging scientists** advise the co-chief scientists on the logging program, for the cruise. They work closely with the Schlumberger field engineer and the Lamont-Doherty Earth Observatory logging scientist in designing, implementing and interpreting the logging program.

# OCEAN DRILLING PROGRAM SAMPLE REQUEST FOR SHIPBOARD AND SHOREBASED CRUISE PARTICIPANTS

(Submit to the Curator at least two months before cruise departs.)

To be completed by the Co-chief Scientists:  
Co-chief scientist please indicate the fate of this request.  
 approved  deferred  rejected  
If this request is rejected please include a brief explanation that can  
be quoted to the requestor.

\_\_\_\_\_ Co-chief signature                      \_\_\_\_\_ Co-chief signature

Please be aware of the current sample distribution policy which is published in recent issues of *Proceedings of the Ocean Drilling Program*. You should complete a separate request form for each research topic you wish to propose.

1. Proposed leg name (include number if known):
2. Name(s), office address, telephone number, fax, email, BITNET (to facilitate contact between investigators), and telex number of investigator(s):
3. Purpose(s) of request. Please summarize the nature of the proposed research concisely in 5-7 lines. [This summary will be included in various official reports.] Provide a detailed description of the proposed research, including techniques of sample preparation and analysis, roles of individual investigators, etc., on an attached sheet. The detailed description of the project will be employed in reviewing the sample request and may be copied to other shipboard scientists.

4. What is the specific cruise related research that you plan to accomplish for this cruise? A specific manuscript title is to be agreed upon by you and the co-Chiefs before the end of the cruise. Investigators who receive samples or data on-board the ship or during the first year post-cruise are obligated to produce a publishable manuscript for the ODP Initial Reports.
  
5. Please describe the proposed core sampling program in sufficient detail so that those who must carry it out onboard ship will understand your needs. Specify the size of samples (cubic centimeters); the number of samples to be taken from each section, core, and/or hole; particular stratigraphic or lithologic units to be sampled; and any other information that will be helpful in conducting your sampling program. Be aware that, if the number of samples which you are requesting is large, sampling for you is likely to be deferred until the cores reach the repository (4 to 6 months following the cruise), so it is to your advantage to keep the total number of samples small. You may choose to propose a two-stage sampling program (i.e. pilot study/follow-up study) now. Or you may elect to get samples only for the pilot study now, with the understanding that you will request additional samples later after you see what is recovered.
  
6. Please describe any specialized sampling or processing techniques that you plan to use. List any specialized supplies or equipment that you want to use during the cruise (will you bring these items with you or do you think they will be available from ODP).
  
7. Please estimate the time it will require for you to obtain publishable results. You must have publishable results within 16 months or less for samples taken on board the ship or during the first year post-cruise, as these must be worked up for the Part B volume.
  
8. In what condition will the samples be once your research is complete? Will they be useful to others? If so, for what kinds of research?
  
9. If you have ever before received samples from DSDP or ODP, please indicate the ODP sample request number (if known), and the number and volumes of samples received. Were all of these samples analyzed? If not, were they returned to DSDP/ODP? If work is still in progress, please attach a brief (2-3 page) progress report. If the work has ended, please return the samples. Micropaleontologists may keep their processed residues until their professional use of the samples is completed, whereupon they must be returned to the Curator.

10. If you have ever before received samples from DSDP or from ODP, please attach a comprehensive list of the publications in journals, outside of the ODP volumes, which resulted from each sample request. If you have recently submitted such a listing, you may update it with only the new publications. If you reference publications which have not yet been forwarded to the Curator, please enclose four (4) reprints of each. If work is still in progress, please attach a brief (2-3 page) progress report. If the work has ended, please return the residues.

11. Please summarize any other information which you feel would be useful in reviewing your request on an attached sheet.

**If you want something other than samples: check one**

thin sections     smear slides     view/photograph

other \_\_\_\_\_

**then skip to last page, for your signature and date**

12. Samples taken on the ship are usually sealed in plastic bags, which are stored and shipped in cardboard boxes at ambient temperatures. If your samples require special storage or shipment handling please describe how you want the samples handled (for example, refrigerated, refrigerated with blue ice, or frozen).

13. If your samples will require special storage or shipment (for example, frozen organic samples) please specify a destination airport which is near your institute. Specify the name, telephone number and telex number of someone who can: re-ice the shipment at the destination airport, clear the shipment from customs and provide transportation to the final destination.

14. Would you prefer that we (circle one):

- a) ship your samples to you,
- b) give them to you at the end of the cruise so that you can put them in your suitcase, or
- c) pack them in a box and give them to you at the end of the cruise?

**Acceptance of samples implies willingness and responsibility on the part of the investigator to fulfill certain obligations:**

- (a) To publish the manuscript you agreed to produce in the ODP *Scientific Results* volume (the title will be listed on the final Cruise Sampling Program in the Hole Summary).
- (b) To acknowledge in all publications that the samples were supplied through the assistance of the international Ocean Drilling Program and others as appropriate.
- (c) To submit (4) copies of reprints of all published works in the outside journals to the Curator, Ocean Drilling Program, Texas A&M Research Park, 1000 Discovery Drive, College Station, Texas 77845-9547, U.S.A. These reprints will be distributed to the repositories and to the ship. The Bibliographies of all reprints received by the Ocean Drilling Program will be sent to the National Science Foundation. You need not send reprints from the ODP Initial Reports.
- (d) To submit all final analytical data obtained from the samples to the Data Base Supervisor, Ocean Drilling Program, Texas A&M University Research Park, 1000 Discovery Drive, College Station, Texas 77845-9547, U.S.A. Please consult recent issues of the *JOIDES Journal* or call 409-845-2673 for information on acceptable data formats. Investigators should be aware that they may have other data obligations under NSF's Ocean Science Data Policy or under relevant policies of other funding agencies which require submission of data to national data centers.
- (e) To return all unused or residual samples, in good condition and with a detailed explanation of any processing they may have experienced, upon termination of the proposed research. In particular, all thin sections and smear slides manufactured onboard the vessel or in the repositories are to be returned to the Curator. Thin sections and smear slides used to describe the cores are unique representatives of the materials and as such they are kept as members of the ODP reference collection. All unused or dry residual paleontological materials may be returned either to the Curator at ODP or to one of designed paleontological reference centers upon completion of the investigators' use of the materials.

**It is understood that failure to honor these obligations will prejudice future applications for samples.**

All requests will be reviewed by the Assistant Curator, by the ODP Staff Scientist assigned to the leg, and by the Co-chief Scientists, before the cruise, to begin preparing a preliminary sampling scheme. Approval/disapproval will be based upon the scientific requirements of the cruise as determined by the appropriate JOIDES advisory panel(s). In the case of duplicate proposals, shipboard scientists will have priority over shorebased scientists. Requests for samples for post-cruise studies will be handled separately. Completion of this form in no way implies acceptance of your proposed investigation.

Date: \_\_\_\_\_

Date: \_\_\_\_\_

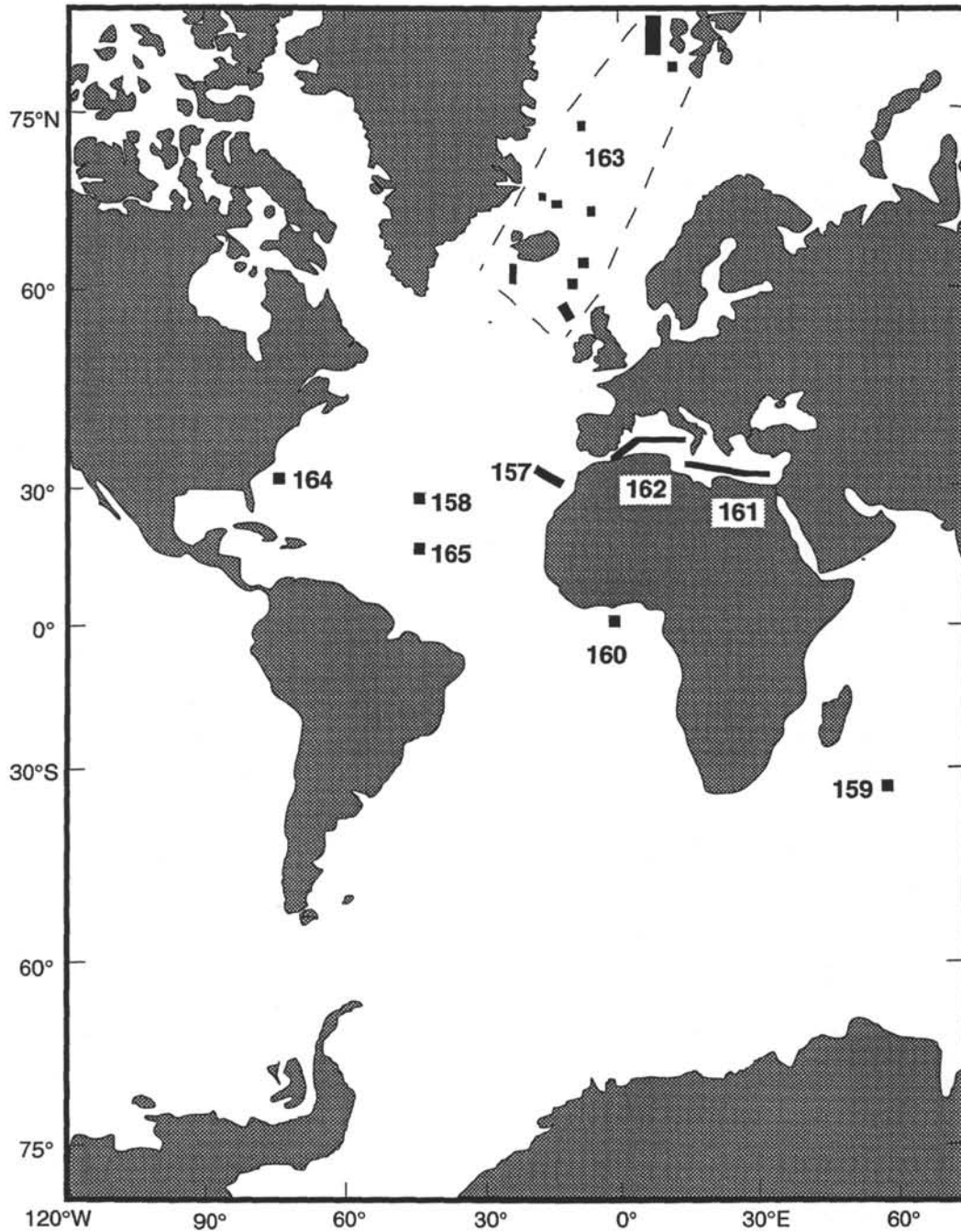
Date: \_\_\_\_\_

Signatures of Investigators

Send this completed form to the Curator **at least two months** in advance of the cruise departure date. The Curator's address:

**Curator  
Ocean Drilling Program  
Texas A&M University Research Park  
1000 Discovery Drive  
College Station, TX 77845-9547**

**bitnet: Chris@TAMODP  
internet: Chris@nelson.tamu.edu  
fax: (409) 845-4857  
phone: (409) 845-4819**



**Location Map of Scheduled Legs 157 through 165**

## OPERATIONS SCHEDULE

LEG	PORT OF ORIGIN	CRUISE DATES	DAYS AT SEA	DAYS: TRANSIT/SITE (Estimated)
157 VICAP-MAP	Barbados 24 - 28 July 1994	29 July - 23 September 1994	56	12/44
158 TAG	Las Palmas 23 - 27 September 1994	28 September - 23 November 1994	56	
<b>DRYDOCK</b>				
159 Site 735	Capetown	January - February 1995	56	16/40
160 Eastern Equatorial Atlantic Transform	Capetown	March - April 1995	56	15/41
161 Mediterranean I	Dakar	May - June 1995	56	18/38
162 Mediterranean II	Napoli	July - August 1995	56	11/45
163 * Atlantic Arctic Gateways II	Aberdeen	September - October 1995	56	15/41
164 Gas Hydrates	Reykjavik	November - December 1995	56	13/43
165 DCS Engineering	Miami	January - February 1996	56	

PRECISE DATES FOR LEG 159 TO LEG 165 CAN NOT BE DETERMINED  
UNTIL THE DRYDOCK PORT HAS BEEN FIXED

\* Atlantic Arctic Gateways II may be scheduled between Mediterranean I and Mediterranean II  
should this provide a better ice/weather window

*LEG 157*

*VICAP - MAP*

## LEG 157

### DRILLING INTO THE CLASTIC APRON OF GRAN CANARIA AND THE MADEIRA ABYSSAL PLAIN

---

Modified From Proposals 380 and 59A Submitted By

Hans-Ulrich Schmincke, Philip P.E. Weaver, P. van der Bogaard, Sierd Cloetingh,  
Ray E. Cranston, Juan J. Dañobeitia, Armin Freundt, Hans Hirschleber, Kaj Hoernle,  
Ian Jarvis, Robert B. Kidd, Roland Rihm, M. Schnaubelt, R.T.E. Schuttenhelm,  
Karl Stattegger, Hubert Staudigel, John Thomson, Anthony B. Watts,  
Wilfried Weigel, Gerd Wissmann, and Rainer Zahn

To Be Named: Co-Chief Scientists and Staff Scientist

---

#### ABSTRACT

The Volcanic Island Clastic Apron Project (VICAP) entails a case history study of a coupled system, "oceanic island - volcanoclastic apron". The source area has a long-term record of chemically distinct rocks/deposits with physically datable mineral phases, so that the submarine and subaerial growth and destruction is reflected in sufficient detail in the volcanoclastic apron. The seamount/island evolution as deduced from deep drilling into the apron can then be compared to the volcanic evolution reconstructed from the study of products exposed on land. Gran Canaria, one of the best studied oceanic volcanic islands, is the most suitable candidate for such a case history study.

The Madeira Abyssal Plain Project (MAP) is aimed at testing the hypothesis that ocean basin sedimentation is controlled by sealevel changes which affect the stability of sediments on continental margins including those on the flanks of volcanic islands. The products of mass wasting events accumulate on the continental slope and on the abyssal plains, but the abyssal plain is the only place where a complete record can be obtained in one drillsite. The combined VICAP-MAP project will study the development of the Canary Basin in terms of the history of volcanic activity in the Canary hotspot, the detailed evolution of the large volcanic oceanic islands of Gran Canaria and Tenerife (Canary Islands), and the filling of the Madeira Abyssal Plain.

## INTRODUCTION

### VICAP

VICAP (Fig. 1) concerns the physical and chemical evolution of the confined system "asthenosphere - lithosphere - seamount - volcanic island - clastic apron - sedimentary basin" by drilling into the proximal, medial and distal facies of a volcanoclastic wedge. The clastic apron is composed largely of material representing the evolution of the volcanic complex, including material no longer present on the island (Figs. 2 and 3). Most importantly, it includes material from the unexposed and inaccessible submarine stages. The volcanic islands produce a large sediment supply with slopes that are at or near the critical angle of repose. They are prone to mass wasting, enhancing the probability that sea-level control vs. volcanic eruption and earthquake control can be distinguished. A major element of the program will be high precision single-crystal  $^{40}\text{Ar}/^{39}\text{Ar}$  age dating with the aim of monitoring the island and basin evolution in detailed time slices as small as 100,000 years. The most distal sites on the Madeira Abyssal Plain will enable us to date major volcanogenic turbidites and hence large events in the Canary Island archipelago. We will achieve a quantitative analysis of a remarkably confined system. The magmatically governed sedimentary apron, which consists of material generated during more than 15 m.y. of volcanic and erosional activity, interfingers with nonvolcanic, continent-derived clastic and biogenic material.

The proposed drilling operation provides a case study of an intraplate volcanic system and its mantle source evolution. It is accompanied by a massive land program, now underway, and is preceded by detailed geophysical pre-site monitoring. With VICAP, an attempt will be made to combine the temporal, spatial, compositional and volumetric evolution of the terrestrial-subaerial and submarine parts of a closely coupled geological system. The project is designed to provide a case history study and therefore a practical calibration system that will allow a more realistic assessment of the past volcanic, petrologic and plate tectonic environments of sedimentary basins adjacent to other productive volcanic source areas. This should serve as a model for the interpretation of many ancient marine sections as well as marine volcanoclastic successions drilled in the DSDP/ODP programs. This fundamental aspect of the proposal cannot, by definition, be solved by drilling on land.

Gran Canaria is extremely well-exposed and well studied. The island has been volcanically active intermittently throughout the past 15 m.y. Igneous rocks, both mafic and evolved, show an extreme spectrum in chemical and mineralogical composition, exhibiting the greatest variability in volcanic rock types known on a single volcano. The island has experienced several stages of high degree of magma differentiation, unique among volcanic islands, generating both frequent explosive fallout ashes and many ash flow deposits. The distinct composition of individual ash flows as well as other volcanic rocks throughout the island's evolution will greatly facilitate stratigraphic subdivision in the cores. The evolved magmas have abundant K-rich mineral phases (feldspar and mica) - a prerequisite for high-resolution age studies.

The neighboring islands of Tenerife (volcanically active for greater than 8 m.y.; Ancochea et al., 1990), Fuerteventura and Lanzarote (both for greater than 20 m.y.; Le Bas et al., 1986), which also contribute to the sediments in the area, have not yet been studied in as great detail as Gran Canaria but show similarly wide and characteristic compositional variations. Extensive on-land study of Tenerife by several international research teams in the framework of the European EPOCH program on "Laboratory Volcanoes" is in progress.

## **MAP**

MAP drilling (Fig. 1) is aimed at testing the hypothesis that ocean basin sedimentation is controlled by sealevel changes which affect the stability of sediments on continental margins including those on the flanks of volcanic islands. The products of mass wasting events accumulate on the continental slope and on the abyssal plains, but the abyssal plain is the only place where a complete record can be obtained in one drillsite. We predict that most sealevel changes, both rises and falls, will be associated with mass wasting events. Thus periods of oscillating sealevels, such as during the last 2.5 m.y., should be represented on the abyssal plains by sequences of turbidites, and periods of stable sealevels should be represented by continuous hemipelagic accumulation. Our evidence suggests that the abyssal plain is a young feature with the whole 350-m thick turbidite sequence (20,000 km<sup>3</sup>) being deposited in just a few million years. The drilling of four sites on the Madeira Abyssal Plain will allow mass balance calculations of sediment transported from the continental margins to the deep-sea, including mass balances for volcanogenic sediments derived from Madeira and the Canary Islands. The history of volcanogenic turbidites will be closely tied to the history of the volcanic islands and should provide information on the initiation of hotspot

*...Leg 157 - Gran Canaria and the Madeira Abyssal Plain...*

activity, on phases of increased volcanic activity and major island-flank collapse events. The frequency of turbidite input and composition of the units on the Madeira Abyssal Plain is ideal for studies of long term diagenesis and sediment burial. We will also be able to study the fate of unstable volcanic glass in the clastic aprons under varying heat-flow regimes.

During Leg 157, we will also attempt to determine sediment budgets for the transport of sediment from the continental slopes to the deep-sea, possible because we have calculated the area of the abyssal plain from our detailed surveys and determined the area of deeper layers from our extensive seismic data. We have been able to show from piston cores that individual turbidites form simple stacked layers on the plain. Individual turbidites can be up to 5 m thick representing single flows of over 190 km<sup>3</sup> in volume. Deep drilling will enable calculations of the volumes of material transported over the last several million years, and allow us to compare transport rates during periods of sealevel change and sealevel stability (i.e. to see if there is a fundamental link between deep-sea sedimentation and the Vail sealevel curves).

The study of early diagenesis in sediments accumulating under non-steady state conditions will also be advanced by study of these sediment sequences. The concept of a "progressive oxidation front" was first proposed following studies of the MAP turbidites (Wilson et al. 1985, 1986; Thomson et al., 1987). When the turbidite top is in diffusive contact with bottom waters following deposition, several elements redistribute themselves around the oxic/postoxic (or sub-oxic) boundary at the front. This results in layers of metal concentrations, with some metals persisting long after conditions have become reducing and some metals disappearing quite quickly. We need to know more about the long term persistence of these signatures to aid in interpreting paleo-redox conditions and the presence of multiple fronts will allow successively older signatures to be examined. The diagenesis and maturation of organic matter can also be examined in the turbidites by techniques such as Rock-Eval pyrolysis.

## **STUDY AREA - GRAN CANARIA**

### **Submarine Growth Stages of the Canary Islands**

Structure, composition and evolution of the submarine part of the Canary Islands is largely unknown except for La Palma, where a 3.5 km-thick section of the uplifted submarine part is well

exposed (Schmincke and Staudigel, 1976; Staudigel and Schmincke, 1984). The submarine section consists of a central plutonic complex, a sheeted dike swarm with minor "metatrachyte" to alkali basalt screens and abundant sills, a lower extrusive section (~ 650 m thick) made up almost exclusively of pillow lavas, and an upper extrusive section (~ 1150 m thick) made up of >50% of pillow fragment breccias and several types of mass flow deposits, many consisting of resedimented, shallow water-derived, vesicular hyaloclastites. The lavas in the uppermost part were probably erupted in shallow water as well.

Although submarine portions of Gomera and Fuerteventura have also been uplifted, the basal complexes on these islands are not well exposed and are heavily overprinted by later magmatic activity (Le Bas et al., 1986). Therefore, it is difficult to decipher the structure, composition, and evolution of the submarine stages on these islands.

The hyaloclastites on La Palma are overlain by *volcaniclastic debris flows* which contain abundant tachylite and a wide variety of subaerial volcanic and subvolcanic rock fragments (ranging from microgabbro to trachyte) but are dominated by alkali basalt. Such debris flows form excellent seismic reflectors and their volume south of Gran Canaria probably exceeds 50 km<sup>3</sup> (Wissmann, unpublished seismic data). Seismic refraction data indicate a 1.5 to 2.0-km thick low velocity (2-3 km/s) upper section beneath some islands such as Tenerife (Dash and Bosshard, 1968). This is similar to the submarine La Palma section where low velocities of this magnitude, reflecting the dominance of hyaloclastites and pillow breccias, would be expected to characterize the upper part of a seamount precursor.

Another approach for monitoring the submarine development of the Canary Islands is the study of volcaniclastic sediments encountered in drill holes, such as those of DSDP Site 397, >100 km SSE of Gran Canaria (Schmincke and von Rad, 1979) (Fig. 4). In this hole, hyaloclastite debris flows (V3, Fig. 5) are interpreted to represent material from the submarine stage of an island (probably Fuerteventura) transported for more than 100 km to the south and southwest. The overlying alkali basalt-fragment rich debris flows (V1, V2, Fig. 5), consisting largely of tachylitic and highly vesicular clasts, are interpreted to represent the shallow-water and shield stages of emerging Gran Canaria, judging from their chemical and mineralogical composition (Fig. 6a). They form the bulk of the debris flows mapped seismically by Wissmann (1979) and thus are thought to reflect the rapid growth of an island during the shield stage (Fig. 2). A very large amount of clastic debris is

generated during the transition period seamount/island by phreatomagmatic and magmatic explosive activity as well as erosion of freshly formed pyroclastic deposits.

Younger ash layers of DSDP Sites 369 and 397 reflect later, differentiated, subaerial stages of an island (Fig. 5), such as the 13- to 14-Ma-old rhyolite ashes from Gran Canaria or the phonolitic Pliocene/Pleistocene ash layers, most of which are probably the result of Plinian eruptions on Tenerife (Rothe and Koch, 1978; Schmincke and von Rad, 1979).

The temporal evolution and regional age progression of Canary Island volcanism is based largely on the subaerially exposed rocks because the much greater volume of submarine volcanics is hidden at depth. Holik et al. (1991) recently interpreted a zone of high layer 3 velocities and units of chaotic seismic facies between 31°N and 33°N as evidence for the location of a Canary Islands hot spot at 50 to 60 Ma and suggest a northeast-southwest age progression of the hot spot. Fossils in sediments interfingering with volcanoclastics in the subaerially exposed Fuerteventura basal complex, however, suggest that volcanism on the easternmost islands may have begun at 70-80 Ma (Le Bas et al., 1986). Detailed information about the submarine stages is badly needed to quantify any model of the age progression in the archipelago.

The geochemical evolution of ocean islands provides important insights into mantle dynamics and evolution. The subaerial stages of volcanism on many ocean islands have been studied in great detail, but little is known about the geochemical evolution of the submarine (seamount) stages of ocean island volcanoes, which make up >90% of the volume of the volcanos. To date, most studies of the submarine stages have either been conducted by dredging seamounts or the flanks of ocean island volcanoes or by studying uplifted basal (submarine) complexes. Both methods have serious shortcomings. Since dredged samples are confined to the surface of the volcanic edifice, they only represent a brief period in the evolution of the submarine stage. Furthermore, it is difficult to evaluate relative differences in age between dredged samples. The temporal history of basal complexes (e.g. Staudigel and Schmincke, 1984; Le Bas et al., 1986), as well as the primary geochemical composition (e.g. Hoernle and Tilton, 1991; Hoernle, et al., 1991), are also difficult to decipher, due to extensive intrusion and moderately high temperature hydrothermal metamorphism related to intrusive activity.

The excellent stratigraphic control, coupled with detailed  $^{40}\text{Ar}/^{39}\text{Ar}$  dating, of samples from drill cores into the volcanic apron around an island will provide a unique opportunity to study the geochemical evolution of the early (submarine) stage of ocean island volcanism. The major element, trace element and isotopic composition of the volcanics can be determined by microprobe, ionprobe and mass spectrometric analyses of carefully-selected, fresh glass and mineral separates. Combined with the detailed geochemical studies on the subaerial portion of Gran Canaria (Schmincke 1976, 1982, 1990; Cousens et al., 1990; Hoernle et al., 1991; Hoernle and Schmincke, 1993a, b, and references therein), the geochemical evolution of the submarine stage will serve as a case study of the passage of the lithosphere over a mantle plume.

### **Geology of Gran Canaria**

Gran Canaria (28° 00'N, 15° 35'W) is the central island of the volcanic Canarian archipelago in the central eastern Atlantic, some 100 km off the northwestern African passive continental margin. It is one of the best-studied oceanic islands with respect to stratigraphy, volcanology, geochemistry, and geochronology. All subaerially exposed volcanic and intrusive rocks were formed within the last 15 m.y. (McDougall and Schmincke, 1976). The most recent dated eruption on Gran Canaria took place approximately 3,500 years ago (Nogales and Schmincke, 1969), but younger prehistoric eruptions are likely (Schmincke, 1987).

Three major magmatic/volcanic cycles have been distinguished on Gran Canaria, which have been further subdivided into several stages (Schmincke, 1976; 1982; 1987; Hoernle and Schmincke, 1993 a and b) (Fig. 7).

The Miocene Cycle started with the rapid formation (~ 0.5 Ma) of the subaerial volcanic shield. Composition and age of the submarine part of the island are unknown. Lavas of the subaerial shield phase are tholeiitic to mildly alkalic basalts. Recently Hawaiian-type tholeiites have been discovered in the shield stage (Hoernle and Schmincke, 1993 a and b). At 14 Ma, the basaltic shield phase was followed by 0.5 m.y.-long volcanism of trachytic to rhyolitic composition (~ 15 cooling units, all chemically and mineralogically distinct) generating what is by far the largest volume of silicic volcanic rocks on any oceanic intraplate volcanic island. A large caldera (~ 15 km in diameter) was formed during the beginning of this phase. High precision single-crystal  $^{40}\text{Ar}/^{39}\text{Ar}$  dating has shown that the ash flows erupted at intervals of 0.03-0.04 m.y. (Bogaard et al., 1988). After the

rhyolitic stage, >500 km<sup>3</sup> of silica-undersaturated nepheline trachyphonolitic ash flows, lava flows and fallout tephra and rare basanite and nephelinite dikes and lavas were erupted between 13 and 9.5 Ma, followed by intrusive activity of syenites and a large cone sheet swarm in the central caldera complex lasting until ~ 8 Ma. Following a major nonvolcanic hiatus lasting approximately 4 m.y., the Pliocene Cycle began with the local emplacement of small volumes of nephelinites and basanites at ~ 5 Ma. With decreasing age from 5 to 4 Ma, the eruption rate increased and the lavas became systematically more SiO<sub>2</sub>-saturated from basanites to alkali basalts to tholeiites. Between 4 and 3.4 Ma, lavas, ranging in composition from alkali basalts through trachytes and basanites through phonolites, were intercalated with massive hauyne-phonolite breccia flows, fallout ashes and pumice flows, which were intruded by trachytic and hauyne phonolite domes (Roque Nublo Group). Following a possible brief hiatus in volcanism, there was a resurgence in volcanism, during which only highly undersaturated mafic volcanics were erupted. These mafic volcanics (3.2-1.7 Ma), ranging in composition from melilite nephelinites to basanites, probably represent the largest volume of highly undersaturated mafic lava flows on any oceanic island.

During the Quaternary, volcanism occurred almost exclusively in the northern half of the island. The oldest dated Quaternary Cycle volcanics are 1 Ma-old nephelinites, whereas the more recent Quaternary volcanics are predominantly basanites, with rarer eruptions of alkali basalt, tephrite and hauyne phonolite. The island can be considered volcanically active, as testified by numerous prehistoric basanite scoria cones, maars, and lava flows as young as 1,000 ka.

Important aspects of the volcanic and chemical evolution of Gran Canaria are 1) the striking differences in compositions of mafic rocks (tholeiites, alkali basalts, basanites, tephrites, nephelinites) erupted in temporally well-defined episodes over a period of ~ 15 Ma, which can be chemically distinguished in the reworked clastic rocks as well (Fig. 6a), 2) the very large volume of evolved magmas erupted between 14 to 13.5 Ma (silica-oversaturated trachytes and peralkaline rhyolites), 13 to 9.5 Ma (trachyphonolites), 4 to 3.4 Ma (trachytes through strongly silica-undersaturated hauyne phonolites) and ~ 1 Ma (hauyne phonolites), whose explosive eruptions generated excellent widespread marker beds, 3) the identification of individual units or groups of units by their characteristic bulk rock and mineral chemical composition and mineral modes and their distinction from volcanic rocks derived from the other Canary Islands (e.g. Fig. 6a, 6b, 6c), 4) the systematic variation in isotopic compositions with bulk rock composition and age on Gran Canaria (Fig. 6d) and other Canary Islands (Hoernle and Tilton, 1991; Hoernle et al., 1991) (rocks

of roughly known age can thus be correlated with volcanic cycles of different islands), and 5) most importantly, the abundant K-bearing phenocrysts (anorthoclase, sanidine and, in the Fataga trachyphonolites, biotite), contained within the evolved lavas, that allow precise single crystal dating.

## STUDY AREA - MADEIRA ABYSSAL PLAIN

### Background

The MAP (Fig. 1) lies at the center of the Canary Basin which is bounded by the lower flank of the Mid-Atlantic Ridge to the west, the Azores-Gibraltar Rise (part of the European/African plate boundary) to the north, the Northwest African Continental Rise in the east, and the Cape Verde Rise in the south. At its western end the abyssal plain extends westward between the abyssal hills of the Mid-Atlantic Ridge flank via fracture zone valleys which trend west-northwest-east-southeast. Further to the west are a series of seamounts which reach to within 300 m of the sea surface. The eastern boundary of the plain is marked by a break in slope from between 1:300 and 1:1000 above 5400 m at the foot of the North West African Continental Rise to less than 1:2000 below 5400 m.

The late Quaternary geological history of the MAP is known in greater detail than any other abyssal plain. During the last 730,000 years very large turbidity flows entered the MAP with a frequency related to climate changes - they appear to have been initiated during periods of both rising and falling sealevels. Between these flows, sedimentation reverted to hemipelagic deposition which alternated between carbonate-poor sediment (mainly clays) during glacials and carbonate-rich (mainly marls and oozes) during interglacials. This pattern of sedimentation does not fit the Vail model for rapid basin infilling (Vail et al., 1977) which suggests that turbidite emplacement should occur dominantly during low stands of sealevel.

### Lithology

#### *Hemipelagic Sediments*

The hemipelagic sediments alternate between clays/marly clays deposited during glacial intervals, and oozes/marly oozes deposited during interglacial conditions. The distinction between these

sediment types is dictated by the water depth of the site, placing it above the carbonate compensation depth (CCD) during interglacials, but below the CCD during glacials, when bottom water changes allow the spread of corrosive Antarctic Bottom Water into the area. This pelagic sediment sequence is clearly displayed in cores from the small hills which protrude above the plain; they show alternating marls and clays with some ooze layers. Each layer is at maximum a few tens of centimeters thick, with the clays usually being just a few centimeters thick. Average accumulation rates are between 0.3-1.5 cm/1000 years. Sediments older than about 2 Ma contain decreasing percentages of calcium carbonate and, by about 3.5 Ma, the sediment has become continuous red clay which is expected to continue to at least the Cretaceous or possibly to the basement (Weaver et al., 1986).

### *Turbidites*

The turbidites form the thickest layers and have been studied in great detail. Individual turbidites can be recognized by their mineralogical composition, micro-floral components, stratigraphic position and color. Individual flows have been designated by letter from *a* at the top down to turbidite *y* which has an age of about 730,000 years (Weaver et al., 1989). They fall into three compositional groups governed by their source area.

Organic-rich turbidites derive from the upwelling cells off the northwest African margin and have two sources, one north and one south of the Canaries. They contain more than 0.3% organic carbon and 45-60% CaCO<sub>3</sub> (de Lange et al., 1987). They are represented over most of the plain by very fine grained sediment (Mz 8-9 phi). The basal layers of these turbidites are often coarser, although in the west this usually means a slight coarsening of the basal few centimeters only. In the east of the area, particularly adjacent to the break of slope at the foot of the continental rise, the basal layers, represented by sands, may be over 1 m thick (Weaver and Rothwell, 1987). The oxidation front mechanism discussed later results in bi-colored turbidite units, usually olive green below the relict oxidation front where the organic material remains, and pale green above where the organic material has been oxidized.

Volcanic turbidites have high TiO<sub>2</sub> contents (about 1.5% CFB), low organic carbon (<0.3%), and 50-60% CaCO<sub>3</sub> (de Lange et al., 1987). They are fine grained over most of the plain, coarsening to the east and north-east. Their volcanic component is derived from the volcanic islands of the

Canaries and/or Madeira. These turbidites are buff brown in color without well developed relict oxidation fronts.

The white calcareous turbidites contain over 75% CaCO<sub>3</sub> and show chemical compositions more akin to the pelagic sediments of the area than to the other two groups (de Lange et al., 1987). Sediment coring has shown them to thicken to the west along the Cruiser fracture zone valley (Weaver et al., 1992) and they are believed to derive from the Cruiser/Hyeres seamount chain.

## **Geological History**

### *Stratigraphy*

The prerequisite of any geological history is a detailed stratigraphy. The MAP lies at a fortuitous water depth in relation to the CCD, which, as mentioned above, causes the pelagic lithology to vary in response to changes between glacial and interglacial conditions. These glacials and interglacials can be correlated with the oxygen isotope stage chronology and several isotope stages can be identified micropaleontologically using nannofossils (Weaver, 1983). Weaver and Kuijpers (1983) used this bio-lithostratigraphy to show that the incoming turbidity currents did not erode the seabed, and that the turbidites entered the area with a frequency related to climate change. Sedimentation fits a regular pattern, with thick turbidites lying between the successive hemipelagic units (clays and oozes). Thus the turbidites are deposited both during the transitions from glacial to interglacial conditions and from interglacial to glacial conditions with a frequency of one turbidite every 20-40 k.y. Twelve of the last eighteen isotope stage boundaries are represented by a turbidite from a single source and two have turbidites from two sources. Each of the four sources operates for a limited time period, supplying several turbidites, before giving way to one of the other sources. The reasons for this are unclear but may be related to recharge times or changes in accumulation rate in the source areas with time. The Canary Island source may be activated during times of increased volcanic activity in the islands, and the marine record may therefore give the best constrained information on these active phases.

### *Deeper Structure*

The longest cores so far recovered from the MAP represent about 730,000 years. The geological history of the area before this time must therefore be determined from an assessment of the structure

of the basin from seismic records. The seismic structure has been described by Duin and Kok (1984), Weaver et al. (1986) and Searle (1987). Four seismic units have been identified, overlying a basement of Late Cretaceous age (80-100 Ma). The deepest unit (Unit D) is seismically transparent and only intermittently present and may represent a facies change within Unit C.

Unit C represents pelagic sediment since it drapes over the underlying basement. We believe Unit C to represent red clay since the area has lain below the CCD almost continuously throughout its history (Weaver et al., 1986), and cores into the local abyssal hills show red clay sediments below about 3 Ma. The upper two units (A and B) probably both represent turbidite sediments, the distinction being in the strength of the reflectors which are much weaker in the lower Unit B. The combined thickness of Unit A/B varies between 120 and 530 m, but averages about 350 m.

Weaver et al. (1986) interpreted the seismic stratigraphy with reference to the geological history determined from core data and found a plausible explanation for the origin of the abyssal plain. Seismic Unit C is about 200 m thick and would have required a long time for its deposition if it is all or mainly red clay. The turbidite Unit A/B fills the depressions in Unit C and levels off the seafloor to give the flat plain. Unit A/B has accumulated rapidly - at about 100 m/m.y. for the last 300,000 years calculated from piston cores, although we have a lesser rate of 50 m/m.y. from the ESOPE cores for the last 730,000 years. These accumulation rates suggest that the abyssal plain could be formed in just a few million years. Von Rad and Wissmann (1982) have shown that the adjacent continental margin off northwest Africa built up by steady accumulation throughout the late Miocene, but this was followed by a period of erosion of the shelf and upper slope in the Pliocene, giving rise to an angular unconformity. During the late Quaternary there was considerable erosion of the shelf and upper slope with massive slope failures, slides and debris flows. The lateral equivalents of these slides and debris flows are found on the plain as turbidites.

## **Geochemistry**

### *The Redox Status of the Sediments*

Difficulties with the direct measurement of Eh in sediments have led to the adoption of a proxy geochemical convention for defining the redox status, based on the chemical species found in pore water solution. This is feasible because the oxidation of organic carbon, the principal reductant buried in sediments, progresses with bacterial mediation using a sequence of electron acceptors in

order of decreasing thermodynamic advantage. Thus oxygen is utilized first, followed by nitrate, manganese and iron oxyhydroxides and sulphate in that order (Froelich et al., 1979).

The pelagic sediments on the topographic highs of the GME area have low accumulation rates, contain only refractory organic carbon, and are oxic (i.e. free oxygen in pore water solution) to several meters. In contrast, the turbiditic sediments only a few hundred meters deeper on the plain below are oxic to only a few decimeters depth. The upper two, near-surface turbidites on the plain are of the organic-rich type. Turbidite a forms the uppermost sedimentary unit over most of the area studied, is oxic to  $20 \pm 2$  cm (Wilson et al., 1986; Thomson et al., 1987), and the oxic/anoxic boundary is marked by a color change from pale brown to light grey at this depth. To the east, turbidite a is very thin, (< 20 cm) and here the oxic/anoxic boundary is located at 40-50 cm in turbidite a1 and is marked by a color change from brown grey to olive grey (Wilson et al., 1985).

These observations have led to the concept of a progressive oxidation front which is formed as bottom water oxygen diffuses down into the turbidite from the sediment/water interface after emplacement, oxidizing as it does so the organic carbon introduced with the turbidite (Wilson et al., 1985, 1986). Various redox-sensitive pore water species show gradients into the front, which appears to be coincident with the color changes in both turbidites. The abrupt redoxcline implied across this front (Sorensen et al., 1987) is in contrast to the succession proposed by Froelich et al. (1979) which is often taken as the general case for deep-sea sediments. The progressive oxidation front is interpreted to be principally a diffusion phenomenon, because bioturbation is present only to 10 cm below the sediment water interface (Thomson et al. 1988).

Several redox sensitive elements (Mn, Fe, P, Co, Cu, Ni, U, V, I, and Zn) redistribute about the progressive oxidation front when it is active. Some of these redistribution profiles persist in buried turbidites, where the oxic depths achieved when the fronts were active can be recognized by color contrasts near the tops of individual units (Jarvis and Higgs, 1987). These color contrasts are therefore preserved in anoxic pore water conditions experienced following emplacement of later turbidites.

The deepest pore water investigations made in the GME sediments are those made on the 30 m cores retrieved on the ESOPE expedition (Schuttenhelm et al., 1988). These data demonstrate that the pore waters between the active progressive front at < 50 cm and the maximum depth cored are post-oxic on Berner's (1981) definition, i.e. negligible free oxygen or sulphide in solution.

Extrapolation of the decrease in the near-linear pore water sulphate profiles suggests zero sulphate at 100-m depth. Such a long diffusion path length limits the supply of sulphate for sulphide production. It is unclear why the large amount of reactive organic carbon buried in the GME turbidites does not drive sulphate reduction at shallow depths in the sediments, as is observed in sediments in shallower water. In the face of a similar problem, Waples and Sloan (1980) speculated that bacterial activity will be at the maximum level possible and that electron-acceptor supply may be the rate-limiting step. Lovely and Phillips (1987) have demonstrated in laboratory experiments that Fe (III) reducing bacteria out-compete sulphate reducers and methanogens when all three types are present. Certainly, some level of organic degradation is proceeding at depth in the GME sediments as evidenced by the increasing pore water  $\text{NH}_4^+$  levels with depth (Schuttenhelm et al., 1988). The post-oxic condition observed in the deeper sediments is consistent with ferric oxyhydroxides as terminal electron acceptors to at least 30 m.

## **SCIENTIFIC OBJECTIVES AND METHODOLOGY**

### **Summary of Objectives**

- 1) To investigate mantle source evolution.
- 2) To conduct high resolution stratigraphic, compositional, temporal, structural, and sedimentological analysis of a large volcanoclastic apron surrounding an intraplate volcanic island system and of the more distal abyssal plain sediments.
- 3) To carry out 3-D basin modelling.
- 4) To determine the response of the lithosphere to loading and heating during magmatic activity and enhanced levels of stress associated with temporal changes in plate dynamics.
- 5) To carry out paleoceanographic and bathymetric reconstructions by identification of dissolution interfaces, benthic organisms, and isotope studies.

- 6) To determine the frequency of turbidite emplacement on the Madeira Abyssal Plain and, through comparison of these frequencies with standard paleo-sealevel curves, correlate emplacement with sealevel oscillations through the whole interval of turbidite input to the plain (12 to 15 Ma).
- 7) To determine the provenance of the turbidite sediments using geochemical, mineralogical, and micropalaeontological methods.
- 8) To calculate sediment budgets for the growth evolution and unroofing of Gran Canaria and organic carbon and volcanoclastic components throughout the Canary Basin by measuring the volume of sediment, and the percentage of  $C_{org}$ , in each turbidite on the abyssal plain.
- 9) To quantify the long-term effects of sediment burial and diagenesis in a sequence of mixed organic-poor and organic-rich sediments and to assess chemical fluxes between components (especially volcanic glass and seawater), maturation of organic matter at elevated temperatures in the proximal facies near the hotter interior of the island as well as during low temperature diagenetic conditions away from the hot spot.

## **Specific Objectives and Methodology**

### *Mantle Source Evolution*

Major changes in the composition of several distinct mantle sources for primitive magmas have been found throughout the subaerial development of Gran Canaria (Fig. 6d). The structure and chemical composition of the non-exposed initial seamount and submarine shield phase comprising ~ 95 vol% of the island are virtually unknown. Obviously, the observed variations in the subaerial portion, making up only 5% of the volcano, are not representative of the whole volcano. Isotopic studies of the subaerial volcanics on Gran Canaria show that the isotopic composition changes significantly with age (e.g. Hoernle et al., 1991; Hoernle and Schmincke, 1993a, b), possibly reflecting greater influence of lithospheric/asthenospheric assimilation in the late stages of ocean island volcanism as in Hawaii (Chen and Frey, 1985). If this is the case, then the voluminous submarine volcanics, formed when the volcano was directly above the plume, whose roots have been identified as deep as 400 km (Anderson et al., 1992), should more closely reflect the true isotopic composition of the plume. Recently-analyzed samples from the uplifted basal (submarine)

complex on La Palma have the most radiogenic Pb yet found in the Canary islands, consistent with this hypothesis (Hoernle et al., in prep). Knowledge of the chemical composition and age of the submarine stage on Gran Canaria will allow us to more clearly characterize (1) the composition of different mantle reservoirs (i.e. plume, asthenosphere and lithosphere), (2) the compositional variability of these reservoirs, (3) the generation of melts from these reservoirs, and (4) mixing of magmas/material from these reservoirs. Grain size and freshness of some clasts should be sufficient to obtain reliable radiogenic isotope ratios.

### *High-Resolution Stratigraphic, Compositional, Temporal, Structural, and Sedimentological Analysis*

#### Stratigraphy

Widespread conspicuous seismic reflectors in marine sediments around the Canary Islands and volcanic islands in general are mostly volcanoclastic debris flow sheets (Wissmann, 1979; Schmincke and von Rad, 1979). The seismic stratigraphy on the continental slope southeast and east of the Canary Islands is well established. South of the Canaries, DSDP Sites 369 and 397 on the West Sahara slope reach Lower Cretaceous. In the north, DSDP Site 415 reaches Late Albian, a Tithonian reflector can be traced from DSDP Site 416. This seismic stratigraphy cannot yet be carried across the island chain into the sedimentary basins north and southwest of Gran Canaria but the current processing of the data collected in 1991 (Meteor 16-4) has revealed a number of well developed reflectors west and southwest of Gran Canaria that are promising for correlation to the southeastern basin. The very detailed additional seismic surveys carried out in 1993 will allow a nearly complete seismic stratigraphy of the entire apron area surrounding Gran Canaria. Age and composition of such volcanoclastic marker beds can be identified in drill cores. This becomes especially important closer to an island, where the volcanoclastic debris flow sheets are interbedded with other volcanoclastic sediments of the apron and are then very difficult to resolve by seismic methods.

#### Composition

A major objective is the detailed geochemical analysis of bulk rocks and single components in all sections drilled using bulk rock analytical methods such as XRF and ICPMS as well as mass spectrometry for isotope ratios and microprobe and ion probe methods for glass and mineral

components. Volcanic clasts from various sources can be distinguished by chemical (especially isotopic) and mineralogical differences. The compositional database for Gran Canaria is unique since it contains several thousand mineral, >1000 rock, and >100 isotope analyses. Rocks from Tenerife are less extensively analyzed to date but data from many current projects will be available by 1994. Volcanic rocks from Madeira and the Canary Islands can be unequivocally distinguished by major and trace elements as well as isotope ratios (Hoernle et al., in prep.).

### Dating

The volcanic nature of widespread reflectors in both basins is a major bonus in providing a gross stratigraphic framework. This, coupled with the basic more detailed stratigraphic framework obtained from long piston cores in the MAP and the good biostratigraphic record of the nonvolcanic sediments, should allow a very good time resolution for the bulk of the sedimentary fill. In the VICAP-MAP project we will attempt a very high resolution temporal analysis of those major parts of all sections drilled containing distal deposits of explosive eruptions. This is feasible as a result of the development of methods to date single crystals by laser heating and the abundance of K-feldspar and biotite-bearing highly evolved rhyolitic, trachytic, and phonolitic magmas especially on Gran Canaria (some 50 to 100 volcanic explosive events (ash flows and fallout layers) between 14 and 3.5 Ma whose products are widespread in the sedimentary basins as shown by previous drilling (DSDP Sites 369, 397) (Schmincke, 1982; Schmincke and von Rad, 1979). This will be complemented by K-feldspar bearing ash layers from Tenerife, expected to be abundant in the southwestern and possibly also northern apron in deposits younger than ~ 2 Ma.

### Inception of Volcanism with Implications for Hot Spot Migration

A major problem in dating the inception of oceanic intraplate volcanism is the lack of records and the fact that most of the evolution by volume occurs under water. We expect to be able to much more precisely date the beginning of volcanism of Gran Canaria and (probably much younger) Tenerife and, with proposed site VICAP- 5, that of the eastern Canaries, through drilling to the base of the volcanic apron. These data provide important constraints for calculating progression of volcanism across the island chain and therefore plate kinematics.

Evidence is increasing from many ocean basins that evolved magmas also erupt at great water depth, sometimes explosively when the magmas are volatile-rich. Although we cannot exclude that

such volcanic eruptions also occurred in the Canary Islands, we suspect that the bulk of the evolved magmas were emplaced during more mature evolutionary phases on land. Our published and unpublished data from DSDP Sites 369 and 397 indicate that clinopyroxenes and feldspar phenocrysts, and even most glass shards, are generally fresh in all evolved tephra layers as old as 14 Ma. This will enable high resolution compositional correlation with major units on land most of which can be distinguished from each other by their glass and mineral compositions.

The proposed focussed drilling strategy aims to identify many of the Miocene and Pliocene evolved ignimbrites and fallout ashes on Gran Canaria with their counterpart marine flow and fallout tephra layers, contributing to better volume calculations of magmatic events and quantifying a unique prototype scenario of land-sea correlations. We also expect to distinguish primary from secondary volcanoclastic fragments and deposits and thus be able to date and quantify erosional and volcanic episodes and compare the computed rates and volumes with those derived from the more accessible, but less complete, record that remains on land.

The entire chemical/petrological, volumetric, and temporal evolution of an intraplate volcanic system can be quantified. Early stages of the volcanic and magmatic evolution of a "hot-spot volcano" can be dated and reconstructed. In contrast to Hawaii, detailed studies of the subaerial volcanics on Gran Canaria provide evidence for the existence of at least three distinct volcanic cycles, which may have evolved similarly from SiO<sub>2</sub>-undersaturated, to SiO<sub>2</sub>-saturated, back to SiO<sub>2</sub>-undersaturated magmas. If the submarine portion of the volcano also represent multiple cycles of volcanism, then the evolution of a Canary Volcano may be significantly different from the evolution of a Hawaiian volcano. These differences may ultimately reflect differences in rates of plate motion and plume flux rate. The Hawaiian Islands, the end member for Pacific-type ocean island volcanoes, were formed on a very rapidly moving plate by a plume with an extremely high flux rate. The Canary Islands, a possible end member for Atlantic-type ocean islands, on the other hand, were formed on a very slowly moving plate by a very weak, possibly intermittent plume (Hoernle and Schmincke, 1993b).

The Madeira Abyssal Plain, the deepest part of the Canary basin, is the ultimate sink for all clastic material, and is located more than 750 km from the island. The proposed drill site MAP-1 is expected to contain the very distal facies of Canary Islands volcanoclastic sediments intercalated

with detritus derived from Madeira, the Atlantis-Meteor seamount complex, and the W-African continental slope.

Very thin distal turbidites and fallout ashes, potentially extending to more than 1000 km, are recorded in the MAP based on preliminary data from giant piston cores and the Canary slide extending from Hierro into the MAP has recently been studied in some detail (Masson et al., in press). Single mass flows and turbidites that travelled into the very distal abyssal plain must record major events on the island, most likely giant slumps of the type recently documented in detail in the Hawaiian Islands (Moore et al., 1989) or major volcanic events such as emergence of an island, caldera collapse and accompanied huge ash flow eruptions or on land volcanic debris avalanches of the type recorded for the Middle Pliocene on Gran Canaria (Mehl and Schmincke, 1992).

The volcanic and morphological evolution of Gran Canaria throughout its 15-m.y. subaerial history has differed significantly in the north and south, the vast majority of the Miocene ash flows accumulating in the south while the northern half was much more heavily eroded during the Miocene but was covered with several hundred meters of Pliocene to sub-Recent mafic lava flows and cones. Drilling of proposed sites VICAP-4 and 5 will enable us to establish a seismic stratigraphy in the north and shed light on the evolution and age of this basin where the compositional spectrum and relative amounts of volcanically and erosionally produced detritus for similar time slices probably differs appreciably from the south. This basin could also be considerably younger than the Triassic/Early Jurassic rift basin (with salt diapirs) to the east of Fuerteventura, if the Atlantic opened by multistage episodic rifting. A refinement of the seismic stratigraphy in the basins north and southwest of Gran Canaria and west of Fuerteventura would substantially help to constrain these conclusions. Penetration of the volcanoclastic apron by drilling should provide important data for the spatial and temporal extent and origin of the major unconformity separating Lower Cretaceous from Neogene sediments.

### *3-D Modelling of Basin Evolution*

The proposed drilling operation and seismic surveys will provide an excellent data base for 3-D modeling of the clastic apron of Gran Canaria. The limited size of this clastic apron, high resolution stratigraphy from unusually complete and detailed pre-site surveys and the drilling operation, identification of sediment geometry from seismic surveys, and point source of sediment fluxes will

facilitate the development of a model. The main topic is the reconstruction of the system, i.e. sediment source, dispersion, and fill, the history of deposition of the clastic apron, and unroofing Gran Canaria.

Model development will include 1) a database of all available data with spatial and time coordinates, 2) end-member modeling of various sedimentological, geochemical, and petrological parameters to specify sediment-source relations within the stratigraphic framework, 3) a time series approach based on the recovered material to analyze and correlate series of volcanic and sedimentary events with emphasis on the major volcanic input-pulses (volcanic cycles) building up the volcanoclastic apron, 4) areal and volume modeling of the different stratigraphic units (cycles) including seismic results using geostatistics and other volume-modeling techniques, and 5) a reconstruction of the apron-building history compared to the Gran Canaria deroofting, and calculation of the sediment budget by stacking of single stratigraphic units to reconstruct the spatial evolution of the volcanoclastic apron in an overlay model and numerical simulation of volcanoclastic dispersion and deposition from the central volcanic area based on volcanological parameters (eruption styles, eruption intensities etc.), and comparison to the reconstruction.

### *Response of the Lithosphere*

The bathymetry around oceanic intraplate volcanic complexes is determined by 1) the density-, thickness- and age-dependant static equilibrium of underlying oceanic basement, 2) subsidence by loading with the volcanic edifices and their volcanoclastic aprons (e.g. Watts et al. 1985; Brocher and ten Brink, 1987; Watts and ten Brink, 1989), 3) subsidence by loading with continent-derived sediments, and 4) uplift by reheating of the lithosphere due to thermal anomalies in the mantle associated with intraplate volcanism (McNutt, 1984).

In the case of the Canary Islands, the relative scale of these effects is a matter of ongoing debate. The Moho was found to lie at a rather constant depth of 15 to 16 km below the central Canary Islands by Banda et al. (1981). Filmer and McNutt (1988) in their study on geoid anomalies did not find evidence for shallow reheating or presence of a mantle plume while Dañobeitia (1988) postulated a depth anomaly in the order of 500 to 1,000 m. He assumed that uplift of the lithosphere by reheating during the beginning of Canary Islands volcanism at 50 Ma almost balances the subsidence resulting from lithosphere thickening by cooling and loading with sediments.

The zone of intraplate deformation offers the prospect of making quantitative progress in the study of lithospheric response to enhanced levels of stress associated with temporal changes in plate dynamics. Identification of marker beds enables volumetric interpretations and reconstruction of the three-dimensional structure of the volcanoclastic apron, which in turn allows deduction of the spatial and temporal response of the lithosphere/mantle system (intraplate deformation and mechanics of flexure) to gravitational loading. It can also reveal the tectonics related to the growth of a volcanic island and the tectonic evolution of a volcanoclastic basin next to a volcanic island. The sediment aprons around the islands preserve direct and indirect evidence of volcano growth and vertical movements. The area provides an interesting analogy to the northeastern Indian Ocean where integrated marine geophysical and modeling studies have demonstrated the crucial role that intraplate stresses (Cloetingh and Wortel, 1985) play in causing a concentration of extensional and compressional deformation in the oceanic lithosphere (Stein et al., 1989, 1990). VICAP-MAP will study the interplay of vertical loading and in-plane stresses using high-resolution data on the temporal evolution of the area. For this purpose, the flexural behavior of the lithosphere using depth-dependant rheologies and variations in stress level associated with this particular tectonic setting will be modelled using state of the art numerical modelling techniques (Cloetingh et al., 1989).

#### *Paleobathymetry and Paleoceanography*

The VICAP drill holes provide important perspectives for the reconstruction of paleobathymetry and paleoceanography of the eastern North Atlantic Ocean in the surroundings of the Canary Islands. It will be of particular importance to investigate the paleobathymetry of the volcanoclastic apron by means of 1) reconstructing the CCD and other dissolution interfaces, 2) analyzing, in detail, the communities of benthic organisms, particularly benthic foraminifera, as qualitative depth indicators, and 3) comparing carbon isotope ratios in the shells of calcareous benthic organisms and planctic surface water dwelling organisms (particularly the carbon isotopes of benthic organisms during periods of elevated carbon contributions in the course of volcanic activity maxima).

Inferences on sea level changes will allow us to separate local from global, tectonically-related effects. The system of currents in the vicinity of the Canary Islands during the past 15 m.y. (stratigraphy of deep-water circulation) can be reconstructed and the response of currents (direction,

*...Leg 157 - Gran Canaria and the Madeira Abyssal Plain...*

velocity, composition, temperature, stratification, etc.) to the evolution of the Canary Islands evaluated.

Important paleoceanographic problems can be addressed when drill holes successfully sample the old Mesozoic part of the Atlantic Ocean. The youngest sediments will permit detailed studies of the Neogene sedimentary sequence with emphasis on the Messinian salinity crisis, which is developed in the Mediterranean but also seems to leave a trace in the isotope signals of the entire Atlantic.

Information on paleo-wind directions can be gained by reconstruction of depositional fans of Plinian fallout ashes. Late Tertiary and Quaternary climatic evolution in the Sahara and Sahel Zone may be deduced from silica dust fluxes (Tiedemann et al., 1989).

#### *Frequency of Turbidite Emplacement*

Determining rates and frequencies of sedimentary processes depends on high resolution stratigraphy. For the late Quaternary in the MAP, we have been able to tie turbidite depositional events to periods of changing bottom water mass, which have elsewhere been linked to climate change. Our resolution is in the order of a few thousand years, and while recognizing that our integrated stratigraphy in this area will never have the resolution now available from recent paleoceanographic legs, it is likely to provide the best stratigraphy for any abyssal plain studies.

We propose to use the same stratigraphic methods for the upper part of the sequence to at least 2.5 Ma because hemipelagic cores from the area show similar alternating carbonate rich and poor layers for the whole of this interval. Thus the methods of high resolution stratigraphy, involving calcareous nannofossils and a lithostratigraphy, should be applicable to at least this age. Beyond 2.5 Ma, the hemipelagic sequence becomes rapidly more carbonate-poor due to dissolution although good paleomagnetic signals can be found throughout.

High-resolution stratigraphy therefore becomes more complicated beyond 2.5 Ma but it is possible to analyze calcareous nannofossils from the turbidites which were originally deposited well above the CCD, and, due to rapid burial, have had their carbonate preserved. They obviously contain a reworked mixture of nannofossils but first occurrence data (FAD's) will not be affected. The FAD of a species will simply occur in the first turbidite to be laid down after its appearance, and, since turbidites occur frequently on the plain, this age will be close to the true age of this datum. Weaver

et al. (1992) has shown that the turbidites contain mainly contemporaneous material representing a mixture of only one or two hundred thousand years (the events that initiated them did not erode deeply into older sediments). By using FAD data alone, half of the datum planes used in standard nannofossil zonations of the last 15 m.y. would be available. This would enable us to divide the sequence into approximately one million year long intervals, within which it would be possible to determine the total number of turbidites.

The method therefore divides into a high frequency correlation for the last 2.5 m.y. where we can compare individual turbidites with individual sealevel changes, and, beyond 2.5 Ma, a lower frequency comparison of periods of turbidite input with lowstands on accepted sealevel curves. By drilling beyond 2.5 Ma, we will test whether the plain sediments are built up from packets of turbidites separated by long intervals of hemipelagic accumulation and whether these turbidite packets correlate with sealevel lowstands. If the correlation of turbidite input with sealevel change holds, intervals such as the early and middle Pliocene, representing about 2.5 m.y., would be represented by just a few meters of pelagic clay. On seismic records these would be indistinguishable from a single turbidite layer. If such a correlation exists, it would indicate that periods of non-oscillating sealevels represent periods of stable sediment accumulation on the continental margin. We know that the margin was stable in this way for much of its history before the initiation of the abyssal plain.

#### *Provenance of Turbidite Sediments*

Work to date (Weaver et al., 1992) has shown four distinct sources of turbidites, volcanic-rich turbidites derived from the oceanic islands, organic-rich ones from the continental margin both north and south of the Canaries, and carbonate-rich ones from seamounts to the west of the plain. This analysis is based on geochemical analyses and mapping the entry points on the plain using grain size analyses.

We expect there to be a strong correlation between volcanic turbidite emplacement and active volcanic phases on the Canary Islands and Madeira. Some of our other work around the Canaries is aimed at determining whether single volcanic eruptions initiate mass wasting or whether material first accumulates on the island slopes until it becomes unstable. These volcanic-rich turbidites nevertheless seem to be tied to sealevel change and there could be a link between climate (sealevel) change and volcanic activity as well as sealevel change and slope stability.

We still do not understand why only one turbidite is contributed at each sealevel change when there are four widely separated independent sources. The answer to how these sources communicate may lie in recharge times in the source areas or in initiation of mass wasting by earthquake activity. Earthquakes are not frequent on this passive margin but during, or following, sealevel change, there may be a period of crustal readjustment when earthquakes are more frequent and larger. Thus sealevel change could be an indirect cause of sediment instability.

### *Sediment Budgets*

#### Volcanic Apron

To determine sediment budgets for material transferred from the submarine and subaerial stages of the Canary Islands by volcanic processes and erosion, as well as for filling of the abyssal plain, it will be necessary to (a) drill the different facies areas of the apron on the two contrasting sedimentation basins north and south of Gran canaria as well as the abyssal plain, (b) identify the volcanic-rich turbidites and their source areas, (c) obtain a nannofossil stratigraphy from the turbidites, (d) radiometrically date their volcanic minerals, and (e) estimate the area covered by individual flows from seismic data as done for several recent turbidites by Weaver and Rothwell (1987). Calculation of the sediment budget through time is necessary for determining the size of the Canary Islands, particularly how they have expanded and contracted during periods of activity and periods of increased erosion.

#### Canary Basin

Sufficient data on the MAP exists to enable the construction of isopach maps for each sedimentary unit through the last 300,000 years (Weaver and Rothwell, 1987; Rothwell et al., in prep). These maps have allowed us to calculate the volumes of material in each flow, showing that the largest turbidites have volumes in the order of 190 km<sup>3</sup>. We have used large numbers of piston cores for these calculations but a consistent pattern has emerged with turbidites thickening either to the east or the west and being fairly constant from north to south. To determine the volumes of each flow in the deeper parts of the sequence a minimum of four drill sites is required. Since we know the boundaries of the plain, back in time through our dense seismic grid, we will be able to extrapolate

from the measured thicknesses of each turbidite in each drillsite. Identification of the same turbidite in different cores is based upon the fact that each one usually has its own microfloral and geochemical signature. Once the turbidite sequence is dated, we will be able to use the seismic data to follow time planes across the whole plain and, in this way, determine volumes of turbidite material for each time interval.

Mass-wasting produces slides, debris flows, and turbidites, and so the turbidite volumes will not be equivalent to the total volume of transported material. However, our work has shown that mass wasting occurs along large tracts of the margin and it would be impossible to drill each set of mass wasting deposits on the continental slope. The Northwest African margin is unlikely to be exceptional in this respect, and debris flows are expected on most continental margins. Drilling abyssal plains, therefore, offers the best opportunity to determine sediment budgets for whole basins, but we must understand the relationship of debris flows to turbidites. Work carried out by the UK and EEC on the Northwest African margin has shown that for turbidite *b*, deposited at the end of the last glacial, the turbidite on the plain has a volume of 120 km<sup>3</sup> and debris flows on the continental slope a volume of 400 km<sup>3</sup>. As a percentage of the total mass-wasted deposits of this event, the volume of turbidite *b* is rather small, but this event appears exceptional in the size of its debris flow content, in that the debris flow reached to the edge of the abyssal plain, over 700 km from source, (Masson et al., in press). Preliminary data suggests the turbidite may represent between 50 and 100% of most flows.

### *Geochemistry*

The VICAP-MAP project will pursue the geochemical identification of turbidite provenance as demonstrated by de Lange et al. (1987) and work in progress by Jarvis. This is relevant to possible variation of source areas and source frequencies over time. Interpretation would be facilitated by the spectral gamma logging of the holes and potentially an intercalibration of this physical response with chemical analyses of the solid phase by IP-AES and IP-MS.

Long-term persistence of the record of oxidation fronts in the turbidites will also be investigated (Thomson et al. 1987). This includes examination of the long-term persistence of metal relocations, particularly of uranium (Colley and Thomson, 1985, 1990; Colley et al., 1989; Jarvis and Higgs, 1987). The more mobile redox active elements, such as iron and manganese, migrate away after

conditions become reducing, so that the interpretation of paleoredox conditions requires an understanding of elements which do not remobilize and thus are expected to provide persistent signatures in the sedimentary record. VICAP-MAP studies will evaluate the stability of such signatures in sediments older than the 700-ka examples studied to date (Colley, and Thomson, 1990).

This project will also investigate authigenic minerals which have been suggested to accompany diagenesis of organic-rich turbidites, e.g. iron silicates (de Lange and Rispen, 1986). This work requires high quality pore-water samples, fully protected from atmospheric oxidation. To date, such samples have only been obtained from the upper 10 m at the GME site. Because the relevant diagenetic processes are quite slow, it is likely that deeper high quality samples will provide more useful information on the active mechanisms. This investigation would combine shipboard pore-water analysis with later laboratory extraction experiments and electron microscopy and microprobe studies. In this way the mechanism of utilization and development of cementation in a mixed pelagic/turbidite sequence with varying proportions of  $\text{CaCO}_3$  can be examined.

Investigations will also be made on pore water geochemistry. Large quantities of organic carbon are buried with the upper turbidites: concentrations in the range 0.5-1.5% are found in the organic-rich turbidites (de Lange et al. 1987; Jarvis and Higgs, 1987). This carbon is not inherently refractory, since it is readily remineralized in those parts of the turbidites which have been in prolonged contact with bottom water oxygen (Wilson et al. 1985, 1986). Nevertheless, buried organic carbon appears to undergo only very slow oxidation once oxygen and nitrate are exhausted. Even though theory suggests that active sulphate reduction and sulphide production should occur, it does not; high levels of pore water sulphate persist. Existing theory is therefore inadequate. Extrapolations from existing pore water data (30-m cores) suggest that pore water sulphate is not in fact consumed until a depth of about 100 m below the sediment-water interface is reached. Such a gradient length limits the potential sulphate supply and sulphide formation. The pore water concentrations of ammonium and phosphate ions, however, both increase linearly with depth over 30 m, suggesting that organic remineralization may be active at greater depth, although again the calculated transport ratios are not consistent with a sulphate reduction stoichiometry. The long-term fate of this reactive organic carbon in the deep-sea requires elucidation, and the most promising approach is an investigation of a comprehensive suite of pore water species at depth.

The diagenesis and maturation of the organic component of the sediment will also be studied by techniques such as Rock-Eval pyrolysis both above and below the level of sulphate reduction.

The VICAP-MAP project will also permit assessment of chemical fluxes between components, especially volcanic glass and seawater, maturation of organic matter at elevated temperatures in the proximal facies near the hotter interior of the island as well as during low temperature diagenetic conditions away from the hot spot.

The timing of hydrothermal and low-temperature circulation and the mass budget of element exchanges related to the submarine growth stage of Gran Canaria will be investigated by determination of diagenetic gradients, authigenic phases, and alteration of volcanic glass along radial profiles (e.g. Bednarz and Schmincke, 1989). The glassy nature of volcanoclastic debris makes it an especially sensitive indicator of diagenetic processes.

## **DRILLING PLAN/STRATEGY**

Locations and descriptions of the proposed VICAP and MAP sites are given in Table 1 and shown in Figs. 8 and 9, respectively.

### **Southern Sites (VICAP)**

We propose to drill four holes south and southwest of Gran Canaria, penetrating the proximal (proposed site VICAP-5), medial (proposed sites VICAP-4 and -7), and distal facies (proposed site VICAP-8) in the South Canary Basin.

These sites should provide a fairly complete sequence of volcanoclastic deposits derived from the submarine and southern subaerial volcanic stages, especially many submarine equivalents of the large ash flows that entered the sea along the paleocoastline of the island between ~ 14 and 10 Ma, as well as younger fallout layers. The seismic lines available show a clear separation of an upper and lower group of sediments, interpreted as the main boundary between the bulk of the submarine growth stage of the Gran Canaria volcanoclastic apron, overlain by younger volcanoclastic Gran Canaria apron deposits (subaerial stages?) and the much younger Tenerife volcanoclastic apron, distinguishable by age and composition from those derived from Gran Canaria. Very abundant fallout tephra (ash) layers and distal submarine extensions of ash flows that entered the sea at the

southwestern coast of Tenerife during the past 2 m.y. should dominate the uppermost part of the section. The excellent recovery of Miocene and younger fallout ash layers at ODP Sites 369 and 397, southeast of Gran Canaria, makes us confident that many ash layers will be recovered. The number and ages of fallout ashes from Gran Canaria recovered will be largely dependant on the (unknown) paleowind direction. Those erupted from the Pico de Teide Complex on Tenerife should be very abundant, because the sites are downwind from the island.

### **Northern Sites (VICAP)**

We propose to drill three sites north and northeast of Gran Canaria to penetrate the "seismic apron" on the island flank (proposed site VICAP-2) and the proximal (proposed site VICAP-6) medial/distal facies (proposed site VICAP-1) in the North Canary Basin.

The northern sites are expected to reflect volcanism, erosion and sedimentation that differ significantly from the south. We hope to penetrate the lowermost part of the Gran Canaria as well as Fuerteventura (?) aprons. These data will show if the age of volcanism in the eastern Canary islands is compatible with a hot spot location at 20 to 30 Ma and an age progression of volcanism from northeast to southwest as proposed by Holik et al. (1991). A similar age progression was proposed by Dañobeitia and Collette (1989) from interpretations of seismic reflection profiles. While the deposits from the submarine stage of Gran Canaria may, or may not, differ in composition and type from those in the south, the younger volcanoclastic deposits should reflect a volcanic and erosional evolution that differs appreciably from that in the south. We expect sufficient fallout layers and distal submarine equivalents of ash flows to date the deposits by single crystal laser heating because ash flows were also erupted from the northern ring fissures of the Miocene caldera but in lesser amounts. Phonolitic deposits from the Fataga Group (~ 13-10 Ma) should dominate. We also expect much more erosional detritus from the Miocene rhyolitic and trachytic stages. By far the largest difference should show up in the Pliocene to Recent deposits. Primary and eroded products from the > 100 km<sup>3</sup> Roque Nublo Stratovolcano (comparable to present day Tenerife in size but not in composition) ash flows, lavas, debris flows, lahars were largely channeled to the north and northeast, the thick Las Palmas clastic fan on land indicating the huge volume of these deposits. Ash layers from the Roque Nublo phase of volcanic activity (~ 5-3.5 Ma) should be abundant at these sites. Detritus from eroded basanitic to nephelinitic flows should dominate the volcanoclastic deposits from the last 2 m.y., probably interspersed with some fallout

tephra layers from Tenerife. We do not expect thick volcanoclastic apron deposits from Tenerife at these sites, however.

### **Cross-Channel Sites (VICAP)**

Two sites will be drilled to establish a correlation between North and South Canary Basin across the channels separating Gran Canaria from Tenerife (proposed site VICAP-9) and Gran Canaria from Fuerteventura (proposed site VICAP-3).

### **Deep Objectives (MAP)**

Drilling this site (proposed site MAP-1; Fig. 9) in the deepest part of the Madeira Abyssal Plain will provide information on the timing and frequency of mass wasting events for the whole Canary Basin.

### **Shallow Objectives (MAP)**

Drilling these sites (proposed sites MAP-2, -3, and -4; Fig. 9) will allow calculations to be made of volumes of individual sediment flows which can be used to determine sediment budgets for the whole Canary basin. We propose to drill three sites in addition to proposed site MAP-1 at locations distributed across the abyssal plain, penetrating as far as the base of the turbidite sequence (350 m maximum). This set of sites would allow the first mapping of the build-up of an ocean basin on a layer by layer basis, thus providing the information for calculating the volumes of sediment transported to the deep ocean per unit time. The extensive knowledge of the area already obtained will allow precise estimates of the volumes of individual turbidite flows from just the four sites. When this is combined with estimates of the amount of material deposited as debris flows on the continental rise calculations of sediment budgets for the whole Canary Basin can be made. Since some of the turbidites have a volcanic origin, we will also be able to calculate erosion rates for the Canary Islands and Madeira.

## **PROPOSED SITES**

### **VICAP**

Proposed site VICAP-1 is located in the North Canary basin and will be drilled to a depth of approximately 1000 m in an attempt to determine the thickness of the medial/distal facies of the shield stage and the younger volcanoclastic deposits north of Gran Canaria.

Proposed site VICAP-2 is located on the outermost edge of the massive island flank, i.e. the "seismic apron". VICAP-2 will be drilled to a depth of approximately 800 m to test the validity of dating initiation of the volcanic island/seamount by the stratigraphic position of the base of the apron.

Proposed site VICAP-3, east of Gran Canaria, is located in the channel between Gran Canaria and Fuerteventura on the top of a major volcanoclastic debris avalanche deposit that has been well dated on land. VICAP-3 will be drilled to a depth of approximately 700 m through a sediment pocket in an attempt to correlate North to South Canary Basin stratigraphy across channel.

Proposed site VICAP-4, and its alternate proposed site VICAP-4a, is located S-SE of Gran Canaria. This site will be drilled to a depth of approximately 500 m to determine the thickness of the volcanoclastic deposits (i.e. the medial facies). DSDP Site 397, located further south, will be used as a reference site for the distal facies. An attempt will be made to verify the correlation of DSDP Site 397 stratigraphy with the MCS M16-4 and M 24 records in the deep part of the South Canary Basin well away from the continental slope.

Proposed site VICAP-5 will be drilled to a depth of approximately 300 m and will penetrate the volcanoclastic deposits (proximal facies) south of Gran Canaria. The site is located at the continuation of a large on-land canyon. By drilling this site, we aim to determine the sedimentation rates for a major drainage system that has operated since the Miocene shield stage.

Proposed site VICAP-6 is located directly north of Gran Canaria and will penetrate volcanic/volcanoclastic deposits (proximal facies). This site will be drilled to an approximate depth of 300 m in an attempt to establish the thickness of individual volcanic layers down to the top of the shield stage on the island flank (i.e. the "seismic apron") as close as possible to Gran Canaria.

Proposed site VICAP-7 is located southwest of Gran Canaria. This site will be drilled to an approximate depth of 1000 m in an attempt to identify and determine the thickness of the Gran Canaria shield stage and the younger Gran Canaria and Tenerife deposits (the medial facies). Furthermore, we will compare the stratigraphy recorded at this site, close to Gran Canaria and Tenerife, to that at the more distant DSDP Site 397 and proposed site VICAP-4.

Proposed site VICAP-8 is located southwest of Gran Canaria and directly south of Tenerife. This site will be drilled to an approximate depth of 1300 m and furthers the primary objective at proposed site VICAP-7, identifying and establishing the thickness of the Gran Canaria shield stage and the younger Gran Canaria and Tenerife deposits.

Proposed site VICAP-9 is located in a channel between Gran Canaria and Tenerife. This site will be drilled to a depth of approximately 500 m in an attempt to penetrate a sediment pocket next to a small (young) volcanic island within the channel. Stratigraphy recorded at this site will augment the cross-channel stratigraphic correlation obtained from proposed site VICAP-3.

## **MAP**

Proposed site MAP-1 has been chosen from 9,600 km of airgun, watergun, and 3.5 kHz profiles in the abyssal plain because all the seismic reflector units are well developed. This ensures that the base of each seismic unit should be dateable at its oldest point (particularly important where units may onlap onto basement highs). The site also lies in a fracture zone valley which, throughout its history, has had a connection through to the continental rise to the east. Thus, as far as we can tell, there has never been an obstruction to turbidity current flow. This site, therefore, provides the best opportunity to ascertain the relationship of turbidite input to sea-level change prior to 300,000 years BP. It is also intended to sample the complete record of volcanoclastics derived from the Canary Islands, from the Madeira Archipelago, and from the Atlantis-Meteor Seamount complex, with the unique opportunity to date the earliest input, and thus minimum age, of each volcanic area.

Estimates of the total thickness of turbidites in the area vary because there are two models for the seismic structures as discussed by Weaver et al. (1986). Duin and Kok (1984) and Searle et al (1985) both divide the sequence into four units. They agree that the deepest unit (D) which occurs in basement troughs, probably represents locally derived turbidites, volcanoclastic deposits or fluid

lava flows and lies on basement of 80-100 Ma age. The next unit (C) probably represents pelagic clay with an average of 200-m thickness and an average accumulation rate in excess of 2.2 m/my. The top two units (A and B) are both regarded as turbidites by Searle et al., but Duin and Kok regarded only Unit A as of turbidity origin, with Unit B consisting of pelagics and some interbedded turbidites. Unit B is about 225-m thick and less well stratified with fewer reflectors (Duin et al, in press). Unit A averages about 125 m in thickness and is strongly laminated. Searle et al have shown that Units A and B are conformable, while Unit A/B is unconformable on the underlying Unit C. The reflectors visible in Unit B are sub-horizontal and parallel to those in Unit A. The true origin of Unit B will be revealed by deep drilling.

Proposed site MAP-1 is located at the site of piston core 82PCS13 which shows a complete turbidite sequence through the last 190 k.y., including turbidites *a* to *g*. The site lies 25 km to the west-southwest of the site of a 34-m long giant piston core MD10 which contains a complete turbidite sequence through the last 690 k.y. (isotope stages 1 to 17) including turbidites *a* to *u*. The average accumulation rate of this giant piston core is 50 m/m.y., although other IOSDL cores from the abyssal plain show accumulation rates of up to 100 m/m.y. Taking the seismic unit A/B as representing turbidites and an accumulation rate of 50 m/m.y., about 7 m.y. would be required to create the area of abyssal plain we see today. This late Miocene age for the initiation of the plain does not agree with the depositional history of the northwest African margin. Von Rad and Wissmann (1982) suggest quiet continuous deposition from the earliest Miocene to the mid Pliocene, with little erosion or canyon cutting. The Pliocene, however, was a time of major canyon cutting and erosion, giving rise to an angular unconformity under the shelf and upper slope. This erosion was continued through the Pleistocene when old canyons were re-excavated and major submarine slides and debris flows were initiated. This Plio-Pleistocene erosive phase is almost certainly linked with Northern Hemisphere glaciation and associated sealevel changes.

Since the onset of Northern Hemisphere glaciation was at 2.5 Ma, either the early turbidite deposition was at much higher rates than during the last 700 k.y., or older turbidite packages are also incorporated in the sediment sequence. Such high deposition rates would agree with the Pliocene period of strong erosion which gave rise to the Pliocene angular unconformity described by von Rad and Wissmann (1982). It is possible that the long period of quiet sedimentation through the Miocene was followed by large scale erosion associated with the initiation of glaciation and associated sealevel oscillations. Earlier turbidite packets could include the Late Miocene and

Late Oligocene (von Rad and Wissmann, 1982). Drilling the abyssal plain will determine which hypothesis is correct and effect budget calculations for the whole Canary Basin.

Proposed sites MAP-2 and 3 will be located proximally near the base of the Lower Continental Rise, both at water depths of 5430 m, and will encounter silty and sandy turbidite bases. Experience suggests that, in this area, no more than 30% of each turbidite will be coarse, and thus we hope to achieve good recovery. The two sites have been chosen to identify one of two possible entry routes for turbidites into the abyssal plain (one from the south and one from the north) by examination of the thickness and coarseness of basal layers of each turbidite.

Proposed site MAP-4 is located to the north of the central basin (5440 m water depth) in an area where additional small turbidites are common. It will provide information on thickness of both large and small turbidites.

The MAP has lain below the CCD through most of its history, and calcareous fossils are therefore rare or absent in the hemipelagic sediments, giving rise to problems of stratigraphic interpretations. This can, however, be overcome by obtaining a nannofossil stratigraphy from the turbidites themselves, and secondly by radiometric dating of potassium-bearing volcanic minerals in the turbidites. Examination of first occurrences of marker species in the turbidites, and not last occurrences, can be expected to give true age information.

## REFERENCES

- Ancochea, E., Fuster, J.M., Ibarrola, E., Cendrero, A., Coello, J., Hernan, F., Cantagrel, J.M., and Jamond, C., 1990. Volcanic evolution of the island of Tenerife (Canary Islands) in the light of new K-Ar data. *J. Volcanol. Geotherm. Res.*, 44:231-249.
- Angevine, C.L., Heller, P.L., and Paola, C., 1990. Quantitative sedimentary basin modeling. *AAPG Course Note Series.*, 32:1-133.
- Banda, E., Dañobeitia, J.J., Surinach, E., and Ansorge, J., 1981. Features of crustal structure under the Canary Islands. *Earth Planet. Sci. Lett.*, 55:11-24.
- Bednarz, U., and Schmincke, H.-U., 1989. Mass transfer during sub-seafloor alteration of the upper Troodos crust (Cyprus). *Contrib. Mineral. Petrol.*, 102:93-101.
- Bogaard, Pvd., Schmincke, H.-U., Freundt, A., Hall, Ch., and York, D., 1988. Eruption ages and magma supply rates during the Miocene evolution of Gran Canaria: single crystal  $^{40}\text{Ar}/^{39}\text{Ar}$  laser ages. *Naturwissenschaften*, 75:616-617.
- Brocher, T.M., and ten Brink, U.S., 1987. Variations in Layer 2 elastic velocities near Hawaii and their correlation to lithospheric flexure. *J. Geophys. Res.*, 92:2647-2661.
- Chen, C.Y., and Frey, F.A., 1985. Trace element and isotopic geochemistry of lavas from Haleakala volcano, East Maui, Hawaii: implications for the origin of Hawaiian basalts. *J. Geophys. Res.*, 90:8743-8768.
- Cloetingh, S., Kooi, H., and Groenewoud, W., 1989. Intraplate stresses and sedimentary basin evolution. *Am. Geophys. Union Monog.*, 48:1-16.
- Cloetingh, S., and Wortel, R., 1985. Regional stress field of the Indian Plate. *Geophys. Res. Lett.*, 12:77-80.
- Colley, S., and Thomson, J., 1985. Recurrent uranium relocations in distal turbidites emplaced in pelagic conditions. *Geochim. Cosmochim. Acta*, 49:2339-2348.
- Colley, S., and Thomson, J., 1990. Diffusion of U-series radionuclides at depth in deep-sea sediments. *Nature*, 346:260-263.
- Colley, S., Thomson, J., and Toole, J., 1989. Uranium relocations and derivation of quasi-isochrons for a turbidite/pelagic sequence in the Northeast Atlantic. *Geochim. Cosmochim. Acta*, 53:1223-1234.
- Cousens, B.L., Spera, F.J., and Tilton, G.R., 1990. Isotopic patterns in silicic ignimbrites and lava flows of the Mogan and lower Fataga Formations, Gran Canaria, Canary Islands: temporal changes in mantle source composition. *Earth Planet. Sci. Lett.*, 96:319-335.
- Dañobeitia, J.J., 1988. Reconocimiento geofísico de estructuras submarinas situadas al norte y sur del Archipiélago Canario. *Rev. Soc. Geol. España*, 1:143-155.
- Dañobeitia, J.J., and Collette, B.J., 1989. Estudio mediante sísmica de reflexión de un grupo de estructuras submarinas situadas al norte y sur del archipiélago Canario. *Acta Geológica Hispánica*, 24:147-163.
- Dash, B.P., and Bosshard, E., 1968. Crustal studies around the Canary Islands. *Proc. Int. Geol. Congr.*, 23rd Session:Prague, 1:249-260.
- Filmer, P.E., and McNutt, M.K., 1988. Geoid anomalies over the Canary Islands group. *Mar. Geophys. Res.*, 11:77-87.
- Froelich, P.N., Klinkhammer, G.P., Bender, M.L., Heath, G.R., Cullin, D., Dauphin, P., Hammond, D., Hartman, B., and Maynard, V., 1979. Early oxidation of organic matter in pelagic sediments of the eastern equatorial Atlantic: suboxic diagenesis. *Geochim. Cosmochim. Acta*, 43:1075-1090.
- Hoernle, K., and Schmincke, H.-U., 1993a. The petrology of the tholeiites through melilite nephelinites on Gran Canaria, Canary Islands: Crystal fractionation, accumulation, and depths of melting. *J. Petrol.*, 34:573-578.

- Hoernle, K.A., and Schmincke, H.-U., 1993b.** The role of partial melting in the 15 Ma geochemical evolution of Gran Canaria: A blob model for the Canary Hotspot. *J. Petrol.*, 34:599-626.
- Hoernle, K., and Tilton, G., 1991.** Sr, Nd, and Pb isotope data for Fuerteventura (Canary Islands) basal complex and subaerial volcanics: applications to magma genesis and evolution. *Schweiz. Mineral. Petrogr. Mitt.*, 71:3-18.
- Hoernle, K.A., Tilton, G., and Schmincke, H.-U., 1991.** The Sr-Nd-Pb isotopic evolution of Gran Canaria: Evidence for shallow enriched mantle beneath the Canary Islands. *Earth Planet. Sci. Lett.*, 106:44-63.
- Holik, J.S., Rabinowitz, P.D., and Austin, J.A., 1991.** Effects of Canary Hot Spot volcanism on structure of oceanic crust off Morocco. *J. Geophys. Res.*, 96, B7:12,039-12,067.
- Isaaks, E.H., and Srivastava, R.M., 1989.** *An Introduction to Applied Geostatistics*: Oxford (Oxford Univ. Press).
- Jarvis, I., and Higgs, N.C., 1987.** Trace-element mobility during early diagenesis in distal turbidites: late Quaternary of the Madeira Abyssal Plain, N. Atlantic. In Weaver, P.P.E., and Thomson, J. (Eds.), *Geology and Geochemistry of Abyssal Plains*. Spec. Publ. - Geol. Soc. London, 31:179-214.
- Kaufman, P., Grotzinger, J.P., and McCormick, D.S., 1991.** Depth-dependent diffusion algorithm for simulation of sedimentation in shallow marine depositional systems. In Franseen, E.K., Watney, W.L., and Kendall, C.G.St.C., and Ross, W. (Eds.), *Sedimentary Modeling*. Kansas Geol. Survey Bull., 233:489-508.
- Kendall, C.G.St.C., Moore, P., Strobel, J., Cannon, R., Perlmutter, M., Bezdek, J., and Biswas, G., 1991.** Simulation of the sedimentary fill of basins. In Franseen, E.K., Watney, W.L., Kendall, C.G.St.C., and Ross, W. (Eds.), *Sedimentary Modeling*. Kansas Geol. Survey Bull., 233:9-30.
- Le Bas, M.J., Rex, D.C., and Stillman, C.J., 1986.** The early magmatic chronology of Fuerteventura, Canary Islands. *Geol. Mag.*, 123 (3):287-298.
- MacDonald, G.A., and Katsura, T., 1964.** Chemical compositions of Hawaiian lavas. *J. Petrol.*, 5:82-133.
- Masson, D.G., Kidd, R.B., Gardner, J.V., Huggett, Q.J., and Weaver, P.P.E., 1992.** Saharan Continental Rise: Sediment facies distribution and sediment slides. In Poag, C.W., and de Graciansky, P.C. (Eds.), *Geologic Evolution of Atlantic Continental Rises*: New York (Van Nostrand Reinhold).
- McDougall, I., and Schmincke, H.-U., 1976.** Geochronology of Gran Canaria, Canary Islands: Age of shield-building volcanism and other magmatic phases. *Bull. Volcanol.*, 40:1-21.
- McNutt, M.K., 1984.** Lithospheric flexure and thermal anomalies. *J. Geophys. Res.*, 89:11180-11194.
- Moore, J.G., Clague, D.A., Holcomb, R.T., Lipman, P.W., Normark, W.R., and Torresan, M.E., 1989.** Prodigious submarine landslides on the Hawaiian Ridge. *J. Geophys. Res.*, 94:17465-17484.
- Moore, J.G., and Fiske, R.S., 1969.** Volcanic substructure inferred from dredge samples and ocean-bottom photographs, *Hawaii Geol. Soc. Am. Bull.*, 80:1191-1202.
- Nogales, J., and Schmincke, H.-U., 1969.** El Pino enterrado de la Canada de las Arenas (Gran Canaria). *Cuadernos de Botanica*, 5:23-25.
- Saggerson, E.P., and Williams, L.A.J., 1968.** Ngurumanite from southern Kenya and its bearing on the origin of rocks in the northern Tanganyika alkaline district. *J. Petrol.*, 5:40-81.
- Schmincke, H.-U., 1976.** Geology of the Canary Islands. In Kunkel, G. (Ed.), *Biogeography and Ecology in the Canary Islands*: the Hague (W. Junk), 67-184.
- Schmincke, H.-U., 1979.** Age and crustal structure of the Canary Islands. *J. Geophys.*, 46:217-224.
- Schmincke, H.-U., 1982.** Volcanic and chemical evolution off the Canary Islands. In von Rad, U., et al. (Eds.), *Geology of the Northwest African Continental Margin*: Berlin Heidelberg New York (Springer Verlag), 273-306.
- Schmincke, H.-U., 1990.** *Geological Field Guide of Gran Canaria*; Witten (Pluto Press).
- Schmincke, H.-U., and Staudigel, H., 1976.** Pillow lavas on central and eastern Atlantic Islands (La Palma, Gran Canaria, Porto Santo, Santa Maria). *Bull. Soc. Geol. France*, 18:871-883.

- Schmincke, H.-U., and von Rad, U., 1979. Neogene evolution of Canary Island volcanism inferred from ash layers and volcanoclastic sandstones of DSDP Site 397 (Leg 47 A). In von Rad, U., Ryan, W.B.F., et al., *Init. Repts. DSDP, 47, Part 1*: Washington (U.S. Govt. Printing Office), 703-725.
- Schuttenhelm, R.T.E., Auffret, G.A., Buckley, D.E., Cranston, R.E., Murray, C.N., Shephard, L.E., and Spijkstra, A.E. (Eds.), 1988. *Geoscience Investigations of Two North Atlantic Abyssal Plains - the ESOPE International Expedition*, Vols 1 and 2, CEC-Joint Research Centre, JRC Report, EUR.
- Searle, R.C., 1987. Regional setting and geophysical characterization of the Great Meteor East area in the Madeira Abyssal Plain. In Weaver, P.P.E., and Thomson, J. (Eds.), *Geology and Geochemistry of Abyssal Plains*. Spec. Publ. - Geol. Soc. London, 31:49-70.
- Searle, R.C., Schultheiss, P.J., Weaver, P.P.E., Noel, M., Kidd, R.B., Jacobs, C.L., and Huggett, Q.J., 1985. *Great Meteor East (distal Madeira Abyssal Plain): Geologic Studies of its Suitability for Disposal of Heat Emitting Radioactive Wastes*. IOS Internal Document, 193:1-161.
- Sorensen, J., Jorgensen, K.S., Colley, S., Hydes, D.J., Thomson, J., and Wilson, T.R.S., 1987. Depth localisation of denitrification in a deep sea sediment from the Madeira Abyssal Plain. *Limnol. Oceanogr.*, 32:758-762.
- Stattegger, K., 1987. Heavy minerals and provenance of sands: Modeling of lithological end members from river sands of northern Austria and from sandstones of the Austroalpine Gosau formation. *J. Sediment. Petrol.*, 57:301-310.
- Staudigel, H., and Schmincke, H.-U., 1984. The Pliocene seamount series of La Palma/Canary Islands. *J. Geophys. Res.*, 89:11,195-11,215.
- Stein, C.A., Cloetingh, S., and Wortel, R., 1989. Seasat-derived gravity constraints on stress and deformation in the northeastern Indian Ocean. *Geophys. Res. Lett.*, 16:823-826.
- Stein, C.A., Cloetingh, S., and Wortel, R., 1990. Kinematics and mechanics of the Indian Ocean diffuse plate boundary zone. In Cochran, J.R., Stow, D.A.V., et al., *Proc. ODP, Sci. Results*, 116:College Station, TX(Ocean Drilling Program), 261-277.
- Strong, D.F., 1972. Petrology of the island of Moheli, Western Indian Ocean. *Geol. Soc. Am. Bull.*, 83:389-406.
- Tetzlaff, D.M., and Harbaugh, J.W., 1989. *Simulating Clastic Sedimentation*:New York (Van Norstrand Reinhold).
- Thomson, J., Colley, S., Higgs, N.C., Hydes, D.J., Wilson, T.R.S., and Sorensen, J., 1987. Geochemical oxidation fronts in NE Atlantic distal turbidites and their effects in the sedimentary record. In Weaver, P.P.E., and Thomson, J. (Eds.), *Geology and Geochemistry of Abyssal Plains*. Spec. Publ. - Geol. Soc. London., 31:167-177.
- Thomson, J., Colley, S., and Weaver, P.P.E., 1988. Bioturbation into a recently emplaced deep-sea turbidite as revealed by <sup>210</sup>Pb excess, <sup>230</sup>Th excess and planktonic foraminifera distributions. *Earth Planet. Sci. Lett.*, 90:157-173.
- Vail, P.R., Mitchum, R.M., and Thompson, S., 1977. Seismic stratigraphy and global changes of sealevel, part 4; Global cycles of relative changes of sea-level. *AAPG Mem.*, 26:83-97.
- von Rad, U., and Wissmann, G., 1982. Cretaceous-Cenozoic history of the West Saharan continental margin (NW Africa): Development, destruction and gravitational sediment. In von Rad, U., Hinz, K., Sarnthein, M., and Seibold, E. (Eds.), *Geology off the Northwest African Continental Margin*:Berlin (Springer Verlag), 106-131.
- Waples, D.W., and Sloan, J.R., 1980. Carbon and nitrogen diagenesis in deep sea sediments. *Geochim. Cosmochim. Acta*, 44:1463-1470.
- Watts, A.B., and ten Brink, U.S., 1989. Crustal structure, flexure, and subsidence history of the Hawaiian Islands. *J. Geophys. Res.*, 94:10473-10500.
- Watts, A.B., ten Brink, U.S., Buhl, P., and Brocher, T.M., 1985. A multichannel seismic study of lithospheric flexure across the Hawaiian-Emperor seamount chain. *Nature*, 315:105-111.

- Weaver, P.P.E., 1983.** An integrated stratigraphy of the upper Quaternary of the King's Trough Flank area, N.E. Atlantic. *Oceanol. Acta*, 6:451-456.
- Weaver, P.P.E., and Kuijpers, A., 1983.** Climatic control of turbidite deposition on the Madeira Abyssal Plain. *Nature*, 306:360-363.
- Weaver, P.P.E., and Rothwell, R.G., 1987.** Sedimentation on the Madeira Abyssal Plain over the last 300,000 years. In Weaver, P.P.E., and Thomson, J. (Eds.), *Geology and Geochemistry of Abyssal Plains*. Spec. Publ. - Geol. Soc. London, 31:71-86.
- Weaver, P.P.E., Rothwell, R.G., Ebbing, J., Gunn, D., and Hunter, P.M., 1992.** Correlation, frequency of emplacement and source directions of megaturbidites on the Madeira Abyssal Plain. *Mar. Geol.*, 109:1-20.
- Weaver, P.P.E., Searle, R.C., and Kuijpers, A., 1986.** Turbidite deposition and the origin of the Madeira Abyssal Plain. In Summerhayes, C.P., and Shackleton, N.J. (Eds.), *North Atlantic Palaeoceanography*. Spec. Publ. - Geol. Soc. London, 21:131-143.
- Weaver, P.P.E., Thomson, J., and Jarvis, I., 1989.** The geology and geochemistry of the Madeira Abyssal Plain sediments : a review. In *Advances in Underwater Technology, Ocean Science and Offshore Engineering - Disposal of Radioactive Waste in Seabed Sediments*: London (Graham and Trotman), 18: 51-78.
- Wilson, T.R.S., Thomson, J., Colley, S., Hydes, D.J., Higgs, N.C., and Sorensen, J., 1985.** Early organic diagenesis: the significance of progressive subsurface oxidation fronts in pelagic sediments. *Geochim. Cosmochim. Acta*, 49:811-822.
- Wilson, T.R.S., Thomson, J., Hydes, D.J., Colley, S., Culkin, F., and Sorensen, J., 1986.** Oxidation fronts in pelagic sediments: diagenetic formation of metal-rich layers. *Science*, 232:972-975.
- Wissmann, G., 1979.** Cape Bojador slope, an example for potential pitfalls in seismic interpretation without the information of outer margin drilling. In von Rad, U., Ryan, W.B.F., et al. (Eds.), *Init. Repts. DSDP*, 47: Washington (U.S. Govt. Printing Office), 491-500.

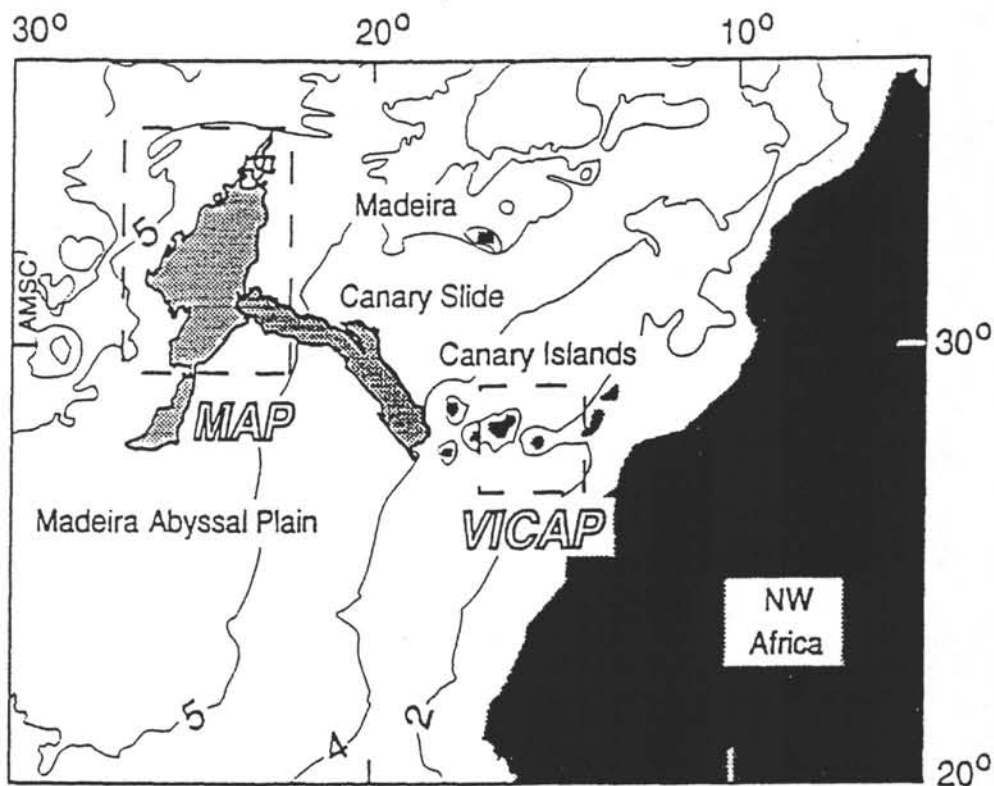


**Figure 1.** Location of VICAP and MAP study areas. Distribution of Holocene Canary slide after Masson et al. (in press). AMSC= Atlantis-Meteor seamount complex. Isobaths in km.

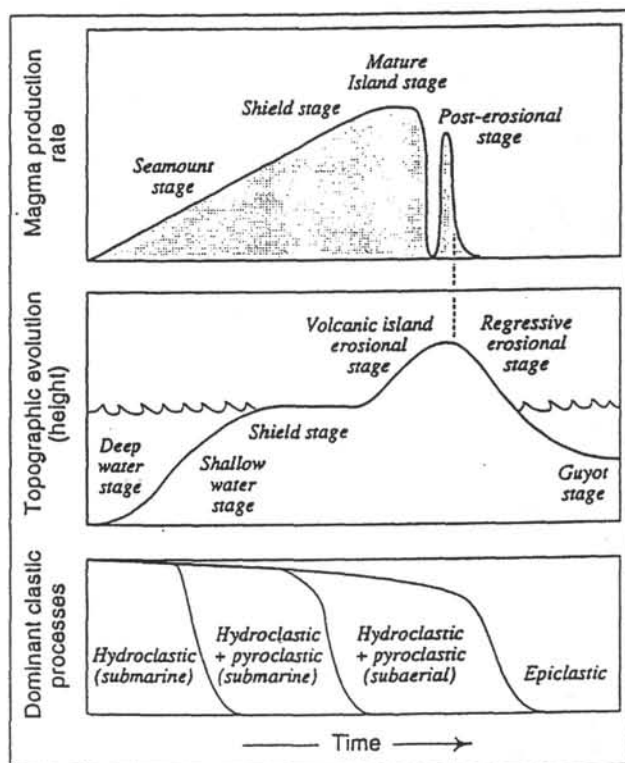


**Figure 2.** General scheme of temporal volcanic ocean island evolution showing variations in magma production, topography, and deposits formed.

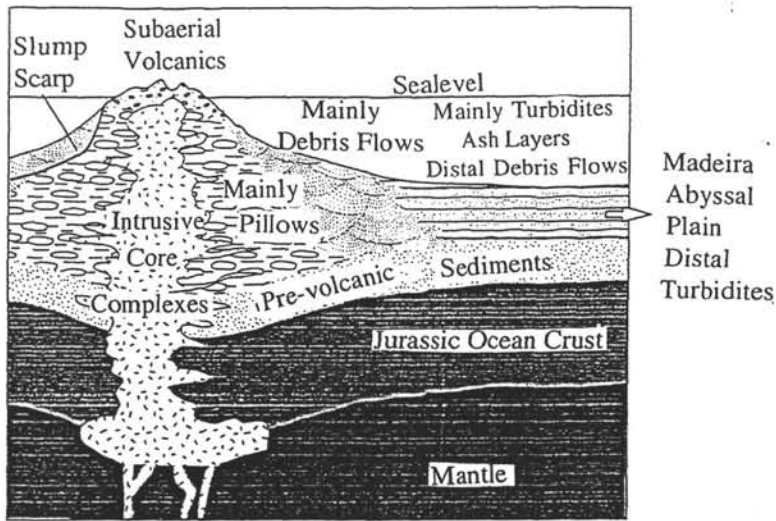


**Figure 3.** Schematic drawing of ocean island and its clastic apron. The volume of the clastic apron may exceed the volume of the island itself.

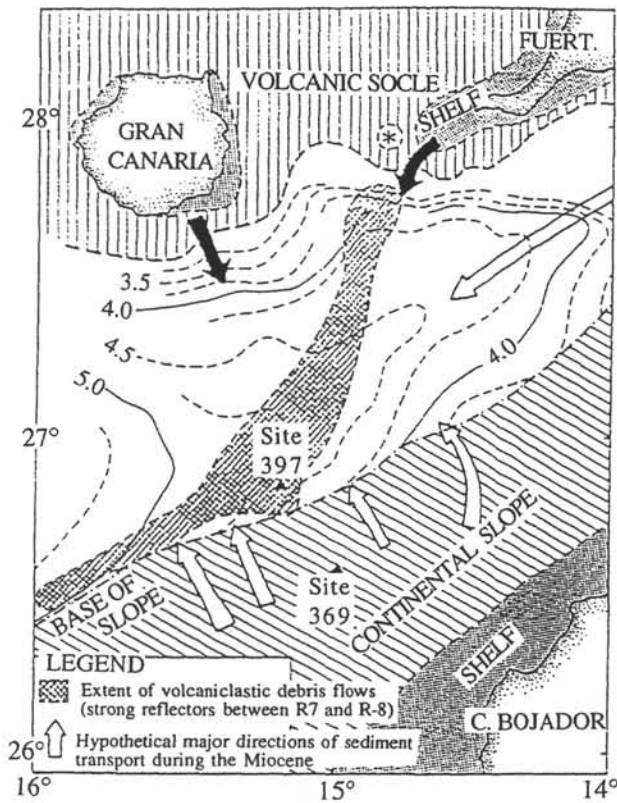


**Figure 4.** Map of the sedimentary basin between Gran Canaria and the northwest African coast, showing depth contours (in seconds of twt) of seismic reflector R-7 on top of the middle Miocene volcanoclastic debris flows. Black arrows indicate island derived sediment transport directions. Asterisk indicates basement high. Modified after Wissmann (1979).

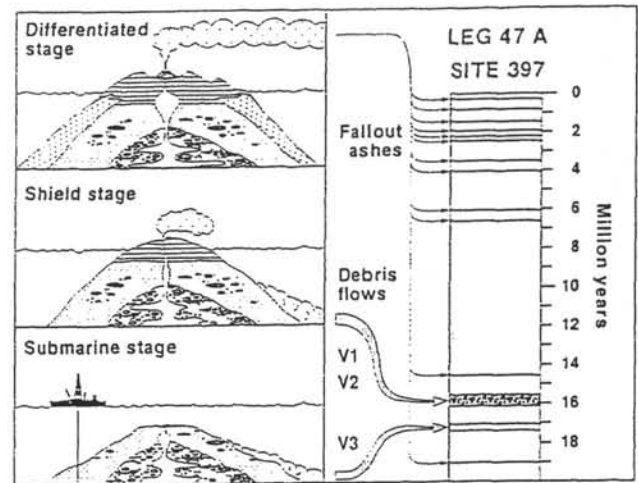


**Figure 5.** Three schematic growth stages of a volcanic ocean island as reflected in three main types of submarine volcanoclastic rocks drilled in DSDP Site 397 south of the Canary Islands. From Schmincke and v. Rad (1979).

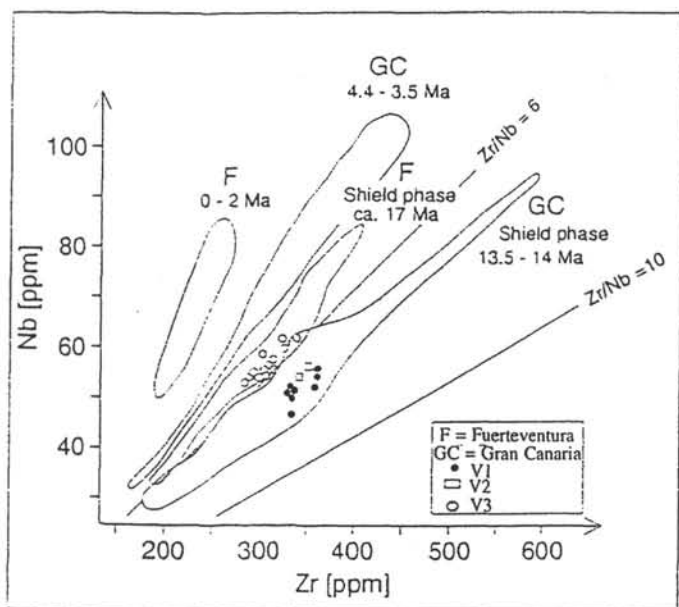


**Figure 6a.** Zr versus Nb variation diagram for rocks from the shield and later magmatic phases of Gran Canaria (GC) and Fuerteventura (F) and volcaniclastic flows V1 to V3 from DSDP Site 397. Hyaloclastite flow V3 probably derived from Fuerteventura. Debris flows V1 and V2 probably generated during the shield phase of Gran Canaria.

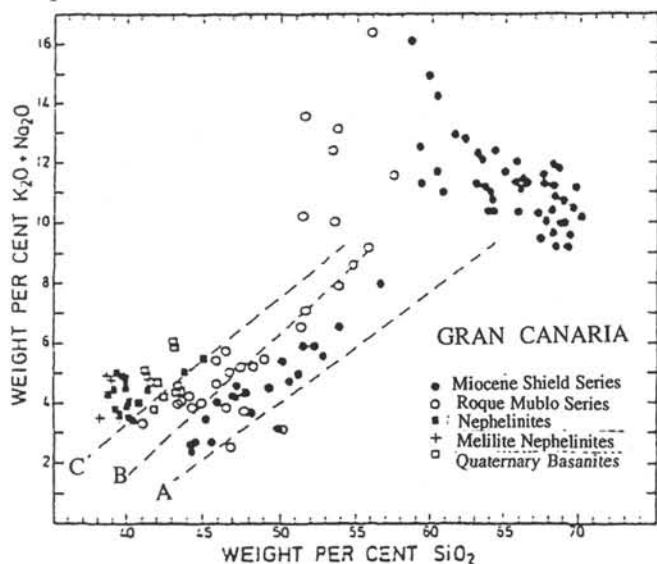


**Figure 6b.** Total alkalis versus silica diagram for the Miocene and Pliocene (Roque Nublo) shield series and post erosional nephelinites, melilite nephelinites, and basanites. Dashed lines separate tholeiites from alkalibasalts (A) in Hawaii (Macdonald and Katsura, 1964), alkalibasalts and basanites (B) on Moheli Islands (Indian Ocean) (Strong, 1972), and basanites and nephelinites (C) in East Africa (Saggerson and Williams, 1968).

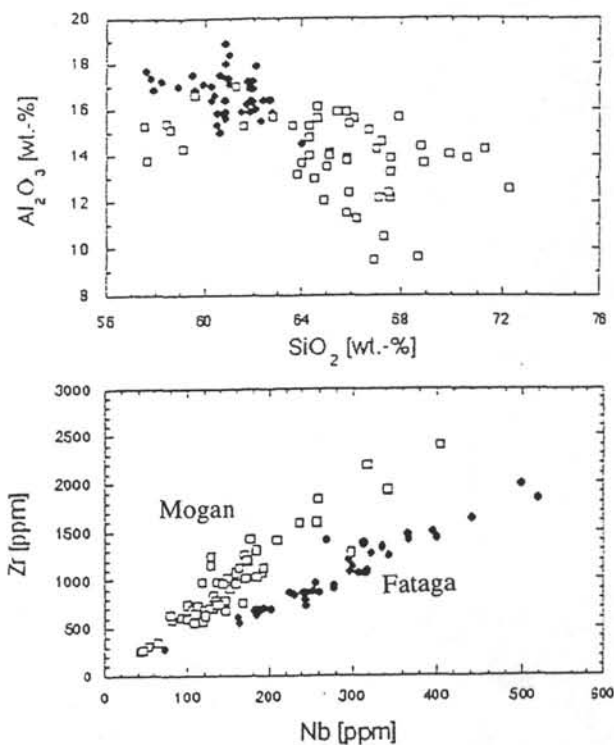


**Figure 6c.** Comparison of some chemical parameters of trachytic and rhyolitic cooling units of the Mogan Formation with trachyphonolitic ignimbrite and lava cooling units of the Fataga Formation (Gran Canaria).

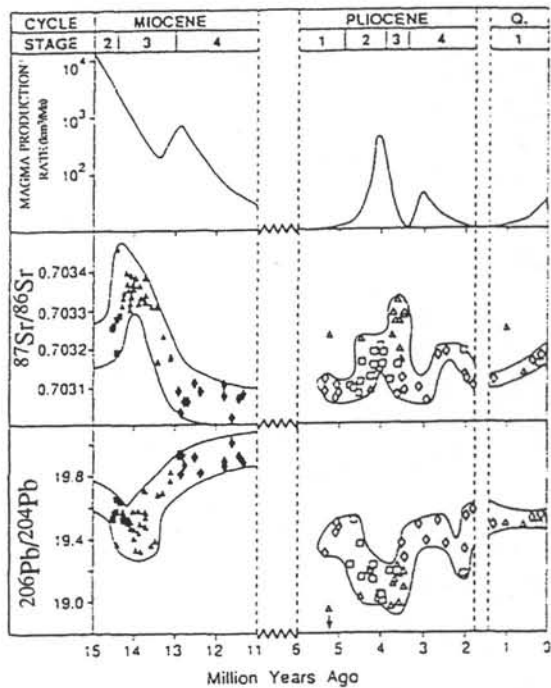


**Figure 6d.** Sr- and Pb-isotope variations with age of Gran Canaria volcanic rocks, and magma production rates derived from eruption rates with a correction for volume loss due to crystal fractionation. From Hoernle et al. (1991).

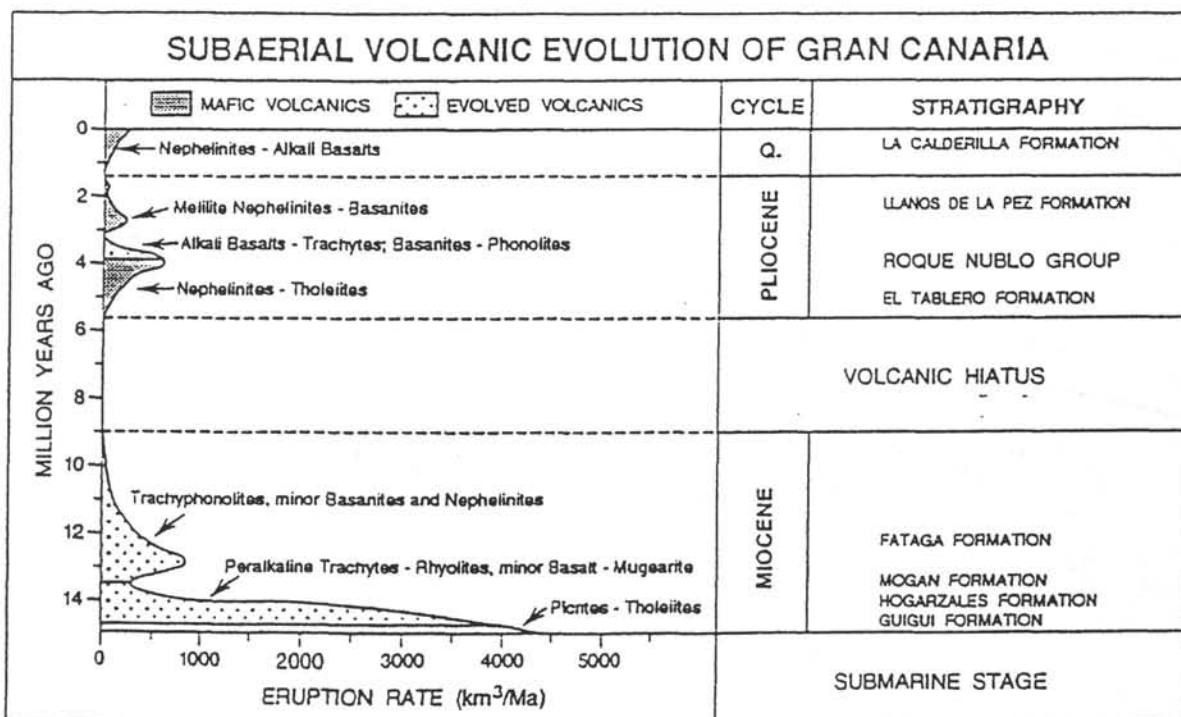


**Figure 7.** Volume-eruption rate relationship of major magmatic phases during the Miocene, Pliocene, and Quaternary (Q) volcanic cycles on Gran Canaria. Stratigraphic names are given on the right. Not high compositional variability within and strong compositional differences between cycles.

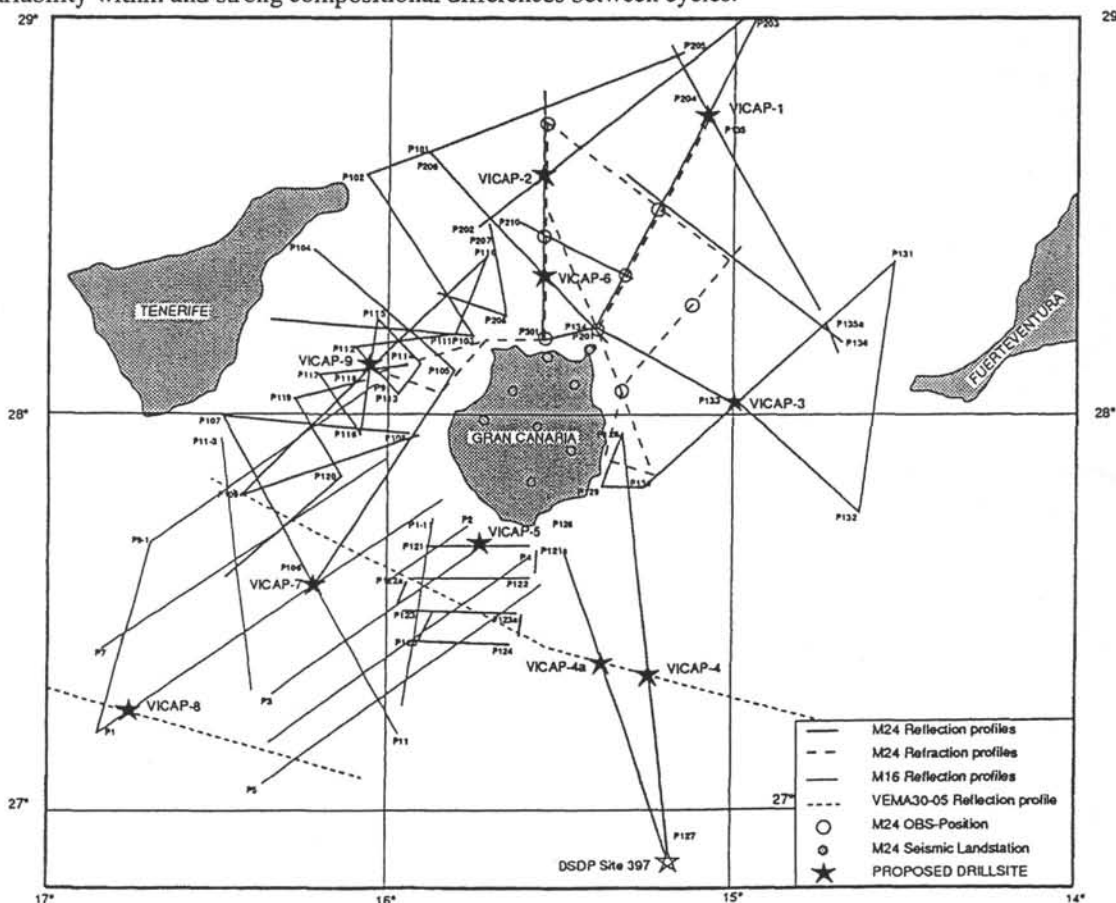


**Figure 8.** Map with location of the proposed VICAP drill sites.

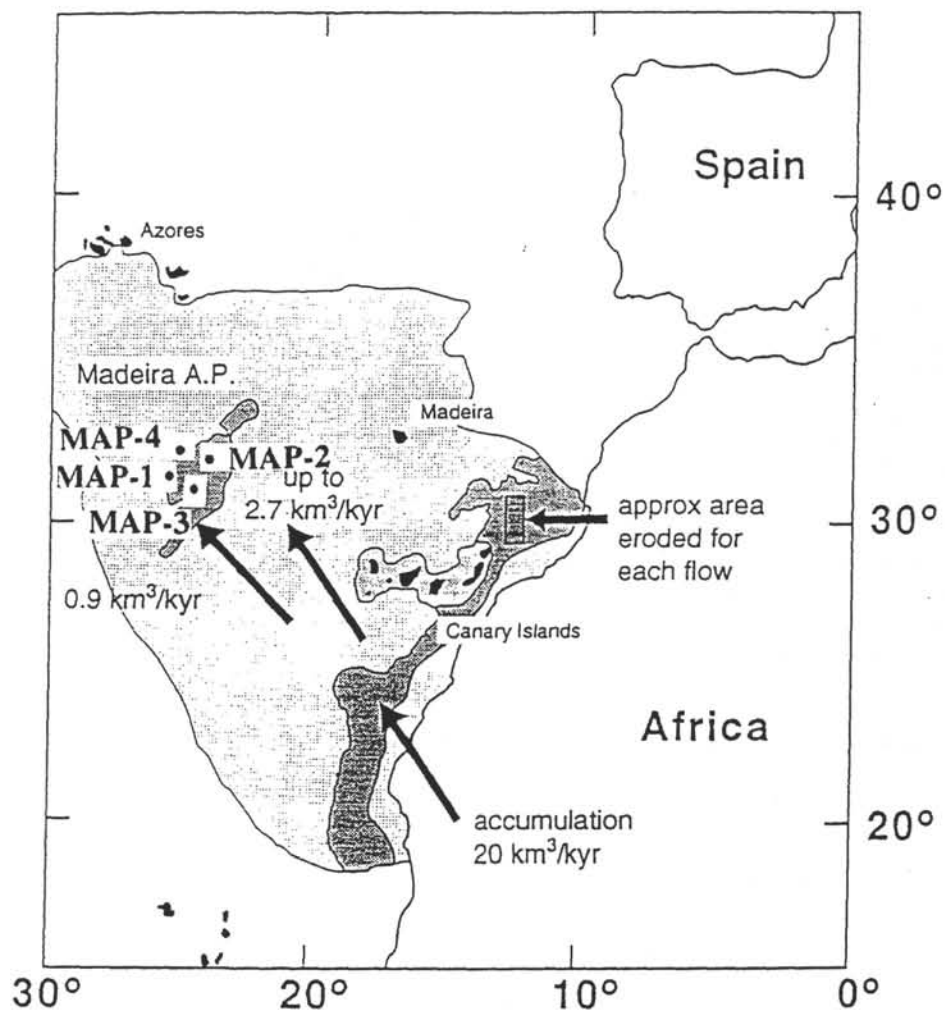


**Figure 9.** Source areas and general flow direction of mass wasting events on the northwest African continental margin.

**TABLE 1**  
**PROPOSED SITE INFORMATION**  
**and**  
**DRILLING STRATEGY**

<b>SITE:</b> VICAP-1	<b>PRIORITY:</b> 1	<b>POSITION:</b> 28°44'N, 15°04'W
<b>WATER DEPTH:</b> 3560m	<b>SEDIMENT THICKNESS:</b> ~4000m	<b>TOTAL PENETRATION:</b> ~4000m
<b>SEISMIC COVERAGE:</b> MCS lines M 24, P 134/203, and 135/204.		

**Objectives:** To establish a high resolution lithostratigraphy of North Canary Basin sediments and identify volcanoclastic deposits as stratigraphic events. To determine the thickness of the medial/distal facies of the shield stage and younger volcanoclastic deposits north of Gran Canaria.

**Drilling Program:** APC, XCB, and RCB coring.

**Logging and Downhole Operations:**

**Nature of Rock Anticipated:** Volcaniclastics and hemipelagic.

<b>SITE:</b> VICAP-2	<b>PRIORITY:</b> 1	<b>POSITION:</b> 28°34'N, 35°W
<b>WATER DEPTH:</b> 3580m	<b>SEDIMENT THICKNESS:</b> ~3800m	<b>TOTAL PENETRATION:</b> ~800m
<b>SEISMIC COVERAGE:</b> MCS lines M 24, P 202, and 301.		

**Objectives:** To establish the stratigraphic sequence of the North Canary Basin and to identify the volcanoclastic deposits as stratigraphic events. To drill through the outermost edge of the massive island flank ("seismic apron") and test the method of dating the initiation of a volcanic island/seamount by the stratigraphic position of the base of the apron.

**Drilling Program:** APC, XCB, and RCB coring.

**Logging and Downhole Operations:**

**Nature of Rock Anticipated:** Volcaniclastics and hemipelagic.

<b>SITE:</b> VICAP-3	<b>PRIORITY:</b> 1	<b>POSITION:</b> 28°02'N, 14°59'W
<b>WATER DEPTH:</b> 1540m	<b>SEDIMENT THICKNESS:</b> ~700m	<b>TOTAL PENETRATION:</b> ~700m
<b>SEISMIC COVERAGE:</b> MCS lines M24, P 130, and 132/133.		

**Objectives:** To drill through a sediment pocket in the channel between Gran Canaria and Fuerteventura (condensed stratigraphy?) on top of a major volcanic debris avalanche deposit well dated on land. To correlate North to South Canary Basin stratigraphy across channel.

**Drilling Program:** APC, XCB, and RCB coring

**Logging and Downhole Operations:**

**Nature of Rock Anticipated:** Volcaniclastics and hemipelagic.

<b>SITE:</b> VICAP-4	<b>PRIORITY:</b> 1	<b>POSITION:</b> 27°18'N, 15°13'W	<b>WATER DEPTH:</b> 2950m
<b>SEDIMENT THICKNESS:</b> total unknown, to R7 ~400m		<b>TOTAL PENETRATION:</b> ~500m	
<b>SEISMIC COVERAGE:</b> MCS lines M 24, VEMA 30-05, and P 127.			

**Objectives:** To determine the thickness of volcanoclastic deposits (medial facies) south/southeast of Gran Canaria with DSDP Site 397 as a reference site for distal facies. To verify correlation of Site 397 stratigraphy with M 16-4 and M 24 MCS records in the deep part of South Canary Basin well away from the continental slope.

**Drilling Program:** APC, XCB, and RCB coring.

**Logging and Downhole Operations:**

**Nature of Rock Anticipated:** Volcaniclastics and hemipelagic.

OR

<b>SITE:</b> VICAP-4a	<b>PRIORITY:</b> 2	<b>POSITION:</b> 27°19'N, 15°23'W	<b>WATER DEPTH:</b> 2950m
<b>SEDIMENT THICKNESS:</b> total unknown, to R7 ~400m		<b>TOTAL PENETRATION:</b> ~500m	
<b>SEISMIC COVERAGE:</b> MCS lines M 24, VEMA 30-05, and P 126.			

**Objectives:** To determine the thickness of volcanoclastic deposits (medial facies) south/southeast of Gran Canaria with DSDP Site 397 as a reference site for distal facies. To verify correlation of Site 397 stratigraphy with M 16-4 and M 24 MCS records in the deep part of South Canary Basin well away from the continental slope.

**Drilling Program:** APC, XCB, and RCB coring.

**Logging and Downhole Operations:**

**Nature of Rock Anticipated:** Volcaniclastics and hemipelagic.

<b>SITE:</b> VICAP-5	<b>PRIORITY:</b> 1	<b>POSITION:</b> 27°40'N, 15°41'W
<b>WATER DEPTH:</b> 375m	<b>SEDIMENT THICKNESS:</b> ~300m*	<b>TOTAL PENETRATION:</b> ~300m
<b>SEISMIC COVERAGE:</b> MCS lines M 24 and P 121.		

\* to top of island flank

**Objectives:** To drill through the continuation of a large on-land canyon to determine sedimentation rates for a major drainage system that has operated since the Miocene shield stage. To identify volcanoclastic deposits (proximal facies) south of Gran Canaria.

**Drilling Program:** APC, XCB, and RCB coring.

**Logging and Downhole Operations:**

**Nature of Rock Anticipated:** Volcaniclastics and hemipelagic.

<b>SITE:</b> VICAP-6	<b>PRIORITY:</b> 1	<b>POSITION:</b> 28°24'N, 15°36'W
<b>WATER DEPTH:</b> 3400m	<b>SEDIMENT THICKNESS:</b> ~4000m	<b>TOTAL PENETRATION:</b> ~300m
<b>SEISMIC COVERAGE:</b> MCS lines M 24, P 201, and 301.		

**Objectives:** To identify volcanic/volcaniclastic deposits (proximal facies) to the north of Gran Canaria. To determine the thickness of individual volcanic layers down to the top of the shield stage island flank ("seismic apron") as close to Gran Canaria as possible.

**Drilling Program:** APC, XCB, and RCB coring.

**Logging and Downhole Operations:**

**Nature of Rock Anticipated:** Volcaniclastics and hemipelagic.

<b>SITE:</b> VICAP-7	<b>PRIORITY:</b> 2	<b>POSITION:</b> 27°27'N, 16°23'W
<b>WATER DEPTH:</b> 3560m	<b>SEDIMENT THICKNESS:</b> ~4500m	<b>TOTAL PENETRATION:</b> ~1000m
<b>SEISMIC COVERAGE:</b> MCS lines M 16-4, P 1, and 113.		

**Objectives:** To determine the thickness of the Gran Canaria shield stage and younger Gran Canaria and Tenerife deposits (medial facies) southwest of Gran Canaria and southeast of Tenerife. To determine the stratigraphic changes nearer to Tenerife (and Gran Canaria) and further off the continent compared to proposed site VICAP-4 and DSDP Site 397 and to identify Gran Canaria and Tenerife shield stages within the South Canary Basin stratigraphy.

**Drilling Program:** APC, XCB, and RCB coring.

**Logging and Downhole Operations:**

**Nature of Rock Anticipated:** Volcaniclastics and hemipelagic.

<b>SITE:</b> VICAP-8	<b>PRIORITY:</b> 2	<b>POSITION:</b> 27°16'N, 16°42'W
<b>WATER DEPTH:</b> 3620m	<b>SEDIMENT THICKNESS:</b> ~4000m	<b>TOTAL PENETRATION:</b> ~1300m
<b>SEISMIC COVERAGE:</b> MCS lines M 16-4, V 30-05, and P 1.		

**Objectives:** To determine the thickness of the Gran Canaria shield stage and younger Gran Canaria and Tenerife deposits (distal facies) southwest of Gran Canaria and south of Tenerife. To identify the position of Gran Canaria and Tenerife shield stages within the South Canary Basin stratigraphy.

**Drilling Program:** APC, XCB, and RCB coring.

**Logging and Downhole Operations:**

**Nature of Rock Anticipated:** Volcaniclastics and hemipelagic.

<b>SITE:</b> VICAP-9	<b>PRIORITY:</b> 2	<b>POSITION:</b> 28°06'N, 16°03'W
<b>WATER DEPTH:</b> 2510m	<b>SEDIMENT THICKNESS:</b> ~500m*	<b>TOTAL PENETRATION:</b> ~500m
<b>SEISMIC COVERAGE:</b> MCS lines M 24, P 109, 115, and 117.		

\* to volcanics

**Objectives:** To drill through a sediment pocket next to a small (young) volcano in the channel between Gran Canaria and Tenerife (condensed stratigraphy?). To correlate North to South Canary Basin stratigraphy across channel.

**Drilling Program:** APC, XCB, and RCB coring.

**Logging and Downhole Operations:**

**Nature of Rock Anticipated:** Volcaniclastics and hemipelagic.

<b>SITE:</b> MAP-1	<b>PRIORITY:</b> 1	<b>POSITION:</b> 31°09'N, 25°26.2'W
<b>WATER DEPTH:</b> 5440m	<b>SEDIMENT THICKNESS:</b> 580m	<b>TOTAL PENETRATION:</b> 500m
<b>SEISMIC COVERAGE:</b> SCS high resolution Tyro 1982 airgun/watergun, IOS Farnella 3/81 + various		

**Objectives:** To determine the high resolution stratigraphy for Pliocene-Quaternary turbidite fill of the Madeira Abyssal Plain. To conduct geochemical logging of the sequence to determine the sedimentary diagenetic history and provenance.

**Drilling Program:** APC and XCB coring.

**Logging and Downhole Operations:** Logging for geochemical properties.

**Nature of Rock Anticipated:** Distal turbidites and pelagic oozes, marls, and clays.

<b>SITE:</b> MAP-2	<b>PRIORITY:</b> 2	<b>POSITION:</b> 31°56'N, 24°05'W
<b>WATER DEPTH:</b> 5430m	<b>SEDIMENT THICKNESS:</b> 1000m	<b>TOTAL PENETRATION:</b> 300m
<b>SEISMIC COVERAGE:</b> Tyddeman 1980 watergun, RGO Tyro 1982 SCS deep penetration + various		

**Objectives:** To determine the high resolution stratigraphy for Pliocene-Quaternary turbidite fill of the Madeira Abyssal Plain. To conduct geochemical logging of the sequence to determine the sedimentary diagenetic history and provenance.

**Drilling Program:** APC, VPC, and XCB coring.

**Logging and Downhole Operations:** Logging for geochemical properties.

**Nature of Rock Anticipated:** Distal turbidites and pelagic oozes, marls, and clays.

<b>SITE:</b> MAP-3	<b>PRIORITY:</b> 1	<b>POSITION:</b> 30°47'N, 24°24'W
<b>WATER DEPTH:</b> 5430m	<b>SEDIMENT THICKNESS:</b> 750m	<b>TOTAL PENETRATION:</b> 500m
<b>SEISMIC COVERAGE:</b> SCS high resolution Tyddeman 1980 watergun, IOS Farnella 3/81 + various		

**Objectives:** To determine the high resolution stratigraphy for Pliocene-Quaternary turbidite fill of the Madeira Abyssal Plain. To conduct geochemical logging of the sequence to determine the sedimentary diagenetic history and provenance.

**Drilling Program:** APC, and XCB coring.

**Logging and Downhole Operations:** Logging for geochemical properties.

**Nature of Rock Anticipated:** Distal turbidites and pelagic oozes, marls, and clays.

<b>SITE:</b> MAP-4	<b>PRIORITY:</b> 1	<b>POSITION:</b> 31°59'N, 25°02'W
<b>WATER DEPTH:</b> 5440m	<b>SEDIMENT THICKNESS:</b> 750m	<b>TOTAL PENETRATION:</b> 300m
<b>SEISMIC COVERAGE:</b> RGO Tyro 1982 SCS deep penetration + various		

**Objectives:** To determine the high resolution stratigraphy for Pliocene-Quaternary turbidite fill of the Madeira Abyssal Plain. To conduct geochemical logging of the sequence to determine the sedimentary diagenetic history and provenance.

**Drilling Program:** APC, and XCB coring.

**Logging and Downhole Operations:** Logging for geochemical properties.

**Nature of Rock Anticipated:** Distal turbidites and pelagic oozes, marls, and clays.

*LEG 158*

*TAG Hydrothermal Mound*

## LEG 158

### DRILLING AN ACTIVE HYDROTHERMAL SYSTEM ON A SLOW-SPREADING RIDGE: MAR 26°N (TAG)

Modified From Proposal 361-Rev 2

Susan Humphris: Co-Chief

Peter Herzig: Co-Chief

Laura Stokking: Staff Scientist

#### ABSTRACT

The overall scientific objectives of Leg 158 are to investigate the fluid flow, geochemical fluxes and associated alteration and mineralization, and the subsurface nature of an active hydrothermal system on a slow-spreading ridge. The TAG active mound is a large, mature deposit of varying mineralogy with emanating fluids displaying a wide range of temperatures and distinct chemistries. The large size and age argue for a reasonably large and altered crustal root zone suitable for good drill penetration and recovery with conventional drill bits. Studies of this feature will give insight into fluid flow, structure, and "zone-refining" in active hydrothermal systems, and clarify how large deposits, similar in size to those mined on land today, are formed on the modern seafloor.

A transect of three holes, one penetrating into the stockwork zone, is proposed to investigate the nature of fluids, deposits, and altered crust in the near-surface part of the hydrothermal system and in the stockwork and root zone underlying the surface deposit. Although it is anticipated that these objectives can be achieved with the currently available technology in this hostile environment, the nearby inactive MIR mound is proposed as a back-up drilling site. The size and primary sulfide features of the MIR mound are similar to that of TAG, but the MIR mound has undergone extensive recrystallization, being entirely indurated by late-stage fluids that have replaced anhydrite and filled all voids with silica.

Drilling at TAG will directly address the processes occurring during hydrothermal circulation. Understanding these processes, and the implications for energy transfer, geochemical fluxes, and the formation of ore deposits is of fundamental importance to our knowledge of crustal accretion.

## INTRODUCTION

Ridge-crest hydrothermal systems play a fundamental role in transferring a large fraction of the heat from the earth's interior to its surface. Through thermally-induced flow of seawater in fractures and fissures in the permeable portion of the crust and upper mantle, much of the mantle-derived thermal energy is dissipated into the lithosphere, hydrosphere, and biosphere along the global mid-ocean ridges. This circulation gives rise to a complex series of physical, chemical, and biological interactions that affect the composition of both seawater and the oceanic crust, and lead to the creation of many types of seafloor ore deposits, and to the existence of unusual biological communities.

Although a considerable amount of surficial sampling has been completed on a number of ridge hydrothermal systems, only drilling an active system on a mid-ocean ridge can clarify 1) the permeability, pressure, and temperature structure within the upflow zone beneath an active hydrothermal system, 2) the nature of the chemical reactions between water and rock in both the upflow zone and the underlying reaction zone, 3) the method of sulfide precipitation and subsequent modification below the seafloor, 4) the structural control on the plumbing system within both the upflow and reaction zones, and 5) the evolution of major black smoker systems.

To date, attempts to answer such questions have relied upon the chemistry of waters from natural systems, samples collected from surface outcrops, experimental and theoretical analyses of basalt/seawater systems, and observations of fossil systems in ophiolites. These sources of evidence make assumptions about the conditions which are present in the sub-seafloor part of an active system, sometimes about which rocks are in equilibrium with which fluids, and sometimes about the nature of the physical structure of an active system. All of these arguments have been carried to their highest level for sediment-free systems, which are predicted to be considerably simpler than sedimented hydrothermal systems. Drilling of a major, sediment-free black smoker system will provide the necessary evidence to discriminate between the many current models.

Hydrothermal systems on unsedimented ridge axes dominate global hydrothermal activity, and hence are an important contributor to global mass and energy fluxes. All previous drilling has been carried out in areas where large deposits have been, or are, developing, such as sedimented-ridge hydrothermal systems. Drilling the interior of a mature, large volcanic-hosted deposit such as the

TAG mound will clarify the processes of recrystallization and "zone-refining", the distribution of minerals, the hydrothermal circulation and plumbing, the nature of the root zone, and the processes occurring during ore formation and deposition.

The TAG area has many features that make it the prime target for drilling an active volcanic-hosted hydrothermal deposit. Firstly, it is located in a slow-spreading environment, a major characteristic of the global rift system, and the hydrothermal field is situated in the central part of a ridge segment bounded by small non-transform offsets or axial discontinuities, typical of many such segments on slow-spreading ridges. The mound represents a good drill target as the combination of size and maturity argues for a large surface areal target, with a well-developed root zone. The presently active mound is approximately 200 m in diameter and 50 m in height. It is composed of massive sulfides probably well in excess of  $5 \times 10^6$  tons, being equivalent in size to some of the deposits in the Cyprus, Oman, and other ophiolites. No basalt has been observed outcropping either on the surface of the mound or on the 20-m high talus slopes that bound the mound to the west, north, and east. Furthermore, the deposit is mature. Geochronological studies indicate the mound to be of the order of 40-50,000 years old, and to have undergone intermittent activity, possibly every 5-6,000 years over the last 20,000 years. Duration of an active cycle still has to be resolved but the present day activity is of, at least, 50 years duration based on radiometric dating. The TAG mound exhibits a wide range of polymetallic sulfides with predominantly Fe-Cu-Zn varieties. A recent series of *Alvin* dives indicates the active mound is zoned, both in terms of type of activity and mineralogy, thereby providing the opportunity to study relationships of mineral alteration. There is also evidence of supergene reactions resulting in enrichment in metals such as gold. Exiting hydrothermal solutions range from high (363°C), through medium to low temperatures at the boundaries of the active mound. These fluids are somewhat different from EPR fluids and have been hypothesized as showing interaction with weathered crust (Campbell et al., 1988). This may be a feature of slow-spreading ridges which can be tested by drilling.

The nearby MIR mound is proposed as a back-up drilling target. It is of similar size to the TAG mound, although not active. Primary sulfide features are similar to TAG, but there has been extensive recrystallization and the whole mound has been indurated by late-stage fluids that have replaced anhydrite and filled all voids with silica. Such an indurated feature will also allow conventional drilling.

## STUDY AREA

### Regional Geologic and Tectonic Setting

The ridge segment along which the TAG hydrothermal field is located, is about 40 km long, trends north-northeasterly, and is bounded by non-transform discontinuities to the south and north at 25°55'N and 26°17'N, respectively (Sempéré, Purdy, and Schouten, 1990; Purdy et al., 1990; Smith and Cann, 1992). Seafloor spreading has been asymmetric over the last 10 m.y.; half spreading rates are 13 mm/yr to the east and 11 mm/yr to the west (McGregor et al., 1977).

The seafloor morphology of the TAG ridge segment is well defined by SeaBeam bathymetric surveys of the Mid-Atlantic Ridge (MAR) in this area (Rona et al., 1986a; Sempéré et al., 1990; Purdy et al., 1990). The segment has a morphology typical of the 15-18 ridge segments lying between the Kane and Atlantis Fracture Zones (Sempéré et al., 1990; Smith and Cann, 1992). In plan view, the floor of the median valley has an hour-glass shape, narrowing and shallowing towards the center of the segment at about 26°10'N. In cross section, the median valley has an asymmetrical shape, the eastern wall being higher, steeper, and less rough than the western wall (Karson and Rona, 1990; Zonenshain et al., 1989). Using SeaBeam and high-resolution deep-towed side-scan sonar data, Smith and Cann (1990, 1992) and Smith et al. (1992) have documented the style of crustal accretion from 24°-30°N. Along this section of the MAR, the floor of the median valley is built of superposed, small-scale seamounts, with the axial volcanic ridges being formed by overlapping individual volcanic edifices (Smith and Cann, 1990, 1992). However, the data are insufficient to resolve the critical geological features needed to establish the distribution of hydrothermal activity and hence its relation to volcanism and tectonism.

Additional data on the geological structure of this segment, primarily concentrated in the vicinity of the hydrothermal field, has been collected from deep-towed camera profiles, piston-coring, water temperature profiling, dredging, and submersible dives (Eberhart et al., 1988; Karson and Rona, 1990; Rona, 1980; Rona et al., 1984, 1986b; Thompson et al., 1988). The western wall of the median valley consists of fault-controlled basaltic scarps and sediment-covered terraces (Eberhart et al., 1988; Zonenshain et al., 1989). Much of the eastern wall is covered with debris-slide deposits partly buried by calcareous ooze; fault scarps range in height from 10 to 20 m but are locally up to 150 m (Karson and Rona, 1990). Outcrops of pillow lavas were also observed on

the eastern wall (Zonenshain et al., 1989). Karson and Rona (1990) have suggested that an east-west trending scarp on the eastern wall represents a structural accommodation zone resulting from differential extension and rotation of crustal blocks to the north and south.

Important constraints on the along-axis changes in stress state and seismic velocity structure are provided by a microearthquake survey and seismic refraction experiment carried out on this ridge segment (Kong, 1990; Kong et al., 1992). These studies suggest that most of the micro-earthquake activity occurs at the axial high at the center of the segment; earthquakes are also distributed along-axis and in the eastern rift valley walls. No seismic events were detected in the immediate vicinity of the TAG hydrothermal field. The maximum depth of seismicity shoals toward the center of the segment, and a low velocity zone is observed there as well. The distribution of seismicity, the low velocity zone, and the recent hydrothermal activity suggest recent crustal injection near the axial high.

Magnetic field data from regional surface ship studies (Tivey et al., 1989) indicate that a broad north-northeast-south-southwest-oriented, elongate magnetic low is associated with the TAG hydrothermal field. A more detailed magnetic study of the mound has also been completed during the Alvin diving program, and has defined the mound as a localized low.

Sea surface gravity data indicate that the TAG segment contains a "bull's eye" anomaly (Lin et al., 1990), suggesting that either the crust is anomalously thick or that there is anomalously warm mantle upwelling buoyantly beneath this ridge segment. There may be a relation between the presence of the bull's eye and the presence of the TAG hydrothermal system on this segment.

## **Geologic and Tectonic Setting of the TAG Hydrothermal Field**

### *Tectonic Setting*

Hydrothermal activity in the TAG field is located on a 10-km-long segment of the eastern wall of the MAR. At this location, the east wall forms a broad salient toward the spreading axis and rises from the valley floor, near 4,000-m depth, to a height of 2,000 m through a series of steps formed by fault blocks (Temple et al., 1979).

The TAG hydrothermal field consists of presently active low and high temperature zones, as well as a number of relict deposits. The zone of low temperature activity occurs between 2,400- and 3,100-m depth on the east wall (Rona et al., 1984). The metalliferous deposits of this low temperature zone include widespread surficial metal-rich staining of carbonate ooze, as well as discrete, massive layered deposits of manganese oxide (birnessite), iron oxide (amorphous), and iron silicate (nontronite). The stratiform deposits range from less than 1 m across to about 15 x 20 m. They vary in composition from thick, laminated, crystalline birnessite precipitates, through Fe-rich tubular vents, to deposits of loose, earthy, interlayered birnessite, nontronite, and amorphous Fe-oxides (Thompson et al., 1985). Anomalous temperatures (Rona et al., 1984) and excessive  $^3\text{He}$  (Jenkins et al., 1980) were recorded in near bottom waters above the low-temperature field. Metal enrichments in the sediments have been recorded both at the surface and at 30-cm depth (Cu and Zn >1,000 ppm, Fe >8%); these enrichments were attributed to past and recent episodes of high-temperature venting in the area (Shearman et al., 1983). The hydrothermal deposits in this low-temperature field exhibit a linear distribution along fault zones, trending sub-parallel to the valley floor, that are inferred to focus hydrothermal discharge (Scott et al., 1974; Rona et al., 1984; Thompson et al., 1985).

The presently active black-smoker system occurs at the juncture between the rift-valley floor and the east wall at a depth of 3,620-3,700 m and at approximately 26°08'N, 44°49'W. The low-temperature field described above lies 3.7 km upslope to the east; the bathymetric axis of the rift valley is 1.5 km to the west. The active high-temperature field lies on oceanic crust at least 100,000 years old, based on the present seafloor-spreading rate. Sediment thickness around the active mound is variable depending on the local morphology. *Alvin* studies show that local basins may have >1 m of ooze, steep slopes are bare, less steep areas have 30-60 cm of sediment.

It is clear that both volcanism and tectonism play an important role in the spatial and temporal distribution of hydrothermal activity in this area, and three hypotheses have been presented addressing their interactions. Based primarily on observations in the low temperature field, Scott et al. (1974), Temple et al. (1979), and Thompson et al. (1985) hypothesized that hydrothermal activity was associated with ridge axis-parallel faults. They suggested these listric faults were the pathways for fluids and that the heat source was probably at the zero-age neovolcanic axis. More recently, based on observations of east-west faults high on the eastern wall in the vicinity of the low temperature field, Karson and Rona (1990) suggested that these transfer faults may intersect the ridge-parallel faults, concentrating hydrothermal activity at the intersections. However, due to

lack of data, no direct evidence exists for, or against, the extension of east-west faults in the low-temperature field to the presently active TAG mound.

SeaBeam bathymetry suggests that the active TAG mound is located on the edge of a dome-shaped high. The domes are suggested to be discrete volcanic centers that may act as heat sources for localized hydrothermal activity. Support for this hypothesis comes from a number of observations. Zonenshain et al. (1989) noted very recent volcanics, as well as older basalt outcrops, located on the volcanic dome to the southeast of the presently active hydrothermal mound, suggesting intermittent volcanic activity with a very recent eruption. Rocks have been observed and collected from at least two older eruptions at this site, although not of the very recent age observed by the Russians. Some of the other volcanic domes are also known to have relict sulfide mounds associated with them, e.g. the MIR mound, and the Alvin mound; others have relict sulfides photographed on their edges. Samples recovered from the Alvin hydrothermal mound have been dated at 10,000, 50,000, and 100,000 years, suggesting a long and complex history similar to the presently active mound. The MIR mound, discovered in July 1991, is a large (200 x 50 m) mound with chimney structures >5 m tall that has been described by Rona et al. (1992). It probably only recently became inactive because the mound appears bare even though carbonate deposition is of the order of 1.8 cm/103 yrs.

### *Geologic Setting*

The black smokers are located on top of an elliptical-shaped, compound mound consisting of concentric inner and outer portions (Rona et al., 1986b, Figure 2). The outer low-lying mound is composed of carbonate ooze, metalliferous sediment, sulfide blocks, and basalt talus and is about 500 m in diameter. The inner mound is about 200 m in diameter and rises 50 m above the outer mound between depths of 3,640 and 3,690 m. It is composed of massive sulfides, with distinct sample types being distributed from the interior to exterior of the mound. A cluster of chalcopyrite-anhydrite-rich black smoker chimneys emitting fluids up to 363°C caps the mound at about 3640-m depth. This chimney cluster sits on the top of a 10-20- m-high, 40-50-m-diameter cone, the surface of which is covered by a 3-6-cm-thick plate-like layer of massive pyrite and chalcopyrite, with interspersed blocks of corroded massive anhydrite and pyrite. The remainder of the top of the inner mound (at a depth of 3660-3665 m) is composed of both fragile Fe-oxide crusts and blocky to bulbous mixed Zn, Fe, and Cu-Fe sulfides with amorphous silica filling cavities.

...Leg 158 - TAG Hydrothermal Mound...

A complex of white smokers venting fluids up to 300°C is located in the southeast quadrant of the mound; these "Kremlin"-like spires are composed dominantly of low-Fe sphalerite with minor amounts of chalcopyrite, pyrite, and amorphous silica. Fluids from the white smokers have a very low pH, contain no magnesium, and lesser amounts of iron than the black smoker fluids. They are thought to be derived from the black smoker fluids by conductive cooling and precipitation of sulfides within the mound.

Mass-wasting of the edges of the inner mound results in steep outer slopes to the west, north, and east. Two sample types are exposed: pyrite-rich blocks with trace amounts of late-stage amorphous silica, quartz, and goethite and with outer oxidized layers that include atacamite, and deep-red to orange-brown blocks of amorphous Fe-oxide, goethite, hematite, and silica (as both amorphous silica and quartz). Analogues for these sample types are not found in other known seafloor vent sites, but are present in massive sulfide deposits of Cyprus (Tivey et al., 1992).

The distribution of sample types, their mineralogy, and the distinct compositions exhibited at the black smoker and Kremlin locations, suggest a flow pattern within the mound similar to that shown in Figure 2. Fluid exiting the black smoker complex is extremely focused. Fluid emanating from the Kremlin area has undergone conductive cooling as evidenced both by the presence of amorphous silica and the chemistry of the fluids (Edmond et al., 1990). As the fluid cools and circulates within the mound, pyrite is precipitated. Blocks of this material are exposed during mass-wasting.

Preliminary geochronological studies suggest that the mound is on the order of 40-50,000 years old, and that activity has been intermittent over the past 20,000 years, with a periodicity of 5,000-6,000 years (Lalou et al., 1990). The presence of late-stage quartz in pyritic and iron oxide blocks exposed on the steep slopes of the inner mound are consistent with such episodicity. Present activity commenced about 50 years ago after a hiatus of about 5,000 years (Lalou et al., 1992).

Previous studies of ongoing hydrothermal activity documented by water column studies of Mn and/or particulate anomalies suggest that there are other presently active sites in the TAG area (H. Elderfield and T. Nelsen, pers. comm.). The location of these sites will be addressed in the site survey cruise. Limited photographic coverage (lacking good navigation or correlation with a structural framework) has shown the presence of relict sulfides in other areas of the TAG field, and recent submersible dives by *Alvin* and the Russian *MIR* vessels discovered two other relict sulfide

mounds (Eberhart et al., 1988; Rona et al., 1990; Rona et al., 1992). The site survey will collect the data that is needed to place the proposed drilling in the context of the regional time distribution and spatial geometry of hydrothermal activity in the entire field.

Previous magnetic studies (Rona, 1980) and the more recent magnetic data from the 1988 MARNOK cruise (Tivey et al., 1989) reveal that the TAG area is the site of a distinctive anomaly in sea-surface magnetics data. This anomaly indicates an unusually pronounced, point-style magnetization low located in the general vicinity of the TAG mound. Four different hypotheses have been proposed for the cause of the sea-surface magnetic low measured at TAG. Three of these hypotheses propose hydrothermal or thermal demagnetization as the cause, while the fourth proposes structural thinning of the source layer by local normal faulting. A 1990 *Alvin* survey over the TAG mound showed a magnetization low located directly beneath the mound with a possible dip to the south, which has been interpreted as the upflow zone beneath the mound (Tivey et al., 1991; Tivey et al., 1992). The survey also showed that the magnetic low beneath the TAG mound cannot itself produce the observed sea-surface anomaly low. Either there are many more magnetic low source regions caused by hydrothermal demagnetization, as suggested by the presence of relict mounds, or a more regional magnetic low is present due to some thermal effect, as suggested by the recent volcanics and the seismic data. Near-bottom magnetic surveys, to be conducted during the site survey, offer the chance to discriminate between these hypotheses and possibly help in determining the occurrence and distribution of active and relict hydrothermal vent systems in the TAG region as a whole.

Only a few heat flow measurements near the active mound and on the relict mounds have been made (Rona, in prep.). Thermal output from the active mound has been estimated to be about  $120 \times 10^6$  W using a transistor array and a grid survey at a height of 20 m above the mound (Rona et al., 1991). Measurements at conductive heat stations on the mound ranged between 1.6 and 4.3 W/m<sup>2</sup>.

## SCIENTIFIC OBJECTIVES AND METHODOLOGY

The overall scientific objectives of drilling at TAG are to investigate fluid flow, geochemical fluxes and associated alteration and mineralization, and the subsurface nature of an active hydrothermal system on a slow-spreading mid-ocean ridge. Understanding the processes operating within a

hydrothermal system, and their interrelations, requires answering a number of questions that can be addressed only by drilling. Although studies of fossil hydrothermal deposits preserved in ophiolites have provided valuable insights into their subsurface geometry and composition, the hypothesis that these systems provide a useful analogue for mid-ocean ridge hydrothermal processes still needs to be tested. In addition, a number of critical parameters cannot be determined from extinct systems; for example, variations in permeability and porosity of the host rocks, the composition of the circulating fluid, and the dynamics of the water-rock interface.

Within the near-surface part of the hydrothermal system, Leg 158 will investigate:

- 1) the temporal and spatial variation in the mineralogy, chemistry, and physical properties of the hydrothermal precipitates;
- 2) the spatial and temporal variation in the composition of the circulating fluids and the effects of conductive cooling on the composition of these fluids and their relationships to mineralogical variations within the deposits;
- 3) the method of fluid circulation within the deposit and the spatial characteristics (focused or diffuse) of the flow;
- 4) the effects of fluid circulation within the mound, e.g. are metals remobilized and concentrated in distinct horizons?; and
- 5) the physical and chemical effects of epigene and supergene alteration reactions on the deposits, and on the fluxes of elements between the deposits and seawater.

In the stockwork and root zone below the surface deposits, studies aim to clarify:

- 1) the variation in mineralogical and chemical composition of deposits in this zone;
- 2) the degree to which fluids have reacted with the adjacent host rocks, the nature of the rock-seawater interactions, and subsequent affects upon the magnetics;
- 3) the physical and hydrogeological properties of the upper crust in this zone;

- 4) the chemical composition of the hydrothermal fluid in this zone;
- 5) the mechanism focusing the fluid flow within this part of the hydrothermal cell; and
- 6) the amount of heat exchanged in the system and the associated energy fluxes.

### **DRILLING PLAN/STRATEGY**

Complete characterization of the subsurface nature of an active hydrothermal system requires a drilling program of more than one leg, since determining the location and nature of the reaction zone would require drilling a deep hole to the base of the sheeted dikes (i.e. to a depth of about 1.5-2 km). However, this one-leg program will demonstrate that it is possible to successfully drill and attain the scientific objectives in this type of environment.

The size and maturity of the deposit, and its compositional variability in terms of both the mineralogy of the deposits and the circulating fluid makes TAG the only currently known site where questions concerning the near-surface part and stockwork and root zones of the hydrothermal system can be addressed. In addition, capping of one (or more) of the holes will allow their future use for time-series measurements and monitoring fluid composition variability. As future technology develops, particularly the capability to sample high-temperature fluids downhole, these holes could be used for a number of different measurements that will help to clarify temporal variability of hydrothermal systems.

From previous drilling experience, there are a number of arguments which suggest that conventional drilling can accomplish the scientific objectives at TAG. TAG may be situated on crust possibly as old as 100,000 years (calculated from spreading rates) If that is the case, the crust (whether altered through hydrothermal circulation or not) is likely to be weathered, with some of the fractures infilled with minerals of various kinds. Previous experience with drilling weathered and hydrothermally-altered crust (for example, at Hole 504B) has demonstrated that conventional drilling is feasible. Although not as young as TAG, weathering and alteration processes clearly played an important role in achieving penetration through the upper pillow lavas at this site. However, if the TAG hydrothermal mound is associated with a younger volcanic dome, there is a

...Leg 158 - TAG Hydrothermal Mound...

possibility of encountering basalts of a younger age. It is proposed to drill through the basalt directly beneath the TAG hydrothermal mound, a major feature that has been active over at least the last 40-50,000 years. The size of the mound and duration of the activity argue strongly for a highly altered crust, with all veins and fissures completely infilled with secondary minerals. This is also consistent with the magnetic low zone directly beneath the mound. Such altered crust has been successfully drilled at Holes 417A and 418A in the North Atlantic, and at Hole 504B in the Pacific.

The likely thickness of the hydrothermal precipitates at TAG is 50-70 m given the analogous shape and size of the deposits of the Troodos ophiolite. Recent drilling during Leg 139 has provided some evidence that conventional drilling technology can drill through short sections of sulfide deposits, although difficulties are encountered with clearing cuttings for long sections. This suggests that the TAG sulfide deposits should not present a problem in terms of penetration and, if a comprehensive logging program is carried out, the recovery will be sufficient to address the objectives.

Problems were encountered on Leg 106 during attempts to drill into the active sulfide mound in the Snakepit hydrothermal field. The problems consisted of both difficult drilling conditions and extremely poor recovery, and were caused by alternating hard and soft, unconsolidated layers of sulfides. Comparison of these two fields from direct *Alvin* observations and inspection of samples from the two areas indicates distinct differences in their structure. The TAG mound is composed of more massive blocks of sulfide that appear to be more homogeneous in nature. Some of the blocks exposed on the steep talus slopes, which offer a window into the interior of the mound, contain late-stage amorphous silica and quartz. Given the age of the TAG mound (Snakepit is considerably younger), and the evidence for circulating fluids and conductive cooling with precipitation within the mound, the interior of TAG is most likely indurated and recrystallized from its long and complex evolution and will consequently provide a hard and massive target for drilling.

Drilling in stockwork zones has been demonstrated to be possible with the available technology. In Hole 504B, the top of a stockwork zone was encountered in 5.9-Ma basalts at a depth of 910 m below the sea floor. Coring in this interval was very successful, with recoveries up to 42%. Good recovery is particularly critical in the stockwork zone if the chemical reactions and their spatial and temporal relationships are to be understood and unravelled.

To meet the objectives of drilling in an active hydrothermal area, a variety of downhole measurements are critical at each site, especially as the recovery might not be high. Important measurements include subbottom formation temperatures, pore pressures and fluid fluxes, formation chemistry, sonic velocity porosity, resistivity, permeability, and stress. A full logging program that will include the standard logs and specialty tools will be run at each site, and will be important to the fluid chemistry and flow objectives of the program.

In addition, these drillholes will provide opportunities for time-series experiments at a hydrothermal system. The instrumentation of these holes for temperature measurements and fluid sampling, such as the CORK system, is encouraged to continue after the drilling is completed. As additional technologies become available, other measurements and experiments can be done at this site. The European community is interested in deploying an instrumented station at a hydrothermal site in the Atlantic, so this may prove to be an advantageous site for continued long-term observations and measurements.

### **PROPOSED DRILL SITES**

Leg 158 will complete a transect of three sites across the TAG mound (Figure 1, Table 1).

Proposed site TAG-1 is located near the center of the mound on the shoulder of the central cone in an area that has a slope of less than 10° and is roughly 20-30 m wide. This is the area closest to the black smokers that, from submersible observations, is the most suitable for drilling near the region of high temperature activity. It is designed to penetrate through the entire section of hydrothermal deposits and into the uppermost portion of the highly altered crust. In this region, large black smoker chimneys occur, from which hot (363°C) fluids are emanating. The chemistry of the fluids suggests that they have not mixed with seawater in the subsurface region of the mound, and it is likely that the ascending flow is well-focused beneath the chimneys (Figure 1). This site provides the best opportunity to recover a stratigraphic section of the hydrothermal mound, and to determine the nature of the fluid flow beneath the most active part of the mound.

Proposed site TAG-2 is located off-center to the southeast of TAG-1 in the "Kremlin" area, where warm (250°C) waters are discharging from small (1-2 m) high chimneys composed dominantly of Zn-Fe sulfides. The surface of the mound at this location is relatively flat, less than 5 m of relief

over an area of roughly 80 x 80 m, and is suitable for setting a guidebase. Fluids emanating from this region have undergone conductive cooling within the mound (Figure 1); consequently, this site will provide information on the mineralogical and chemical variability within the mound related to these different fluids and physical controls. In addition, any differences in the alteration of the upper crust and the minerals precipitated within veins and fractures within it, will be determined.

Proposed site TAG-3 is located at the edge of the mound, where cool (<100°C) waters are diffusing out of the deposits and older, weathered sulfides are observed on the surface. It is also located over the magnetic low, and thus has a high probability of intersecting the stockwork. Drilling at this site will allow differences in the plumbing system within the mound related to diffuse, rather than focused, flow to be determined. In addition, the extent of the oxidation of the deposits, which is seen on the exposed surfaces of the mound, will be investigated, as well as the composition of the fluids present in this region.

Two of these proposed sites will be shallow (200 m), non-reentry holes and will be designed to penetrate through the hydrothermal deposits and into the top of the altered basaltic crust. The third proposed site (most likely TAG-2) will be a reentry hole that will penetrate into the stockwork zone and will be drilled to at least 500 m on this leg, with the possibility of being deepened further to the reaction zone at a later date. Determination of the exact locations of these sites, and confirmation of which will be the reentry site, will be made from the pending site survey cruises, which include bathymetry, deep-tow magnetics, geothermal and geoelectrical data.

There is the possibility that drilling into this active system may prove difficult, e.g. it may not be well-consolidated, and/or the high temperatures may cause problems (although similar high temperature fluids posed no problems on Leg 139). Consequently, a back-up site should be considered that will allow most of the objectives to be accomplished, except for those addressing fluid composition and flow. The MIR mound is proposed as the back-up site should drilling at TAG prove not to be feasible. Observations from the *MIR* submersibles in 1991 located the MIR mound on the lower part of the east wall of the rift valley about 2 km northeast of the TAG mound. Rona et al. (1992) have described the mound as consisting of two concentric zones: an inner zone, about 400 m in diameter, consisting of discontinuous sulfide outcrops with groups of inactive chimneys with intervening metalliferous sediment; and an outer zone of low temperature Fe and Mn oxide deposits 150-200 m wide. It appears to be associated with a volcanic dome and is consequently in a similar tectonic setting to TAG. It is also about the same size as TAG and has

similar primary sulfide features. However, unlike TAG, it is inactive, and the whole mound has been extensively recrystallized (Rona et al., 1992), and has been indurated by late-stage fluids that have replaced anhydrite and filled all voids with silica. Such an indurated feature will be considerably easier to drill.

## **ADDITIONAL CONSIDERATIONS**

### **Safety**

The sulfide deposit is volcanogenic-hosted, so hydrocarbons are not expected to pose a problem. The hot circulating solutions and their hydrogen sulfide concentrations have already been demonstrated not to pose a problem with drilling in these system. TAG is significantly deeper than the drilling at Middle Valley on Leg 139, when no problems were encountered. However, precautions for early detection of high levels of hydrogen sulfide will be necessary.

## REFERENCES

- Campbell, A.C., Palmer, M.R., Klinkhammer, G.P., Bower, T.S., Edmond, J.M., Lawrence, J.R., Casey, J.F., Thompson, G., Humphris, S.R., Rona, P.A., and Karson, J.A., 1988. Chemistry of hot springs on the Mid-Atlantic Ridge: TAG and MARK sites. *Nature*, 335:514--519.
- Eberhart, G.L., Rona, P.A., and Honnorez, J., 1988. Geologic controls of hydrothermal activity in the Mid-Atlantic Ridge rift valley: tectonics and volcanics. *Mar. Geophys. Res.*, 10:233--259.
- Edmond, J.M., Campbell, A.C., Palmer, M.R., and German, C.R., 1990. Geochemistry of hydrothermal fluids from the Mid-Atlantic Ridge: TAG and MARK. *Eos*, 71:1650-1651.
- Jenkins, W.J., Rona, P.A., and Edmond, J.M., 1980. Excess He in the deep water over the Mid-Atlantic Ridge at 26°N: Evidence of hydrothermal activity. *Earth Planet. Sci. Lett.*, 49:39--44.
- Karson, J.A., and Rona, P.A., 1990. Block tilting, transfer faults and structural control of magmatic and hydrothermal processes in the TAG area, Mid-Atlantic Ridge, 26°N. *Geol. Soc. Am. Bull.*, 102:1635--1645.
- Kong, L.S.L., 1990. Variations in structure and tectonics along the Mid-Atlantic Ridge, 23°N and 26°N [Ph.D. dissert.]. MIT/WHOI Joint Program, Woods Hole, Mass.
- Kong, L.S.L., Solomon, S.C., and Purdy, G.M., 1992. Microearthquake characteristics of a mid-ocean ridge along axis. *J. Geophys. Res.*, 97:1659--1685.
- Lalou, C., Thompson, G., Arnold, M., Bricquet, E., Druffel, E., and Rona, P.A., 1990. Geochronology of TAG and Snakepit hydrothermal fields, Mid-Atlantic Ridge: Witness to a long and complex hydrothermal history. *Earth Planet. Sci. Lett.*, 97:113--128.
- Lalou, C., Reyss, J.L., Bricquet, E., Arnold, M., Thompson, G., Fouquet, Y., and Rona, P., 1992. New age data for Mid-Atlantic Ridge hydrothermal sites: TAG and Snakepit chronology revisited. *J. Geophys. Res.*, in press.
- Lin, J., Purdy, G.M., Schouten, H., Sempéré, J.-C., and Zervas, C., 1990. Evidence from gravity data for focused magmatic accretion along the Mid-Atlantic Ridge. *Nature*, 344:627-632.
- McGregor, B.A., Harrison, C.G.A., Lavelle, J.W., and Rona, P.A., 1977. Magnetic anomaly pattern on the Mid-Atlantic Ridge crest at 26°N. *J. Geophys. Res.*, 82:231-238.
- Purdy, G.M., Sempéré, J.-C., Schouten, H., DuBois, D.L., and Goldsmith, R., 1990. Bathymetry of the Mid-Atlantic Ridge, 24-31°N: a Map Series. *Mar. Geophys. Res.*, 12:247-252.
- Rona, P.A., 1980. TAG hydrothermal field: Mid-Atlantic Ridge at latitude 26°N. *J. Geol. Soc. Lond.*, 137: 385--402.
- Rona, P.A., Thompson, G., Mottl, M.J., Karson, J.A., Jenkins, W.J., Graham, D., Mallette, M., Von Damm, K., and Edmond, J.M., 1984. Hydrothermal activity at the TAG hydrothermal field, Mid-Atlantic Ridge crest at 26°N. *J. Geophys. Res.*, 89:11365--11377.
- Rona, P.A., Pockalny, R.A., and Thompson, G., 1986a. Geologic setting and heat transfer of black smokers and TAG Hydrothermal field. *Eos*, 67:1021.
- Rona, P.A., Klinkhammer, G., Nelson, T.A., Trefry, J.H., and Elderfield, H., 1986b. Black smokers, massive sulfides and vent biota on the Mid-Atlantic Ridge. *Nature*, 321:33--37.
- Rona, P.A., Hannington, M.D., and Thompson, G., 1990. Evolution of hydrothermal mounds, TAG Hydrothermal field. *Eos*, 71:1650.
- Rona, P.A., Bogdanov, Y.A., Gurvich, E.G., Minski-Korsakov, N.A., Sagalevitch, A.M., and Hannington, M.D., 1992. Relict hydrothermal mounds at TAG hydrothermal field, Mid-Atlantic Ridge 26°N, 45°W. *Earth Planet. Sci. Lett.*, (submitted).
- Scott, M.R., Scott, R.B., Rona, P.A., Butler, L.W., and Nalwalk, A.J., 1974. Rapidly accumulating manganese deposit from the median valley of the Mid-Atlantic Ridge. *Geophys. Res. Lett.*, 1: 355--358.
- Sempéré, J.-C., Purdy, G.M., and Schouten, H., 1990. Segmentation of the Mid-Atlantic Ridge between 34°N and 30°40'N. *Nature*, 344:427--431.
- Shearme, S., Cronan, D.S., and Rona, P.A., 1983. Geochemistry of sediments from the TAG hydrothermal field, M.A.R. at latitude 26°N. *Mar. Geol.*, 51:269-291.
- Smith, D.K., and Cann, J.R., 1990. Hundreds of small volcanoes on the median valley floor of the Mid-Atlantic Ridge at 24°--30°N. *Nature*, 348:152-155.

- Smith, D.K., and Cann, J.R., 1992.** The role of seamount volcanism in crustal construction at the Mid-Atlantic Ridge (24°--30°N). *J. Geophys. Res.*, 97:1645-1658.
- Smith, D.K., Cann, J.R., et al., 1992.** Building the crust of the Mid-Atlantic Ridge (24-30°N). *Nature* (submitted).
- Temple, D.G., Scott, R.B., and Rona, P.A., 1979.** Geology of a submarine hydrothermal field, Mid-Atlantic Ridge 26°N latitude. *J. Geophys. Res.*, 84:7453--7466.
- Thompson, G., Mottl, M.J., and Rona, P.A., 1985.** Morphology, mineralogy and chemistry of hydrothermal deposits from the TAG area, 26°N Mid-Atlantic Ridge. *Chem. Geol.*, 49:243--257.
- Thompson, G., Humphris, S.E., Schroeder, B., Sulanowska, M., and Rona, P.A., 1988.** Active vents and massive sulfides at 26°N (TAG) and 23°N (Snakepit) on the Mid-Atlantic Ridge. *Can. Mineral.*, 26:697--711.
- Tivey, M.A., Schouten, H., Sempéré, J.-C., and Wooldridge, A., 1989.** Implications of the 3D structure of the TAG magnetic anomaly on the Mid-Atlantic Ridge. *Eos*, 70:455.
- Tivey, M.A., Rona, P.A., and Schouten, H., 1991.** A submersible investigation of the magnetic field over the TAG hydrothermal mound on the Mid-Atlantic Ridge at 26°08'N. *Eos*, 72:265.
- Tivey, M.A., Rona, P.A., and Schouten, H., in prep. (1992).** A magnetic low beneath the active sulfide mound, TAG hydrothermal field, Mid-Atlantic Ridge 26°N.
- Tivey, M.K., Thompson, G., Humphris, S.E., Hannington, M.D., and Rona, P.A., 1992.** Similarities between the active TAG hydrothermal mound, Mid-Atlantic Ridge 26°N, and ore deposits of the Troodos ophiolite. *Eos*, 73:360.
- Zonenshain, Z.P., Kuzmin, M.I., Lisitsin, A.P., Bogdanov, Yu.A., and Baranov, B.V., 1989.** Tectonics of the Mid-Atlantic rift valley between TAG and MARK areas (26--24°N): Evidence for vertical tectonism. *Tectonophysics*, 159:1--23.

...Leg 158 - TAG Hydrothermal Mound...

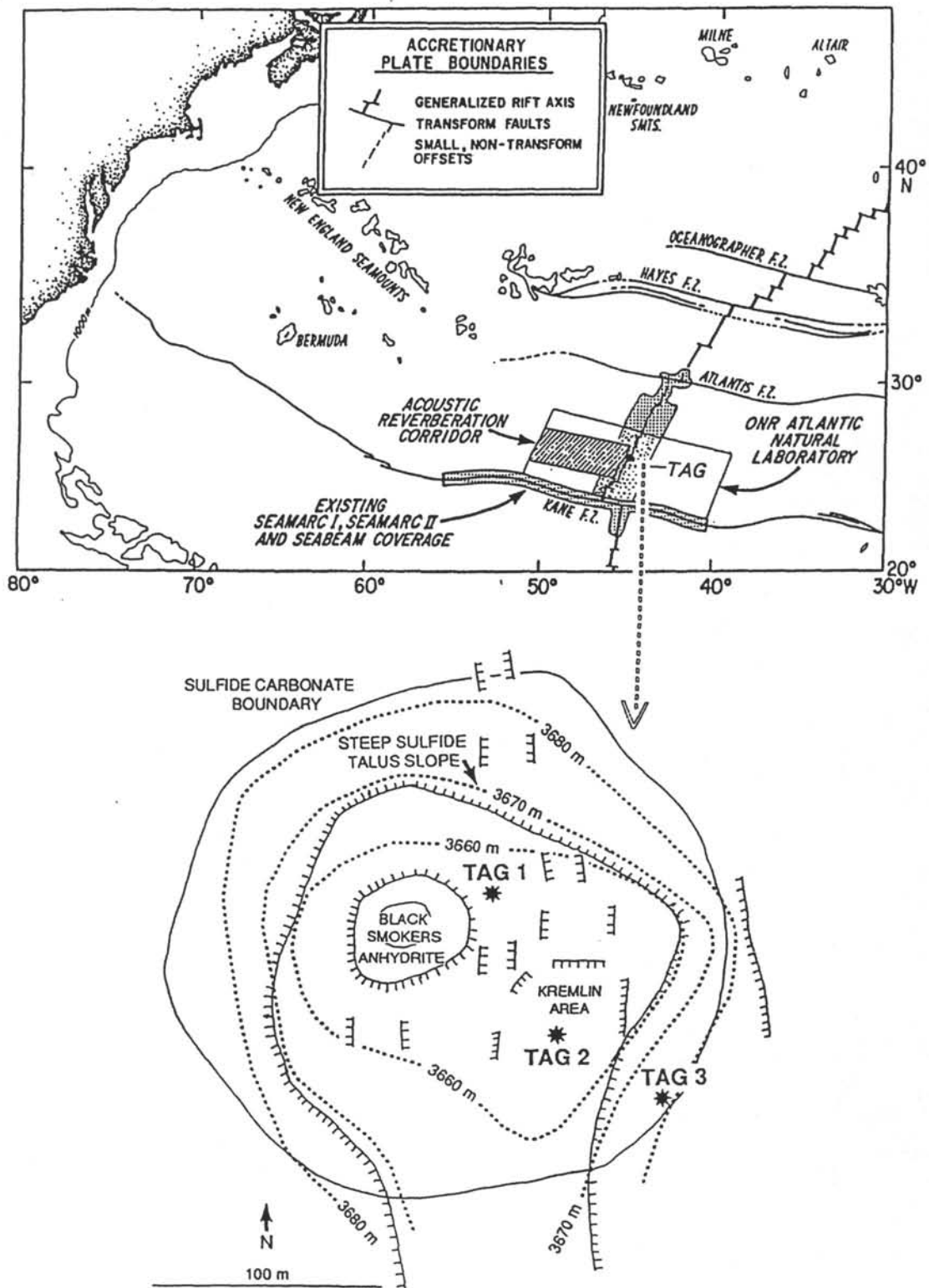


**Figure 1.** Location of the ONR Atlantic Natural Laboratory on the Mid-Atlantic Ridge (modified from Tucholke et al., 1991) and plan view of the active TAG mound showing the principal boundaries and tectonic features as derived from submersible observations and photography. The locations of the three proposed drill sites are shown.

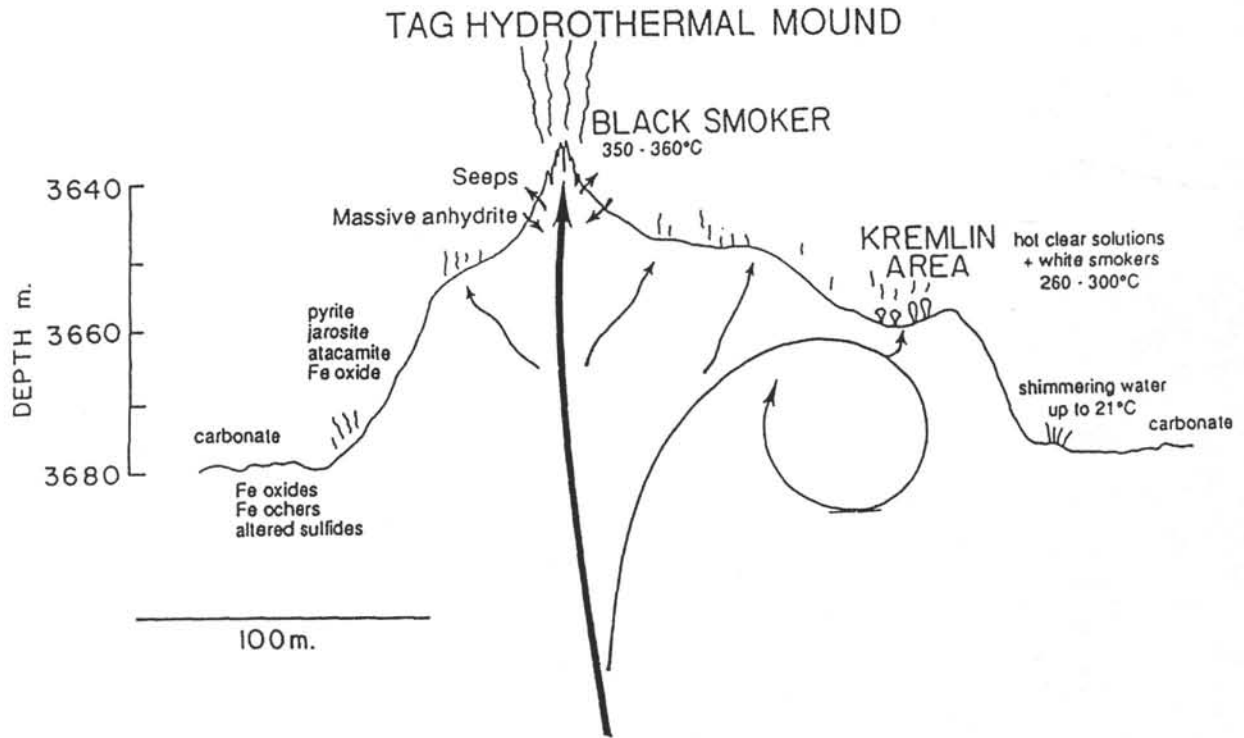


**Figure 2.** Cross section of the active TAG mound with observations derived from submersible observations. The suggested flow pattern within the mound is derived from the mineralogy of the deposits and the fluid chemistry.

**TABLE 1**  
**PROPOSED SITE INFORMATION**  
**and**  
**DRILLING STRATEGY**

<b>SITE: TAG-1</b>	<b>POSITION: 26°08'N, 44° 49'W</b>	
<b>WATER DEPTH: 3660 m</b>	<b>SEDIMENT THICKNESS: 50-70 m</b>	<b>BASEMENT PENETRATION: 140 m</b>

**Objectives:** Sample the entire section of the TAG hydrothermal mound near the black smokers where fluid flow is focused, and into the upper part of the highly altered crust.

**Drilling Program:** RCB coring.

**Logging and Downhole Operations:** Standard logs and specialty tools to measure sub-bottom formation temperatures, pore pressures and fluid fluxes, formation chemistry, sonic velocity porosity, resistivity, permeability, and stress.

**Nature of Rock Anticipated:** Massive sulfide deposits and hydrothermally altered and veined basalts.

<b>SITE: TAG-2</b>	<b>POSITION: 26°08'N, 44° 49'W</b>	
<b>WATER DEPTH: 3660 m</b>	<b>SEDIMENT THICKNESS: 50-70 m</b>	<b>BASEMENT PENETRATION: 450 m</b>

**Objectives:** Sample the section of the TAG hydrothermal mound in an area where fluids have undergone conductive cooling within the mound, and extend penetration into the underlying stockwork zone.

**Drilling Program:** RCB coring and reentry.

**Logging and Downhole Operations:** Standard logs and specialty tools to measure sub-bottom formation temperatures, pore pressures and fluid fluxes, formation chemistry, sonic velocity porosity, resistivity, permeability, and stress.

**Nature of Rock Anticipated:** Massive sulfide deposits, stockwork zone and hydrothermally altered basalts.

<b>SITE: TAG-3</b>	<b>POSITION: 26°08'N, 44° 49'W</b>	
<b>WATER DEPTH: 3680 m</b>	<b>SEDIMENT THICKNESS: 20 m</b>	<b>BASEMENT PENETRATION: 180 m</b>

**Objectives:** Drill through the older, weathered sulfides where there is diffuse flow and into the stockwork, the existence of which is suggested by the magnetization low.

**Drilling Program:** RCB coring.

**Logging and Downhole Operations:** Standard logs and specialty tools to measure sub-bottom formation temperatures, pore pressures and fluid fluxes, formation chemistry, sonic velocity porosity, resistivity, permeability, and stress.

**Nature of Rock Anticipated:** Massive sulfide deposits, stockwork zone and hydrothermally altered basalts.

*LEG 159*

*Return to Hole 735B*

**LEG 159**  
**RETURN TO HOLE 735B**

---

**Modified from Proposal 300-Rev Submitted By:**

**Henry J.B. Dick, Stanley Hart, James H. Natland, Paul Robinson,  
Ralph Stephen, and Richard P. von Herzen**

**To Be Named: Co-Chief Scientists and Staff Scientist**

---

**ABSTRACT**

Hole 735B was previously drilled during ODP Leg 118 on the Southwest Indian Ridge and Leg 159 represents the first leg in a proposed multi-leg program to deepen Hole 735B to a nominal depth of 2 km sub-basement, drill a suite of complementary shorter 500 m holes along a lithospheric flow line at 800 m intervals, and conduct downhole and logging experiments. This program takes advantage of the unique outcrop of the lower crust exposed along a 15-km-long wave-cut terrace 18 km east of the Atlantis II Transform Fault to drill the first systematic transect of the lower ocean crust to directly test the widely hypothesized episodic and discontinuous nature of magmatic, hydrothermal, and tectonic processes in the lower ocean crust at a slow-spreading ocean ridge. A spacing of 800 m along the flow line corresponds to 100,000-year increments and each penetration would overlap the paleo-horizontal with several other holes. The proposed suite of holes thus spans a 400,000-year interval of crustal generation at varying depths, which should reflect many magmatic and amagmatic cycles if current models are correct.

The principle objective of Leg 159 is to explore the lateral and temporal variability of lower crust generated at a slow-spreading ocean ridge. The proposed drilling may reach the petrologic Moho, the boundary between rocks which are the residues of the processes by which magmas form and migrate to the crust and rocks produced by the crystallization of those magmas as they rise out and pool above the upwelling mantle peridotite; however, reaching the petrologic Moho is not a requirement to achieve our objectives as the recovery of a truly representative section of plutonic crust would, by itself, be a major breakthrough in understanding the geologic processes occurring beneath ocean ridges. By deepening Hole 735B and drilling an offset section of holes along a lithospheric flow we will obtain a representative section of the lower ocean crust at one of the two critical ends of the spreading spectrum which, together with seafloor mapping, will permit a true three-dimensional view of the ocean crust and provide a natural laboratory where hole to hole magnetotelluric and permeability experiments can be conducted and the nature of layer 3 may be directly tested.

## INTRODUCTION

The composition, internal stratigraphy, and petrogenesis of the largest and deepest seismic layer of the ocean crust is one of the fundamental questions of earth science. After an initial debate in the late 1950's and early 1960's a consensus was achieved for a fairly straightforward layer cake geologic model. This model was based on the match of density and P and S wave velocities of gabbros, diabase, and tholeiitic basalt dredged from the seafloor and found in ophiolite complexes (fossil sections of ocean crust tectonically emplaced in island arcs and continental margins) to the seismic character of the ocean crust (e.g., Christensen, 1972). An overall stratigraphy was then compiled extrapolating the simple observed layered seismic structure to the vertical lithologic stratigraphy seen in tectonically-disrupted ophiolites.

Based on this layer 3 was expected to consist of a uniform layer of magmatic cumulates deposited on the floor and walls of a large continuous magma chamber, overlain by evolved ferrogabbros along its roof. This internal stratigraphy was in reality more dependent on the documented stratigraphy of the large layered intrusions found on the continents, than it was on the internal stratigraphy of gabbros in ophiolites. These large layered intrusions have dominated the thinking of the petrologic community, with their systematic progression in chemistry from top to bottom, and their historic role in establishing the key role of fractional crystallization in the evolution of magmas. It has been a natural impulse to impose their stratigraphy on that of lower crust in both ophiolites and the present-day ocean basins. Thus, evolved the extremely attractive paradigm of the "infinite onion", a large continuous magma chamber underlying the global ocean ridge system, disrupted only by the largest of ocean fracture zones, from which layers of ocean crust continuously grew at top, sides, and bottom to form a uniform coarse gabbroic layer comprising two thirds of the ocean crust (Cann, 1970).

Two decades of geophysical testing of this model, and study of the stratigraphic structure and chemistry of ophiolites has thrown this simple paradigm into question. The seismic structure has become increasingly complex along the ridges, while the provenance of ophiolites has become increasingly ambiguous, and generally believed to be atypical of ocean crust. Recent work has, in fact, suggested that the ocean crust has a complex, three dimensional structure (e.g., Whitehead et al., 1984) highly dependent on magma supply and spreading rates, and without large steady-state magma chambers (e.g., Sinton and Detrick, 1992). Compilations of dredge results and seismic data have suggested that a continuous gabbroic layer does not exist at slow-spreading ridges (Mutter et

al., 1985; NAT Study Group, 1985; McCarthy et al., 1988; Dick, 1989; Cannat et al., 1992; Tucholke et al., in prep.), and that its internal stratigraphy is governed by dynamic processes of alteration and tectonism as much as by igneous processes. The exceptional abundance of serpentinized peridotite in dredge hauls both from fracture zones and from the walls of rift valleys and in the rift mountains away from fracture zones (Aumento et al., 1971; Rona et al., 1987; Dick, 1989; Cannat et al., 1992; Tucholke, in prep.) is also raising the serious possibility that serpentinite is a major component of layer 3 as originally suggested by Hess (1962). Thus, at this point in time, we have little ground truth as to the internal structure and composition of layer 3 beyond educated supposition.

## STUDY AREA

### Previous Investigations at Site 735

During Leg 118, a large intact 500-m section of gabbros was recovered from Site 735. These gabbros were unroofed and uplifted on the transverse ridge flanking the Atlantis II Fracture Zone. The complex internal structure and stratigraphy of the recovered section provides a first look at the processes of crustal accretion and on-going tectonism, alteration, and ephemeral magmatism at a slow-spreading ocean ridge. The section was not formed in a large steady-state magma chamber, but by continuous intrusion and reintrusion of numerous small, rapidly crystallized bodies of magma. There is little evidence of the process of magmatic sedimentation, so important in layered intrusions. Instead, new batches of magma are intruded into and initially supercooled by a lower ocean crust which consists of wholly crystalline rock and semi-solidified crystal mush. This leads to undercooling and rapid initial crystallization of new magmas to form a highly viscous or rigid crystal mush preventing the formation of magmatic sediments, followed by a longer, and petrologically more important, period of intercumulus melt evolution in a highly viscous crystal mush or rigid melt crystal aggregate.

As a consequence long-lived magma chambers or melt lenses were virtually absent throughout most of crustal formation beneath the Southwest Indian Ridge. Thus, melts in the highly viscous or rigid intrusions were largely uneruptable throughout most of their crystallization. This explains the near absence of highly evolved magmas such as ferrobasalts along the Southwest Indian Ridge (Dick, 1989), as opposed to fast-spreading ridges where they are common and a long-lived melt lens is believed to underlie the ridge axis (e.g., Sinton and Detrick, 1992)

Wall rock assimilation while small batches of melt worked their way up through the partially solidified lower crust appear to have played a major role in the chemical evolution of the section and therefore in the chemistry of the erupted basalt. This process has been largely unevaluated for basalt petrogenesis to date, and throws into questions simple models for the formation of MORB drawn from experimental studies which assume equilibrium crystallization and melting processes throughout magma genesis.

An unanticipated major feature of the drilled section is the evidence for deformation and ductile faulting of the still partially molten gabbros. This deformation apparently occurred over a narrow window, late in the cooling history of the gabbros (probably at 70-90% crystallization) when they became sufficiently rigid to support a shear stress. This produced numerous small and large shear zones, creating zones of enhanced permeability into which the late intercumulus melt moved. This synkinematic igneous differentiation of intercumulus melts into the shear zones transformed the gabbro there into oxide-rich ferrogabbros. The net effect of these magmatic and tectonic processes was to produce a complex igneous stratigraphy with undeformed oxide-free olivine gabbros and microgabbros criss-crossed by bands of sheared ferrogabbro. Synkinematic differentiation is probably ubiquitous in lower ocean crust formed at slow-spreading ocean ridges, and should be recorded in ophiolite suites formed in similar tectonic regimes.

At Site 735, ductile deformation and shearing continued into the sub-solidus regime, causing recrystallization of the primary igneous assemblage under granulite facies conditions, and the formation of amphibole-rich shear zones (Stakes et al., 1991, Dick et al., 1991a, Cannat et al., 1991). Here again, formation of ductile shear zones localized late fluid flow, with the most intense alteration occurring in the ductile faults (Dick et al., 1991a). Undeformed sections of gabbro also underwent enhanced alteration at this time principally by replacement of pyroxene and olivine by amphibole.

A consequence of simultaneous extension and alteration, has been far more extensive alteration at high temperatures than found in layered intrusions which were intruded and cooled in a static environment. An abrupt change in alteration conditions of the Hole 735B gabbros, however, occurred in the middle amphibolite facies with the cessation of shearing and ductile deformation. Mineral vein assemblages changed from amphibole-rich to diopside-rich, reflecting different fluid chemistry. Continued alteration and cooling to low temperature occurred under static conditions similar to those found for large layered intrusions. These changes likely occurred due to an inward

jump of the master faults defining the rift valley walls, thus transferring the section out of the zone of extension and lithospheric necking beneath the rift valley into a zone of simple block uplift in the adjoining rift mountains. Ongoing hydrothermal circulation, no longer enhanced by stresses related to extension, was greatly reduced, driven only by thermal dilation cracking as the section cooled to ambient temperature.

The complex section of rock drilled at Site 735 formed beneath the very slow-spreading Southwest Indian Ridge (0.8 cm/yr half rate) and represents the slow end of the spectrum for crust formation at major ocean ridges far from hot spots. Such ridges have the lowest rates of ocean ridge magma supply, and crustal accretion is most heavily influenced by deformation and alteration. At the opposite end of the spreading rate spectrum (7-9 cm/yr), where the majority of the sea floor has formed, the crustal stratigraphy is likely different. Judging from the results of Hole 735B, the critical brittle-ductile transition has migrated up and down through the lower crust due to the waxing and waning of magmatism beneath the Southwest Indian Ridge. In contrast, this transition may be more stable near the sheeted dike gabbro transition at faster spreading ridges such as the East Pacific Rise, reflecting a near steady-state magma chamber or crystal mush zone. This should produce an internal stratigraphy for the lower crust quite different than that described here.

The rather general conclusions drawn to date from Hole 735B, so different from what was anticipated, are based on study of only a small part of what is likely to be a 2- to 4-km-thick section, and thus may represent only part of a more complex overall stratigraphy. By deepening Hole 735B to greater depth and drilling an offset section of holes along a lithospheric flow we will obtain a representative section of the lower ocean crust at one of the two critical ends of the spreading spectrum which, together with seafloor mapping, will permit a true three-dimensional view of the ocean crust. The suite of holes will also provide a true natural laboratory for downhole geophysical experiments, where hole to hole magnetotelluric and permeability experiments can be conducted, and which will provide a downhole seismic laboratory from which the nature of layer 3 may well be directly tested.

### **Tectonic Setting**

Site 735 is located in the rift mountains of the Southwest Indian Ridge, 18 km east of the present-day axis of the Atlantis II Transform Fault (Fig. 1). The Southwest Indian Ridge has existed since the initial breakup of Gondwanaland in the Mesozoic (e.g., Norton and Sclater, 1979). Shortly

before 80 Ma, plate readjustment in the Indian Ocean connected the newly formed Central Indian Ridge to the Southwest Indian Ridge and the Southeast Indian Ridge to form the Indian Ocean Triple Junction (Fisher and Sclater, 1983). Steady migration of the triple junction to the northeast has created a succession of new ridge segments and fracture zones including the Atlantis II. Thus, the Atlantis II Fracture Zone and the adjacent ocean crust is entirely oceanic in origin, free from complications due to continental breakup as postulated for some equatorial fracture zones along the Mid-Atlantic Ridge (e.g., Bonatti and Honnorez, 1976).

Over the last 34 m.y., the spreading rate along the Southwest Indian Ridge has been relatively constant, near 0.8 cm/yr, at the very slow end of the spreading-rate spectrum (Fisher and Sclater, 1983). All the characteristic features of slow-spreading ridges, including rough topography, deep rift valleys, and abundant exposures of plutonic and mantle rocks, are present on the Southwest Indian Ridge (Dick, 1989). Significantly, two thirds of the rocks dredged from the walls of the active transform valleys are altered mantle peridotites, whereas most of the remainder are weathered pillow basalts. This exceptional abundance of peridotite, compared to dredge collections of similar size from the North Atlantic suggests an unusually thin crustal section in the vicinity of Southwest Indian Ridge transforms. Moreover, the paucity of dredged gabbro along the Southwest Indian Ridge suggests that magma chambers were small or absent near fracture zones.

The thin crust adjacent to fracture zones is thought to reflect segmented magmatism along the Southwest Indian Ridge producing rapid along-strike changes in the structure and stratigraphy of the lower ocean crust (e.g., Whitehead et al., 1984; Francheteau and Ballard, 1983; Crane, 1985; Schouten et al., 1985; MacDonald, 1986). Such a model views the Southwest Indian Ridge as comprised of a series of regularly spaced, long-lived shield volcanoes and underlying magmatic centers, which undergo continuous extension to form the ocean crust (Dick, 1989). Site 735 is situated some 18 km from the Atlantis II Transform Fault, and was accordingly situated near the mid-point of a hypothetical magmatic center beneath the Southwest Indian Ridge at 11.5 Ma (Dick et al., 1991b).

### **Geology of the Atlantis II Fracture Zone**

Hole 735B is located on a shallow bank, informally named Atlantis Bank, on the crest of a 5-km-high mountain range constituting the eastern wall of the Atlantis II Transform valley. This transverse ridge is similar to many other flanking fracture zones on the Southwest Indian Ridge

(e.g., Engel and Fisher, 1975; Sclater et al., 1978, Fisher et al., 1986; Dick, 1989) where abundant plutonic rocks, particularly peridotite, are uplifted to a shallow level and exposed. The bank consists of a platform, roughly 9 km long in a north-south direction and 4 km wide, which is the shallowest of a series of uplifted blocks and connecting saddles that form a long, linear ridge parallel to the transform. The top of the platform is flat, with only about 100 m relief over 20 km<sup>2</sup>. A 200 x 200 m box video survey in the vicinity of the hole showed a smooth flat wave-cut platform exposing foliated and massive jointed gabbro locally covered by sediment drift. The platform probably formed by erosion of an island similar to St. Paul's Rocks in the central Atlantic, and then subsided to its present depth from normal lithospheric cooling (Dick et al., 1991b). A similar wave-cut platform occurs on the ridge flanking the DuToit Fracture Zone (Fisher et al., 1986).

The foliation seen in the video survey and at the top of the drill core appears to strike east-west, parallel to the ridge axis and orthogonal to the fracture zone. The orientation of similarly foliated peridotites exposed on St. Paul's Rocks has been measured and is also parallel to the Mid-Atlantic Ridge and orthogonal to St. Paul's Fracture Zone (Melson and Thompson, 1971). This foliation, projected along strike across the platform, intersects a long ridge coming up the wall of the fracture zone, which is oriented obliquely west-northwest to the transform. Ridges produced by land-slips and debris flows normally are oriented orthogonal to the fracture zone. The suspicion is then, that this oblique ridge, and a similar one 2 km to the north represent the trace of the thick zone of foliated gabbros down the wall of the transform. Given the once shallow water depth, the canyon between the two ridges may be erosional, and the foliated gneissic amphibolites resistant remnants. A three point solution for the dip of the shear zone, based on the trend of this ridge, and an east-west strike gives a dip of approximately 40°, close to that observed in the drilled amphibolites.

This shear zone represents a ductile-fault, and thus does not represent a simple stratigraphic discontinuity. The rocks at the top of the shear zone are gabbro-norites which pass gradually into a zone of olivine gabbro toward its base. The shear sense determined from drill cores is normal. Thus, it would appear that the rocks to the north of the drill site are down-thrown an unspecified amount. Any offset drill sites to the north then would start higher in the stratigraphic section

The site is located between magnetic anomalies 5 and 5a, approximately 93 km south of the present-day axis of the Southwest Indian Ridge and 18.4 km from the inferred axis of transform faulting on the floor of the Atlantis II Fracture Zone (Dick et al., 1991b). Given the position of the site, the

*...Leg 159 - Return to Hole 735B...*

relatively constant spreading direction over the last 11 m.y., and the ridge-parallel strike of the local foliation, the Atlantis Bank gabbros must have crystallized and deformed beneath the median valley of the Southwest Indian Ridge, 15 to 19 km from the ridge-transform intersection, around 11.5 Ma. A single 11.3 Ma Pb-zircon age reported by Stakes et al. (1991) for a trondhjemite in amphibolite near the top of the hole confirms the age determined by plate reconstruction.

The gabbros were subsequently uplifted in a large horst from beneath the rift valley 5 to 6 km up into the transverse ridge (Dick et al., 1991b). The single uniform magnetic inclination throughout the section, demonstrates that there has been no late tectonic disruption of the section, although the relatively steep inclination suggests block rotation of up to 18° (Pariso et al., 1991). Thus, unlike some rocks dredged from fracture-zone walls, those drilled in Hole 735B formed beneath the rift-valley floor away from the transform fault. They likely represent petrologically a typical igneous section of Southwest Indian Ridge ocean crust, with an intact metamorphic and tectonic stratigraphy recording brittle-ductile deformation and alteration at high temperatures beneath the rift valley as well as subsequent unroofing and emplacement on ridge-parallel faults.

The unroofing and exposure of the Hole 735 B section relates to the present-day asymmetric distribution of plutonic and volcanic rocks north and south of the ridge axis near the fracture zone, as well as to the striking physiographic contrast between crust spreading in opposite directions at the ridge-transform intersection (Fig. 2) (Dick et al., 1991b). These features suggest that a crustal weld periodically formed between the shallow levels of the ocean crust and the old, cold lithospheric plate at the ridge-transform intersection. This weld caused the shallow levels of the newly formed ocean crust to spread with the older plate away from the active transform, creating long-lived detachment faults beneath which the deep ocean crust spreading parallel to the transform was unroofed and emplaced up into the rift mountains to form a transverse ridge. A similar model was proposed by Dick et al. (1981) to explain the asymmetric physiography and distribution of plutonic and volcanic rocks at the Kane Fracture Zone in the North Atlantic. In the Kane Fracture Zone, the surface of the detachment fault has actually been observed by submersible (Dick et al., 1981; Mevel et al., 1991). Detachment faults similar to the one proposed to explain unroofing of the lower crust at the Atlantic Fracture Zone have been suggested to occur periodically within rift valleys by fault capture during amagmatic periods (Harper, 1985; Karson, 1991). Thus, the structures and fabrics seen in the Hole 735B core are likely to be representative of the kinds of fabrics generally found in lower crustal sections formed at slow-spreading ridges. It is true,

however, that due to the proximity to the transform, the extent of the ductile shear may be greater than elsewhere beneath the rift valley.

## SCIENTIFIC OBJECTIVES AND METHODOLOGY

### Summary of Objectives

- 1) To investigate the nature of magmatic, hydrothermal, and tectonic processes in the lower ocean crust at a slow-spreading ocean ridge.
- 2) To achieve a detailed sampling of the spatial and temporal variability of the lower crust by examining the extent of both brittle and ductile deformation in the lower ocean crust, the spacing, width and orientation of major and minor fault zones, and the state of internal stress of the lower ocean.
- 3) To establish a natural laboratory with the potential for future hole to hole magnetotelluric and permeability experiments and direct testing of the nature of layer 3.

### Specific Scientific Objectives and Methodology

The principle objective of Leg 159 will be to deepen Hole 735B to a depth of 2 km (Fig. 3). Leg 118 ended with Hole 735B cored to a depth of 500.7 mbsf, penetrating 0.5 m into a coarse-grained troctolite (Fig. 4). Based on the many fine-grained troctolite precursor micro-intrusions in the overlying olivine gabbro, it has been suggested that the coarse-grained troctolite represents the top of a third major intrusive body. The primitive composition and modal mineralogy of this body are similar to that seen in the primitive cumulates overlying the petrologic Moho in many ophiolites. Leg 159 will deepen the hole to confirm the presence of a large body of troctolite and then will drill deeper to determine if there are other intrusions below it. To date, no layered cumulates, as would be expected to form by magmatic sedimentation, have been found in the hole. If these are encountered deeper in the hole, then this would suggest, contrary to the Leg 118 results, that there was a significant long-lived magna chamber present. Only continued drilling can confirm the absence of such rocks in plutonic layer 3 here. An additional objective of Leg 159 will be to determine the spacing of major ductile shear zones. If the faults these represent are listric, then the inclination of the fault plane and the nature of the physical deformation should change with depth as

*...Leg 159 - Return to Hole 735B...*

the faults sole into the brittle-ductile transition. Extensive alteration in the amphibolite facies has been found in Hole 735B to date. A major objective is to define whether or not there is gradational alteration with depth. The existing section is too short to determine this, particularly given its heterogeneous nature. An important objective is to recover a full representation of the major igneous lithofacies to determine the nature and extent of the igneous processes which occurred during formation of the section.

While the exact level of Hole 735B in the lower crust cannot be determined with any accuracy, it is likely that it is fairly deep, and possibly within a short distance of the petrologic Moho. The vertical seismic profile conducted in the hole during Leg 118 showed coherent events at 560 and 760-825 mbsf. These were tentatively interpreted as reflections from the seismic Moho by Swift et al. (1991). A detailed gravity survey was conducted over the Atlantic II Fracture Zone with 13 parallel 300-km lines run at a 5-km spacing down the length of the transform and adjacent ridges (Dick et al., 1991b). These showed that the transverse ridge is isostatically unsupported and composed of high density material, ruling out an origin by serpentinite diapirism similar to other transverse ridges studied by gravity (e.g., Loudon and Forsyth, 1982). Moreover, individual gravity highs were situated over each of the major topographic highs along the ridge. Modeling the gravity field suggested that the structure of the ridge was heterogeneous, with topographic lows underlain by lower density material, and highs underlain by high density, with the gravity over the Atlantic Bank suggesting the presence of virtually no crustal component. The gravity data suggest that the mantle densities exist near the sea floor and that the crustal section drilled on the wave-cut platform is unlikely to extend to great depth (Fig. 5). In addition, troctolites, which were drilled at the bottom of Hole 735B, while they have been found as isolated intrusions at all levels in ophiolites, are generally abundant near the petrologic Moho.

The nature of the basal cumulates in the ocean crust is of fundamental importance to understanding magmatic processes, and the nature of primary magmas. It is widely believed that these rocks represent the first products of crystallization of the primary magmas as they migrate out of the mantle. As such, simple liquid-crystal partitioning and trace and major element modeling can be used to recover the composition of the primary liquids (e.g., Meyer et al., 1989). recent studies of the rare earth elements in abyssal peridotites suggest that the dominant process by which melts form in the mantle is fractional melting rather than batch equilibrium melting as was once widely supposed (Johnson et al., 1990). Mid-ocean ridge basalts, however, by themselves can be modeled equally well by batch equilibrium and fractional melting models.

A single deep penetration of plutonic layer 3 is a purely one-dimensional view, yet the last three decades of research at mid-ocean ridges, particularly at slow-spreading ocean ridges, leads to the conclusion that magmatic and tectonic processes there may be episodic on a variety of scales (Ballard and Van Andel, 1977; Karson et al., 1987; Pockalny et al., 1988; Severinghaus and MacDonald, 1988). Implicit to this is the concept that at the slow end of the spreading spectrum, magma chamber are ephemeral and of limited extent in time in space (e.g., Dick et al., 1991a; Sinton and Detrick, 1992). There are, however, no direct constraints whatsoever on this inference, which can only be done by obtaining an accurate two dimensional cross section of the lower crust along a lithospheric flow line.

In this respect, Hole 735B is unique. The wave-cut platform provides a horizontal section of the lower ocean crust some 7 km long and approximately 3.5 km across. Moreover, due to the results of Leg 118, we know that the rocks in this hole, which crossed through at least one major ductile fault, have the most uniform magnetic inclination of any crustal section ever drilled, giving direct evidence that the block preserves largely intact the internal tectonic-igneous and metamorphic stratigraphy of the ocean crust from the time at which it passed through its Curie point. This data also gives us an estimate of paleo-horizontal through the site (Fig. 3). Based on this information, phase two of investigations, to be conducted at some future date, should consist of a suite of 500 m drill holes which should represent a paleo-stratigraphic overlapping transect of crust generated over a 400,000 interval (defined by the spreading rate). While we do not know the lateral extent of the one dimensional stratigraphy determined from Hole 735B, this can be determined from the proposed drilling. Holes 735C and 735D, for example, both should drill into a crustal section stratigraphically overlying and overlapping with the upper portion of the section drilled in Hole 735B. Hole 735E, on the other hand, should largely overlap the upper 500 m of Hole 735B, while Hole 735F should drill a section stratigraphically immediately below the present depth of Hole 735B, but overlapping the section we propose to drill on Leg 159. It will be noted that the section we propose to drill contains at least one major ductile fault. While its orientation and dip are known from a combination of bottom TV survey and drilling, the throw on this fault is not known. While this is one of the objectives of drilling Hole 735D, it can be reasonably assumed that since this fault occurs within a major tectonic block along the transverse ridge, that the throw is not large. As we show it (note the offset of paleo-horizontal), the total throw is 200 m.

Thus, the proposed drilling would capitalize on the unique opportunity presented by the wave-cut terrace at the Atlantis Bank, to directly test the two-dimensional structure of the ocean crust. While

...Leg 159 - Return to Hole 735B...

wave-cut terraces exist along other great transverse ridges, such as the Vema, those accessible for drilling in the Atlantic are either capped by limestone, or have an entirely ambiguous spreading history, and thus the lithospheric section can not be related to its paleo-position along the ocean ridge where it was generated.

Given the highly three-dimensional structure believed to exist in the lower ocean crust beneath ocean ridges the proximity of the section to the mid-point or distal end of a magmatic cell is critical. A section drilled far from the mid-point of such a cell for example, may have a petrologic Moho where highly evolved ferrogabbros are intruded over residual mantle peridotite. Such a section would not resolve any of the major petrologic questions about the nature of primary magmas at ocean ridges, and would likely provide answers entirely parochial to the distal ends of spreading segments close to large offset fracture zones. A section generated near the mid-point of a magmatic cell, on the other hand, as we anticipate at Site 735 (Fig. 6), is likely to not only have a thicker plutonic section, and longer-lived more slowly cooled magma chambers, but is also likely to contain the products of crystallization of the most primitive melts erupted from the mantle as basal cumulates. Such a section would be far more diagnostic of the magmatic processes affecting the composition of mid-ocean ridge basalts within the crust. Moreover, residual mantle peridotites drilled beneath such a section are likely to record evidence of the mantle conduits through which melts flowed and the processes effecting melts at shallow depths in the mantle if current models for the focusing of melt flow out of the mantle toward the mid-points of ocean ridge segments are correct.

The section we propose at the Atlantis Bank, can be accurately placed due to the extremely good magnetic survey made by the *RV Conrad* along the walls and flanks of the fracture zone, to lie 18 km from the present and paleo-transform. Based on this, the section originally formed beneath the paleo-Southwest Indian Ridge at 11.5 Ma (Dick et al., 1991b) close to the mid-point of an average magmatic cell for this spreading rate (e.g., Schouten et al., 1985). This age and the paleomagnetic reconstruction have been confirmed by an 11.5-Ma U-Pb zircon age date (Stakes et al., 1991) on a trondhjemite vein from Hole 735B. This, as far as we know, is the only plate reconstruction so confirmed to date, and gives it an exceptionally high degree of reliability.

The objective of Leg 159 is not to directly test the composition of layer 3, a problem in seismic stratigraphy. At the present time, there is probably no suitable site know for offset drilling in the oceans where that problem can be directly addressed, requiring a site where a known seismic

stratigraphy can be traced into it from seismically "normal" ocean crust. By their nature, tectonically exposed sections of the lower ocean crust generally occur where the crustal topography and tectonics is too complex to do this. However, a long continuous section of lower crustal rocks, and documentation of the nature of the magmatic, tectonic and hydrothermal processes occurring therein, is of immeasurable value in trying to indirectly reconstruct the nature of layer 3 in the oceans and the reflectors therein, and is thus invaluable in constraining new models for its nature and origin.

### *Tectonic Objectives*

The rocks cored on Leg 118 showed a remarkable structural geology, with both hydrothermal alteration and late magmatic processes uniquely controlled by brittle-ductile deformation. The rocks recovered included 100 m of amphibolites from a brittle-ductile shear zone representing a ductile fault believed to have formed beneath the rift valley of the Southwest Indian Ridge, as well as rocks deformed by shear while the gabbros were still partially molten. The drilled section provided us with the first look at tectonic processes within an in-situ section of ocean crust. Moreover it was shown that alteration of the entire section was tectonically enhanced. The strong interrelationship of deformation and igneous and metamorphic process is unique in many ways to the mid-ocean ridges. During Leg 159, we will examine the extent of both brittle and ductile deformation in the lower ocean crust, the spacing, width and orientation of major and minor fault zones, and the state of internal stress of the lower ocean

Hole 735D is situated in such a way that it should pass through the ductile fault encountered at the top of Hole 735B if the fault is listric, which would be expected from the block rotation postulated from the magnetic study of the core, or drill into the top of it if the fault plane remains at a constant angle with depth. Moreover, as the stratigraphy immediately below the footwall of the fault was drilled during Leg 118, we may be able to determine the total throw on the fault when we have recovered a stratigraphic section from above the hanging wall in Hole 735D. The orientation and nature of the major fault planes bounding mid-ocean ridge rift valleys at depth is a major question, which this program will directly address.

The formation of transverse ridges has been the subject of great speculation (Severinghaus and MacDonald, 1988). These ridges consist of a series of connected tectonic blocks generated by block uplift at the inside-corner highs of the great fracture zones where the active transform valley

intersects the active rift valley. For whatever reason, it has been now widely documented that at these intersections the crust is periodically unroofed and uplifted as much as 6 km. The Atlantis Bank is one such tectonic block. Drilling within the block may tell us little of the uplift process, however, as the actual displacements which occurred in the crust at the level of the rocks we propose to drill were largely confined to the faults bounding the block. The geologic structures drilled may have been influenced by this process, as these faults are likely to form and root within the brittle-ductile transition zone beneath the rift valley. As a result the extent of brittle-ductile deformation may be enhanced. Nonetheless, similar faulting is postulated to occur beneath slow-spreading rift valleys far from transforms as well (e.g., Karson et al., 1987), and the presence of such faults has also been inferred seismically (Toomey et al., 1988). Thus, while the degree of ductile faulting and alteration found in the proposed drilling transect may be accentuated compared to ocean crust further from a transform, the processes involved are likely to be the same, and most conclusions drawn from the drilling are likely to be valid for the ocean crust formed at slow-spreading ridges as a whole.

### **DRILLING PLAN/STRATEGY**

Hole 735B is unique in the history of crustal drilling in the oceans in that it is the only hole in which drilling conditions continuously improved with depth. At the end of Leg 118, when operations were discontinued for logging, it was being drilled at a rate of 60 m/day with 100% recovery. The hole was left open with no evidence of any significant breakouts or rubble, and no junk due to drilling mishaps. No bits were destroyed or even seriously damaged during drilling, and the average bit retrieved could have been rerun in the hole.

A major operational consideration is the shallow water depth at the site. Situated in only 700 m of water, drilling operations are extremely easy. The superb drilling conditions at the site can be attributed to its location in the center of a large keystone horst block on the crest of the transverse ridge, and its emplacement from the zone of ductile and brittle ductile deformation due to detachment faulting directly into the zone of block uplift at the inside-corner high of the ridge-transform intersection (Fig. 2). As a consequence, the section did not pass through a zone of brittle extensional tectonics at the ridge axis, which would have created extensive fracturing and the formation of rubble. This latter process, is reasonably the cause of most of the drilling problems encountered in the pillow lava and sheeted dike sections drilled at slow-spreading ridges to date. Moreover, the medium to coarse grained gabbros have large individual mineral grains with well

defined cleavage planes and significant stored internal thermal strain. These rocks proved, unlike fine to very fine-grained basalts and diabases in Hole 504B, to be uniquely suited to rotary drilling, as each mineral grain has sufficient stored elastic strain, that they shatter under percussion drilling. During Leg 140 at Hole 504B, drilling conditions and recovery both correlated positively with grain size in the recovered core (Dick, Erzinger, Stokking, et al., 1992).

It is reasonable to assume that drilling conditions will remain roughly constant from the holes present depth until thermal problems occur, or when serpentinitized peridotite is encountered. While the depth at which the latter will occur is difficult to predict, thermal problems would not reasonably be expected until about 2000 m sub-basement, based on experience at Hole 504B where the present temperature is now close to 190°C. Conditions in drilling serpentinite at Hole 670 in the MARK area and Galicia Margin also have proved to be good, and thus, even if encountered, serpentinite should pose no problems, though it could slow drilling.

The present temperature at the bottom of the hole is 11°C, with a very low gradient, which appears to be increasing with depth. An accurate projection of temperature with depth below the hole, therefore, is difficult, but will almost certainly be lower than that of Hole 504B at a given depth (R.P. Von Herzen, pers. comm.).

Based on the hypothesis that brittle fracture and brecciation decrease with depth in plutonic layer 3 due to the steep geotherm beneath an ocean ridge, and that fine-grained rocks are unlikely to be encountered lower in the section, it is reasonable to suspect that the overall penetration rate would remain close to that for Leg 118. Five hundred meters were drilled at Hole 735B in 19 days, including setting a guide base and starting with the mud motor rather than the top drive, and using minimum bit weights and extreme conservatism. With virtually no wear on the bits and improved bit design, Leg 159 should have markedly longer bit life which should more than make up for increased trip time as the hole is deepened.

During Leg 159, Hole 735B will be deepened to 2 km depth or until drilling conditions force the hole to be abandoned. Following this, we will offset 800 m due south and spud in a second hole, Hole 735C, in crust 100,000 years older, and drill to 500 m. Given the paleomagnetic evidence from Hole 735B that the section is back tilted 18° (Pariso et al., 1991), it is believed that this would drill into rocks representing part of the upper missing section at Hole 735B, possibly intersecting the upper levels of the gabbro norite and about 250 m of the underlying olivine gabbro previously

*...Leg 159 - Return to Hole 735B...*

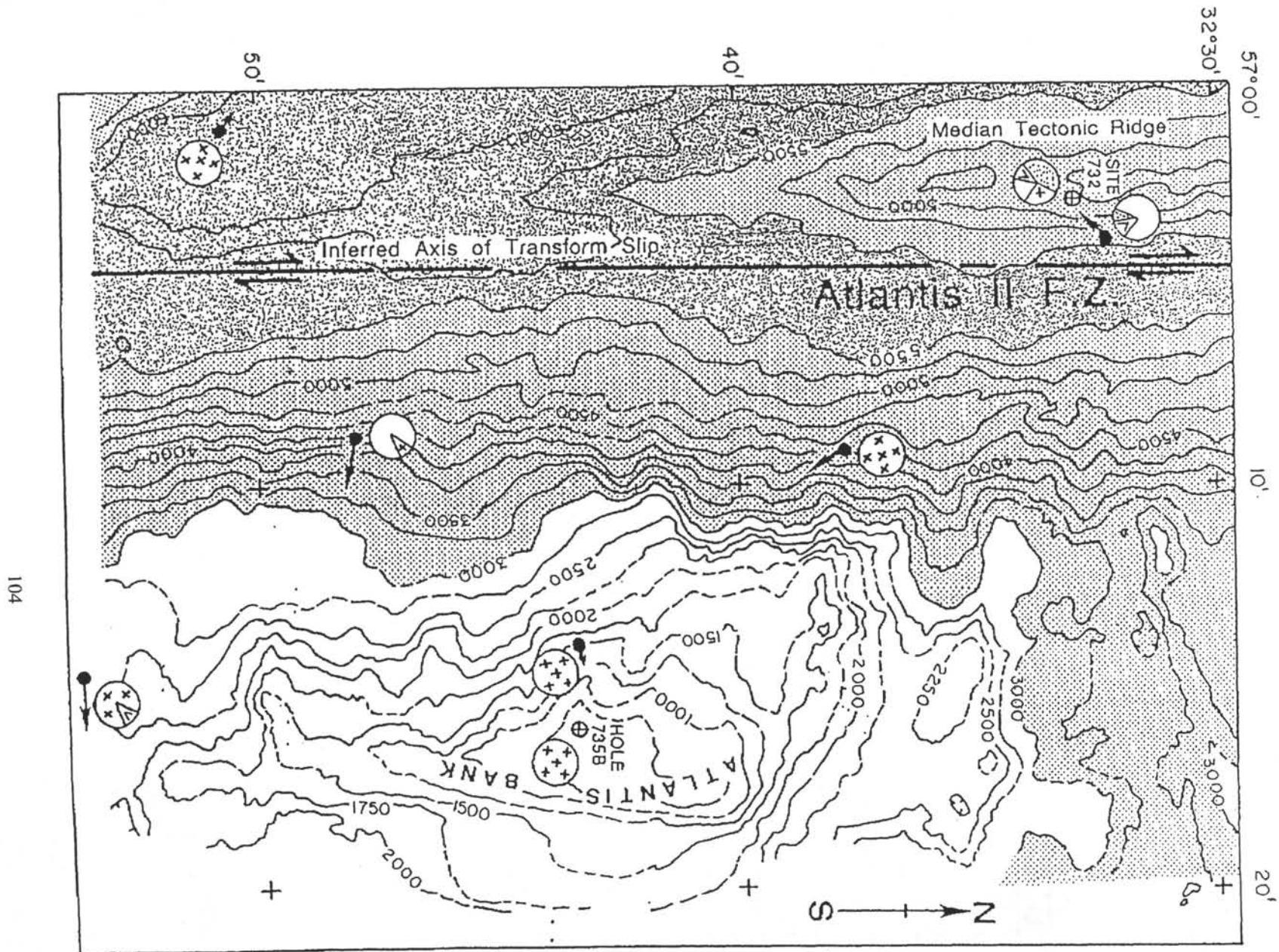
drilled, provided that these intrusions extend this far south. Logging of hole would be deferred to a future program. Leg 159 is devoted entirely to drilling except for logging the temperature profile in Hole 735B prior to disturbing the hole with additional drilling. Hole 735C will be drilled if time permits. A future program would re-occupy Hole 735B and deepen it to 2 km if that depth had not been reached on Leg 159, or re-occupy or spud in Hole 735C if the latter had not reached its target depth of 500 m. Drilling, logging and geophysical downhole experiments would then be conducted at Holes 735D, 735E, and 735F.

## REFERENCES

- Aumento, F., Loncarevic, B.D., and Ross, D.I., 1971.** Hudson Geotraverse: Geology of the MidAtlantic Ridge at 45°N. *Philos. Trans. R. Soc. London (A)*, 268:623-650.
- Ballard, R.D., and Van Andel, Tj.H., 1977.** Project FAMOUS: Morphology and tectonics of the inner-rift valley at 36°50'N on the Mid-Atlantic Ridge. *Geol. Soc. Am. Bull.*, 88:507-530.
- Bonatti, E., and Honnorez, J., 1976.** Sections of the Earth's crust in the equatorial Atlantic. *J. Geophys. Res.*, 81:4104-4116.
- Cann, J.P., 1970.** New model for the structure of the ocean crust. *Nature*, 226:928-930.
- Cannat, M., Bideau, D., and Bougault, H., 1992.** Serpentinized peridotites and gabbros in the Mid-Atlantic Ridge axial valley at 15°37'N and 16°52'N. *Earth Planet. Sci. Lett.*, 109:87-106.
- Cannat, M., Mevel, C., and Stakes, D., 1991.** Normal ductile shear zones at an oceanic spreading ridge: tectonic evolution of Site 735 gabbros (southwest Indian Ocean). In Von Herzen, R.P., and Robinson, P.T., et al., *Proc. ODP, Sci. Results*, 118: College Station, TX (Ocean Drilling Program), 415-431.
- Christensen, N.I., 1972.** The abundance of serpentinites in the oceanic crust. *J. Geol.*, 80:709-719.
- Crane, K., 1985.** The spacing of rift axis highs: dependence upon diapiric processes in the underlying asthenosphere? *Earth Planet. Sci. Lett.*, 72: 405-414.
- Dick, H.J.B., 1989.** Abyssal peridotites, very-slow spreading ridges and ocean ridge magmatism. In Saunders, A.D., and Norry, M.J., (Eds.), *Magmatism in the ocean basins*. Spec. Publ. - Geol. Soc. London, 42: 71-105.
- Dick, H.J.B., Bryan, W.B., and Thompson, G., 1981.** Low-angle faulting and steady-state emplacement of plutonic rocks at ridge-transform intersections. *Eos*, 62:406.
- Dick, H.J.B., Erzinger, J., Stokking, L.B., et al., 1992.** *Proc. ODP, Init. Repts.*, 140: College Station, TX (Ocean Drilling Program).
- Dick, H.J.B., Meyer, P.S., Bloomer, S., Kirby, S., Stakes, D., and Mawer, C., 1991a.** Lithostratigraphic evolution of an in-situ section of oceanic layer 3. In Von Herzen, R. P., and Robinson, P.T., et al., *Proc. ODP, Sci. Results*, 118: College Station, TX (Ocean Drilling Program), 439-538.
- Dick, H.J.B., Schouten, H., Meyer, P.S., Gallo, D.G., Bergh, H., Tyce, R., Patriat, P., Johnson, K.T.M., Snow, J, and Fisher, A., 1991b.** Tectonic evolution of the Atlantis II Fracture Zone. In Von Herzen, R. P., and Robinson, P.T., et al., *Proc. ODP, Sci. Results*, 118: College Station, TX (Ocean Drilling Program), 359- 398.
- Engel, C, G., and Fisher, R.L., 1975.** Granitic to ultramafic rock complexes of the Indian Ocean ridge system, western Indian Ocean. *Geol. Soc. Am. Bull.*, 86:1553-1578.
- Fisher, R. L., Dick, H.J.B., Natland, J.H., Meyer, P.S., 1986.** Mafic/ultramafic suites of the slowly spreading SW Indian Ridge: PROTEA exploration of the Antarctic plate boundary, 24°E - 47°E. *Ofioliti*, 11:141-178.
- Fisher, R.L., and Sclater, J.G., 1983.** Tectonic evolution of the Southwest Indian Ocean since the Mid-Cretaceous: plate motions and stability of the pole of Antarctica/Africa for at least 80 myr. *Geophys. J. R. Astron. Soc.*, 73:553-576.
- Francheteau, J., and Ballard, R.D., 1983.** The East Pacific Rise near 21°N, 13°N, and 20°S: Inferences for along-strike variability of axial processes of the mid-ocean ridge. *Earth Planet. Sci. Lett.*, 64:93-116.
- Harper, G.D., 1985.** Tectonics of slow spreading mid-ocean ridges and consequences of a variable depth to the brittle-ductile transition. *Tectonics*, 4:395-409.
- Hess, H.H., 1962.** The history of the ocean basins. In Engel, A.E. J., James, H.L., and Lenord, B.F., (Eds.), *Petrological Studies: A volume in honor of A.F. Budding*, 599-620.
- Johnson, K.T.M., Dick, H.J.B., and Shimizu, N., 1990.** Melting in the oceanic upper mantle: an ion microprobe study of diopside in abyssal peridotites. *J. Geophys. Res.*, 95:2661-2678.

- Karson, J.A., 1991.** Accommodation zones and transfer faults: Integral components of Mid-Atlantic Ridge extensional systems. In Peters, Tj., Nicolas, A., and Coleman, R.G. (Eds.), *Ophiolites Genesis and Evolution of Oceanic Lithosphere*, 21-37.
- Karson, J. A., Thompson, G., Humphris, S.E., Edmond, J.M., Bryan, W.B., Brown, J.R., Winters, A.T., Pockalny, R.A., Casey, J.F., Campbell, A.C., Klinkhammer, G., Palmer, M.R., Kinzler, R.J., and Sulanowska, M.M., 1987.** Along-axis variations in seafloor spreading in the MARK area. *Nature*, 328:681-685.
- Louden, K.E., and Forsyth, D.W., 1982.** Crustal structure and isostatic compensation near the Kane Fracture Zone from topography and gravity measurements: I - Spectral analysis approach. *Geophys. J. R. Astron. Soc.*, 68:725-750.
- MacDonald, K.C., Castillo, D.A., Miller, S.P., Fox, P.J., Kastens, K.A., and Bonatti, E., 1986.** Deep tow studies of the Vema Fracture Zone 1. Tectonics of a major slow slipping transform fault and its intersection with the Mid-Atlantic Ridge. *J. Geophys. Res.*, 91:3334-3354.
- McCarthy, J., Mutter, J.C., Morton, J.L., Sleep, N.H., and Thompson, G.A., 1988.** Relic magma chamber structures preserved within the Mesozoic North Atlantic crust. *Geol. Soc. Am. Bull.*, 100:1423-1436.
- Melson, W.G., and Thompson, G., 1971.** Layered basic complex in oceanic crust, Romanche Fracture, equatorial Atlantic Ocean. *Science*, 168:817-820.
- Mevel, C., Cannat, M., Gente, P., Marion, E., Auzende, J.M., and Karson, J.A., 1991.** Emplacement of deep crustal and mantle rocks on the west wall of the MARK area (Mid-Atlantic Ridge, 23°N). *Tectonophysics*, 190:31-53.
- Meyer, P.S., Dick, H.J.B., and Thompson, G., 1989.** Cumulate gabbros from the Southwest Indian Ridge, 54°S- 17°16'E: Implications for magmatic processes at a slow spreading ridge. *Contrib. Mineral. Petrol.*, 103:44-63.
- NAT Study Group, 1985.** North Atlantic Transect - a wide aperture, two-ship Multichannel seismic investigation of the oceanic crust. *J. Geophys. Res.*, 90:10321-10341.
- Mutter, J.C., and North Atlantic Transect Study Group, 1985.** Multichannel seismic images of the oceanic crust's internal structure: evidence for a magma chamber beneath the Mesozoic Mid-Atlantic Ridge. *Geology*, 13:629-632.
- Norton, I.O., and Sclater, J.G., 1979.** A model for the evolution of the Indian Ocean and the breakup of Gondwanaland. *J. Geophys. Res.*, 84:6803-6830.
- Pariso, J.E., Scott, J.H., Kikawa, E., and Johnson, H.P., 1991.** A magnetic logging study of Hole 735B gabbros at the Southwest Indian Ridge. In Von Herzen, R. P., and Robinson, P.T., et al., *Proc. ODP, Sci. Results*, 118: College Station, TX (Ocean Drilling Program), 309-321.
- Pockalny, R.A., Detrick, R.S., and Fox, P.J., 1988.** The morphology and tectonics of the Kane Transform from SeaBeam bathymetric data. *J. Geophys. Res.*, 93:3179-3194.
- Rona, P.A., Widenfalk, L., and Bostrum, K., 1987.** Serpentinized ultramafics and hydrothermal activity at the Mid-Atlantic Ridge crest near 15°N. *J. Geophys. Res.*, 92:1417-1427.
- Schouten, H., Dick, H.J.B., and Klitgord, K.D., 1987.** Migration of mid-ocean ridge volcanic segments. *Nature*, 326:835-839.
- Schouten, H., Klitgord, K.D., and Whitehead, J.A., 1985.** Segmentation of mid-ocean ridges. *Nature*, 317:225-229.
- Scientific Party, 1989.** Site 735. In Robinson, P.T., Von Herzen, R.P., et al., *Proc. ODP, Init. Repts.*, 118: College Station, TX (Ocean Drilling Program), 89-212.
- Sclater, J.G., Dick, H.J.B., Norton, I.O., and Woodroffe, D., 1978.** Tectonic structure and petrology of the Antarctic plate boundary near the Bouvet Triple Junction. *Earth Planet. Sci. Lett.*, 37:393-400.
- Severinghaus, J.P., and MacDonald, K.C., 1988.** High inside corners at ridge transform intersections. *Mar. Geophys. Res.*, 9:357-367.
- Sinton, J.M., and Detrick, R.S., 1992.** Mid-ocean ridge magma chambers. *J. Geophys. Res.*, 97:197-216.

- Stakes, D., Mevel, C., Cannat, M., and Chaput, T., 1991.** Metamorphic stratigraphy of Hole 735B. *In* Von Herzen, R.P., and Robinson, P.T., et al., *Proc. ODP, Sci. Results*, 118: College Station, TX (Ocean Drilling Program), 153-180.
- Swift, S.A., Hoskins, H., and Stephen, R.A., 1991.** Seismic stratigraphy in a transverse ridge, Atlantis II Fracture Zone. *In* Von Herzen, R.P., and Robinson, P.T., et al., *Proc. ODP, Sci. Results*, 118: College Station, TX (Ocean Drilling Program), 219-226.
- Toomey, D.R., Solomon, S.C., and Purdy, G.M., 1988.** Microearthquakes beneath the median valley of the Mid-Atlantic Ridge near 23°N: Tomography and tectonics. *J. Geophys. Res.*, 93:9093-9112.
- Whitehead, J.A., Dick, H.J.B., and Schouten, H., 1984.** A mechanism for magmatic accretion under spreading centers. *Nature*, 312:146-148



104

**Figure 1.** Hand-contoured bathymetric map of the eastern transverse ridge, showing the location of Site 732 and Hole 735B. SeaBeam tracks hand-shifted by eye to eliminate conflicts in the data. Solid lines indicate actual data, while hatched lines show inferred contours. Contour interval is 250 m. Solid dots and arrows indicate the starting point and approximate track of dredge hauls. Filled circles indicate the approximate proportions of rock types recovered in each dredge - white = altered gabbro; + = gabbro; V = basalt and diabase, stippled = greenstone.

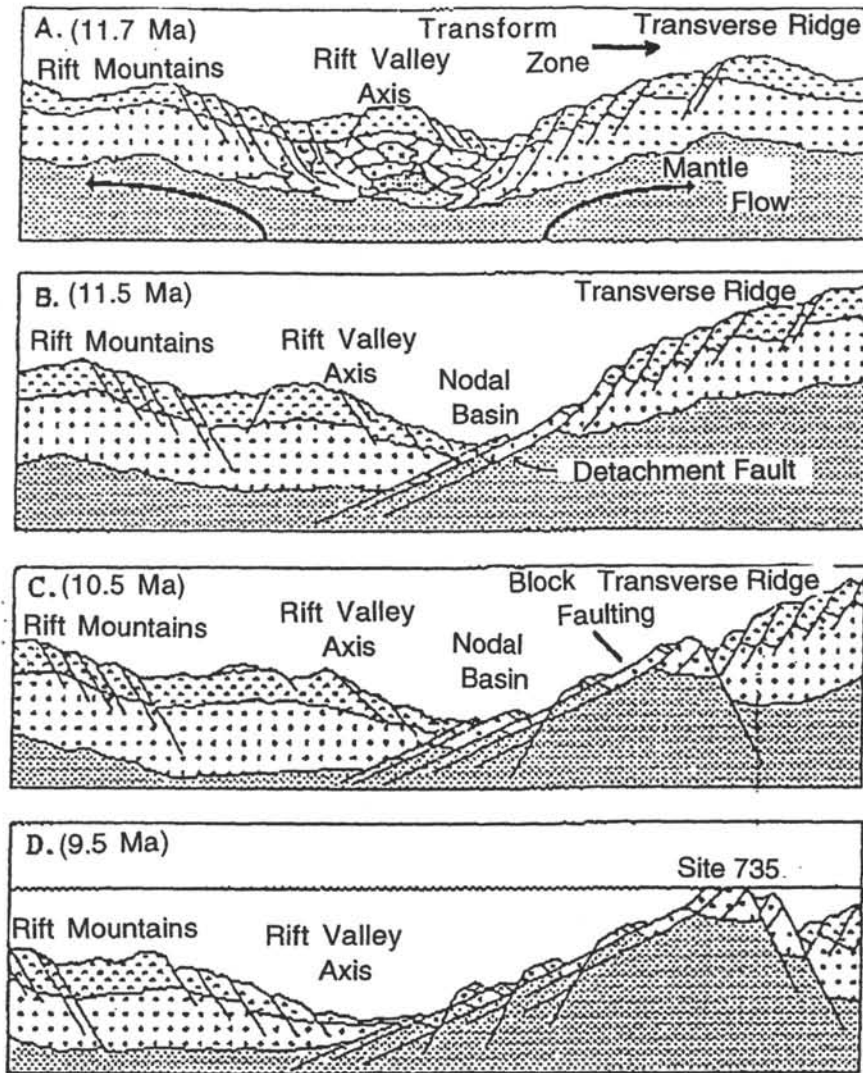


**Figure 2.** Temporal cross sections across the Southwest Indian Ridge rift valley drawn parallel to the spreading direction (not across the fracture zone, but parallel to it), showing the postulated tectonic evolution of the transverse ridge and Hole 735B (Dick et al., 1991). The sequential sections are drawn at about 18 km from the transform fault. Crust spreading to the right passes into the transverse ridge and spreads parallel to the transform valley. Crust spreading to the left spreads into the rift mountains of the Southwest Indian Ridge parallel to the inactive extension of the Atlantis II Fracture Zone.

A. Initial symmetric spreading, possibly at the end of a magmatic pulse. Late magmatic brittle-ductile deformation occurs because of lithospheric necking above (and in the vicinity of whatever passes for a magma chamber at these spreading rates). Hydrothermal alteration at high temperatures accompanies necking and ductile flow in subsolidus regions.

B. At some point, the shallow crust is welded to the old, cold lithosphere to which the ridge axis abuts, causing formation of a detachment fault, and nodal basin, initiation of low-angle faulting, continued brittle-ductile faulting, and amphibolite-facies alteration of rocks drilled at Hole 735B.

C and D. Block uplift of the rift mountains at the ridge-transform corner forms a transverse ridge enhanced by regional isostatic compensation of the local negative mass anomaly at the nodal basin. Initiation of the block uplift terminates the extension driving cracking, and drastically reduces permeability in the Hole 735B rocks, effectively terminating most circulation of seawater and alteration. Greenschist-facies retrograde alteration continues along the faults on which the block is uplifted to account for the greenschist-facies alteration that predominates in dredged gabbros.

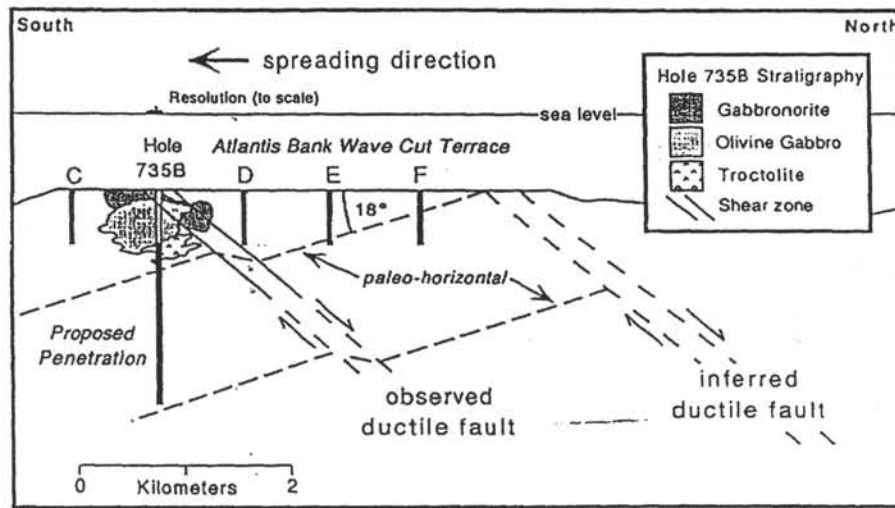
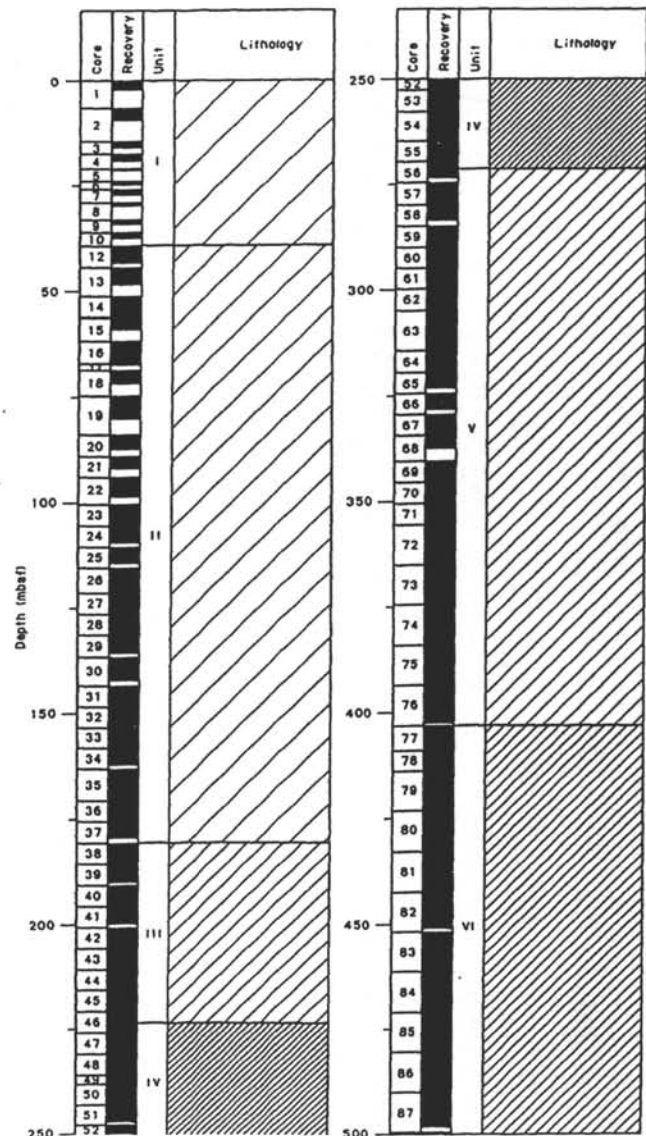


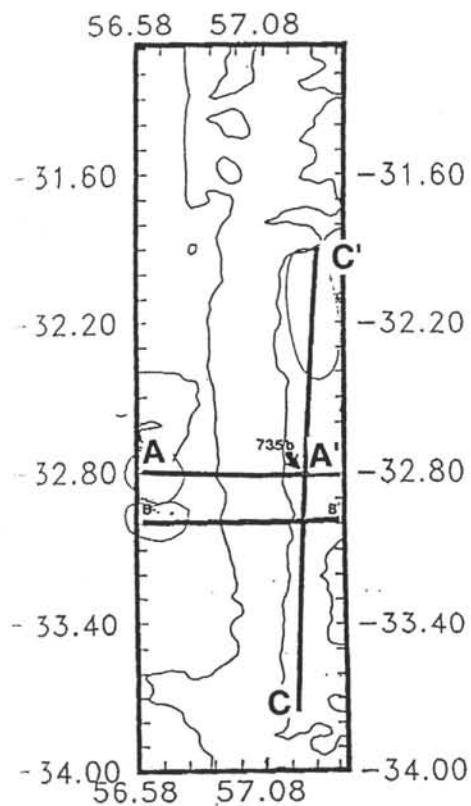
**Figure 3.** Cross section along a lithospheric flow line over the wave-cut platform at Hole 735B, showing the proposed Leg 159 deepening of the hole and drilling transect (no vertical exaggeration). At the observed spreading rate of 0.8 cm/yr, the proposed 800 m offset of the holes equates to 100,000 year spreading increments. Simplified stratigraphy based on Leg 118 lithostratigraphy (Scientific party, 1989; Dick et al., 1991). The inferred ductile fault is based on the bathymetry which suggests the presence of such a structure. The paleo-horizontal is inferred on the basis of the rock rotation needed to explain the deviation of the observed magnetic inclination of 70° from the predicted 52° (Pariso et al., 1991).

**Figure 4.** Basement lithostratigraphy of Hole 735B (Leg 118).

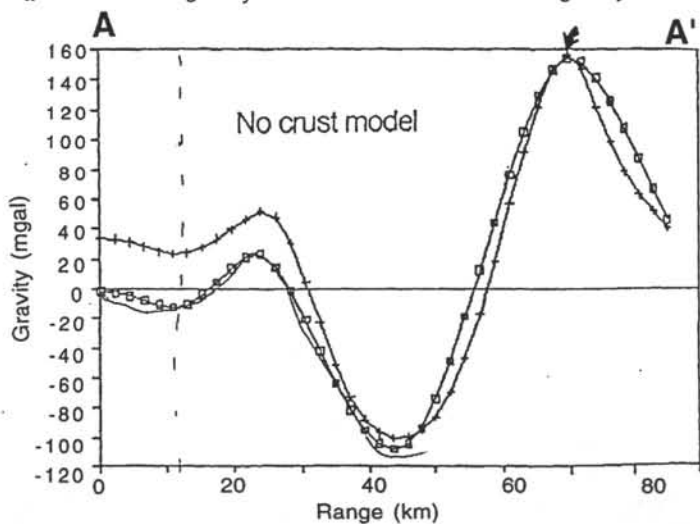
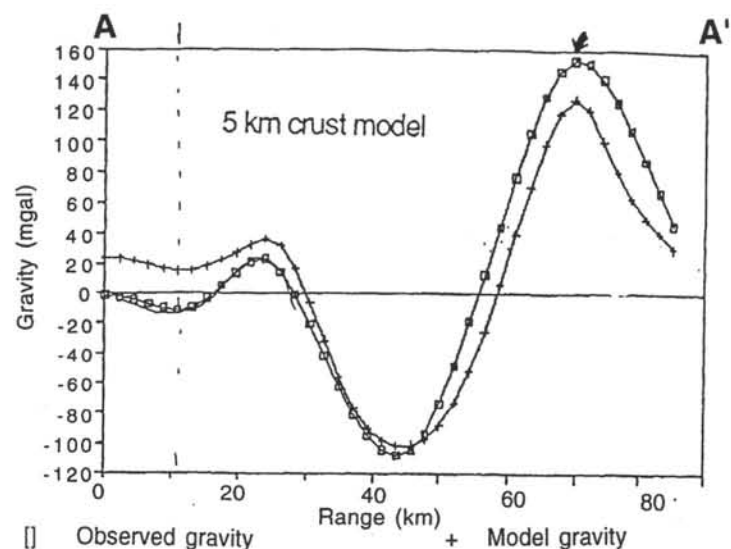
-  Foliated metagabbro
-  Olivine-bearing and olivine gabbro
-  Olivine gabbro
-  Iron-titanium oxide-rich gabbro
-  Olivine-rich gabbro and troctolite



Atlantis II Fracture Zone, profile across 735b.



Atlantis II Fracture Zone, 3800m isobath.



Atlantis II Fracture Zone, Long Profile

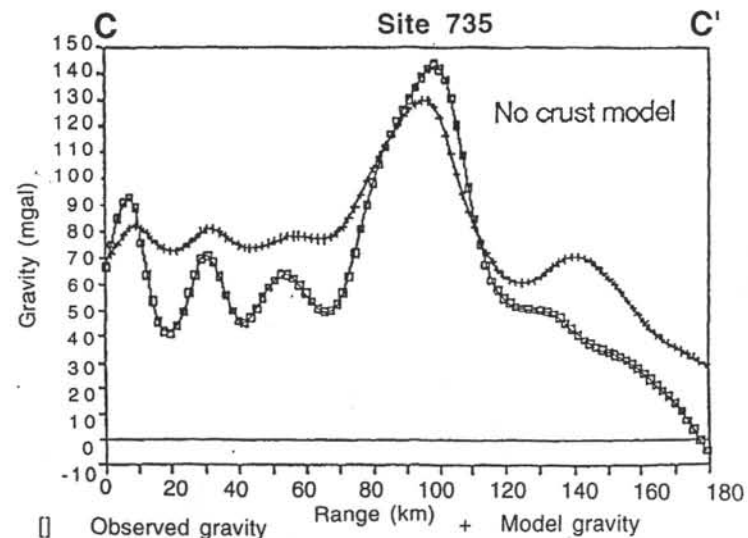
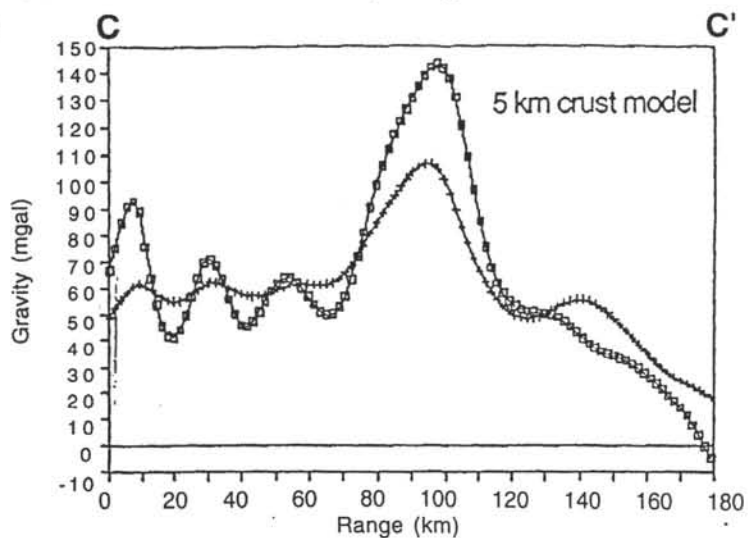


**Figure 5.** Observed and model gravity profile along a lithospheric flow line down the eastern transverse ridge flanking the Atlantis II Fracture Zone and across the transform. The line passes directly over Hole 735B,m as shown, where there is the largest anomaly found anywhere along the ridge. Note that the topographic highs correspond to gravity highs and the topographic lows to gravity lows (counter-intuitive). This agrees with tectonic modeling showing that the walls of inside-corner highs expose deep crustal rocks including gabbro and mantle peridotites, and clearly demonstrates that such highs are not the product of serpentinite diapirism (Dick et al., 1991; Snow et al., in prep.). Curves passing through boxes are the observed gravity field, while curves passing through +’s are the model gravity fields for 5 km and 0 km thick crustal models, respectively.

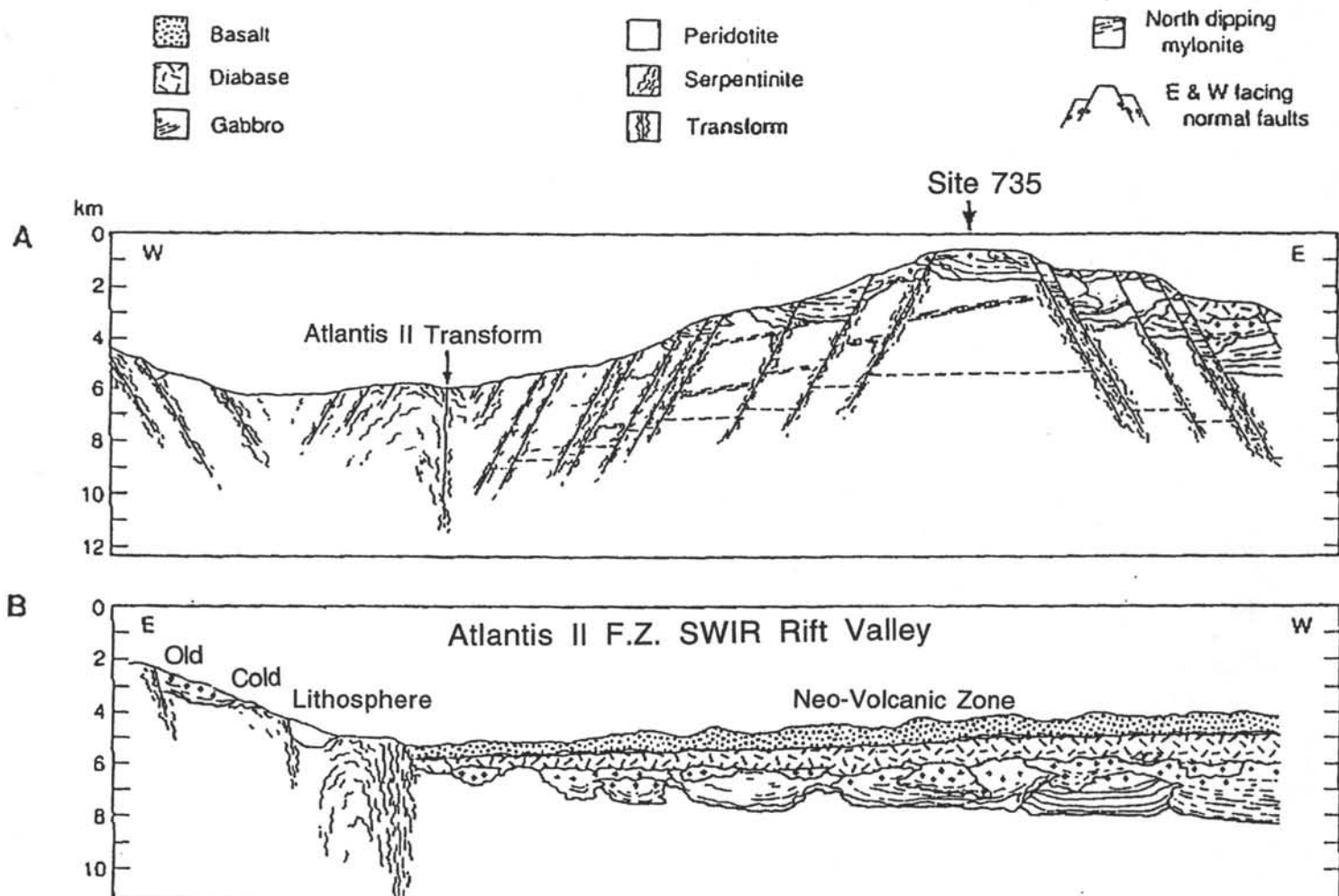


**Figure 6.**

A. Balanced cross section across the Atlantic II transform valley and through Site 735 and the Atlantic Bank showing the interpreted structure as an axial horst situated parallel to the transform valley (from Dick et al., 1991). The geology is based on SeaBeam bathymetry, the distribution of lithologies dredged along the walls of the fracture zone in its vicinity, the televiewer survey at Site 735 and the drilling results at Hole 735B.

B. Restored cross-section based on the topography of the present day Southwest Indian Ridge Rift Valley (southern rift). Faults are inferred on the basis of the location of benches along the walls of the transform. Fault dips are arbitrarily drawn as the drilling encountered no high-angle faults (which would be anticipated from Hole 735B's location near the center of a keystone horst block).

**TABLE 1**  
**PROPOSED SITE INFORMATION**  
**and**  
**DRILLING STRATEGY**

<b>SITE:</b> 735	<b>PRIORITY:</b> 1	<b>POSITION:</b> 57°16.0'E, 32°43.4'S
<b>WATER DEPTH:</b> 700m	<b>SEDIMENT THICKNESS:</b> 0 m	<b>TOTAL PENETRATION:</b> 2000m
<b>SEISMIC COVERAGE:</b> OPD Leg 118 Site 735		

**Objectives:** To drill a 2 km section of plutonic layer 3 starting at the present 500 m depth of Hole 735B. The drilled hole will be used as part of the deep crustal natural laboratory for downhole experiments. Potential Holes 735 C, 735D, 735 E, and 735F lie along a traverse spaced 800 m apart and colinear with Hole 735B and will provide a two-dimensional section of seismic layer 3 which, through downhole experiments, can be used to test the nature of that layer and to provide a detailed sampling of the temporal and spatial variability of the lower crust.

**Drilling Program:** RCB coring to 2000 m in Hole 735B and 500 m in Holes 735C, 735D, 735E, and 735F.

**Logging and Downhole Operations:** Heat flow and standard suite from bottom of present Hole 735B. Standard suite in Holes 735C, 735D, 735E, and 735F and ongoing detailed downhole experiments.

**Nature of Rock Anticipated:** Gabbro and peridotite.

*LEG 160*

*Eastern Equatorial  
Atlantic Transform*

## **LEG 160**

### **THE CÔTE D'IVOIRE-GHANA TRANSFORM MARGIN (EASTERN EQUATORIAL ATLANTIC)**

---

**Modified From Proposal 346 Submitted By**

**Jean Mascle, Christophe Basile, Roger Scrutton, Michel Moullade, and Carolyn Ruppel**

**To Be Named: Co-Chief Scientists and Staff Scientist**

---

#### **ABSTRACT**

Proposals for scientific drilling of transform continental margins have recently received increased attention for two main reasons. Firstly, transform faults represent the third category of major plate boundaries, but are still less understood than the two other major plate boundaries, divergent and convergent. Among transform faults, transform continental margins are still poorly known, and have never been investigated by the potentialities of scientific drilling. Secondly, drilling at a transform margin can constrain the structure and evolution of the ocean-continent transform boundary, particularly deformational history, vertical movements and its effects on the sedimentary records.

The Côte d'Ivoire-Ghana (ICG) Margin in the eastern equatorial Atlantic is considered as one of the best known examples of a transform boundary between continental and oceanic crust. The margin has been created by major transform motion between plate boundaries. This motion is still active today along the Romanche Fracture Zone. Since its creation, the ICG Margin has not experienced any major regional tectonic disruption, and its present day sedimentary and tectonic features are directly inherited from its Cretaceous transform margin history.

Drilling on the ICG Margin will document 1) the relationship between deformation and sedimentation and the development of the transform margin, 2) the nature, structure and deformation history of this transform boundary, and 3) the history of the oceanic gateways between the Central and South Atlantic during the opening of the Equatorial Atlantic, particularly in Cretaceous times.

## INTRODUCTION

The concept of a transform (or sheared/translational) continental margin as a specific type of continent-ocean boundary progressively developed since the 1970s. Geophysical results from several transform margins clearly demonstrate that these margins are drastically different from divergent margins, on the basis of crustal structure, deformation, subsidence and sedimentation history.

Within the past 10 years, several marine geophysical cruises (mainly gravimetry, refraction, and reflection seismic profiling) have been devoted to a few important transform margins, namely a) Agulhas Margin and its conjugate the Falkland Margin (Ewing et al., 1971; Emery et al., 1975; Scrutton, 1976, 1979, 1982; Lorenzo and Mutter, 1989), b) southern Newfoundland Margin (Hayworth and Keen, 1979; Todd et al., 1988; Keen et al., 1990), c) southern margin of the Exmouth Plateau (Lorenzo et al., 1991), d) Spitzbergen Margin (Lowell, 1972; Eldholm and Talwani, 1982; Eldholm et al., 1987), and e) equatorial African transform margins (Fail et al., 1970; Arens et al., 1971; Machens, 1973; Delteil et al., 1974; Emery et al., 1975; Mascle, 1976; Klingebiel, 1976; Blarez, 1986; Blarez et al., 1987; Mascle and Blarez, 1987; Mascle et al., 1988; Mascle, Auroux et al., 1989; Basile, 1990; Basile et al., 1992; Mascle et al., 1993; Basile et al., 1993) and their conjugate, the northern Brazilian Margin (Ponte and Asmus, 1978; Zalan et al., 1985; Costa et al., 1990). Scientific drilling was conducted during DSDP Leg 36 (Barker, Dalziel, et al., 1976) and ODP Leg 114 (Ciesielski, Kristofferson, et al., 1988) in the Falkland area and ODP Leg 122 in the Exmouth Plateau (Haq, von Rad, O'Connell, et al., 1990).

From these results, three main morpho-structural features of transform margin (e.g., The Côte d'Ivoire-Ghana (ICG) Transform Margin, Fig. 1A, 1B, 1C) can be recognized, namely the existence of a) lateral structural continuity between a major oceanic fracture zone and a continental transform margin (the Romanche Fracture Zone and ICG Margin), b) a very steep and narrow continental slope (20-30 km) between a continental shelf and an adjacent oceanic abyssal plain, indicating a very sharp crustal transition between thick or partially thinned continental crust and oceanic lithosphere, and c) a morphologically well expressed marginal ridge, bounding the transform margin, along an adjacent extensional basin (Côte d'Ivoire Basin).

All these features result from a translational stress acting between two continents along active transform faults. During rifting and opening, such evolution can be schematized into three main stages (Fig. 2) (Mascle and Blarez, 1987).

Stage 1 - An intra-continental active transform fault (stage A on Fig. 2). This results in a contact between two thick continental plates of variable thicknesses. In this case, the transform boundary of the extensional basin is submitted to shear stresses and accompanies potential uplift to create a bordering marginal ridge.

Stage 2 - Continent-ocean active transform fault contact (stage B on Fig. 2). In this setting, the proximity of the hot oceanic lithosphere may induce important vertical readjustment of the nearby continental margin border.

Stage 3 - Inactive continent-ocean transform fault (stage C on Fig. 2). This is tectonically a passive transform margin, experiencing relatively homogenous thermal subsidence.

## **STUDY AREA**

The ICG Margin has been created by major transform motion between plate boundaries. This motion is still active today along the Romanche Fracture Zone, which offsets the Mid-Atlantic Ridge by 945 km (Fig 1A) (Fail et al., 1970). Since its creation, the ICG Margin has not experienced any major regional tectonic disruption, and its present day sedimentary and tectonic features are directly inherited from its Cretaceous transform margin history. The area of particular recent investigation along this margin is the Côte d'Ivoire Marginal Ridge, that is located between the divergent margin (i. e. the deep Ivorian Basin) and the transform margin. This area corresponds to a transition between laterally thinned continental crust and adjacent oceanic crust. The setting of the present-day marginal ridge includes a fossil ridge that connects laterally with the extinct Romanche Fracture Zone (Fig. 1B and 1C).

### **Nature of the Continent-Ocean Transform Boundary**

Little is still known about the structure of the continental crust beneath transform margins. Almost nothing is known about the transition between continental and oceanic crust at the transform boundary. The oceanic crust emplaced at the junction between accretionary axis and the transform fault (stage B in Fig. 2) should record strike-slip tectonics.

Along the ICG Transform Margin, there is no evidence of oceanic crust deformation. However, an echelon elongated basement ridges has been discovered at the western termination of the ICG Transform Margin (Basile, 1990) as along the oceanic Romanche Fracture Zone (Masclé, Auroux, et al., 1989) (Fig. 1). Dredging and recent sampling during the diving cruise *Equanaute* have shown that these ridges consist of continental derived rocks (Honnorez et al., 1993).

These rocks are likely related to transform activity at the ocean-continent boundary, although the precise origin and deformation history of the continentally derived rocks and their relationship to the adjacent oceanic crust must still be resolved.

Clear similarities exist between fossil transform margins and inactive oceanic fracture zone. First, and as exposed above, an echelon minor ridges exist between the thinned continental crust and the oceanic crust (length 25 km, width 6 km, height 750-1000 m, spacing 10 km), within the fossil oceanic fracture zone (inactive Romanche: length 25 km, width 7 km, height 500 m, spacing 10 km), and possibly in the active one (median ridges in the active Romanche or Vema Fracture Zone, for example) (active Romanche: length 18-25 km, width 4-6 km, height 300-600 m) (Bowen and White, 1986; MacDonald et al., 1986; Auzende et al., 1989a; Mamaloukas-Frangoulis et al., 1991; Honnorez et al., 1991).

At another scale, the ICG Marginal Ridge as a whole appears to be comparable in size to transverse ridges bordering active oceanic fracture zones (e.g., Vema, Romanche) (Bonatti and Chermak, 1981; Auzende et al., 1989b; Honnorez et al., 1991). The ICG Marginal Ridge, like fracture zone transverse ridges, is an elongated asymmetrical feature, with a steep slope facing the transform boundary and a more gentle slope on its opposite side. Its southern slope (along the transform boundary) exposes an upper crustal section several kilometers thick suggesting that the marginal ridge, like transverse ridges of fracture zones, may result from block tilting.

Similar tectonic processes thus can be active during the formation of both oceanic fracture zones and transform margins. Unfortunately the lack of detailed geological data on transform margin minor ridges, as well as the absence of quantitative information on the rate of uplift and subsidence of transform marginal ridge are insufficient to develop this comparison further.

## **Equatorial Atlantic Gateways**

The history of the continental separation within the equatorial Atlantic area remains a key to understand the events that have led to the establishment of the past (and present) patterns of oceanic water circulation (Berggren and Hollister, 1974; Föster, 1978; Moullade and Guerin, 1982; Moullade et al., 1993).

During its early opening stages, the Central Atlantic was separated to the South Atlantic by a major fracture zones system (Chain, Romanche and Saint Paul Fracture Zone) in the Gulf of Guinea.

The oceanic connection between the Central and South Atlantic occurred through the Equatorial Atlantic in Aptian times. During the Early Cretaceous stages of basin development, water circulation was greatly restricted by both fracture zones and transform margins, leading to deposition of thick carbonaceous shales sequences. Hence, the circulation of dense, saline water in the equatorial basins has been an important factor in controlling deposition along the Atlantic margins, and is likely to have contributed to the development of several unconformities within the Cretaceous sedimentary record.

By Santonian times the equatorial rift had reached a width of about 1200 km, water depths close to the continental margins exceeded 5000 m and the transfer of surface water between the central and south Atlantic was well established.

During Cenozoic times, the Romanche Fracture Zone has acted as an important conduit for the transfer of deep bottom water from the western to the eastern equatorial Atlantic basins.

## **Seismic Stratigraphy of the Côte d'Ivoire Margin Domain**

The seismic stratigraphy of the area is based on investigations by the 1983 *Equamarge I* cruise (Blarez, 1986; Blarez et al., 1987, Mascle and Blarez, 1987, Mascle et al., 1988), the 1990 *Equasis* cruise, the *Equaref* cruise and *C. Darwin* cruise 55 (1990 and 1991, respectively), the 1988 *Equamarge II* cruise (Mascle, Auroux et al., 1989; Basile et al., 1989; Popoff et al., 1989; Pontoise et al., 1990; Basile, 1990; Basile et al., 1992, Basile et al., 1993), the 1992 *Equanaute* cruise (Mascle et al., 1993), and a few results from the Brazilian conjugate margin, chiefly explored by PETROBRAS (Ponte and Asmus, 1978; Zalan et al., 1985; Costa et al., 1990).

The proposed seismic stratigraphy is defined on the basis of angular relationships between several sedimentary units, especially along the northern slope of the marginal ridge. We distinguish six main units, A to F (Fig. 3) (Basile et al, 1993).

The relationship between basal Unit A and the underlying acoustic basement is still not clear. This basal unit is deformed both in the divergent Ivorian Basin and the transform marginal ridge. It can be divided into subunits in A0, A1 and A2. A0 seems to be ante-rift in the whole area. A1 is syn-rift in the divergent Ivorian Basin. A2 is post-rift in the Ivorian Basin, but deformed within the transform margin.

Unit B corresponds to post-rift sediments, and is not deformed within the transform margin. It unconformably overlies both the A sequence of the deep Ivorian Basin and the A2 sequence of the transform margin.

Units C to F lie conformably on the previous units, within and along the eastern side of the transform margin. However, they lie unconformably on the B and A2 sequences that constitute most of the northern slope of the marginal ridge. All units lie almost horizontally in the deep Ivorian Basin, but may progressively pinch out against the marginal ridge, possibly due to coeval ridge uplift.

Sedimentary Units C and D seem to have been deposited both by aggradation within the Ivorian Basin (i. e. distal detrital sedimentation from the African coasts) and by progradation originating from the marginal ridge summit (i. e. proximal detrital sedimentation). Such mechanisms imply that the ridge top was near sea level at that time. The upper part of the C sequence onlaps the ridge top, whereas the lower "D" sequence is restricted to the deepest part of the Ivorian Basin. Such progressive restriction of the area of sedimentation also characterizes E and F sequences. Also, the lower E sequence consists of short-dipping reflectors prograding northward.

## **Lithology**

Only few samples were recovered by coring, or dredging, along the transform margin itself. These all consist of detrital sediments (sandstones or siltstones). Unfortunately these could not be correlated with the seismic stratigraphy. However, during the *Equanaute* dives, 14 geological sections were made along the southern slope of the marginal ridge, and 165 samples were

collected. Most of these are also terrigenous and probably belong to the same thick sandy-clayey formations (mainly sedimentary Units A1 and A2). These rocks include fine-grained to coarse-grained sandstones, greenish, lenticular to wavy-bedded, siltstones and black shales, which show numerous syndiagenetic microfaults and slumps.

Locally, near the foot of the continental slope (sedimentary Unit A1), orthoquartzites and indurated shales characterized by slaty cleavage were sampled. Thin sections show recrystallized phyllosilicates which are synchronous with respect to the slaty cleavage. These recrystallizations, of probable low-grade metamorphic origin, are similar to those observed in Albian deposits of the Lower Benue Basin (Benkhelil, 1986, 1988). However, the deepest dive (4900 m, dive 11) have also yielded black schists and fine-grained quartzites comparable to metasediments of Early Voltaian age (Precambrian), which crop out along the West African shoreline (Affaton et al, 1980). These results question the Proterozoic or Early Cretaceous age of the base of the Ridge.

*Equanaute* dives have documented the A2 unit, made of massive sandstones and siltstones interbedded with pelites. Here, direct in situ observations reveal silty-clayey strata interbedded with large-scale trough cross-bedded sandstones. Both the sedimentary facies and structures favor a very shallow marine environment of deltaic type, quite similar to Lower Cretaceous sediments known in the Lower Benue Basin (Nigeria) (Ojoh, 1990) and in the Potiguar Basin (northeast Brazil) (Neves, 1989).

Only a few samples can be related to the uppermost Units D to F (chiefly collected during dive 14). These consist of clayey limestones, dolomites, and siltstones.

## **Ages**

Only two samples (one core and one dredge) have yet provided reliable age information on the sedimentary units. Both indicate a middle to uppermost Albian age (one dated by palynology (Klingebl, 1976), the second by Ostracoda (Grosdidier, pers. comm., 1989)). As both A1 and A2 sedimentary units are exposed along the slope, it is not possible to determine from which unit the samples were retrieved. Two hypotheses can be considered.

...Leg 160 - Eastern Equatorial Atlantic Transform...

Units	Ages following Hypothesis I	Ages following Hypothesis II	
F	Present to	Present to	
E	Oligocene	Paleocene	
D	Eocene to	upper Cretaceous	
C	upper Cretaceous	Albian	
B	Cenomanian to	Albian	post-transform unconformity
A2	uppermost Albian	Albian	post-rift unconformity
A1	Albian to	Aptian	
A0	Lower Cretaceous	Lower Cretaceous	

In Hypothesis I, the samples were retrieved from A1 unit, as thought by Blarez (1986). From this hypothesis we infer that the syn-rift sedimentary Unit A1 is at least late Albian in age and conceivably may be older (Aptian, like all the equatorial basins, or even Neocomian). In this case, the post-rift sediments (A2 and B unit) were deposited in latest Albian or Cenomanian times, as in the Benue trough (Popoff, 1990), but later than the Aptian/Albian unconformity described in the conjugate Brazilian Margin (Zalan et al., 1985; Costa et al., 1990).

An alternative hypothesis, Hypothesis II assigns an Albian age to the A2 unit. In this case, the syn-rift Unit A1 and post-rift unconformity should be respectively Aptian and Aptian/Albian in age, as indicated on the conjugate Brazilian Margin.

Since no sample was retrieved from the upper sedimentary units (C to F), they can be tentatively dated only from the hypothesis made on their basement age, and calibrated to an offshore borehole located 150 km northwards on the Ivorian shelf (IVCO2, Fig. 1C) (Blarez, 1986).

Since the samples retrieved during the dives consist mainly of sandstones, no easy dating by microfaunas is to be expected. Tentative dating by palynology on a few shales samples are attempted. Radiochronological dating (Ar/Ar) on neomorphic biotite, and fissions track dating on apatites and zircons are currently in progress. Preliminary results from the fissions track of detrital apatites give the following ages of cooling for crossing the isotherm 60°C: 68 Ma (dive EN1, depth 3479 m), 52 Ma (dive EN4, depth 2405 m), and 44 Ma (dive EN9, depth 3905 m).

Correlations can also be made between the main regional tectonic events and the dating of the oceanic opening of the equatorial Atlantic. In this area, the lack of identified magnetic anomalies prevents the determination of an accurate chronology of oceanic opening. The proposed kinematic models are thus chiefly based on fracture zone geometry and tentatively fitted to magnetic reversal chronology derived from the South Atlantic (Le Pichon and Hayes, 1971; Sibuet and Mascle, 1978; Rabinowitz and LaBrecque, 1979; Klitgord and Schouten, 1986; Scotese et al., 1988).

Despite the differences between the proposed rotation poles, all reconstructions agree that rifting of the equatorial Atlantic occurred during the early Cretaceous, maybe in Neocomian-Barremian time according to Doyle et al. (1982) in the Keta Basin, Popoff (1990), and Brunet et al. (1991) in the Benue Trough. The various reconstructions also imply that kinematic parameters were modified in Santonian time. This reorganization has tentatively been correlated with the final disruption of the African and Brazilian cratons within the equatorial area (Mascle and Blarez, 1987).

## **Tectonics**

To the north of the marginal ridge, the deep Ivorian Basin is an extensional margin, thinned by dip-slip faults trending north-south to northeast-southwest. These faults bound tilted blocks and half-grabens, which are infilled by thick syntectonic sediments (Unit A1; Fig. 4). To the south, the fossil marginal ridge is a 130 km long and 25 km wide prominent feature that towers over the Ivorian Basin by 1300 m and over the adjacent oceanic crust by more than 4000 m.

The regional structure of the transform margin seems to be linked to the westward thinning of the adjacent divergent basin (Fig. 4). East of 10°W, the transform border is expressed by a narrow shelf lying at the same depth as the Ivorian Basin. Between 10°W and 45°W, the transform zone is chiefly expressed by the marginal ridge that towers the flat Ivorian Basin by 1300 m. West of 45°W, the ridge top is progressively westward dipping like the bordering Ivorian Basin.

Due to the chaotic facies of the pseudo-acoustic basement little is known about the internal structure of the marginal ridge from single channel seismic lines. Migrated multichannel seismic lines have greatly improved our knowledge of this pseudo-basement.

East of 10°W (MCS line MT3), in the eastern side of the area, transform motion appears as flower structures at the Ivorian Basin - transform margin transition. To the north, these strike-slip become

transpressional and exhibit reverse slip. The folds associated are en échelon disposed, indicating right-lateral movement (Fig. 4). Southward appears a wide (> 10 km) and deep (1 km) channel that is possibly an infilled intracontinental transform valley, such as the Jordan valley in the Dead Sea transform. The southern limit of this valley is probably at the top of the actual southern continental slope. Here the deformation observed during the dives is more important (folding, vertical fracturing, fracture cleavage) than southward, out of the transform valley (strata tilted S-E).

The activity of the strike-slip faults is recorded by the sedimentation of A1, A2 and B units. The reverse strike-slip faults are active from the deposition of the A1 sequence (uplifted during the sedimentation), up to the deposition of A2 (cut by the faults). An additional uplift of the A2 sequence is sealed as strike-slip faulting by the unreformed B unit.

The transform valley is also probably active during A1 and A2 deposition. Here the A1 unit is eroded, and the valley is infilled by the A2 sequence showing thick lenticular bodies prograding to the south.

Between 10°W and 45°W (MCS line MT2), along a N-W cross section of the marginal ridge, three tectonic domain can be distinguished. The western prolongation of the transform valley observed eastward (see above). This transform valley is also located at the boundary between the deep Ivorian Basin and the marginal ridge. The valley erodes the deepest unit (A0). It is infilled partly by the faulted A1, and mainly the unfaulted A2 unit. No deformation can be clearly identified within the northern slope of the marginal ridge because of the lack of continuity of seismic reflectors. However, it appears that the northern slope of the marginal ridge is mainly made by an important thickening of the A2 unit to the south. This thickening results in the edification of a ridge, with at its top sedimentary lenses prograding to the north, and distal fans along its northern slope.

The presence of the deep Ivorian Basin to the north, and the northward progradation, indicate that the detrital material was originate from the Brazilian shelf that was just located southward at that time of intracontinental transform faulting. Even if tectonic styles cannot be easily determined from such seismic sections, *Equanaute* dives tend to substantiate that deformation increases upslope towards the ridge top (fracturing and folding) where strike-slip activity was probably concentrated.

The seismic lines also show that the B unit is restricted to the deep Ivorian Basin and northern ridge slope. Thus, sedimentation proceeded simultaneously by both aggradation in the Ivorian Basin (sediments originating from African coasts) and progradation (probably sediments derived from the ridge top erosion). Units C to F are also restricted to the Ivorian Basin and northern ridge slope.

The progressive westward deepening of the marginal ridge is due to dip-slip faulting. This faulting occurred prior B unit, but cannot be dated with confidence. It could alternatively have been inherited from the Ivorian Basin rifting, or from east-west strike-slip activity and coeval pull-apart basin creation.

West of 45°W (MCS line MT1), to the west of the marginal ridge, the southern border of the transform margin includes several en echelon spaced minor acoustic ridges (Fig. 4). These tower over the oceanic crust to the south and over a thick (about 2 km) syn-transform basin to the north. These minor ridges are believed to originate in connection with transform motion, but different hypothesis can be made about their nature and deformation history. Are these ridges continental or oceanic, basement or sediments? Did these ridges appeared during the rifting of the Ivorian Basin, during intracontinental transform faulting or during the continent-ocean transform faulting?

We cannot determine if the syn-transform sediments that infill the basin lying just north (Unit A2 or B?) are similar and contemporaneous to the sediments that make up the minor ridges. A second question relates to the potential similarity between these lower margin minor ridges and the en echelon ridges mapped to the west, along the inactive Romanche Fracture Zone. Are these similar in nature and origin? If so, this indicates that parts of the continental margin basement (and cover) were tectonically displaced during transform motion (during intracontinental transform contact and even after).

#### *Tectonic Model for the Evolution of the ICG Margin*

From the interpretation of the data discussed above, and according to experimental modelling of the deformations at rift-transform intersection (Basile et al., 1992), we propose the following schematic evolution of the ICG Transform Margin (Figs. 5 and 6).

### Initial Setting (Fig. 5)

During Early Cretaceous times, the African and South American continents were in contact along their equatorial boundaries. The deep Ivorian Basin and the Ghanaian shelf were facing their Brazilian Margin conjugates, respectively the Barreirinhas Basin and the Piauí-Ceará area.

### Early Rifting of the Deep Ivorian Basin (Fig. 5)

According to plate reconstruction and geological field data (Le Pichon and Hayes, 1971; Sibuet and Mascle, 1978; Rabinowitz and Labrecque, 1979; Doyle et al., 1982; Klitgord and Schouten, 1986; Popoff, 1988; Scotese et al., 1988; Brunet et al., 1991), opening of the equatorial Atlantic ocean began during Early Cretaceous time (possibly during the Neocomian). The deep Ivorian Basin was then initiated as the result of an east-west to east-northeast-west-southwest oriented extension, generating north-south syntectonic half-grabens and associated tilted block. The sedimentary infill (syn-rift Unit A1) deposited over the whole basin, was thicker within the half-grabens and along the future transform margin.

Data from *Equanaute* dives, as well as comparison with field data from northeast Brazil and the Benue trough, indicate that the sedimentation was chiefly detrital and probably in a subaerial, deltaic to lacustrine environment. In the future transform area, detrital sedimentation was probably greatly influenced by the vicinity of the Brazilian shelf, and was potentially controlled by rapid subsidence in structures such as pull-apart basins.

### Rifting of the Ivorian Basin and the Shearing of its Southern Border (Fig. 6)

As the stretching of the Ivorian Basin crust progressed, the basin deepened and relative shear motion between the African plate and the South American plate affected its southern border. By that time, this border evolved as an accommodation zone (Fig. 6), concurrently undergoing vertical motion between a thinned Ivorian Basin and the stable Brazilian shelf (within the Ivorian Basin this relative vertical motion increased from east to west following the basin thinning) and an increase in the intensity of horizontal (transcurrent) motion from west to east.

As expected from this assumed kinematic model, the observed strike-slip and dip-slip motions respectively decreased and increased from east to west. The first en échelon strike-slip fault zones were generated at the contact between the rifted basin and its transform boundary. Vertical

displacement, especially in the western area, was recorded by tilting of the northern slope ridge and coeval creation of an east-west syn-rift basin perpendicular to north-south extensional structures of the Ivorian Basin.

In this hypothesis, the accommodation zone activity is necessarily coeval with the syn-rift Unit A1 deposition in both the Ivorian Basin (tilted blocks) and in the transform zone where detrital sediments coming from the Brazil led to the development of a sedimentary wedge. Furthermore, the minor ridges were probably created during this time interval.

#### End of Rifting and Intracontinental Transform Faulting (Fig. 6)

Rifting ceased in the Ivorian Basin when oceanic crust was created along its western edge. Continental break-up there was recorded by a typical post-rift unconformity and by the deposition of B unit in the deepest parts of the main depocenters. Before this event, potential block rotation may have occurred within the deep Ivorian Basin, reworking former extensional features in anticlinal features and strike-slip lineaments. The reason for such structural inversion is unknown, but could be related to local kinematic modification during break-up.

Along the southern border of the Ivorian Basin, initiation of the drift stage induced transform-type displacement between the two continental plates. This event may have been contemporaneous with deposition of post-rift Unit A2, that is restricted to the transform margin. The deposition of A2 unit occurred above and along the northern slope of the marginal ridge, and contributed to its construction.

Before B unit deposition, the transform motion shifted towards the south, to the top of the present continental slope where the different structural features observed during *Equanaute* dives (sets of brittle joints, slaty cleavage, folds and microfolds) are in good agreement with a dextral activation of N60 major faults.

#### Continent/Ocean Transform Faulting (Fig. 6)

Final continental parting between West Africa and North-East Brazil brought into contact the Gulf of Guinea oceanic crust and the continental transform fault, that became, at this time, an active continental transform margin. The active transform system is thought to be rather located within the

*...Leg 160 - Eastern Equatorial Atlantic Transform...*

thin oceanic crust. Differences in depths between the continental border and the oceanic basin could have led to gravitational sliding, progressively creating the southern slope of the marginal ridge.

Moreover, the contact between hot oceanic lithosphere and colder continental crust should have induced strong thermal gradients and results in subsequent marginal ridge uplift (Todd and Keen, 1989; Lorenzo and Vera, 1992). Within the Ivorian Basin, coeval sedimentation (D sequence) recorded such an uplift, while the previous sedimentary units were tilted northwards. This uplift probably increased up to the passage of the oceanic spreading center. At this stage, the vertical motion is estimated in the order of 1 km, 20 km north of the continent / ocean boundary. This uplift is comparable to the thermal uplift estimated and reported by Todd and Keen (1989) for the southern Newfoundland Transform Margin.

#### Passive Margin Evolution

Active tectonism of the transform margin ended when the southern spreading center passed south of the ICG Margin. The transform margin and the adjacent oceanic basin started to subside as a result of thermal subsidence. Afterwards, the strong damming effect of the marginal ridge restricted most of the detrital sediment input to the deep Ivorian Basin. The only striking feature within the subsequent sedimentary cover relates to major Cenozoic lowstand (Oligocene stage, between E and F units) (Vail and Hardenbol, 1979; Haq et al., 1988). This induced strong submarine erosion, still imprinted in the present morphology by canyons and wide submarine valleys.

#### *Alternate Reconstructions*

The evolution proposed above explains the built up of the marginal ridge by successive tilting and sedimentary processes, namely tectonic tilting during the rifting of the Ivorian Basin, thermal tilting during the continental-oceanic transform faulting, and sedimentary accretion mainly during the rifting of the Ivorian Basin.

However the relative importance of these phenomena can not be easily determined from the data available. Moreover, this explanation doesn't take in account other potential mechanisms that can be tested by drilling, such as 1) the marginal ridge can be uplifted by shearing in a transpressional setting, as can be deduced from microtectonic features in cores, 2) the marginal ridge can be

uplifted by block tilting along the transform boundary, like the transverse ridges in the active oceanic transform faults (in this case, the only expected tectonic feature is the tilting of every sedimentary structures), 3) the marginal ridge can be a continental block, not thinned by the opening of the Ivorian Basin, but translated from the west to its southern boundary (in this case, the deformation is not expected within the block, but only along its borders), 4) the marginal ridge can result from rotations (about vertical axis) along the transform area, that may explain both the transtension and transpression features observed along the ridge, respectively eastward and westward (this hypothesis can be tested by paleomagnetism measurements), or 5) the marginal ridge can be a sedimentary wedge, resulting only from accumulation of detrital sediments and modeling by erosional and gravitational processes (in this case, no tectonic deformation is expected, but typical sedimentary features are expected to be observed in drilling cores).

## **SCIENTIFIC OBJECTIVES AND METHODOLOGY**

### **Summary of Objectives**

- 1) To determine the exact tectonic and sedimentary processes that are involved in the creation of the different main morphostructural features generated at ICG Transform Margin, including formation of the marginal ridge, and the nature and structural deformation of the acoustic basement underlying the minor ridges generated at the transform boundary.
- 2) To document the type of deformation (and deformation history) of the ICG Transform Margin during the successive stages of evolution.
- 3) To constrain the timing, rate and degree of vertical motion (subsidence and uplift) occurring on the ICG Transform Margin.
- 4) To investigate the thermal evolution of the transform margin in relationship to the actively spreading oceanic crust, including diagenesis within the transform margin and the heating, hydrothermalism, and possibly magmatism occurring along the transform margin in response to the vicinity of a spreading center that progressively migrated along and then away from the transform margin.

- 5) To accumulate important data on the history of the oceanic gateway across the Equatorial Atlantic, and on the sedimentation of specific facies (anoxic sediments) during the opening phase.

### **Specific Objectives and Methodology**

The main questions to be addressed by the drilled at the three proposed sites IG-1, IG-2, and IG-3 relate to the age, nature and deformation of the sediments and basement, and their vertical behavior. The final objective is, of course, to describe sedimentary, structural and thermal factors operative at transform margin. These parameters will permit a precise description of the tectonic and sedimentary processes involved in creation and evolution of a transform margin, and help to better constrain the succession of events and thermo-mechanical models.

#### *Timing Controls and Evolution of the Sedimentary Cover*

The ages of samples collected on *Equanaute* '92 dives are not yet available. However these dates will concern only discontinuous sedimentary units that are deeper than those expected at proposed sites IG-1 and IG-2 on the marginal ridge. No sample is yet available from the minor ridges (proposed site IG-3). Drilling is essential to provide a continuous sedimentary record, including the clayey beds (where microfauna and/or pollen are to be expected) that were not sampled during dives.

The different timing controls expected from drilling holes concern

- 1) the beginning of extension in the adjacent rifted Ivorian Basin - this will be provided by the post-rift sediments, Unit A2 and B, at proposed site IG-1,
- 2) the beginning of oceanic accretion (south of the transform margin), marking the end of tectonic activity on the margin - this age cannot be obtained directly using the proposed sites, but is expected to be determined by dating the end of the tectonic activity on the continental margin at proposed sites IG-1, IG-2, and IG-3,
- 3) the initiation of strike-slip faulting on the transform margin - such timing can be obtained directly at proposed site IG-2 and probably IG-3, since both holes are located near a strike-slip

fault on an assumed sheared block while the time of ending of strike-slip activity is expected from data at all three proposed sites IG-1, IG-2, and IG-3,

- 4) the age of A1/A2 unconformity associated with the end of strike-slip faulting and related uplift - this can be addressed at proposed site IG-2.

Furthermore, comparisons between the holes will be used to

- 1) correlate the history of subsidence of the margin (proposed site IG-1), with the main tectonic events (e.g., extensional rifting, continent-continent transform faulting, continent-ocean transform faulting, passive transform margin),
- 2) compare the deformation history of both the rifted basin and of its transform boundary (proposed sites IG-1 and IG-2),
- 3) estimate the diachronism of the estimate sedimentary and tectonic events along the transform margin (proposed sites IG-1, IG-2, and IG-3).

#### *Evolution of Sedimentation and Diagenesis*

Continuous coring at all three proposed sites will also determine

- 1) the ages and facies of the sedimentary cover, especially the post-rift sedimentary sequences (Units B to D, proposed site IG-1), necessary to estimate the depth/age curve, i. e. the subsidence history of the margin,
- 2) the origin of detrital sediments (Units B to D), derived from either the north (Africa), or from the south (erosional top of marginal ridge at proposed site IG-1),
- 3) the origin of onlaps and toplaps of the sedimentary cover detected on the northern ICGMR slope (proposed site IG-1) and whether they are related to tectonic or isostatic events (uplift or subsidence of the marginal ridge), or environmental variations (e.g., sedimentation rate, currents, sea level) in a proximal or distal fan,

*...Leg 160 - Eastern Equatorial Atlantic Transform...*

- 4) the history of sedimentation within the active transform margin, including the dynamic of detrital sedimentation in a deltaic environment, the origin of the major unconformity and their control by tectonic processes,
- 5) diagenesis of detrital sediments in the transform margin, during and after tectonic activity, paying special attention to the evolution of organic matter in relation to diagenesis, metamorphism, and heating in the vicinity of the oceanic lithosphere to constrain the thermo-mechanical model of the margin,
- 6) the evolution of water depth during marginal ridge formation - this will be addressed near the top at proposed site IG-1, and along the western extremity of the marginal ridge at proposed site IG-2; the comparison between the two sites showing if the ridge has been uplifted after sedimentary deposition,
- 7) the nature of the bordering minor ridges at proposed site IG-3 will be investigated - if these ridges are similar to those from within the fossil Romanche Fracture Zone, metasandstones would be expected and, if this is the case, timing of sedimentation, depositional environment, dating of metamorphism, and degree of deformation are needed to understand the mechanisms that have created these lower margin en echelon ridges.

*Structural Measurements*

Structural analyses is an important part of this drilling program, and should document

- 1) the type of deformation related to strike-slip faulting at proposed sites IG-1, IG-2, and IG-3 - according to *Equanaute* dives, this includes microfolds, fractures, faults and shear zones,
- 2) paleostresses from small-scale tectonic features at proposed sites IG-1, IG-2, and IG-3 recorded in structural changes within the transform margin - the relative roles of strike-slip faulting and gravitational instabilities on the stress field is particularly important in order to evaluate the influences of those processes on formation of the marginal ridge. [Special attention will be given to paleostress measurements at proposed site IG-3 where changes in the stress field can be expected as a consequence of the transition from a transform fault regime to an extensional

regime related to the oceanic spreading. Furthermore, metamorphism could be expected as a consequence of large-scale shearing (shear heating) that has probably generated the en échelon pattern],

- 3) the importance of gravitational deformation (i. e. syndiagenetic microfaults and slumps) related to detrital sedimentation (i.e. sedimentary Unit A at proposed sites IG-1 and IG-2 - sedimentary unit at proposed site IG-1); samples retrieved during the *Equanaute* dives show syn-depositional, or syn-diagenetic deformation, that can be due to tectonic instability,
- 4) the nature and origin of deeper reflectors (our interpretation of the MCS lines implies that the deep reflectors are unconformities (or sedimentary reflectors), not thrust ramps - this question can be addressed especially at proposed site IG-2, where the deep reflectors can be alternatively interpreted as the top of a tilted (extensional) block, or as a basal thrust below an eroded block.

Microtectonic observations, paleostress measurements, tilting history and paleomagnetic controls will be used together to define the tectonic regime and evolution of the transform margin.

Finally, structural results will be combined with sedimentary data (ages, nature and depths of deposition) in order to

- 1) determine the relative interplay of synrift and postrift-syntransform tectonic and sedimentary processes involved in the formation of a transform margin, and
- 2) quantify, in time and space, the subsidence and tilting history of each main margin area.

All data are needed to define a thermo-mechanical model for transform margin creation and evolution, and potentially to compare the results to models developed for oceanic fracture zones.

#### *Paleoenvironment*

Proposed site IG-1 should constrain the connection between Central and South Atlantic through the Equatorial Atlantic based on the sedimentary record. The drilling results should help to determine

- 1) the age of the gateway (as far back as the Aptian-Albian),

- 2) the nature of the gateway (an Atlantic gateway versus a gateway crossing Africa through the Sahara and the Benue Basin), and
- 3) the bathymetric evolution.

The same site should help determine the middle (from Aptian-Albian) and upper Cretaceous paleoenvironmental evolution, constraining

- 1) the age and nature of the first marine sedimentation,
- 2) the evolution of paleoenvironments (bathymetry, salinity, oxygenation, surface and bottom circulation, upwellings) and biofacies (Atlantic or African gateway) during the middle and upper Cretaceous,
- 3) the age of open marine environment and communication with the open ocean (possibly from Albian),
- 4) the initiation of cold water deep currents originating from the South ("paleo-Benguela Current") and influence on the productivity and dissolution of carbonates,
- 5) the probable sampling of an anoxic event (black shales) at the Cenomanian/Turonian boundary, as a regional event or a global event,
- 6) the origin of sedimentary onlaps and toplaps along the northern ICGMR slope. Are they due to tectonic or isostatic events (uplift or subsidence of the marginal ridge), or to environmental variations (sedimentation rate, currents, sea level) in proximal fans (sediments derived from the south, i. e. from the marginal ridge) or distal fans (detrital sediments from the north, i. e. the African coasts), and
- 7) the record of Cenozoic global events in an area influenced by deep water circulation along the Romanche Fracture Zone.

### *Potential Lithospheric Implications*

Available MCS and refraction data suggest that the oceanic crust emplaced at this ridge / transform intersection was created at a very low magmatic accretion rate, by intrusion of discontinuous differentiated magmatic bodies within partially serpentinized peridotites. Such mechanisms as well as serpentinization should have been controlled by faulting.

Unfortunately, the thickness of the sediments precludes reaching the oceanic crust in this area. However, information on the oceanic crust may be expected from proposed site IG-3, located near the continent-ocean boundary, including the nature of the minor ridges, involvement of magmatic rocks near transform fault, and investigation of hydrothermal activity at the intersection of the accretionary ridge and transform fault

## **DRILLING PLAN/STRATEGY**

Our drilling choice is controlled by the thickness of the sedimentary cover in the Ivorian Basin, on the marginal ridge and in the adjacent oceanic abyssal plain, and by the need to develop a drilling program that can be completed during a single ODP leg (Table 1).

Two sites are proposed on the marginal ridge (proposed sites IG-1 and IG-2, Figs. 1 and 5), in areas where deep targets can be hit with a relatively thin, but continuous, sedimentary cover (1600 and 780 m, respectively). In addition, a shallower hole is proposed on a minor ridge, near the transition between oceanic fracture zone and continental transform margin (proposed site IG-3, Figs. 1 and 5).

These three sites represent an east-west, along-strike transect. They should allow us to study the lateral evolution of the transform margin, from a thick continental crust to a thinned crust. Because proposed site IG-3 is closer to the continent-ocean boundary, comparison with proposed sites IG-1, IG-2 should illustrate the change in tectonic effects as we move across the continent-ocean boundary toward the oceanic crust.

## **PROPOSED SITES**

Proposed site IG-1 is dedicated to study of the northern slope of the ICG Marginal Ridge and of its unreformed sedimentary cover. Complementing the deepest sediments retrieved during the

*Equanaute* submersible dives, a hole drilled at this site will document the entire sedimentary column covering the transform margin, including 1) units coeval with the Ivorian rifting, 2) units subsequent to rifting (but contemporaneous with transform faulting), 3) units posterior to transform faulting (but contemporaneous with thermal uplift), and finally 4) the sedimentary units covering the passive margin after the end of transform faulting.

Information obtained from this site should also constrain 1) the formation and subsidence of the fossil marginal ridge, 2) the style, intensity, and timing of the strike-slip deformation, 3) the timing and nature of rotation about vertical and horizontal axis, and 4) the age and nature of the first marine sediments related to the opening of the Equatorial Atlantic gateway.

Proposed site IG-2 is dedicated to the study of the western extremity of the ICG Marginal Ridge. In this area, the unreformed sedimentary cover is thin, but incomplete (sedimentary Units B, C and E are missing). However the available post-rift cover could allow a comparison between the subsidence of the two sectors of the marginal ridge, proposed site IG-1 (on the eastern side) versus proposed site IG-2 (western extremity near oceanic crust).

The main goal of the proposed IG-2 site is to drill the top of a tilted block that may have undergone extension, strike-slip movements, and potential structural inversion. Information on the style, intensity and timing of deformation are necessary to understand the creation of this part of the marginal ridge.

Paleomagnetic studies within the syn-transform sediments will be used to investigate possible block rotations about a vertical axis.

Finally, the diagenesis and possible metamorphism of the syn-transform sediments can be used to constrain the P-T field, associated with transform shearing and the post-transform heating due to proximity of adjacent oceanic crust.

Proposed site IG-3 is devoted to the study of one of the en echelon minor ridges that characterize the westernmost transform margin, near its junction with the fossil Romanche Fracture Zone. In this area, the lower margin ridges have possibly experienced two transform related events - transform motion within an intracontinental transform fault and transform motion within a continent-ocean transform fault.

The nature of basement (deformed sediments, continental basement, oceanic basement?) of these minor ridges is the main target of drilling at this site and the type of deformation that has generated the en échelon pattern would also be determined from microstructural analysis.

Structural observations will be used to establish the two successive transform events (intracontinental and continent-ocean) and, finally, hydrothermal activity and/or heating processes of the minor ridge sediments and/or basement are expected due to the vicinity of the oceanic lithosphere.

A proposed alternate site IG-1bis is located on the northern slope of the marginal ridge about 2 nmi south of proposed site IG-1. The site is dedicated to the study of the same major topics but cannot document the entire sedimentary column since seismic units are pinching out against the A2 and A1 units. However proposed site IG-1bis may permit penetration deeper into basal ridge units. This site is proposed as an alternate to reduce drilling time operations, if necessary. The site, based on a 800 m penetration (single bit hole) may become a reentry hole in order to document deeper sequences A1-A2.

Proposed site IG-2bis is an alternate for proposed site IG-2. It is located at the intersection of single channel line 35 and MCS line MT 05, on the top of a small tilted block on the western ICG Marginal Ridge. The main objectives at this site are to document style, intensity and timing of deformation undergone by this part of the marginal ridge close from the ocean-continent boundary. Penetration at this site is planned at approximately 800 m to document mostly A1 and A2 units; the unreformed sedimentary cover is incomplete and about 300 m thick.

## REFERENCES

- Affaton, P., Sougy, J., and Trompette, R., 1980. The tectono-stratigraphic relationships between the upper Precambrian and lower Paleozoic Volta basin and the Pan-African Dahomeyide orogenic belt (west Africa). *Am. J. Sci.*, 280:224-248.
- Arens, G., Delteil, J.R., Valery, P., Damotte, B., Montadert, C. and Patriat, P., 1971. The continental margin of the Côte d'Ivoire and Ghana. *Inst. Geol. Sci. London, Rep.*, 70:61-78.
- Auzende, J.M., Bideau, D., Bonatti, E., Cannat, M., Honnorez, J., Lagabrielle, Y., Malavielle, J., Mamaloukas-Frangoulis, V., and Mevel, C., 1989a. L'intersection entre la zone de fracture Vema et la dorsale médio-Atlantique: résultats préliminaires de la campagne Vemanaute. *C. R. Acad. Sci. Paris*, 309:1341-1348.
- Auzende, J.M., Bideau, D., Bonatti, E., Cannat, M., Honnorez, J., Lagabrielle, Y., Malavielle, J., Mamaloukas-Frangoulis, V., and Mevel, C., 1989b. Direct observation of a section through slow-spreading oceanic crust. *Nature*, 337:726-729.
- Barker, P.F., Dalziel, I.W.D., et al., 1976. *Init. Repts. DSDP*, 36:Washington (U.S. Govt. Printing Office).
- Basile, C., 1990. Analyse structurale et modélisation analogique d'une marge transformante: l'exemple de la marge profonde de Côte d'Ivoire-Ghana. *Mém. Doc. CAESS Rennes*, 39.
- Basile, C., Brun, J.P., and Mascle, J., 1992. Structure et formation de la marge transformante de Côte d'Ivoire-Ghana: apports de la sismique réflexion et de la modélisation analogique. *Bull. Soc. Géol. Fr.*, 163:207-216.
- Basile, C., Mascle, J., Auroux, C., Bouillin, J.P., Mascle, G., Gonzalves de Souza, K., and le groupe *Equamarge*, 1989. Une marge transformante type: la marge continentale de Côte d'Ivoire-Ghana : résultats préliminaires de la campagne *Equamarge II*. *C. R. Acad. Sci. Paris*, 308 (II):997-1004.
- Basile, C., Mascle, J., Popoff, M., Bouillin, J.P., and Mascle, G., 1993. The Côte d'Ivoire-Ghana transform margin: a marginal ridge structure deduced from seismic data. *Tectonophysics*, in press.
- Benkhelil, J., 1986. Structure et évolution géodynamique du bassin intracontinental de la Bénoué (Nigeria) [Thesis] Université Nice.
- Benkhelil, J., 1988. Structure and geodynamic evolution of the intracontinental Benue Trough (Nigeria). *Bull. Centres Rech. Expl. Prod. Elf Aquitaine*, 12(1):29-128.
- Berggren, W.A., and Hollister, C.D., 1974. Paleogeography, paleobiogeography and the history of circulation of the Atlantic ocean. *Proc. Symp. Geol. Hist. Oceans. SEPM Mem.*, 20:126-186.
- Blarez, E., 1986. La marge continentale de Côte d'Ivoire-Ghana : structure et évolution d'une marge continentale transformante [Ph. D. Thesis] Univ. Pierre et Marie Curie.
- Blarez, E., Mascle, J., Affaton, P., Robert, C., Herbin, J.P., and Mascle, G., 1987. Géologie de la pente continentale ivoiro-ghanéenne: résultats de dragages de la campagne *Equamarge*. *Bull. Soc. Géol. Fr.*, 5:877-885.
- Bonatti, E., and Chermak, A., 1981. Formerly emerging crustal blocks in the equatorial Atlantic. *Tectonophysics*, 72:165-180.
- Bowen, A. N., and White, R. S., 1986. Deep-tow seismic profiles from the Vema transform and ridge-transform intersection. *J. Geol. Soc. London*, 143:807-817.
- Brunet, M., Dejax, J., Brillanceau, A., Congleton, J., Downs, W., Dupéron-Landoueneix, M., Eisenmann, V., Flanagan, K., Flynn, L., Heintz, E., Hell, J., Jacobs, L., Jehenne, Y., Ndjeng, E., Mouchelin, G., and Pilbeam, D., 1991. Mise en évidence d'une sédimentation précoce d'âge barrémien dans le fossé de la Bénoué en Afrique Occidentale (bassin du Mayo Oulo Léré, Cameroun), en relation avec l'ouverture de l'Atlantique sud. *C. R. Acad. Sci. Paris*, 306:1125-1130.
- Ciesielski, P.F., Kristofferson, Y., et al., 1988. *Proc. ODP, Init. Repts.*, 114:College Station, TX (Ocean Drilling Program).

- Costa, I.G., Beltrami, C.V., and Alves, L.E.M., 1990. A evolução tectono-sedimentar e o habitat do oleo da bacia do Ceara. *B. Geoci. PETROBRAS*, 4:65-74.
- Delteil, J.R., Valery, P., Montadert, C., Fondeur, C., Patriat, P., and Mascle, J., 1974. Continental margin in the northern part of the gulf of Guinea. In C.A. Burk, C.A., and C.L. Drake, C.L. (Eds.), *Geology of Continental Margins*: New York (Springer), 297-311.
- Doyle, J.A., Jardiné, J., and Doerenkamp, A., 1982. *Afropollis*, a new genus of early angiosperm pollen, with notes on the Cretaceous palynostratigraphy and paleoenvironments of northern Gondwana. *Bull. Centres Rech. Explor.-Prod. Elf Aquitaine*, 1:39-117.
- Eldholm, O., Faleide, J.I., and Myhre, A.M., 1987. Continent-ocean transition at the western Barents Sea/Svalbard continental margin. *Geology*, 15:1118-1122.
- Eldholm, O., and Talwani, M., 1982. The passive margins of northern Europe and East-Greenland. In Scrutton, R.A., (Ed.), *Dynamics of Passive Margins. Geodynamics Series*, 6:30-44.
- Emery, K.O., Uchupi, E., Phillips, J., Bowin, C., and Mascle, J., 1975. Continental margin off Western Africa: Angola to Sierra Leone. *AAPG Bull.*, 59:2209-2265.
- Ewing, J.I., Ludwig, W.J., Ewing, M., and Eittreim, S.L., 1971. Structure of the Scotia Sea and Falklands plateau. *J. Geophys. Res.*, 76:7118-7137.
- Fail, J.P., Montadert, L., Delteil, J.R., Valery, P., Patriat, P., and Schlich, R., 1970. Prolongation des zones de fractures de l'océan Atlantique dans le golfe de Guinée. *Earth Planet. Sci. Lett.*, 7:413-419.
- Föster, R., 1978. Evidences for an open seaway between northern and southern proto-Atlantic in Albian times. *Nature*, 272:158-159.
- Gorini, M.A., 1977. The tectonic fabric of equatorial Atlantic and adjoining continental margins, Gulf of Guinea to Brazil [Ph.D. dissert]. Columbia Univ.
- Haq, B.U., Hardenbol, J., and Vail, P.R., 1988. Mesozoic and cenozoic chronostratigraphy and eustatic cycles. In Wilgus, C., et al. (Eds.), *Sea-Level Change - An Integrated Approach*. Spec. Publ. - Soc. Econ. Paleontol. Mineral., 42:71-108.
- Haq, B.U., von Rad, U., O'Connell, S., et al., 1990. *Proc. ODP, Init. Repts.*, 122:College Station, TX (Ocean Drilling Program).
- Hayworth, G., and Keen, C.E., 1979. The Canadian Atlantic margin: a passive continental margin encompassing an active past. *Tectonophysics*, 59:83-126.
- Honnorez, J., Mascle, J., Basile, C., Tricart, P., Villeneuve, M., and Bertrand, H., 1991. Mapping of a segment of the Romanche fracture zone: a morphostructural analysis of a major transform fault of the Equatorial Atlantic. *Geology*, 19:795-798.
- Honnorez, J., Villeneuve, M., and Mascle, J., 1993. Old continent-derived metasedimentary rocks in the Equatorial Atlantic: an acoustic basement outcrop along the fossil trace of the Romanche transform fault at 6°30'W. *Mar. Geol.*, in press.
- Keen, C.E., Kay, W.A., and Roest, W.R., 1990. Crustal anatomy of a transform continental margin. *Tectonophysics*, 173: 527-544.
- Klingebiel, A., 1976. Sédiments et milieux sédimentaires dans le golfe de Bénin. *Bull. Centre Rech. Pau-SNEAP*, 1:129-148.
- Klitgord, K.D., and Schouten, H., 1986. Plate kinematics of the Central Atlantic. In Vogt, P.R., and Tucholke, E. (Eds.), *The Western Atlantic Regions*: Geol. Soc. Am., 351-377.
- Le Pichon, X., and Hayes, D.E., 1971. Marginal offsets, fracture zones and the early opening of the South Atlantic. *J. Geophys. Res.*, 76:6283-6293.
- Lorenzo, J.M., and Mutter, J.C., 1989. Seismic stratigraphy and tectonic evolution of the Falklands/Malvinas plateau. *Rev. Bras. Geoc.*, 18:191-200.
- Lorenzo, J.M., Mutter, J.C., Larzon R.L., and the Northwestern Australia Study Group, 1991. Development of the continent-ocean transform boundary of the southern Exmouth Plateau. *Geology*, 19:843-846.

- Lorenzo, J.M., and Vera, E.E., 1992.** Thermal uplift and erosion across the continent - ocean transform boundary of the southern Exmouth Plateau. *Earth Planet. Sci. Lett.*, 108:79-92.
- Lowell, J.D., 1972.** Spitsbergen Tertiary orogenic belt and the Spitsbergen fracture zone. *Geol. Soc. Am. Bull.*, 83:3091-3102.
- MacDonald, K.C., Castillo, D.A., Miller, S.P., Fox, P.J., Kastens, K.A., and Bonatti, E., 1986.** Deep-tow studies of the Vema Fracture Zone: 1. Tectonics of a major slow-slipping transform fault and its intersection with the Mid-Atlantic Ridge. *J. Geophys. Res.*, 91:3334-3354.
- Machens, E., 1973.** The geological history of the marginal basins along the North shore of the gulf of Guinea. In A.E.M. Nairn, E.M., and F.G. Stehli, F.G. (Eds.), *The Ocean Basins and Margins: the South Atlantic*: New York (Plenum Press), 351-390.
- Mamaloukas-Frangoulis, V., Auzende, J.M., Bideau, D., Bonatti, E., Cannat, M., Honnorez, J., Lagabrielle, Y., Malavieille, J., Mevel, C., and Needham, H.D., 1991.** In-situ study of the eastern ridge-transform intersection of the Vema Fracture Zone. *Tectonophysics*, 190:55-71.
- Mascle, J., 1976.** Le golfe de Guinée: un exemple d'évolution de marge atlantique en cisaillement. *Mém. Soc. Géol. Fr., nouvelle série*, 128.
- Mascle, J., Auroux, C., and the Shipboard Scientific Team, 1989.** *Les marges continentales transformantes ouest-africaines (Guinée, Côte d'Ivoire-Ghana) et la zone de fracture de la Romanche: Campagne Equamarge II (Février-Mars 1988)*. Campagnes Océanographiques Françaises. Publications IFREMER.
- Mascle, J., and Blarez, E., 1987.** Evidence for transform margin evolution from the Côte d'Ivoire-Ghana continental margin. *Nature*, 326:378-381.
- Mascle, J., Blarez, E., and Marinho, M., 1988.** The shallow structures of the Guinea and Côte d'Ivoire-Ghana transform margins: their bearing on the equatorial Atlantic Mesozoic evolution. *Tectonophysics*, 155:193-209.
- Mascle, J., Guiraud, M., Basile, C., Benkhelil, J., Bouillin, J.P., Cousin, M., and Mascle, G., 1993.** The Côte d'Ivoire-Ghana transform margin: preliminary results from the *Equanaute* cruise (June 1992). *C. R. Acad. Sci. Paris*, 316:1255-1261.
- Moullade, M., and Guerin, S., 1982.** Le problème des relations de l'Atlantique Sud et de l'Atlantique central au Crétacé moyen: nouvelles données microfauniques d'après les forages D.S.D.P. *Bull. Soc. Geol. Fr.*, 7:511-517.
- Moullade, M., Mascle, J., Benkhelil, J., Cousin, M., and Tricart, P., 1993.** Occurrence of marine mid-Cretaceous sediments along the Guinean slope (*Equamarge II* cruise): their significance for the evolution of the central Atlantic African margin. *Mar. Geol.*, 110: 63-72.
- Neves, C.A.O., 1989.** Hydrocarbon generation, migration and accumulation in the Early Cretaceous continental sequence of the intracontinental Potiguar rift basin, northeastern Brazil. *B. Geoci. PETROBRAS*, 3(3):131-145.
- Ojoh, K., 1990.** Cretaceous geodynamic evolution of the southern part of the Benue trough (Nigeria) in the equatorial domain of the south Atlantic. Stratigraphy, basin analysis and paleoceanography. *Bull. Centres Rech. Expl. Prod. Elf Aquitaine*, 14(2):419-442.
- Ponte, F.C., and Asmus, H.E., 1978.** Geological framework of the Brazilian continental margin. *Geol. Rundsch.*, 67:201-235.
- Pontoise, B., Bonvalot, S., Mascle, J., and Basile, C., 1990.** Structure crustale de la marge transformante de Côte d'Ivoire-Ghana déduite des observations de gravimétrie en mer. *C. R. Acad. Sci. Paris*, 310:527-534.
- Popoff, M., 1988.** The mid-African rift system; basin evolution, magmatism, and rifting of the Benue Valley. In Mesozoic to Present Magmatism of the African Plate and its Structural Context. *Occasional Publication - International Center for Training and Exchanges in the Geosciences*, 15:180-186.
- Popoff, M., 1990.** Deformations intracontinentales gondwanienne: rifting Mésozoïque en Afrique [Thesis]. Univ. Marseille III.

- Popoff, M., Raillard, S., Mascle, J., Auroux, C., Basile, C., and Equamarge Group, 1989.** Analyse d'un segment de marge transformante du Ghana: résultats de la campagne *Equamarge II* (Mars 1988). *C. R. Acad. Sci. Paris*, 309:481-487.
- Rabinowitz, P.D., and La Brecque, J.L., 1979.** The Mesozoic Atlantic ocean and evolution of its continental margins. *J. Geophys. Res.*, 84:5973-6002.
- Scotese, C.R., Gahagan, L.M., and Larson, R.L., 1988.** Plate tectonic reconstructions of the Cretaceous and Cenozoic ocean basins. *Tectonophysics*, 155:27-48.
- Scrutton, R.A., 1976.** Crustal structure at the continental margin of South Africa. *Geophys. J. R. Astron. Soc.*, 44:601-623.
- Scrutton, R.A., 1979.** On sheared passive continental margins. *Tectonophysics*, 59:293-305.
- Scrutton, R.A., 1982.** Crustal structure and development of sheared passive continental margins. In Scrutton, R.A. (Ed.), *Dynamics of Passive Margins: Geodynamics Series*, 6:133-140.
- Sibuet, J.C., and Mascle, J., 1978.** Plate kinematic implications of Equatorial Fracture Zone trends. *J. Geophys. Res.*, 83:3401-3421.
- Todd, B.J., and Keen, C.E., 1989.** Temperature effects and their geological consequences at transform margins. *Can. J. Earth Sci.*, 26:2591-2603.
- Todd, B.J., Reid, I., and Keen, C.E., 1988.** Crustal structure across the Southwest Newfoundland transform margin. *Can. J. Earth Sci.*, 25:744-759.
- Vail, P.R., and Hardenbol, J., 1979.** Sea-level changes during the Tertiary. *Oceanis.*, 22:71-79.
- Zalan, P.V., Nelson, E.P., Warme, J.E., and Davis, T.L., 1985.** The Piauí Basin: rifting and wrenching in an Equatorial Atlantic transform basin. In Biddle, K.T., and Christie-Blick, N. (Eds.), *Strike-slip Deformation, Basin Formation and Sedimentation*. Spec. Publ. - Soc. Econ. Paleont. Miner., 37:143-158.

...Leg 160 - Eastern Equatorial Atlantic Transform...

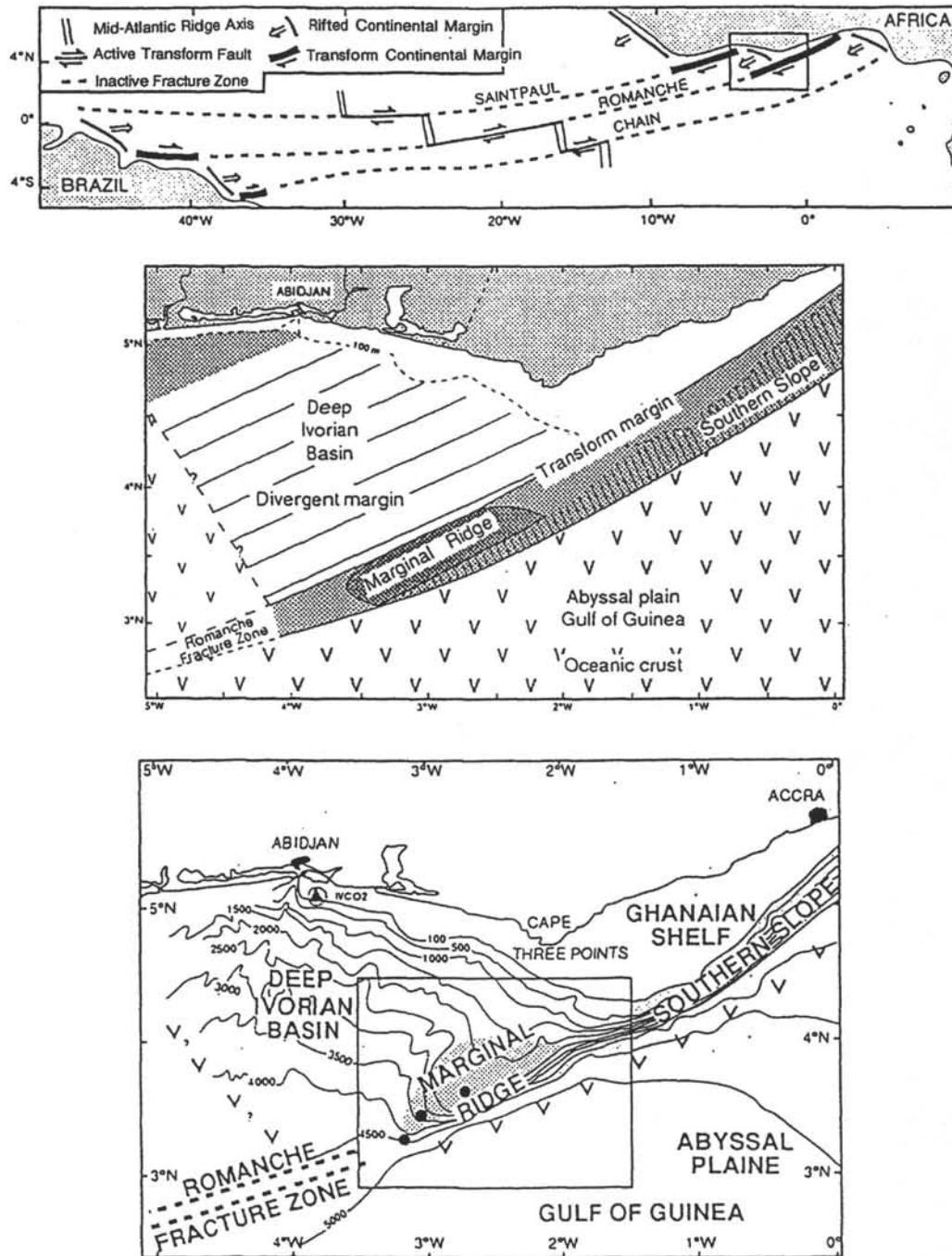


**Figure 1.** Geodynamic, geological and bathymetric framework of the ICG Transform Margin.

- 1A:** Fracture zones in the equatorial Atlantic and associated continental margins (modified from Gorini, 1977).
- 1B:** Structural sketch of the ICG continental margin and the different continent-ocean transitions observed. Shaded: transform margins including the ICG Marginal Ridge. The "V" indicates oceanic crust, older west of the Ivorian Basin than southward in the Gulf of Guinea.
- 1C:** Bathymetry (contour interval, 500 m) and main morphostructural domains of the ICG Transform Margin. The dots show location of proposed bore-holes, the triangle the location of hole IVCO2.

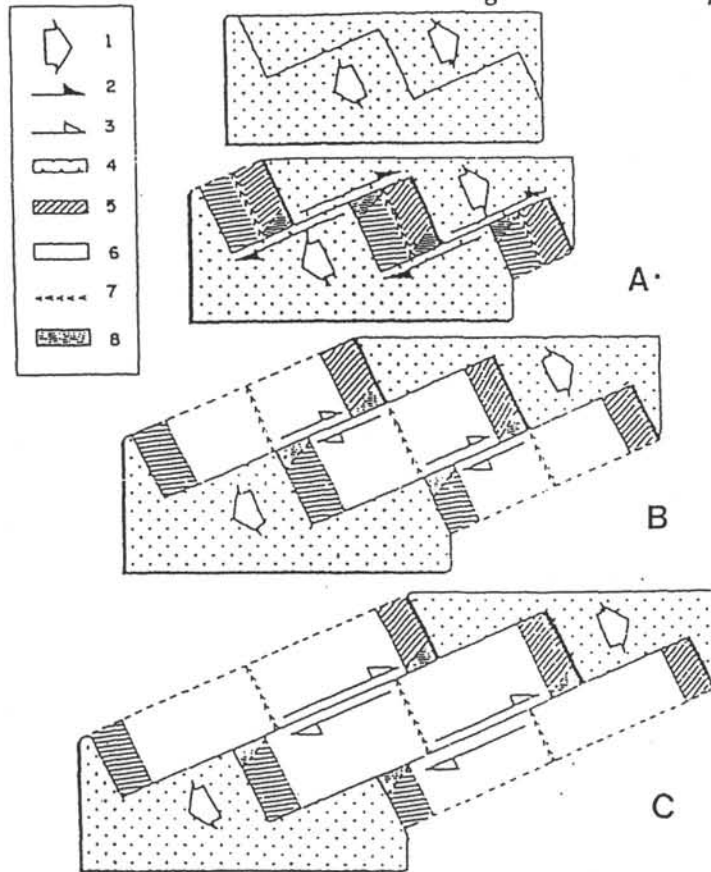


**Figure 2.** Schematic diagram illustrating the main stages in the evolution of a rift-transform margin. (1) divergence, (2) and (3) transform motion between respectively continental and oceanic crust, (4) normal continental crust, (5) thinned continental crust, (6) oceanic crust, (7) ridge axis, and (8) marginal ridge.

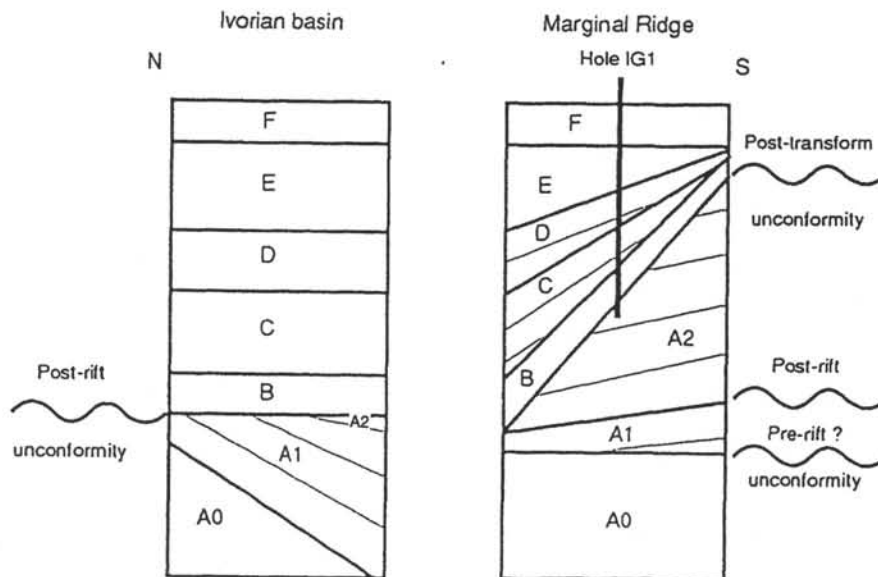


**Figure 3.** Relationship between the sedimentary units in the Ivorian Basin and marginal ridge.

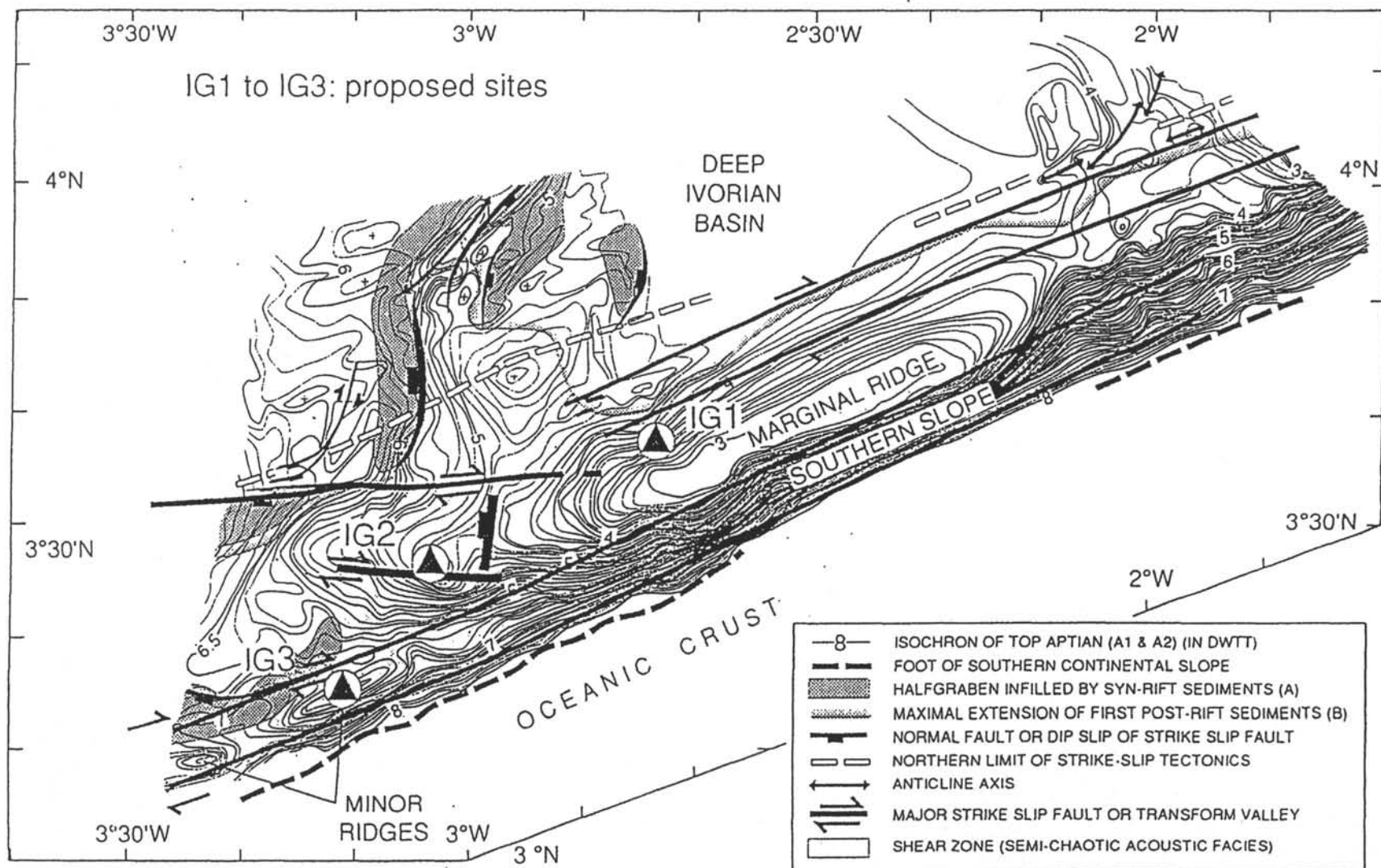
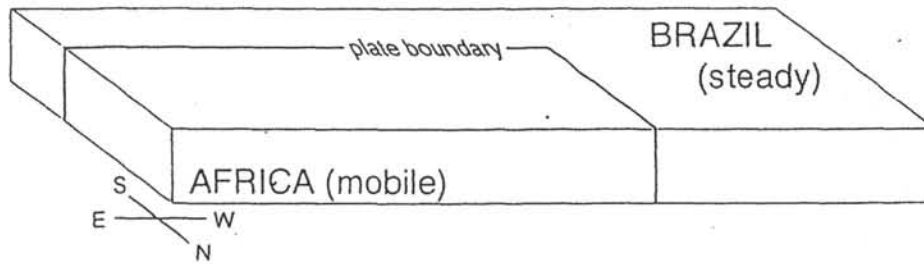
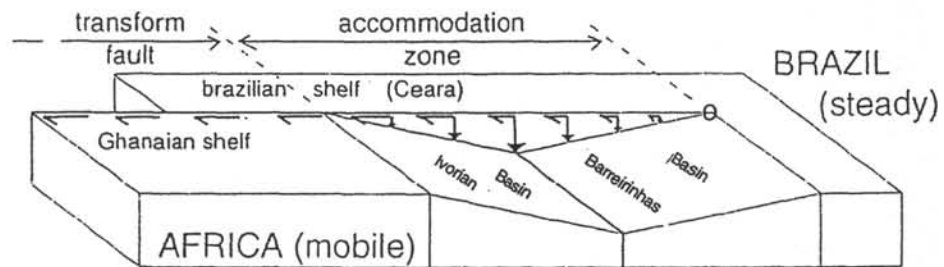


**Figure 4.** Simplified structural map of the ICG deep margin. Depth is shown in two-way travel time to the top of the synrift Unit A. The fossil marginal ridge appears as the prominent feature of the margin. Only the main tectonic elements are shown.

INITIAL SETTING



SYN-RIFT STAGE



POST-RIFT STAGE

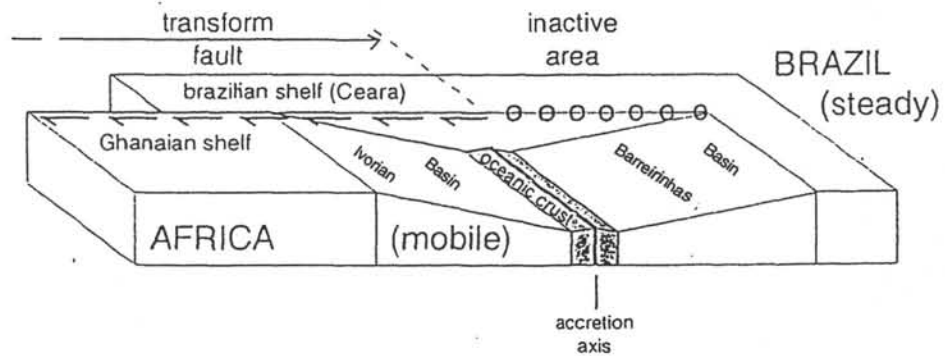


**Figure 5.** Kinematic evolution of the southern border of the deep Ivorian Basin during opening (view from the north). The South American Plate (Brazil) is supposed to be fixed. Arrows show horizontal (strike-slip) and vertical (dip-slip) relative motions between the steady plate and the moving African Plate. 0 indicates no motion.

...Leg 160 - Eastern Equatorial Atlantic Transform...

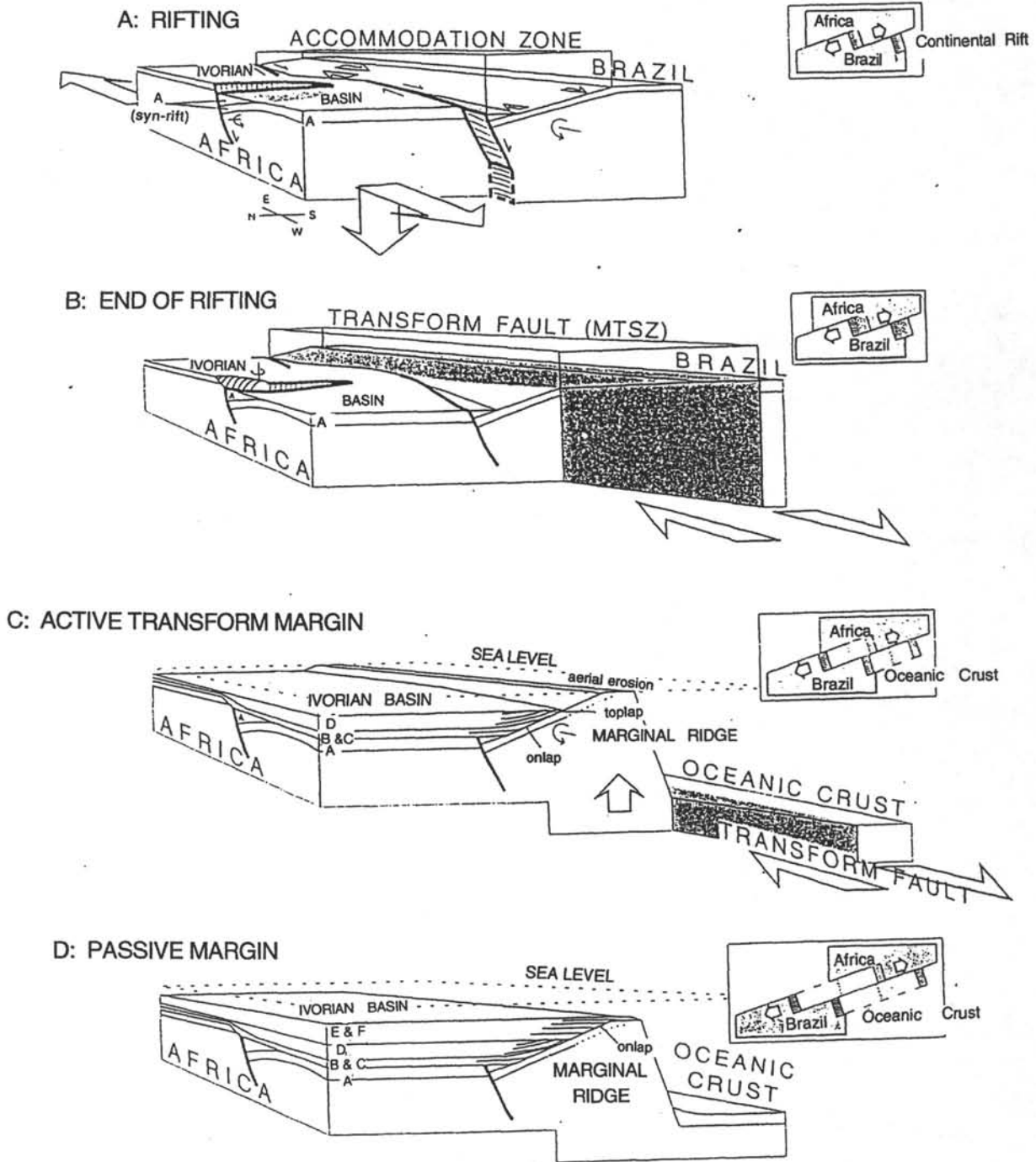


**Figure 6.** Four stages of the formation of the ICG Margin. Views from the WNW. In (A), the shaded area shows the north-south and east-west synrift basins (in the deep Ivorian Basin and along the marginal ridge, respectively) and the white arrows in the accommodation zone show the relative horizontal motion. In (B) and (C), the shaded belt shows the transform fault.

## TABLE 1

### PROPOSED SITE INFORMATION and DRILLING STRATEGY

<b>SITE:</b> IG-1	<b>PRIORITY:</b>	<b>POSITION:</b> 3°37.6'N, 2°44.1'W
<b>WATER DEPTH:</b> 2100m	<b>SEDIMENT THICKNESS:</b> 1600m	<b>TOTAL PENETRATION:</b> 1600m
<b>SEISMIC COVERAGE:</b> MCS line MT2 and SCS line 10 ( <i>Equamarge</i> , 1988)		

**Objectives:** To drill the post-tectonic sedimentary cover (Units C to F), the early post-rift (and syn-transform) sedimentary Units B and A2, in order to elucidate deformation history, vertical movements, and sedimentary evolution of the marginal ridge.

**Drilling Program:** Multiple bit and reentry.

**Logging and Downhole Operations:** FMS, seismo-stratigraphic and geochemical tools.

**Nature of Rock Anticipated:** Post-rift clays, marls, and siltstones and syn-rift sandstones and indurated shales.

OR

<b>SITE:</b> IG-1bis	<b>PRIORITY:</b>	<b>POSITION:</b> 3°35.3'N, 2°43.9'W
<b>WATER DEPTH:</b> 2062m	<b>SEDIMENT THICKNESS:</b> 780m	<b>TOTAL PENETRATION:</b> 780m
<b>SEISMIC COVERAGE:</b> MCS lines MT2 and MT5.		

**Objectives:** To drill the post-tectonic sedimentary cover (Units C to F), the early post-rift (and syn-transform) sedimentary Units B and A2, in order to elucidate deformation history, vertical movements, and sedimentary evolution of the marginal ridge.

**Drilling Program:** Multiple bit and reentry.

**Logging and Downhole Operations:** FMS, seismo-stratigraphic and geochemical tools.

**Nature of Rock Anticipated:** Post-rift clays, marls, and siltstones and syn-rift sandstones and indurated shales.

<b>SITE:</b> IG-2	<b>PRIORITY:</b>	<b>POSITION:</b> 3°26.5'N, 3°03.6'W
<b>WATER DEPTH:</b> 3338m	<b>SEDIMENT THICKNESS:</b> 780m	<b>TOTAL PENETRATION:</b> 780m
<b>SEISMIC COVERAGE:</b> MCS line MT5 and SCS line 24 ( <i>Equamarge</i> , 1988)		

**Objectives:** To investigate the diagenesis and strike-slip deformation of syn-rift Units A1 and A2, the nature of dipping reflectors (sedimentary layers, unconformity, thrust fault?), the subsidence of the marginal basin, and syn-rift or syn-transform faulting.

**Drilling Program:** Single bit coring.

**Logging and Downhole Operations:** FMS, seismo-stratigraphic and geochemical tools.

**Nature of Rock Anticipated:** Oozes, sandstones, and shales

**OR**

<b>SITE:</b> IG-2bis	<b>PRIORITY:</b>	<b>POSITION:</b> 3°18.1'N, 3°22.9'W
<b>WATER DEPTH:</b> 4500m	<b>SEDIMENT THICKNESS:</b> 800m	<b>TOTAL PENETRATION:</b> 800m
<b>SEISMIC COVERAGE:</b> MCS line MT5 and SCS line 35 ( <i>Equamarge</i> , 1988)		

**Objectives:** To investigate the diagenesis and strike-slip deformation of syn-rift Units A1 and A2, the nature of dipping reflectors (sedimentary layers, unconformity, thrust fault?), the subsidence of the marginal basin, and syn-rift or syn-transform faulting.

**Drilling Program:** Single bit coring.

**Logging and Downhole Operations:** FMS, seismo-stratigraphic and geochemical tools.

**Nature of Rock Anticipated:** Oozes, sandstones, and shales.

<b>SITE:</b> IG-3	<b>PRIORITY:</b>	<b>POSITION:</b> 3°15.4'N, 3°11.1'W
<b>WATER DEPTH:</b> 4650m	<b>SEDIMENT THICKNESS:</b> 550-700m	<b>TOTAL PENETRATION:</b> 700m
<b>SEISMIC COVERAGE:</b> MCS line MT1 and SCS lines 28 and 37 ( <i>Equamarge</i> , 1988)		

**Objectives:** To investigate the lithology, nature, deformation history and metamorphism of the acoustic basement of the minor ridges along strike of a transform margin, near its junction with an extinct fracture zone and to investigate hydrothermalism and thermal effects of the adjacent oceanic crust.

**Drilling Program:** Single bit coring

**Logging and Downhole Operations:** FMS, seismo-stratigraphic and geochemical tools.

**Nature of Rock Anticipated:** Oozes, clays, and metasediments and 0-150 m of continental gneiss or magmatic basalt.

*LEG 161*

*Mediterranean Sea I -  
The Eastern Mediterranean*

# LEG 161

## MEDITERRANEAN SEA I - THE EASTERN MEDITERRANEAN

---

Modified from Proposals 330-Rev and 391-Rev2 Submitted By:

Angelo Camerlenghi, Nicolas Chamot-Rooke, Maria-Bianca Cita, Bruno Della Vedova,  
Ditza Kempler, Werner Hieke, Hans Hirschleber, Kim Kastens, Yossi Mart,  
Floyd McCoy, Lorenzo Mirabile, A. Polonia, M. Rebesco, Alastair H.F. Robertson  
and Rainer Zahn, Maria-Bianca Cita, Gert de Lange, Kay-Christian Emeis, and Adrian Cramp

To Be Named: Co-Chief Scientists and Staff Scientist

---

### ABSTRACT

Leg 161 represents the first in a two-leg program to investigate the tectonic and paleoceanographic history of the Mediterranean Sea and focuses upon the processes associated with accretion at incipient continental collision on a salt-bearing accretionary complex, and the origin of sapropels, laminated organic-rich layers deposited in the eastern Mediterranean Basin. To achieve the tectonic objectives of identifying the incoming sediment, rates of outward growth and uplift of the deformation front, and the influence of the Messinian evaporites on the interstitial fluid circulation, drilling will be conducted in zones of terminal subduction at near-orthogonal and low-angle plate convergence, and of initial continental collision where the deformed sediments of the Mediterranean Ridge override the African continental slope. Drilling on the Napoli mud volcano on the crest of the ridge will provide insight into diapiric processes while a transect of sites from the top of the Eratosthenes Seamount to the Cyprus Margin will identify the tectonic phases that led to the present structure of the seamount.

Sapropels are deposited in a rhythmic fashion unrelated to global glacial-interglacial cycles but driven by distinctive changes in physical circulation and biogeochemical cycling possibly related to precession-induced fluctuations of monsoonal atmospheric circulation. One hypothesis for their origin postulates that the deeper water column went anoxic during their formation, fostering preservation of organic carbon at the sea floor. A second hypothesis favors increased primary productivity as the ultimate stimulus through increased rates of carbon flux to the sea floor. Variations in sediment texture, dilution, and the settling flux of carbon exert a dominant control on the carbon contents of sediments and water column redox conditions may play only a secondary role (Pedersen and Calvert, 1990). Recent evidence that the early-Holocene sapropel found in the Black Sea, the "type" euxinic basin in the stagnation/anoxia hypothesis, has accumulated under well-ventilated conditions, appears to underscore the importance of productivity over anoxia.

## INTRODUCTION

### **Tectonics of the Eastern Mediterranean**

This leg represents the first phase of a drilling program to investigate the collisional margin of the eastern Mediterranean. This current program of shallow-drilling addresses the fundamental processes associated with accretion during incipient continental collision on a salt-bearing accretionary complex through a number transects along the entire collisional margin. (Fig. 1A).

Continental collision is the final stage of the opening and closing of an oceanic basin. The eastern Mediterranean is a unique example of closure of an ocean basin, the Mesozoic Tethys, namely Mesogea (Biju-Duval et al., 1978; Boccaletti, 1979; Dewey and Sengor, 1979; Le Pichon, 1982; Dewey et al., 1986). The transition between the remnants of a thick Mesozoic oceanic crust, located in the Ionian Basin (de Voogd et al. 1992) and perhaps in the Levantine Basin (Garfunkel and Derin, 1984), and the African continental margin enters the Aegean Subduction Zone (Dewey et al., 1973; MacKenzie, 1978). A large accretionary complex, the Mediterranean Ridge (Kastens 1991; Kastens et al., in press), formed in a complicated setting of alternating zones of continental collision, the Pelagian Promontory, the Cyrenaica Promontory and the Eratosthenes Seamount (Nur and Ben Avraham, 1978; Kempler and Ben-Avraham, 1987; Robertson et al., 1991), and terminal subduction (Fig. 1A).

Consumption of an oceanic basin implies that lateral heterogeneities in the incoming lithospheric plate (seamounts, fracture zones, basement ridges, the mid-ocean ridge) progressively reach the trench and interact with the structure of the convergent continental margin, causing a complex style of deformation of the offscraped sediments (e.g., Tonga Kermadec Trench, New Hebrides, Japan, and Peru convergent margins) and changes in the uplift rates and thermal regime of the accretionary complex (e.g., Aleutian margin, Chile Ridge, and Pacific margin of the Antarctic Peninsula). Examples of these cases are rather frequent in the present day narrowing oceanic basins.

There are very few places on Earth where the ocean-continent crustal transition at a passive continental margin approaches the subduction zone; two of these are the eastern Indonesian Arc and the eastern Mediterranean Sea, both belonging to the same "collisional-type" orogenic belt (Alpine-Himalayan), in contrast to the "cordilleran-type" orogenic belts. The two zones of continental collision bear some similarities. A large continental plate (Australia and Africa, respectively)

collided with a continental block in approximately north-south direction and a thick pile of sediments, as old as Mesozoic, is being deformed at the collisional margin (Timor/Sumba Ridges and Mediterranean Ridge, respectively); lateral transition between continental and oceanic crust occurs in the collisional area (Argo Abyssal Plain and Ionian/Herodotus Abyssal Plains, respectively). The processes of collisional deformation are in a more advanced stage in the Indian Ocean (e.g., the accretionary complex has emerged at Timor) while, in the eastern Mediterranean, a wide spectrum of collisional settings is present, including incipient collision, due to the very irregular shape of the eastern Mediterranean convergent margin.

### **The Origin of Sapropels**

Depositional sequences retrieved in sediment cores from the eastern Mediterranean and exposed on land in Neogene sections in southern Italy, Sicily, and Crete have revealed the existence of numerous dark to black colored layers which are intercalated in "normal" hemipelagic sediments. These layers are enriched in organic carbon and often laminated, and are referred to as sapropels. Sapropels are believed to be deposits characteristic for restricted basins of marginal seas, a contention which has been supported by ODP Legs 127 and 128 which discovered numerous alternating layers of "normal" pelagic oozes and laminated organic-rich sections in Miocene through Holocene sediments of the Japan Sea (Cramp and Lewis, 1992; Föllmi et al., 1992; Tada et al., 1992). However, laminated organic-rich sediments have recently also been found during ODP Leg 138 in the eastern equatorial Pacific (Kemp and Baldauf, 1993) i.e., in an open-ocean environment. In all cases it seems that the deposition of organic-rich sediments occurred in response to unusual, very distinctive changes of the regional water mass circulation and marine chemical cycling.

According to traditional models laminated organic-rich facies accumulates under stagnant, anoxic conditions as was originally proposed by Kullenberg (1952) and later by Olausson (1961). This thinking model was based on the supposition that organic matter is more amendable to oxic as compared to anoxic degradation, leading to the conclusion that organic carbon preservation should be greatly enhanced during oceanic anoxia. Laminated organic-rich facies is found throughout the Black Sea which is considered the type-euxinic basin with little or no oxygen at depth, thus also supporting the axiomatic association between laminated organic-rich sediments and anoxic deep-water conditions. The absence of benthic foraminifera in most sapropels is further used as a strong indication for bottom water anoxia.

However, the tenet that the deposition of organic-rich sediments is primarily a function of deep water anoxia is open to question. For instance, it is well documented that the accumulation of organic carbon at coastal upwelling sites throughout the world ocean varied by up to one order of magnitude during glacial-interglacial times even though the organic-rich sediments at these sites accumulate in dynamic flow regimes of local bottom currents where bottom waters are neither anoxic nor stagnant (e.g., Calvert and Price, 1983; Reimers and Suess, 1983; Pedersen, 1983; Müller et al., 1983; Morris et al., 1984; Sarnthein et al., 1988; Zahn and Pedersen, 1991; Sancetta et al., 1992). Furthermore, the early-Holocene sapropels found in Black Sea sediment cores have conceivably accumulated under well-oxygenated conditions as is implied by the distribution of manganese, iodine and bromine in these sediments (Calvert, 1990). A systematic reevaluation of published data suggests that organic carbon levels in marine sediments are primarily a function of sediment texture, dilution and carbon flux, rather than of water column oxygen levels (Pedersen and Calvert, 1990). Thus, these studies are now calling attention to biological productivity combined with distinctive changes in physical water mass circulation as important controls of the formation of organic-rich, sapropelic deposits.

The Mediterranean sapropels represent paleoceanographic windows through which we may study, in great detail, key processes which lead to the burial and preservation of carbon at the sea floor in relation to marine chemical cycling and physical water mass circulation. During Leg 161 (Fig. 1B), we will undertake a systematic stable isotope, geochemical and micropaleontological survey of the Mediterranean sapropels in a concerted program using stable isotope stratigraphy and paleoceanography (foraminiferal  $\delta^{18}\text{O}$  and  $\delta^{13}\text{C}$ ), geochemical oxygen, nutrient and productivity tracers (Ba, Br, Cd, I, Mn), carbon source biomarkers (long-chain alkenones, dinosterol, plantwax lipids,  $\delta^{13}\text{C}_{\text{org}}$ ,  $\delta^{15}\text{N}_{\text{org}}$ ), and microfaunal assemblage analysis.

The timing of the eastern Mediterranean sapropel events apparently correlates with maxima of the precession-related monsoonal index (Rossignol-Strick, 1983; Hilgen, 1991). To examine this apparent correlation, we will investigate the influence of the long-term development of monsoonal circulation over the Indian Ocean on the formation of the Mediterranean sapropels as far back as the Miocene when the monsoonal circulation evolved in response to the tectonic uplift of the Himalayas and the Tibetan Plateau.

## STUDY AREA

### Regional Framework

The Mediterranean Ridge is a 1300-km-long, 300- to 150-km-wide arcuate submerged relief (Fig. 1A). To the southeast and southwest of the ridge, narrow abyssal plains (Ionian, Sirte, and Herodotus) separate the deformation front from the African continental slope. South of the central section of the ridge, the folded sediments of the deformation front lean directly against the African continental slope of the Cyrenaica Peninsula. North of the ridge is a complex system of deep trenches, on average deeper than the southern abyssal plains, called the Hellenic Trench System. The minimum water depth on the ridge crest is around 1200 m. The maximum depth in the Hellenic Trench is 5100 m, and the depths of the outer abyssal plains are between 4150 and 3200 m, shallowing toward the Nile deep-sea fan. The topography of the ridge is characterized by the alternation of small rimmed basins and ridges oriented roughly parallel to the deformation front which produces a hummocky acoustic reflection (cobblestone topography of Emery in Hersey, 1965).

Convergence in the eastern Mediterranean is produced by the relative plate motion among Africa, Eurasia, and the Aegean microplate. According to kinematic analysis (Le Pichon and Angelier, 1979; Jongsma et al., 1987), subduction is near-orthogonal in a northeast direction in the Ionian Basin, at low-angle in the western Levantine Basin (prevailing left-lateral strike slip), and again near orthogonal in the easternmost Levantine Basin (Cyprus Arc).

Crustal thickness of the incoming plate indicates that southwest and southeast of the Mediterranean Ridge, oceanic or thinned continental crust exists, while crustal thickening occurs under the Mediterranean Ridge and the Hellenic Trench system (Rabinowitz and Ryan, 1970; Woodside and Bowin, 1970; Finetti, 1976; Makris, 1977; Giese et al., 1982; Makris et al., 1983; Makris and Stobbe, 1984; Underhill, 1989; deVoogd et al., 1992; and Hipkins et al., submitted). The crust is thicker between the Cyrenaica Promontory and Crete Island (the narrower segment of the eastern Mediterranean with no abyssal plain seaward of the deformation front) where continental collision occurs. North of the Hellenic Trench System, are the non-volcanic arc of Crete (continental crust) and the Aegean back arc basin (Horvath and Berckhemer, 1982) in which andesitic volcanism has developed (Fytikas et al., 1984). The horizontal component of the gravity vector (Brennecke and Lelgemann, 1986) clearly evidences the horizontal heterogeneities in the mass distribution of depth

related to the continental convergence. The seismological evidence of the African-Eurasian plate boundary in the eastern Mediterranean is located along the Hellenic Trench System, where a broad zone of intermediate depth earthquakes (not exceeding the depth of 200 km) roughly delineate a generally northward dipping subducting lithospheric slab (Wortel et al., 1990). The biggest uncertainty in the Hellenic subduction zone concerns the age of onset of subduction, which has been estimated in the range between 5 Ma (McKenzie, 1978; Kissel and Lay, 1988) and about 100 Ma (Wortel et al., 1990).

The accretionary nature of the Mediterranean Ridge has been defined through gradual recognition of the compressional tectonics which moved the ridge from the role of Outer Swell to that of Accretionary Complex. Offscraping of sediments from the African plate must be older than 33 Ma (Kastens, 1991) and occurs with development of two deformation fronts with opposite vergence (Fig. 2). The Outer Deformation Front is located along the abrupt morphologic change between the flat abyssal plains and the rough topography of the ridge, and provides generally southward vergence of tectonic structures. The Inner Deformation Front is located along the escarpment that delimits to the north the ridge crestal plateau, and provides generally northward vergence and wide spread evidence of mud diapirism. The Inner Deformation Front causes the deformed sediments of the Mediterranean Ridge to thrust over the rather flat and undeformed continental plateau (Inner Plateau ) where a Messinian sedimentary depocenter provides the evidence of an ancient fore-arc basin (Camerlenghi et al., in preparation).

Reliable and accurate temperature measurements were taken at DSDP Sites 374 (Ionian Abyssal Plain, seaward of the Western Deformation Front of the Mediterranean Ridge), 376 (Florence Rise, Cyprus Arc), and 378 (Southern Aegean Sea) (Erickson and von Herzen, 1978). The low heat flow obtained from Sites 374 and 376 ( $33.5 \text{ mWm}^{-2}$  and  $39.4 \text{ mWm}^{-2}$ , respectively) and from the other conventional measurements available in the area provide a valuable constraint to the regional thermal regime of the eastern Mediterranean. The few heat flow measurements located on the Mediterranean Ridge show, on average, values lower than  $30 \text{ mWm}^{-2}$  that could be caused by widespread downward flux of seawater in the sediments overlying the evaporites. Local positive anomalies, however, can be expected where fluid expulsion or mud diapirism occur (e.g., Barbados Ridge). Heat-flow measurements in the drill holes across the eastern Mediterranean area may thus provide valuable in reconstructing fluid paths within the accretionary complex.

## **Frontal Deformation**

The style of initial deformation of the sediments on the outer edge of the Mediterranean Ridge is different in the three different settings which are related to the angle of plate convergence.

### *Ionian Deformation*

The deformation front (Fig. 3) is defined by the sudden change from the flat and layered reflections of the Ionian Abyssal Plain to the hyperbolic patterns produced by the "cobblestone topography" of the Mediterranean Ridge. A 10.5-km-long, 310-m-high seahill strongly oriented in southwest-northeast direction (about 45° with respect to the regional trend of the Mediterranean Ridge) is located a few kilometers seaward of the deformation front (Victor Hensen Seahill, Hieke, 1978). It is the highest part of the Victor Hensen Structure which can be traced in the subbottom over 60 km in a southwest-northeast direction.

Recently acquired MCS lines (Cruise *Valdivia* 120 MEDRAC, 1992) provide evidence of several elongated structures indicating intense pre-Messinian tectonic activity under the Ionian Abyssal Plain, seaward of the Ionian Deformation Front. The structures are elevated from a sequence of partly tilted pre-Messinian sediments. However, the tops of the elongated structures are sometimes free of evaporites. At this stage of the data processing, the style of deformation can be either indicative of extensional block-faulting or of faulted and thrust anticlines separated by tilted piggy-back basins.

Since Messinian evaporites and overlying P-Q turbidites show less evidence of deformation, the main part of the tectonic phase that produced these structures must be, at the latest, of Messinian age (about 5 Ma). However, the deformation continued during the Pliocene-Quaternary with synsedimentary extensional faulting (Avedik and Hieke, 1981; Hieke and Wanninger, 1985; Hieke, in preparation).

The Victor Hensen Structure interacts with the present day deformation front, indicating that a complicated pattern of varying lithologies and thickness of sediments become incorporated in the Mediterranean Ridge accretionary complex. The styles of initial deformation are thus expected to be correspondingly different.

The proposed transect of shallow holes is intended to sample the incoming sediment section overlying the buried Victor Hensen Structure in the abyssal plain and the post-Messinian deformed sediment of the ridge.

### **Mud Diapirism**

Mud diapirism on the Mediterranean Ridge has been recently identified through high resolution seismic reflection profiles and gravity coring (Cita et al., 1989; Camerlenghi et al., 1992) in a narrow area of the northern edge of the 'upper plateau', the flat crestral area of the ridge, although at present there are no multibeam bathymetric, side scan sonar, and deep-towed camera data to describe the phenomenon. Extensive Mark 2 Gloria surveys of the Mediterranean Ridge (Kenyon et al., 1982) outlined the presence on the central crestral area of the Mediterranean Ridge of numerous tectonic trends with relief up to 130 m, but these were interpreted as outcrops of thrusts. We now correlate that evidence to mud diapirism.

There is indirect (seismic only) evidence of mud diapirism also on the escarpment (northern boundary of the 'Upper Plateau') and in the 'Inner Plateau', a flat floored, undeformed sedimentary basin located between the crest of the Mediterranean Ridge and the Hellenic Trench. The seismic and morphological evidence of northward vergent thrusting and the occurrence of mud diapirism associated to the escarpment suggest that this is in fact an active deformation front with arcward vergence (Camerlenghi et al., in prep.).

Both mud diapirs and mud volcanoes have been identified on the Mediterranean Ridge. For the first time in the study of mud diapirism, several cores have been taken on the domes in order to analyze the diapiric material in terms of lithology, sedimentology, micropaleontological content, geochemistry and geotechnical properties (Camerlenghi, 1990). Heat flow measurements, taken in the area of the mud diapir fields (Pellis, pers. comm.; Cruise Report BAN-89), returned evidence that the diapiric material is a grey clay- and silt-sized, matrix-supported breccia with centimeter-size subrounded clasts of semi-indurated sediment, that the age of the source formation is Oligocene-Neogene (Cretaceous age has been documented for the westernmost diapiric field according to Cita et al., 1981), and that the clay mineral composition of the diapiric material reflects the Nile sediment composition, with stronger affinity (high smectite content) in the easternmost fields (closer to the Nile cone); higher illite/smectite ratio found in the "Napoli" mud volcano can be tentatively explained by dehydration of smectite. Sedimentary structures and textures permitted identification

of reworked mud flow deposits, mud lake deposits, and 'primitive' (intrusive) diapiric material. Gas-escape sedimentary structures are common and a strong salinity gradient has been found in the pore fluids of the 'Napoli' mud volcano, suggesting interaction of the diapiric material with the Messinian evaporites during the ascent to the surface. The diapiric material displays lower porosity than the hemipelagic surface host sediments and consolidate like a remolded specimen. Calculations on the depth of provenance of the diapirs, based on hydrostatic equilibrium between the diapiric mass and the surrounding host sediments, indicates a minimum depth ranging between 600 and 1000 mbsf (Fig. 4), and both thermogenic and biogenic methane has been detected in the pore fluids of the diapiric material. The geothermal gradient obtained from the heat flow measured in the diapiric area ( $20\text{-}30\text{ }^{\circ}\text{Ckm}^{-1}$  and  $12\text{-}30\text{ mWm}^{-2}$ , respectively) suggests that the  $75^{\circ}\text{C}$  isotherm, the temperature generally assumed for cessation of methanogenic bacterial activity (Fuex, 1977), will be found between 2.0 and 3.1 km below seafloor. Many of these conclusions, supported by seismic evidence, clearly indicate that the diapirs come from below the Messinian evaporites.

Although the information provided by the mud diapirs on the lithological composition of the pre-evaporitic strata are scarce due to their chaotic internal structures (they can be described as sedimentary mélanges), the composition of the pore fluids of the diapiric material may provide useful information on the deep fluid composition of the Mediterranean Ridge accretionary complex.

### **The Eratosthenes Seamount**

The Eratosthenes Seamount, the most prominent bathymetric feature between the Nile Cone and Cyprus, is an elevated structure surrounded by a deep moat, which rises to more than 1500 m above its surroundings. The seamount forms the highest part of a much larger structural high interpreted as a partly volcanic construction over a continental block, which was stranded in the Levant Basin following Early Mesozoic Neo-Tethys rifting (Kempler and Garfunkel, in press). This interpretation agrees with past studies, which indicated that the crust beneath the Eratosthenes is continental, comparable with that of Cyprus and Israel (Makris et al., 1983). The seamount is also associated with a big positive magnetic anomaly, caused by a bigger and deeper-located structure (Ben-Avraham et al., 1976). Attached to the African Plate since Early Mesozoic times, the Eratosthenes Structural High witnessed the opening and the closure of the Neo-Tethys Ocean, and the evolution of the eastern Mediterranean Sea throughout its geologic history. The seamount

recorded, by superposition of a number of structural elements, the different phases of this evolution (Kempler and Garfunkel, in prep.).

A quadrilateral graben, delimited by steep fault scarps that probably originated as Miocene strike-slip faults, is superimposed on the Eratosthenes Structural High. Downfaulting of the central area of this graben through post-Messinian reactivation of the steep faults in a vertical sense, produces the moat around the topographic high (Kempler and Garfunkel, in press). Messinian evaporites pinch out outside the graben and seem to be absent in the graben and on the seamount, indicating that the Eratosthenes was a well expressed physiographic feature in Messinian times, its peak (the present seamount) more than 1500 m higher than the top of the evaporites strata. However, this argument is based only on the interpretation of multichannel seismic reflection profiles, and is therefore a working hypothesis. The proposed drill sites on the Eratosthenes Seamount will reach rock units which may be suspected as non-evaporite equivalents of the Messinian unit, or evidence for subaerial erosion related to the Messinian desiccation and sea-level drop. A thorough identification of these units is important not only for a better understanding of the Messinian event, but because they are probably the best reference marker in the Neogene sedimentary sequence of the Mediterranean. Moreover, the non-deposition of Messinian evaporites on the Eratosthenes Seamount results in the absence of halokinesis, which has distorted the overlaying sediments elsewhere in the eastern Mediterranean. Therefore we expect to drill a non-interrupted Plio-Pleistocene series.

The relatively flat summit of the seamount is delimited by scarps of normal faults that form a series of terraces around the summit. We presume that the rock units which form the Eratosthenes summit have recorded sea-level fluctuations, changes in intermediate water-mass levels, and evidence for tectonic and seismic activity since the Cretaceous. Therefore these strata thoroughly represent the paleosedimentology, paleoceanography, and tectonic events in the eastern Mediterranean. Moreover, the Eratosthenes summit seems to be unaffected by high-rate deposition of Nile-derived sediments and their blurring effect; therefore, its sedimentary cover is thinner than the Plio-Pleistocene sedimentary sequence elsewhere in the eastern Mediterranean. This reduced thickness of the sedimentary cover guarantees efficient drilling. The smooth topography indicates that slumping was not significant here. Unconformities in the sedimentary record on the Eratosthenes summit may therefore be attributed to regional phenomena rather than local disruptions.

Due to its mid-water and geographically central location, the sedimentary cover of the Eratosthenes is expected to be especially sensitive to Plio-Pleistocene anoxic events. Sapropels deposited under anoxic conditions would show up as changes in color and organic carbon content, reflecting changing chemistry and water circulation changes. Biostratigraphic components should be particularly good indicators of anoxia from mass mortality of benthic life, to modification of planktonic assemblages of foraminifera, calcareous nannoplankton, and diatoms. Interpretations derived from these biostratigraphic indicators should document changes in surface-water circulation. These changes could be attributed to various causes, such as drop in surface water productivity in response to an influx of fluvial and/or melt water into the Mediterranean by monsoonal activity or melting of glaciers, or surface water modifications derived from upwelling, related to periodic overturning of the anoxic basin. The proximity of the Nile is particularly advantageous to testing the hypothesis of monsoonal control as the cause of the regional anoxia via increased fluvial discharge from the Nile.

Intensive diffusive exchange of many elements occurs at the water-sediment interface, and clays are notably reactive. The alkalinity/chlorinity ratio of the interstitial water of Quaternary sediments is much higher than that of the present Mediterranean water (Emelyanov and Shimkus, 1986). Considerable fluctuations in this ratio reflect not only different intensities of sulphate reduction, but indicate carbonate precipitation as well, and contribute to the reconstruction of the environmental physicochemical conditions in the eastern Mediterranean.

The Eratosthenes summit today lies in the Levantine Intermediate Watermass, where bottom current erosion should be insignificant (Wust, 1961). Therefore, the summit sediments should be sensitive to changes in the position of this watermass over time, especially over the past few million years, since the Mediterranean Sea evolved to have only a western outlet to the world ocean system at Gibraltar.

### **Circulation and Water Mass Distribution in the Mediterranean Sea**

The Mediterranean's physical circulation is mainly driven by the surface wind field and modulated by its complex bottom topography. Its principal features resemble those of an open-ocean sub-basin (100-km-scale) and mesoscale (10-km-scale) eddy circulation which is driven by seasonal winds and thermohaline gradients. This circulation pattern defines the distribution of nutrients in the

Mediterranean, which tend to be highest in the western basin and lowest in the eastern basin (Fig. 5), thus leading to inter-basin differences in primary production.

In the present situation evaporation exceeds precipitation and river runoff, the negative water balance being compensated by the inflow of Atlantic waters through the Strait of Gibraltar. Inflowing Atlantic waters are nutrient-enriched, warmer (15°C), and less saline (36.3‰) compared to the outflowing deeper water masses (13°C, 38.2‰). Inflowing Atlantic waters affect the circulation of the entire Mediterranean basin in that they generate cyclonic gyres in the Balearic and Tyrrhenian Seas. Atlantic water is transported into the eastern Mediterranean Basin by way of the North African Current which flows along the African coast and passes through the Sicily Channel. Once they have reached the far eastern parts of the eastern basin, evaporation is high enough to increase surface salinities to an extent that convection of the surface water to greater depth occurs. This way, Levantine Intermediate Water is formed which flows westward into the western Mediterranean and further through the Strait of Gibraltar into the Gulf of Cadiz and North Atlantic. Bottom waters are also generated in the eastern basin; they are restricted in areal extent to the eastern basin since the shallow topography of the Sicily Channel prevents any exchange of abyssal water masses between the eastern and western basins.

Besides their influence on the Mediterranean's physical circulation, inflowing Atlantic waters also define the biogeochemical and physical inventory of the upper layer (50 m) which drives the primary production in the Mediterranean and controls the flux of biologically-cycled constituents to the seafloor and into the sediments. The close connection between the Mediterranean's general circulation and the asymmetric distribution of trophic levels between its western and eastern basins points to the importance of understanding the past variability of the Mediterranean's physical oceanography as a whole so as to unravel the origin of sapropel formation in the east. In particular, inversions of the evaporation-precipitation balance could have resulted in the development of a much stronger pycnocline and altered the physical circulation throughout the Mediterranean. This could ultimately have increased the rates of primary production in some areas, thus altering the Mediterranean's gross nutrient budget. Understanding the Mediterranean's past circulation plays therefore a fundamental role in determining the origin of sapropels.

Sapropel formation occurred basin-wide within the eastern Mediterranean throughout Miocene-Pliocene-Pleistocene times. Correlation with standard oxygen isotope stratigraphy provides an excellent framework to evaluate the occurrence of the late Pleistocene sapropels with respect to the

state of global climate (Fig. 6A). Apparently, sapropels formed rather unsystematically during full-glacial stages (sapropels S6, S12), full-interglacial stages (sapropels S8, S10, S11), and during interstadial stages (e.g., Vergnaud-Grazzini et al., 1977; Cita et al., 1977).

A more systematic correlation has been obtained between the distribution of sapropels and maxima of the so-called orbital insolation monsoon index (Rossignol-Strick, 1983) (Fig. 6B). Maxima in the monsoon index point to an intensified Indian Ocean summer monsoon leading to enhanced continental humidity in tropical Africa and ultimately enhanced discharge rates of the Nile. Increased rates of continental runoff would possibly have changed the circulation of the Mediterranean from today's anti-estuarine system towards an estuarine pattern, thereby preconditioning the eastern Mediterranean towards sapropel formation (Fig. 7). New compilations of paleoclimatologic data also point to the importance of humid phases in the northern borderlands of the eastern Mediterranean for stimulating the formation of sapropels (Rohling and Hilgen, 1991). Apparently, increased summer precipitation along the borderlands was due to increased activity of Mediterranean depressions which tend to lower evaporation rates over the eastern Mediterranean thus redistributing freshwater between the eastern and western Mediterranean basins.

The existence of early Pleistocene, Pliocene, and Miocene sapropels is known from eastern Mediterranean DSDP sites which have been drilled during *Glomar Challenger* Legs 13 and 42A (Ryan et al., 1973; Hsü et al., 1978; Kidd et al., 1978) and from exposed sections in southern Italy, Sicily and Crete (for a recent review see Hilgen, 1991). The western most occurrence of sapropels has been documented at Leg 109 drilling sites in the Tyrrhenian Sea (Emeis et al., 1991). However, a detailed evaluation of these old sapropels with respect to the state of Mediterranean climate, water mass and atmosphere circulation is to date not possible because we do not have the required continuous multi-proxy records at hand. Sampling of sapropel deposits in on-land sites is not adequate since many geochemical tracers to be used in our program are labile and their alteration due to exposure to the atmosphere and ground waters would make the interpretation of the data very difficult if not impossible. Thus the required records must come from long time-series of sapropel deposition and water mass variability to be obtained from multiple hydraulic piston cores at eastern Mediterranean drill sites.

#### *The Deep-Water Stagnation Hypothesis*

According to traditional thinking, preservation of organic carbon should be enhanced during oceanic anoxia. The most viable means to deplete oxygen in deep waters is by way of extremely

strong gravitational stability of the water column; this would shut off thermohaline overturn and thus terminate deep water ventilation (Fig. 7C). Strongest support for this model comes from negative oxygen isotope anomalies recorded in planktonic foraminifera which are associated with the sapropels (e.g., Williams et al., 1978; Vergnaud-Grazzini et al., 1986). These anomalies imply the existence of a low-salinity and, thus, low-density surface layer in the eastern Mediterranean at times of sapropel deposition.

High abundances of planktonic foraminiferal species in most of the upper Pleistocene sapropels, which calcify preferentially under low-salinity conditions, provided additional evidence for marine-brackish surface waters during these times (Thunell et al., 1984) (although an association of these planktonic assemblages with increased nutrient scenarios can to date not be excluded; see Rohling and Gieskes, 1989). Presumed sources for the fresh water diluent are the Black Sea, which conceivably exported large volumes of glacial meltwaters to the eastern Mediterranean as the sea level rose above the depth of the Bosphorus sill, the Nile (Rossignol-Strick, 1983) and the inflowing Atlantic waters (Müller, 1990). Rossignol-Strick (1983) demonstrated that the temporal distribution of the eastern Mediterranean sapropels correlates with maximum potential strength of the African monsoons which would have resulted in maximum discharge from the Nile. This could have finally resulted in a periodic reversal of flow patterns between the eastern and western Mediterranean which would have caused the eastern Mediterranean to become a nutrient trap, thereby increasing the oxygen demand and resulting in episodic anoxia (Sarmiento et al, 1988).

This stagnation hypothesis has been recently questioned for several reasons. First, the modern Mediterranean receives largely all of its waters from inflowing Atlantic surface-subsurface waters, which are intrinsically nutrient-depleted (Fig. 7A). Thus, overall nutrient concentrations are low and the Mediterranean is an oligotrophic system in which no major productive areas exist (e.g., Murdoch and Onuf, 1974). Estimates of the annual primary production range from 25-50 gCm<sup>-2</sup> for the open Mediterranean to 60-75 gCm<sup>-2</sup> in some coastal zones. At this low rate of biosynthetic marine organic carbon input, sedimentary organic carbon concentrations would barely reach the elevated levels observed in the sapropels (Calvert, 1983). Only in localities such as the Bannock and Tyro Basins, in which anoxic and hypersaline bottom waters prevail (Jongsma et al., 1983; de Lange and ten Haven, 1983; Cita et al., 1985; Parisi et al., 1987), is the preservation of organic carbon in the sediments distinctly enhanced. Organic carbon contents there are higher (up to 1.3% C<sub>org</sub>) than in normal Mediterranean sediments (0.3% C<sub>org</sub>) probably due to the "red herring/

pickling effect" of the deep-seated brines which suppress bacterial activity and decomposition of the organic sediment fraction (Klinkhammer and Lambert, 1989); but they are still much lower than the values often encountered in sapropels (3-17%  $C_{org}$ ).

Second, areal mapping of the negative oxygen isotope anomalies observed in sediment cores from around the Nile cone suggests that the low-salinity surface layer extant during the formation of sapropel S1 was strongest in the immediate vicinity of the river mouth, presumably because the fresh waters mixed rapidly with the highly saline waters of the easternmost Mediterranean (Jenkins and Williams, 1984). Thus, the potential stabilizing effect of the low-salinity surface layer could have been restricted to the area closest to the Nile cone, whereas thermohaline overturn could have still prevailed in the easternmost Mediterranean.

Third, the stagnation hypothesis is seriously challenged by geochemical evidence that the early-Holocene sapropel (containing up to 14% organic carbon) in the Black Sea must have formed under well-ventilated, fully-oxic conditions (Calvert, 1990) and by the fact that there are no sapropels forming there at present, even though the modern Black Sea is regarded as the type fully-anoxic basin. Thus, reduction of organic matter degradation alone appears unlikely to have promoted the formation of sapropels in the eastern Mediterranean.

### *The Productivity Hypothesis*

Enhanced rates of biosynthetic carbon fixation are well recognized to be the primary factor controlling elevated levels of carbon in seafloor sediments. Organic carbon variations in sediment cores from high-productivity areas of equatorial divergence and coastal upwelling systems have been attributed to climate-controlled variations of primary productivity (Arrhenius, 1952; Pedersen, 1983; Müller et al., 1983; Morris et al., 1984; Zahn et al., 1986; Lyle et al., 1988; Prahl et al., 1989a, 1989b; Sancetta et al., 1992). Using empirically-derived relationships between carbon production in the surface waters and carbon burial rates at the seafloor (Müller and Suess, 1979), and assuming average physical properties of the sapropels, implies that productivity rates of 100-200  $gCm^{-2}yr^{-1}$  are required for the Mediterranean to produce carbon concentrations of 5-15% at depth, which are typically found in the eastern Mediterranean sapropels. These estimated production rates are similar to low to moderate primary production rates observed, for example, in the upwelling system off Northwest Africa. Although new cadmium and barium data (Boyle and

Lea, 1989) suggest a possible contribution of riverine carbon input to early-Holocene sapropel S1, other isotopic and geochemical tracers point to a predominantly marine origin of the sapropel organic carbon (Sutherland et al., 1984; Smith et al., 1986; ten Haven et al., 1987). Therefore, formation of the Mediterranean sapropels was probably promoted by enhanced rates of marine productivity rather than increased supplies of terrestrial carbon.

Several models have been put forward to explain how higher productivity levels in the otherwise oligotrophic Mediterranean could have been brought about. It has been postulated, for instance, that enhanced volumes of freshwater input during deglacial meltwater surges and/or monsoon-controlled river floodings would have reversed the Mediterranean circulation towards an anti-estuarine system (Fig. 7B) (Sarmiento et al., 1988; Lohmann and Pride, 1989; Thunell and Williams, 1989). In this case, the Mediterranean would have imported nutrients via an inflow of nutrient-enriched subthermocline waters from the Atlantic, which would have upwelled in the eastern Mediterranean (Fig. 7B). This is likely to have increased primary productivity. However, the circulation reversal postulated by this model would be in apparent contradiction with benthic foraminiferal  $\delta^{13}\text{C}$  signatures obtained from sediment cores to the west of the Strait of Gibraltar which imply that the outflow of deeper waters from the Mediterranean to the North Atlantic, though at reduced rates, continued also during the formation of sapropel S1 (Zahn et al., 1987).

Rohling and Gieskes (1989) recently envisioned a causal link between the development of deep chlorophyll maxima at the base of the euphotic zone and the formation of sapropels. Accordingly, the development of a marine-brackish, low-density surface layer in the Mediterranean would have resulted in a shoaling of the pycnocline and its associated nutrient maxima into the euphotic zone, thereby promoting enhanced primary production of deep phytoplankton and stimulating the development of a deep chlorophyll maximum.

The deep-chlorophyll-maximum model appears to be constrained by unusually high abundances of neogloboquadrinids (*N. dutertrei* and *N. pachyderma*) in the sapropels, deep-dwelling planktonic foraminiferal species which are typically associated with deep chlorophyll maxima extant in the modern open ocean (Rohling and Gieskes, 1989). However, this species appears to be absent from the Holocene sapropel S1 and, thus, the model does not provide a unique solution to the problem of sapropel formation. Nevertheless, the model has recently been supported by quantitative analyses of calcareous nannofossil assemblages in eastern Mediterranean sediment cores. The core

profiles show salient maxima of deep-dwelling floral species during sapropel events S4, S5, and S7 thus also pointing to the existence of deep chlorophyll maxima (Castradori, 1993). Sapropel events S1 and S6 do not show as distinctive a nannofloral distribution as the other events again hinting at different origins for the different sapropels.

Salient maxima of dinosterols and long-chain alkenones which are associated with sapropels S1 and S7 (Smith et al., 1986; Ten Haven et al., 1987) were used to infer that coccolithophorid and dinoflagellate productivity was high during sapropel formation, thus pointing to the potential importance of primary productivity for the formation of the Mediterranean sapropels.

## **SCIENTIFIC OBJECTIVES AND METHODOLOGY**

### **Summary of Objectives**

- 1) To estimate deformation rates in relation to different stages of continental collision.
- 2) To investigate the influence of salt in sediment deformation.
- 3) To study the diagenesis of the sediments.
- 4) To study the circulation of interstitial fluids, using brines as geochemical tracers.
- 5) To study the development of depositional environments that accompany continental collision.
- 6) To investigate the long-term history of sapropel formation in relation to the history of atmospheric circulation and water mass variability in the Mediterranean, the inter-sapropel geochemical variability as a function of different environmental boundary conditions, and the water column redox conditions and (paleo-) productivity levels during sapropel formation.

### **Specific Tectonic Objectives and Methodology**

Drilling in the continental collisional setting of the eastern Mediterranean will investigate processes at two structural environments - 1) terminal subduction-initial collision (subduction of the last remnants of African oceanic lithosphere and related sediment deformation in the accretionary

complex of the Ionian and Herodotus abyssal plains) and 2 ) incipient continental collision (collision of continental promontories of the African margin off the Cyrenaica Peninsula and on the Eratosthenes Seamount).

### *1) Terminal Subduction-Initial Collision*

#### Accretionary Processes

Offscraping of the thick, terrigenous sedimentary sequence of the African foredeep should produce a deep décollement, seaward-vergent thrusting in the outer portion of the deformed area resembling the style of deformation of fold and thrust belts, and possibly landward thrusting in the inner portions (Seely, 1977; MacKay et al., 1992). The style of initial deformation should also vary between the Ionian and Herodotus abyssal plains in response of the different angle of incidence of the incoming plate with respect to the plate boundary (near-orthogonal and low angle, respectively - Le Pichon et al., 1979; Le Pichon et al., 1982; and Mascle et al., 1986). Furthermore, underthrusting of the thick, terrigenous sedimentary sequence of the African foredeep under the Hellenic Arc should produce coherent underplating with possible duplex formation at depth and consequent high uplift rates on the Mediterranean Ridge. The structural styles of the Mediterranean Ridge will be compared with adjacent on-land, older accretionary prisms of the Pindos thrust belt of mainland Greece in order to understand how structural styles may be related to incipient continental collision.

#### Depositional Settings

A valuable time frame for recent accretionary processes of the Mediterranean Ridge can be provided by the lateral transition of sedimentary facies. The clastic sedimentary input to the eastern Mediterranean subduction zone is provided mostly by the incoming subducting plate (sediments from the overriding plate are trapped in the Black , Marmora , and Aegean seas). An additional characteristic of the developing accretionary complex is that the "trench sediments" (abyssal plains are trenches with no morphological expression) are high-sedimentation rate sand-rich clastics, while the "slope sediments" (on the ridge) are low sedimentation rate fine-grained pelagics and hemipelagics (Blechs Schmidt et al., 1982; Cita et al., 1982). The high-resolution litho-biostratigraphic control provided by the Pliocene-Quaternary (younger than 5 Ma) hemipelagic slope deposits of the Mediterranean Ridge will be used for tracking the transition between trench

and slope sedimentary facies and to calculate rates of outward growth and uplift of the toe of the accretionary complex.

### Dewatering

The initiation of shearing is strongly dependent on the state of effective stress of the sedimentary sequence (Hubbert and Rubey, 1959; von Huene and Lee, 1982). Pore-water pressure greater than hydrostatic can be found in sedimentary rocks due to a number of processes other than tectonic stress, including high sedimentation rates, hydrocarbon gases formation, dehydration of smectite, and osmosis (Hanshaw and Zen, 1965; Rieke and Chalingarian, 1974). A number of these processes are acting within the African continental foredeep approaching the Aegean subduction zone.

The Nile River deep sea fan produces fine-grained turbiditic sediments, with rates of sedimentation as high as 55 cm/k.y. and smectite-dominant clay mineral composition (Nesteroff, 1973), that enter the subduction zone in the Herodotus Abyssal Plain. In addition, a salt body is present in the upper part of the incoming sedimentary sequence (Messinian Evaporites, Hsü et al., 1973) which may trigger osmotic pressure gradients in the overlying sediment sequence (Camerlenghi, 1988; 1990) and evidence of biogenic and thermogenic hydrocarbon gases has been found in the Oligocene-Miocene mud breccia sampled on the mud diapirs of the crest of the Mediterranean Ridge (Camerlenghi et al., 1992).

The amount of interstitial water that enters the subduction zone must be anomalously high because the thickness of the incoming sedimentary sequence (10<sup>4</sup> m) is one order of magnitude larger than average oceanic cases (10<sup>3</sup> m). Conditions are thus favorable for sediment underconsolidation within the incoming sedimentary sequence of the eastern Mediterranean. This is particularly relevant for the pre-salt sediment section, because the upward drainage of pore water in response to sediment compaction might be prevented by the widespread impermeable Messinian halite layer.

### Role of Salt

The mechanical properties of salt affect the style of post-Messinian (younger than 5 Ma) sediment deformation, and seem to cause a geometric anomaly of the Mediterranean Ridge (large width, 150-

300 km, and low taper angle,  $\sim 2.2^\circ$ ; Kastens et al., in press). Similarly, the presence of salt in other fold and thrust belts, like the Appalachian Plateau, the Franklin Mountains, or the Jura belt (Davis and Engelder, 1985), seem to affect the style of deformation, determining narrow taper and inconsistency of vergence of tectonic structures as most characterizing properties. A direct comparison will be made with Eocene-Oligocene thrust tectonics of Crete which has developed on Triassic (Carnian) evaporitic layers.

The interaction between the highly soluble rocks contained within the shallow-buried evaporitic sequence and seawater causes widespread phenomena of dissolution-collapse, such as the regional "cobblestone topography" and the deep-sea anoxic brine lakes (Cita, 1991). In addition, an osmotic gradient between buried brines and seawater, separated by a layer of semi-permeable hemipelagic sediments, may potentially trigger a wide-scale fluid circulation from the ridge to the abyssal plains within the post-Messinian sedimentary sequence (Camerlenghi, 1988; 1990). The geochemical anomalies in the interstitial fluids produced by salt-water interaction will be used as tracers of fluid migration within the post-evaporitic sediment section.

The impermeable nature of the salt layer should also prevent dissipation of excess interstitial pore pressure through upward fluid migration, which is generally materialized in the open ocean (where temperature conditions are favorable) with the formation of the near surface layer of solid state gas hydrates (BSR). The presence of overpressured sediments below the Messinian salt layer of the Mediterranean Ridge has been recognized through the seismic and geological identification of mud diapirism (Camerlenghi et al., 1992). However, the distribution of mud diapirism seems to differ from what is generally observed on oceanic accretionary prism without salt in the deforming sediment sequence. In these areas, and particularly on south Barbados Ridge, mud volcanoes occur also seaward of the deformation front in response to the propagation of the pore-water pressure field induced by the prism (Westbrook and Smith, 1983; Brown and Westbrook, 1988). On the Mediterranean Ridge, mud mobilization has been observed so far exclusively on a narrow corridor along the crest of the ridge and it appears to be concentrated where continental collision occurs.

It can be inferred that both pervasive flux and channelized fluid flow may be prevented by the presence of an impermeable layer near the surface of the ridge. The evaporitic layer, whose thickness is larger toward the Herodotus and Ionian abyssal plains (Montadert et al., 1978), prevents the mud from outcropping to the sediment surface, while on the ridge crest, where salt is thinner and the pressure field is likely to be the highest, underconsolidated mud breaks through the

evaporites to form mud diapirs and mud volcanoes. If this happened, the extremely high pore-water pressure below the evaporites could lower the shear strength of the sediments and contribute to the widening of the ridge (increase in outward growth rate) and narrowing of the taper angle (decrease in uplift rate).

## 2) *Incipient Continental Collision Processes*

Incipient collision implies that a thick sedimentary sequence deposited on the North African passive continental margin enters the subduction zone. This sequence is expected to include a variety of lithologies with a prevailing fine-grained siliciclastic component, also including basal shallow water carbonates or evaporites, and retaining high quantities of organic material (Mitchell and Reading, 1989; Bradley and Kidd, 1991). In this environment, critical factors to the sediment deformation and failure, like porosity reduction with depth, anisotropy of permeability, flow rates of interstitial fluids, mud diapirism and hydrocarbon gas production will be affected by the lateral and vertical lithologic variability. In particular, porosity reduction and fluid mobilization will be more intense in the upper, less consolidated, terrigenous sequence. The initiation of shearing will probably depend upon both the presence of regional discontinuities along lithologic boundaries and the response of sediment consolidation to the stress field within the accretionary complex of homogeneous sedimentary units, according to the Mohr-Coulomb failure criteria (Bray and Karig, 1985; Moore and Byrne, 1987; Taira et al., 1992).

The style of deformation of the incoming lithosphere will be different from the typical horst and graben style of deformation in the oceanic crust, due to lithospheric bending seaward and below the trench axis (Karig and Sharman, 1975). Collisional foredeeps on continental lithosphere show a style of deformation which implies sets of synthetic planar downward-terminating normal faults dipping at high angle toward the arc (observations at Taconic and Ouachita foredeeps and Timor Trough), referred to as continental lithosphere flexural extension by Bradley and Kidd (1991). The geometry of the deformed foredeep affects the tectonic processes in the accretionary wedge and determines the predominance of accretion and underplating versus subcretion and tectonic erosion (McMillen and Bachman, 1981)

Evidence for lithospheric flexural extension on the African foredeep is provided by a few published multichannel seismic profiles (Finetti, 1982) and is particularly evident on the Cyrenaica continental

slope and on the Eratosthenes Seamount, where extensional faulting is an example of local extension at a convergent boundary.

Basically almost normal crustal thickness (~ 30 km) between the Cyrenaica continental promontory and the island of Crete provide evidence for continental collision. Other observations on this part of the margin support the incipient collisional setting; 1) the arcward concavity of the southwest and southeast Mediterranean Ridge (where the last remnants of the oceanic crust enter subduction) is reverted to arcward convexity in response to the adjustment of the accretionary complex to the shape of the collided African margin (Cyrenaica Promontory); 2) the Mediterranean Ridge reaches the maximum elevation; 3) the outer deformation front of the Mediterranean Ridge is shallowest and is in contact with the continental slope of the incoming African margin (there are no abyssal plains facing the outer deformation front); 4) the continuity of the inner deformation front and of the inner plateau are interrupted by a physiographic promontory; 5) the distribution of mud diapirism and mud volcanism on the Mediterranean Ridge crest is maximum; and 6) extremely high uplift rates have been recorded on the island of Crete during the Quaternary.

An abrupt change from subduction to continental collision occurs between the western and central segments of the Cypriot Arc (Kempfer, 1986; Kempfer and Ben-Avraham, 1987). The western segment is characterized by normal subduction beneath the Anatolian plate, as implied by seismic and gravity data, whilst the approach of a thick, buoyant, probably partly-volcanic continental block (whose mere top is the Eratosthenes Seamount to the central segment south of Cyprus) interrupts the subduction and results in a head-on collision between Eratosthenes and the arc. This collision post-dates the Pleistocene uplift of the Troodos Massif in Cyprus (Robertson, 1991), i.e. it is younger than 2 Ma.

The Eratosthenes Seamount serves as a dip-stick to the superimposed geological history represented by the compact sequence of sediments that is equivalent to the extraordinarily thick sedimentary section of the eastern Mediterranean (Lort et al., 1974; Ginzburg et al., 1979; Makris et al., 1983).

Within the post-Miocene tectonic regime, the relatively thick and buoyant Eratosthenes block in the thinner crust of the eastern Mediterranean causes the younger uplifting phases in Cyprus (Kempfer, 1986; Robertson, 1991). The collision of Eratosthenes with the Cypriot Arc is comparable with that of seamounts and ridges at various stages of subduction accompanied by deformation along Pacific arcs (e.g., Yamazaki and Okamura, 1986), in particular, the Dai-ichi Kashima Seamount, which

presently interacts with the overriding plate at the Japan Trench (Mogi and Nishizawa, 1980; Kempler, 1986). Fragmentation and erosion of the accreted seamounts typically accompanies the morphological expressions of this process. Therefore, considerable amounts of rock fragments in the sedimentary sequence may yield critical information about the time and evolution of this collision. Nevertheless, since the Eratosthenes Seamount differs from Pacific seamounts in its crustal structure, differences in the style of the deformation should be expected. A northward tilt was discerned on the top strata of Eratosthenes and the lower area to the north (G.B. Udintsev, pers. comm. 1990), suggesting that compression and collision are presently active.

A comprehensive model for the evolution of Eratosthenes within the eastern Mediterranean tectonic framework integrates the available seismic reflection profiles from the Eratosthenes area with other geophysical data and with plate kinematic considerations (Kempler and Garfunkel, in press). The model shows that the initiation of continental collision in the eastern Mediterranean takes place after a long history of oceanic crust consumption due to the Neo-Tethys closure between the African and Eurasian plates. The analysis of the geology of the southeastern Mediterranean Basin suggests that the northern tectonic boundary of the African Plate occurs between the Eratosthenes Seamount and Cyprus (Mart, 1987). Therefore, the tectonic collision between Eratosthenes and Cyprus represents a rare example for the early stages of continental collision. Drilling at Eratosthenes will therefore provide rock samples that will reveal details of incipient collision. The Mesozoic block that underlies the Eratosthenes Seamount is probably located at a depth of 3-4 km, beyond the scope of the present project. We propose to sample the Late Miocene and subsequent units to understand their tectonic evolution and the paleoceanographic, paleoclimatic, and paleosedimentary changes, recorded in the upper parts of the seamount and its vicinity.

### **Specific Paleoceanographic Objectives and Methodology**

#### *Testing the Stratification Model*

Foraminiferal oxygen isotope profiles provide the primary evidence for global climatic change. In addition to the climate-controlled "ice-effect", foraminiferal  $\delta^{18}\text{O}$  data combine the signals of regional temperature and salinity effects. Because the Mediterranean acts as a concentration basin in which evaporation exceeds precipitation and riverine freshwater input, salinity effects - in addition to the global ice-effect - may be expected to be the dominant contributors to the glacial-interglacial

amplitudes of foraminiferal oxygen isotope records (e.g., Thunell and Williams, 1989). Negative  $\delta^{18}\text{O}$  anomalies in planktonic isotope records from the eastern Mediterranean, for instance, have been largely ascribed to pulses of freshwater supply, either from deglacial meltwater surges or in response to varying intensities of monsoonal rainfall over tropical East Africa which, in turn, control the discharge rates of the Nile (Rossignol-Strick, 1983; Vergnaud-Grazzini et al., 1986).

If indeed regional salinity anomalies existed, they could also have been brought about in part by a redistribution of freshwater between the eastern and western Mediterranean due to changes in atmospheric circulation (Rohling and Hilgen, 1991). In both cases - increased river runoff and/or precipitation - we would expect a gradual decrease in magnitude of the associated foraminiferal  $\delta^{18}\text{O}$  anomalies from the eastern to the western basin. This would also mean that thermohaline overturn would have decreased during these periods because of weaker salinity gradients between the western and eastern basins. Whether or not this led to stagnation of the deep waters depends on the resulting density contrasts in the Mediterranean. This would be tested using traditional temperature-salinity-density diagrams in combination with  $\delta^{18}\text{O}$ -equilibrium fractionation scenarios (see Zahn and Mix, 1991). That is, synoptic mapping of contemporaneous planktonic  $\delta^{18}\text{O}$  signals in the eastern and western Mediterranean will be an essential part in detecting possible inter-basin density contrasts and determining their effects as triggers for sapropel formation.

Statistical analysis of planktonic assemblages which are associated with the Mediterranean sapropels provides a further, independent constraint on surface water conditions during sapropel formation. Planktonic foraminiferal species which are adapted to low-salinity conditions have been found to be the dominant faunal constituents in the sapropel samples, thus supporting the contention that sapropel formation occurred during times of enhanced static stability of the water column (Thunell et al., 1984). Quantitative analysis of the nanoplankton assemblages will further constrain the reconstruction of the vertical architecture of the upper water by revealing the distribution of lower-photic-zone species as compared to surface-dwelling species (Castradori, 1993). In addition, variations of the faunal and floral assemblages just below and above the sapropel horizons are needed to document possible re-organizations of the deep-thermocline before and after periods of sapropel formation (Lohmann and Pride, 1989).

### *Testing the Anoxia Model*

The ratio of the two halogens bromine (Br) and iodine (I) in marine sediments is directly controlled by the redox conditions prevailing during sediment deposition. This is because I-speciation varies as a function of the prevailing redox conditions (iodide is the stable species under anoxic conditions, whereas iodate is the stable species under oxic conditions), and because iodate is the only species that reacts with sedimentary organic matter (Francois, 1988). In contrast, Br does not display such a redox behavior since it exists as the bromide ion under all oceanic redox conditions. Hence, unlike I, the Br content of sediments is linearly related to the organic carbon concentration regardless of the redox state of the overlying water column or the sediment-water interface. Therefore, even though some Br and I is lost from the degrading organic host to the porewaters during early diagenetic reactions, the relative abundances of Br and I in the sediments can be used to determine whether the sediments originally accumulated under oxic or anoxic conditions (e.g., Calvert, 1990).

The distribution of solid-phase manganese (Mn) can also be used to decipher the redox conditions at the sediment/water interface. The behavior of solid-phase  $Mn^{4+}$  and dissolved  $Mn^{2+}$  during early diagenesis in marine sediments is well understood. Sub-surface anoxic sediments which have originally accumulated under oxic conditions generally contain high concentrations of solid-phase Mn due to the burial of surface oxides and their dissolution under the lowered redox potentials at depth. High interstitial alkalinities in these same porewaters promote the precipitation of high-Mn carbonate phases. On the other hand, sediments accumulating under anoxic conditions tend to have solid-phase Mn concentrations which are close to crustal abundance levels; there is no surface enrichment of Mn oxides which can be buried to produce the high interstitial  $Mn^{2+}$  concentrations required for the formation of diagenetic carbonate phases.

### *Testing the Productivity Model*

Most organic compounds of marine origin are intrinsically labile and are, as such, removed from the sedimentary record during early diagenesis. Of the few original biomarkers that persist in the sediments, long-chain alkenones and dinosterol are the clearest indicators of marine carbon sources (e.g., Prahl, 1992). Both compounds are biosynthetic products characteristic of coccolithophorid and dinoflagellate productivity, respectively. They appear to be important components of the

organic fraction in Mediterranean sapropels S1 and S7 (Smith et al., 1986; ten Haven et al., 1987). This has been attributed either to higher degrees of preservation, or to enhanced levels of biological productivity during sapropel formation. The productivity-specific interpretation is supported by the observation that organic carbon and long-chain alkenones covary along a sediment core from the open equatorial Pacific, suggesting that marine primary production is the ultimate signal recorded by alkenones there (Prahl et al., 1989b). Evaluation of the long-term stability of these biomarker signals suggests that even if >85% of the total alkenone concentration is lost by post-depositional decomposition, the alkenone isomer ratio remains virtually unchanged (Prahl et al., 1989b). Consequently, UK37 and other alkenone biomarkers can be used as paleo-environmental indicators.

Atmospheric and riverine input of continentally-derived particulate carbon represents another potentially important source contributing to the sapropel organic carbon. Plantwax lipids are considered the most powerful indicator of terrestrial carbon. They are remarkably stable in the marine environment and are readily identified by capillary gas chromatography. Stable carbon isotope analysis of the organic sediment fraction also has a great potential for separating organic carbon derived from terrestrial and marine sources. Source-specific  $\delta^{13}\text{C}_{\text{org}}$  fractionation between terrestrial and marine organic matter is about 10‰ (terrestrial:  $-20\text{‰} > \delta^{13}\text{C}_{\text{org}}$  (PDB)  $> -30\text{‰}$ ; marine:  $-6\text{‰} > \delta^{13}\text{C}_{\text{org}}$  (PDB)  $> -20\text{‰}$ ) which can be easily distinguished by mass spectrometry. Modulation of the terrestrial  $\delta^{13}\text{C}_{\text{org}}$  signal largely depends on photosynthetic carbon fixation pathways, the C3 pathway (Calvin-Benson cycling) leading to greater depletion in  $\delta^{13}\text{C}_{\text{org}}$  than the C4 pathway (Hatch-Slack cycling).  $\delta^{13}\text{C}_{\text{org}}$  values of marine phytoplankton, on the other hand, show some fractionation in response to varying temperature ( $\Delta\delta^{13}\text{C}_{\text{org}} \sim 0.4\text{‰}$  per  $\Delta T$  of  $1^\circ\text{C}$ ; Fontugne and Duplessy, 1981).

In addition, the  $\delta^{13}\text{C}$  composition of bulk marine carbon carries the imprint of aqueous  $\text{CO}_2$  concentration (Rau et al., 1991) which in turn is related to the rate of photosynthesis and ocean-atmosphere gas exchange. Furthermore, compound-specific  $\delta^{13}\text{C}$  analysis of isotopic biomarkers derived from primary producers may help to determine the total biomass of the source organisms and thus, of productivity levels (Jasper and Hayes, 1990) during sapropel formation. The carbon isotope composition of this carbon fraction appears to be rather stable (Hayes et al., 1990) and is only insignificantly affected by carbon loss due to diagenetic degradation. Therefore, the analysis of

$\delta^{13}\text{C}_{\text{org}}$  will be most helpful (i) in combination with the analysis of plantwax lipids to separate the contribution of terrestrial versus marine carbon sources to the sapropels and (ii) in determining productivity levels during sapropel formation by way of estimating both the concentration of aqueous  $\text{CO}_2$  and total biomass of the signal carrying primary producers.

The isotopic composition of nitrogen in oceanic particulates provides useful information on the sources of nitrogen in, and export from, the mixed layer and on the recycling of particles throughout the water column. Altabet (1988) has shown, for instance, that  $\delta^{15}\text{N}$  values of settling particulate matter (sampled by sediment traps) and the suspensate (the fine fraction sampled by pumps or bottles) in the same area of the North Atlantic may differ significantly from each other. This may signify food-chain fractionation by way of amplification of the heavier isotope, producing  $^{15}\text{N}$  enrichments of  $\sim 3\%$  for each trophic step (DeNiro and Epstein, 1981; Minagawa and Wada, 1984). Consequently, oligotrophic ocean systems which are usually associated with relatively extensive food-chain fractionations should have more positive  $\delta^{15}\text{N}$  values of the organic fraction, whereas eutrophic systems with fewer trophic steps should have more negative  $\delta^{15}\text{N}$  values. On the other hand, there is new evidence that the fractionation between  $^{15}\text{N}$  and  $^{14}\text{N}$  is also influenced by the availability of nitrate as a nutrient (Altabet and Francois, 1992), thus probably allowing the use of  $\delta^{15}\text{N}$  values as an indicator of nutrient concentration and thus, primary production.

The concentration of barium (Ba) in marine sediments appears to be directly related to the rate of primary production at the sea surface as revealed by high Ba concentrations in pelagic sediments which accumulate beneath areas of high productivity (Goldberg, 1958; Goldberg and Arrhenius, 1958; Schmitz, 1987). As a possible mechanistic link between surface productivity and Ba contents at depth, it has been suggested that barite is precipitated in decomposing organic detritus in the upper water column (Bishop, 1988). Alternatively, Ba might be delivered to the sediments because of the secretion of barite microcrystals by marine flagellates (Suess, pers. comm. in Calvert, 1990). Water depth and sedimentation rates seem to exert some control on the preservation of Ba signals in the sediments (Van Os et al., 1991).

Lattice-bound cadmium (Cd) in the shells of calcareous foraminifera has been shown to be a sensitive tracer of changes in the nutrient content of ambient water masses (Boyle, 1988). Continuous Cd/Ca profiles along sediment cores from the open North Atlantic and the Caribbean Sea have been successfully correlated with foraminiferal  $\delta^{13}\text{C}$  records, thus demonstrating the great

potential of Cd as a tracer of ocean circulation and primary production studies. This potential is further augmented by the close, linear relation of Cd and phosphorus in the ocean (Boyle, 1988; Frew and Hunter, 1992). Thus, both Ba and Cd may be used to further constrain possible productivity scenarios.

#### *An Example for the Proposed Multi-Proxy Survey*

In a recent study Fontugne and Calvert (1992) analyzed the chemical composition of the sediments which have been cored at site MD 84641 in the eastern Mediterranean (33°02'N, 32°38'E, 1375 m; total core length 11.61 m). They carried out measurements of some of the tracers to be used in our multi-proxy study and we use their work here to exemplify the great potential of such multi-proxy surveys.

Correlation of the oxygen isotope record at site MD 84641 which was obtained from the planktonic foraminifera *Globigerinoides ruber* with the global mean  $\delta^{18}\text{O}$  Specmap record shows that core MD 84641 extends back to oxygen isotope stage 11, i.e., approximately 460 ka, yielding sedimentation rates between 1.3 and 5.3 cmk.y.<sup>-1</sup> (Fig. 8).

These data are a first step to constrain whether the formation of the sapropels was driven primarily by an increase in biological productivity or by enhanced carbon preservation with no increase in productivity relative to the levels extant prior to and after the sapropel events. New nitrogen isotope data measured on the organic nitrogen fraction in the same core MD 84641 provide some clues to this effect. The nitrogen isotope record shows that each of the sapropels is associated with a marked negative  $\delta^{15}\text{N}_{\text{org}}$  anomaly (S.E. Calvert, unpublished data). As has been suggested by studies of  $\delta^{15}\text{N}_{\text{org}}$  in trapped particles at open ocean sites such variations may be due to food chain amplification of the heavier nitrogen isotope, producing  $^{15}\text{N}$  enrichments of some 3‰ for each trophic step (DeNiro and Epstein, 1981; Minagawa and Wada, 1984). Newer data also hint at the possibility, that enhanced fractionation of nitrogen isotopes occurs in response to increased concentration of nitrate, which in turn would stimulate biological primary production in the surface waters. Thus the  $\delta^{15}\text{N}_{\text{org}}$  record of core MD 84641 would support the contention that sapropel formation in the eastern Mediterranean went along with production increases thus resulting in higher fluxes of marine organic material from the surface waters to the sea floor.

These data very clearly demonstrate the rich potential of multi-proxy strategies to decipher the origin of organic-rich sapropels. The study by Fontugne and Calvert produced a wealth of information on the tracer distribution within the more recent sapropels. The Leg 161 and 162 program will extend this type of work back to times of changing environmental conditions during the Miocene and Pliocene.

### **DRILLING PLAN/STRATEGY**

During Leg 161 (Fig. 1A, Table 1), we will drill three transects of sites across different settings of the outer deformation front of the Mediterranean Ridge accretionary complex (proposed sites MR-1, MR-2, and MR-3). Transects are located in zones of terminal subduction at near-orthogonal plate convergence (Ionian deformation front) and at initial continental collision (Katia Deformation Front), where the deformed sediments of the Mediterranean Ridge override the African continental slope. At these sites, we aim to identify the incoming sediment section, the rates of outward growth and uplift of the deformation front, the fluid flow paths, and the influence of the Messinian evaporites (which include a salt body) on the tectonic structure and the interstitial fluid circulation, using brines as geochemical tracers.

We will also drill one site on the Napoli mud volcano (proposed site MV-1) in order to date the diapiric intrusions, and record the physical properties of the diapiric material and the composition of deep interstitial fluids brought to the surface by the diapiric processes along the inner deformation front of the Mediterranean Ridge. The diapirs of the inner deformation front constitute an excellent opportunity to sample fluids expelled from below the impermeable salt layer. Proposed site MV-1 will be drilled on the flank of the "Napoli" mud volcano in the Olimpi mud diapir field (Cita et al., 1989; Camerlenghi et al., 1992; de Lange et al., 1991; Camerlenghi et al., in preparation). Penetration in the mud volcano will establish the lithologic composition of the mud, its diagenetic history, and age. Interstitial water analysis, so far conducted only on one piston core (de Lange et al., 1991), will allow us to determine whether fluid is currently advecting through this structure, and if so, the nature of the fluid source. Analysis of diagenetic alterations within the sediments will provide information on the history of fluid-flow pathways. A CORK will also be installed at this site and will monitor long-term variations in fluid and temperature regime.

Four sites are planned to be drilled along a transect from the top of the Eratosthenes Seamount (proposed sites ESM-1, ESM-2, ESM-3, and ESM-4) to the Cyprus Margin to identify the tectonic

phases, vertical displacements, and the variation in sediment provenance and depositional environments that accompanied the collision between the seamount and the margin.

All the proposed sites require two APC/XCB holes and heat flow measurements. The use of RCB will be necessary for a third hole (one for each transect) to run the standard geophysical tools and conduct geochemical logging. Downhole measurements, like Adara, WSTP, and LAST-II will be widely employed. The deployment of borehole seals is foreseen at two sites.

In order to determine the hydrology and characterize the fluid regime, we will measure the bulk sediment properties and sample the pore fluids at in situ conditions. Consequently, the complete standard logging package is to be run at each site, even though the proposed holes will be shallow. The lateral stress tool can be used to measure stress and deformation in the soft sediments in the top portion of the hole, and the borehole televiewer will provide stress orientation in the more consolidated sediments in the bottom portion of the hole.

In situ temperature measurements have provided valuable information pertaining to the hydrological regime in accretionary prisms along continental margins. We will use the Adara tool and the WSTP in conjunction with the standard logging runs to establish anomalies in the thermal structure which may be indicative of advective versus conductive temperature regimes.

Hydrocarbon gases obtained in mud diapir samples indicate a partial thermogenic origin. Characterization of methane and other hydrocarbons at close to in situ conditions will require the use of the WSTP sampler.

In order to determine the influence of the various factors on sapropel formation, we must obtain multi-proxy records along an east-west transect across the entire Mediterranean (Fig. 1B, Table 1). Such transect would allow to synoptically map the hydrographic and climatic conditions throughout the Mediterranean both at the sites of sapropel formation in the eastern basin and at sites in the western basin where no sapropels formed. Only this Mediterranean-wide data base will allow to determine the driving force behind sapropel formation at different times, and how the Mediterranean's physical circulation and chemical cycling preconditioned the eastern basin towards sapropel formation. That is, the paleoceanography of the entire Mediterranean must be understood if we are to unravel the origin of sapropel formation in its eastern basin.

To achieve these scientific goals, the drill sites must fulfill four essential requirements.

- 1) Stratigraphic continuity. Sedimentary sections at targeted sites have to be complete, undisturbed, hemipelagic and pelagic, and shielded from the occasionally drastic effects of submarine karstification and tectonics of the Mediterranean.
- 2) High stratigraphic resolution. Sedimentation rates must be high enough to allow for a detailed documentation of the transition into and out of the various sapropels as well as possible internal variability within individual sapropels. High-resolution records are also important for accurate cross-correlation of the multi-proxy records along the drilling transect.
- 3) Long stratigraphic range. Sapropels did form under very different global climatic settings. For instance, between 800 k.y. and 1 Ma the period of glacial-interglacial climate cycles shifted from 40,000 years to 100,000 years (e.g., Ruddiman et al., 1989). Numerical simulations which are constrained by paleoclimate data indicate that monsoons as strong as today occurred only after 7 to 8 Ma when the elevation of the Himalayas and the Tibetan plateau has risen to about half their modern elevation. Documentation of sapropel formation before, across, and after these periods of changing environmental boundary conditions is needed to pin down the influence of these parameters on the formation of sapropels. The APC coring must be conducted at least into the Miocene.
- 4) Optimum areal coverage. The drill sites must cover the entire Mediterranean basin in order to permit evaluation of paleoceanographic, paleochemical, and paleontological zonality and teleconnections throughout the entire basin. Key locations are close to the Nile cone (but far enough away from it to avoid its turbidites) as a freshwater source, the Strait of Sicily as the seaway determining water mass exchange between the eastern and western basins, an Alboran Sea site as the watchdog for Atlantic-Mediterranean water exchange, and central western and eastern basin sites to document pelagic environments between these hydrographic boundary end members.

In order to ensure highest-quality information on the depositional environment during sapropel formation, sampling density of the sapropel layers, as well as the "normal" sediments immediately below and above the sapropels, must be on scales of centimeters to millimeters. Such high sampling resolution is essential for determining the factors that have led to the formation of the

sapropels and which have helped in maintaining an environment favorable for the formation of sapropels over time scales of  $10^2$  to  $10^3$  years. Triple HPC/APC coring may be necessary to allow such intense sampling at the proposed eastern Mediterranean sites where sapropels do occur.

## **PROPOSED SITES**

### **Tectonic Objectives**

Proposed site MR-1 on the incoming sediment section will provide the reference section for the post-evaporitic sediments. Recognition of depositional environments (terrigenous turbiditic, pelagic turbiditic, hemipelagic, and pelagic) during the last 5 m.y. and the possibility of timing their changes through the high resolution biostratigraphic record of the Plio-Pleistocene of the eastern Mediterranean (Blechsmidt et al., 1982) will allow us to identify precursors of tectonic activity of the Mediterranean Ridge in the sedimentary section. In addition, lithostratigraphic markers and biostratigraphic events (anoxic layers, mega-turbidites, ash layers, faunal changes due to paleoclimatic modifications) will be identified, dated, and correlated with the sites on the deformation front, thus dating tectonic events. Proposed site MR-1 will reach the top of the shallow-buried tectonic structure called Victor Hensen Seahill, where seismic evidence indicates that the evaporites are absent. Therefore, the site represents a window on pre-evaporitic sediments that will allow us to determine the depositional environment on the structure before the Late Miocene and, hopefully, indications of the tectonic environment at the time of deposition.

Proposed site MR-2 on the lower deformation front will provide a sedimentary section that has been progressively uplifted on the Mediterranean Ridge during the outward propagation of the deformation front. A change in the sedimentary record is expected from terrigenous turbiditic sediments (abyssal plain deposition) to slump and debris flow deposition as a marker of the initial deformation, to hemipelagic or pelagic turbiditic after uplift on the slope has been completed. Similar sequences of sedimentary events related to the tectonic evolution of the deformation front have been identified by Kastens et al. (1992) on the Sirte Deformation Front. The changes in depositional environment will be dated through correlation with marker beds identified in the abyssal plain section or with well known markers of the Mediterranean Ridge biostratigraphic record.

Additionally, the physical properties and the structural fabric recorded at this site will be compared with that at the abyssal plain site to determine whether tectonic stress of the ridge is transmitted to post-evaporitic sediments (in this case anomalous reduction of porosity and development of foliation fabric in the sediments will occur) or confined to pre-evaporite sediments due to the presence of the physical barrier of the plastic salt body (in this case no changes in physical properties and structural fabric are expected between abyssal plain and lower deformation front sites). In the latter case, the outward growth of the deformation front would occur as passive, time-progressive uplift of post evaporite sediments, while shortening would occur within the pre-evaporitic section. The influence of the salt body on the mechanical development of an accretionary prism could thus be evaluated.

Proposed site MR-3 on the upper deformation front will provide a third point of correlation among litho- and bio-stratigraphic markers in identifying changes in depositional environment (being, first, the present day position of the deformation front and, second, the site on the lower deformation front). The rate of outward growth and uplift of the deformation front of the Mediterranean Ridge is, in fact, supposed to be constant during the post-evaporites evolution (Kastens, 1991). Identifying the position of the deformation front in three locations during the post-evaporite deposition time span will allow to compare deformation rates among the three transects, and will provide constraints for the development of a comprehensive model of sediment accretion on the Mediterranean Ridge. In addition, this site has been chosen to intercept the first fault planes that apparently cut across the evaporite layer on the upper deformation front. Recovery of sediments across the fault zone will allow us to establish if the fault is active (mainly through geochemical anomalies) and if there is a substantial change in the physical properties and structural fabric among these sediments, the undeformed sediments of the abyssal plain, and the sediments of the lower deformation front. Again, the development of faults across the salt body will allow us to determine the propagation of stress and deformation across a plastic salt layer in an context of sediment accretion.

### *Mud Volcano*

Proposed site MV-1 will be drilled on the flank of the mud volcano to sample and date deep mud sills propagating outside the mud conduit, and to obtain a detailed section of the physical properties within the mud volcano and as much information as possible on the chemical composition of the interstitial fluids of the diapiric material in order to evaluate depth of origin, fluid migration paths,

and diagenetic alterations. From a geochemical point of view, the site has been incorporated in the Katia transect, since it represents a window to the deep fluid composition along the inner deformation front.

### *Eratosthenes Seamount*

Proposed sites ESM-1 to -4 are located on the southern peak of the seamount to the deformation front at the foot of the Cyprus continental slope and will allow us to identify the tectonic phases that led to the present structure of the seamount through the identification of depositional environments (deep vs. shallow water), to sample the sediments of the collisional trough to identify the sediment source (e.g., from Troodos and Mamonia complexes vs. Nile sources), and to evaluate the rate of vertical motion of different structures along the convergent boundary and the rate of subsidence of the colliding continental crust through transition of sedimentary facies on the seamount. The scientific objectives addressed by the transect of holes across the Eratosthenes Seamount also include paleoceanographic and paleoenvironmental themes that aim at understanding the non-evaporitic Messinian depositional environment and the areal distribution of anoxic marker beds in the Plio-Quaternary record of the eastern Mediterranean.

### **Paleoceanographic Objectives**

A Bannock SCS line exists over proposed site MedSap 2B. Core BAN89-10GC (total length 5 m) which was taken close to the location of proposed site MedSap 2B, retrieved 6 sapropels and implies average sedimentation rates of 2 cmk.y.<sup>-1</sup>.

Proposed site MedSap 3 is located at the Calabrian Ridge, on the Pisano Plateau between Beato Angelico Trough and Raffaello Basin. This site is at the location of core KC01B, taken during the MARFLUX program. Core KC01B (total length 37 m) goes back to the early Pleistocene. First results of micropaleontological and sedimentological studies show that core KC01B contains 11 sapropels and 3 magnetic reversals, and that the planktonic foraminiferal assemblage nicely tracks the Quaternary climatic cycles.

The MedSap 4 proposed sites are on the Gela Bank in the Sicily Channel and will be used as the watchdog for water mass exchange between the eastern and western Mediterranean basins. By and large, the Sicily Channel marks the borderline between sapropel-bearing sediments in the east and sapropel-free sediments in the west. Proposed site MedSap 4A is at the location of cores MT 7 and MT 9 which retrieved 4.7 m of pelagic sediments each. Proposed site MedSap 4C, an alternate site to MedSap 4A, is at the location of core MT 11 which retrieved 10 m of pelagic sediments. Initial inspection of the core and preliminary micropaleontologic results reveal distinct variations of the foraminiferal assemblage which indicates glacial and interglacial stages.

## REFERENCES

- Altabet, M. A., 1988.** Variations in nitrogen isotopic composition between sinking and suspended particles: implications for nitrogen cycling and particle transportation in the open ocean. *Deep-Sea Res.*, 35:535-554.
- Altabet, M.A., and Francois, R., 1992.** Sedimentary nitrogen isotopic ratio records surface ocean nitrate utilization. Submitted.
- Arrhenius, G. O., 1952.** Sediment cores from the East Pacific. In Petterson, H. (Ed.), *Reports of the Swedish Deep-Sea Expedition*, 5(1).
- Avedik, F., and Hieke, W., 1981.** Reflection seismic profiles from the Central Ionian Sea (Mediterranean) and their geodynamic interpretation. *Meteor Forsch. Ergebnisse*, 34:49-64.
- Ben-Avraham, Z., Shoham, Y., and Ginzburg, A., 1976.** Magnetic anomalies in the eastern Mediterranean and the tectonic setting of the Eratosthenes Seamount. *Geophys. J. R. Astron. Soc.*, 45:105-123.
- Biju-Duval, B., Letouzey, J., and Montadert, L., 1978.** Structure and evolution of the Mediterranean basins. In Hsü, K.J., Montadert, L. et al., *Init. Repts. DSDP*, 42: Washington (U.S. Govt. Printing Office), 951-984.
- Bishop, J. K. B., 1988.** The barite-opal-organic carbon association in oceanic particulate matter. *Nature*, 332:341-343.
- Blebschmidt, G., Cita, M.B., Mazzei, R., and Salvatorini, G., 1982.** Stratigraphy of the Western Mediterranean and Southern Calabrian ridges, eastern Mediterranean. *Mar. Micropaleontol.*, 7:101-134.
- Boccaletti M., 1979.** Mesogea, Mesoparatethys, Mediterranean and Paratethys: their possible relations with Tethys Ocean development. *Ofioliti*, 4(2):83-98.
- Boyle, E. A., 1988.** Cadmium: chemical tracer of deep water paleoceanography. *Paleoceanography*, 4:471-489.
- Boyle, E. A., and Lea, D.W., 1989.** Cd and Ba in planktonic foraminifera from the eastern Mediterranean: evidence for river outflow and enriched nutrients during sapropel formation. *Eos*, 43: 1134.
- Bradley, D.C., and Kidd, W.S.F., 1991.** Flexural extension of the upper continental crust in collisional foredeeps. *Geol. Soc. Am. Bull.*, 103:1416-1438.
- Bray, C.J., and Karig, D.E., 1985.** Porosity of sediments in accretionary prisms and some implications for dewatering processes. *J. Geophys. Res.*, 90(B1)10:768-778.
- Brennecke, J., and Lelggemann, D., 1986.** The shape of the European Geoid and the geotectonic structures. In Freeman, R., Mueller, St., and Giese, P. (Eds.), *Proc. Third Workshop on the European Geotraverse (EGT) Project*, The Central Segment, ESF, 241-248.
- Brown, K., and Westbrook, G.K., 1988.** Mud diapirism and subcretion in the Barbados Ridge accretionary complex: the role of fluids in accretionary processes. *Tectonics*, 7:613-640.
- Calvert, S. E., 1983.** Geochemistry of Pleistocene sapropels and associated sediments from the eastern Mediterranean. *Oceanol. Acta*, 6:255-267.
- Calvert, S.E., 1990.** Geochemistry and origin of the Holocene sapropel in the Black Sea. In Ittekkot, V., Kempe, S., Michaelis, W., and Spitzzy, A. (Eds.), *Facets of Modern Biogeochemistry*: Berlin (Springer-Verlag), 328-353.
- Calvert, S. E., and Price, N.B., 1983.** Geochemistry of the recent sediments of the Namibian shelf. In Suess, E., and Thiede, J. (Eds.), *Coastal Upwelling*, Part A: New York (Plenum), 337-375.
- Camerlenghi, A., 1988.** Subsurface dissolution of evaporites in the eastern Mediterranean Sea [MS Thesis]. Texas A&M University, College Station, Texas.
- Camerlenghi, A., 1990.** Anoxic basins of the eastern Mediterranean: Geologic framework. *Mar. Chem.*, 31:1-19.
- Camerlenghi, A., Cita, M.B., Hieke, W., and Ricchiuto, T.S., 1992.** Geological evidence of mud diapirism on the Mediterranean Ridge accretionary complex. *Earth Planet. Sci. Lett.*, 109:493-506.
- Castradori, D., 1993.** Calcareous nannofossils and the origin of eastern Mediterranean sapropels. Submitted to *Paleoceanography*.

- Cita, M.B., 1991. Anoxic basins of the eastern Mediterranean: An overview. *Paleoceanography*, 6(1):133-141.
- Cita, M.B., Broglia, C., Malinverno, A., Spezzibottani, G., Tomadin, L., and Violanti, D., 1982. Late Quaternary pelagic sedimentation on the southern Calabrian Ridge and Western Mediterranean Ridge, eastern Mediterranean. *Mar. Micropaleontol.*, 7:135-162.
- Cita, M.B., Camerlenghi, A., Erba, E., McCoy, F.W., Castradori, D., Cazzani, A., Guasti, G., Giambastiani, M., Lucchi, R., Nolli, V., Pezzi, G., Redaelli, M., Rizzi, E., Torricelli, S., and Violanti, D., 1989. Discovery of mud diapirism in the Mediterranean Ridge - A preliminary report. *Boll. Soc. Geol. It.*, 108:537-543.
- Cita, M.B., et al., 1985. Gypsum precipitation from cold brines in an anoxic basin in the eastern Mediterranean. *Nature*, 314:152-154.
- Cita, M.B., Ryan, W.F.B., and Paggi, L., 1981. Prometheus mud-breccia: An example of shale diapirism in the Western Mediterranean Ridge. *Ann. Geol. Pays Hellen.*, 30:543-570.
- Cita, M.B., Vergnaud-Grazzini, C., Robert, C., Chamley, H., Ciaranfi, N., and D'Onofrio, S., 1977. Paleoclimatic record of a long deep sea core from the eastern Mediterranean. *Quat. Res.*, 8: 205-235.
- Cramp, A., and Lewis, C., 1992. Pliocene-Pleistocene-Holocene trace metal data from Holes 794A, 795A, 797A, and 797B. In Tamakai, K., et al., *Proc. ODP, Sci. Results*, 127/128, Pt. 2: College Station, TX (Ocean Drilling Program), 1361-1364
- Davis, D.M., and Engelder, T., 1985. The role of salt in fold-and-thrust belts. *Tectonophysics*, 119:67-88.
- de Lange, G. and other participants to the MARFLUX Expedition (abstract), 1991. Variability of biogeochemical fluxes in the eastern Mediterranean. *Eos*, 72(15):53.
- de Lange, G.J., and ten Haven, H.L., 1983. Recent sapropel formation in the eastern Mediterranean. *Nature*, 305:797-798.
- DeNiro, M.J., and Epstein, S., 1981. Influence of diet on the distribution of nitrogen isotopes in animals. *Geochim. Cosmochim. Acta*, 45:341-351.
- de Voogd, B., Truffert, C., Chamot-Rooke, N., Huchon, P., Lallemand, S., and Le Pichon, X., 1992. Two-ship deep seismic soundings in the Basins of the eastern Mediterranean Sea (*Pasiphae* cruise). *Geophys. J. Int.*, 109:536-552.
- Dewey, J.F., Hempton, M.R., Kidd, W.S.F., Saroglu, F., and Sengör, A.M., 1986. Shortening of continental lithosphere: the neotectonics of eastern Anatolia. *Geol. Soc. London Spec. Paper*, 19:3-36.
- Dewey, J.F., Pitman, W.C., Ryan, W.B.F., and Bonin, J., 1973. Plate tectonics and the evolution of the Alpine system. *Bull. Geol. Soc. Am.*, 84:3137-3180.
- Dewey, J.F., and Sengör, A.M.C., 1979. Aegean and surrounding regions: Complex multiplate and continuum tectonics in a convergent zone. *Geol. Soc. Am. Bull.*, 90:84-92.
- Emeis, K.-C., Camerlenghi, A., McKenzie, J.A., Rio, D., and Sprovieri, R., 1991. The occurrence and significance of Pleistocene and Upper Pliocene sapropels in the Tyrrhenian Sea. *Mar. Geol.*, 100:155-182.
- Emelyanov, E.M., and Shimkus, K.M., 1986. *Geochemistry and Sedimentology of the Mediterranean Sea*: Rotterdam (D. Riedel Pub. Co.).
- Erickson, A.J., and von Herzen, R.P., 1978. Down-hole temperature measurements, Deep Sea Drilling Project, Leg 42A. In Hsü, K.J., Montadert, L., et al., *Init. Repts. DSDP*, 42: Washington (U.S. Govt. Printing Office), 1114-1118.
- Finetti, I., 1976. Mediterranean Ridge. A young submerged chain associated with the Hellenic arc. *Boll. Geol. Teor. Appl.*, 28(69):31-62
- Finetti, I., 1982. Structure, stratigraphy and evolution of Central Mediterranean. *Boll. Geof. Teor. Appl.*, 24(96):274-315.
- Föllmi, K.B., Cramp, A., Föllmi, K.E., Alexandrovich, J.M., Brunner, C., Burckle, L.H., Casey, M., deMenocal, P., Dunbar, R., et al., 1992. Dark-light rhythms in the sediments of the Japan Sea: Preliminary results from Site 798, with some additional results from Sites 797 and 799. In Tamakai, K., et al. (Eds.), *Proc. ODP, Sci. Results*, 127/128, Pt. 2: College Station, TX (Ocean Drilling Program), 559-576.

- Fontugne, M.R., and Calvert, S.E., 1992. Late Pleistocene variability of the carbon isotopic composition of organic matter in the eastern Mediterranean: monitor of changes in carbon sources and atmospheric CO<sub>2</sub> concentrations. *Paleoceanography*, 7:1-20.
- Fontugne, M.R., and Duplessy, J.-C., 1981. Organic carbon isotopic fractionation by marine plankton in the temperature range -1 to 31°C. *Oceanol. Acta*, 4:85-90.
- Francois, R., 1988. A study on the regulation of the concentrations of some trace metals (Rb, Sr, Zn, Pb, Cu, V, Cr, Ni, Mn and Mo) in Saanich Inlet sediments, British Columbia, Canada. *Mar. Geol.*, 83:285-308.
- Frew, R.D., and Hunter, K.A., 1992. Influence of Southern Ocean waters on the cadmium-phosphate properties of the global ocean. *Nature*, 360:144-146.
- Fuex, A.N., 1977. The use of stable carbon isotopes in hydrocarbon exploration. *J. Geochem. Explor.*, 7:155-188.
- Fytikas, M., Innocenti, P., Manetti, P., Mazzuoli, R., Peccerillo, A., and Villari, L., 1984. Tertiary to Quaternary evolution of volcanism in the Aegean region. In Dixon, J.E., and Robertson, A.H.F. (Eds.), *The Geological Evolution of the Eastern Mediterranean*. Spec. Publ. - Geol. Soc. London, 17:687-700.
- Garfunkel, Z., and Derin, B., 1984. Permian-Early Mesozoic Tectonism and continental margin formation in Israel and its implication for the history of the eastern Mediterranean. In Dixon, J.E., and Robertson, A.M.F. (Eds.), *The Geological Evolution of the Eastern Mediterranean*. Spec. Publ. - Geol. Soc. London, 17:187-201.
- Giese, P., Nicolich, R., and Reutter, K.J., 1982. Explosion seismic crustal studies in the Alpine-Mediterranean region and their implication to tectonic processes. In Berckhemer, H., and Hsü, K. (Eds.), *Alpine-Mediterranean Geodynamics*. AGU-GSA Geodynamic Series, 6:39-74.
- Ginzburg, A., Makris, J., Fuchs, K., Frodehl, C., Kaminski, W., and Amitai, U., 1979. A seismic survey of the crust and upper mantle of the Jordan-Dead Sea rift and their transition throughout the Mediterranean Sea. *J. Geophys. Res.*, 84:569-1582.
- Goldberg, E.D., 1958. Determination of opal in marine sediments. *J. Mar. Res.*, 17:178-182.
- Goldberg, E.D., and Arrhenius, G., 1958. Chemistry of Pacific pelagic sediments. *Geochim. Cosmochim. Acta*, 13:153-212.
- Hanshaw, B.B., and Zen, E., 1965. Osmotic equilibrium and overthrust faulting. *Geol. Soc. Am. Bull.*, 76:1379-1387.
- Hayes, J.M., Freeman, K.H., Popp, B.N., and Hoham, C.H., 1990. Compound-specific isotopic analyses: a novel tool for reconstruction of ancient biogeochemical processes. *Org. Geochem.*, 16:1115-1128.
- Hersey, J.B., 1965. Sedimentary basins of the Mediterranean Sea. In Whitard, W.F., and Bradshaw, W. (Eds.), *Submarine Geology and Geophysics. Proc. 17th Symp. of the Colston Research Society*, London, 75-91.
- Hieke, W., 1978. The "Victor Hensen Seahill"; part of a tectonic structure in the Central Ionian Sea. *Mar. Geol.*, 26:M1-M5.
- Hieke, W., and Wanninger, A., 1985. The Victor Hensen Seahill (Central Ionian Sea)- Morphology and structural aspects. *Mar. Geol.*, 64:343-350.
- Hilgen, F.J., 1991. Astronomical calibration of Gauss to Matuyama sapropels in the Mediterranean and implication for the geomagnetic polarity time scale. *Earth Planet. Sci. Lett.*, 104:226-244.
- Horvath, F., and Berckhemer, H., 1982. Mediterranean back arc basins. In Berckhemer, H., and Hsü, K. (Eds.), *Alpine-Mediterranean Geodynamics*. AGU-GSA Geodynamic Series, 6:141-174.
- Hsü, K. J., Montadert, L., et al., 1978. *Init. Repts. DSDP*, 42: Washington (U.S. Govt. Printing Office).
- Hsü, K.J., Ryan, W.B.F., and Cita, M.B.C., 1973. The origin of the Mediterranean evaporites. In Ryan, W.B.F., Hsü, K.J. et al., *Init. Repts. DSDP*, 13: Washington (U.S. Govt. Printing Office), 1203-1232.
- Hubbert, M.K., and Rubey, W.W., 1959. Role of fluid pressure in mechanics of overthrust faulting. *Geol. Soc. Am. Bull.*, 70:115-166.
- Jasper, J.P., and Hayes, J.M., 1990. A carbon-isotopic record of CO<sub>2</sub> levels during the late Quaternary. *Nature*, 347:462-464.

- Jenkins, P., and Williams, D.F., 1984.** Nile water as a cause of eastern Mediterranean sapropel formation: Evidence for and against. *Mar. Micropaleontol.*, 8:521-534.
- Jongsma, D., 1987.** The geometry and rates of microplate motions in the eastern Mediterranean Sea- Quantitative constraints by using anoxic basins as piercing points. *Mar. Geol.*, 75:1-30.
- Jongsma, D., Fortuin, A.R., Huson, W., Troelstra, S.R., Klaver, G.T., Peters, J.M., van Harten, D., de Lange, G.J., and ten Haven, L., 1983.** Discovery of an anoxic basin within the Strabo Trench, eastern Mediterranean. *Nature*, 305:795-797.
- Jongsma, D., Woodside, J.M., King, G.C.P., and van Hinte, J.E., 1987.** The Medina Wrench: a key to the kinematics of the central and eastern Mediterranean over the past 5 Ma. *Earth Planet. Sci. Lett.*, 82:87-106.
- Karig, D.E., and Sharman, G.F., 1975.** Subduction and accretion in trenches. *Geol. Soc. Am. Bull.*, 86:377-389.
- Kastens, K.A., 1991.** Rate of outward growth of the Mediterranean Ridge accretionary complex. *Tectonophysics*, 199:25-50.
- Kastens, K.A., Breen, N., and Cita, M.B., in press.** Progressive deformation of an evaporite-bearing accretionary complex: SeaMARC I, SeaBeam, and piston-core observations from the Mediterranean Ridge. *Mar. Geophys. Res.*
- Kemp, A.E.S., and Baldauf, J.G., 1993.** Vast Neogene laminated diatom mat deposits from the eastern equatorial Pacific Ocean. *Nature*, 362:141-144.
- Kempler, D., 1986.** The tectonic evolution of the Cyprean Arc [M.Sc. thesis]. Tel-Aviv Univ., Tel-Aviv (in English, Hebrew abstr.).
- Kempler, D., and Ben-Avraham, Z., 1987.** The tectonic evolution of the Cyprean Arc. *Annales Tectonicae*, 1(1):58-71.
- Kempler, D., and Garfunkel, Z., in press.** *The Eratosthenes Seamount: a Fossil Superstructure in the Eastern Mediterranean.* CIESM Abs. Book, Trieste.
- Kenyon, N.H., Belderson, R.H., and Stride, A.H., 1982.** Detailed tectonic trends on the central part of the Hellenic Outer Ridge in the Hellenic Trench System. In Leggett, J.K. (Ed.), *Trench-Forearc Geology*. Spec. Publ. - Geol. Soc., 10:335-343.
- Kidd, R.B., Cita, M.B., and Ryan, W.B.F., 1978.** Stratigraphy of eastern Mediterranean sapropel sequences recovered during DSDP Leg 42 and their paleoenvironmental significance. In Hsü, K.J., Montadert, L., et al., *Init. Repts. DSDP*, 42, Part 1: Washington (U.S. Govt. Printing Office), 421-443.
- Kissel, C., and Lay, C., 1988.** The Tertiary geodynamical evolution of the Aegean Arc: a paleomagnetic reconstruction. *Tectonophysics*, 146:183-201.
- Klinkhammer, G.P., and Lambert, C.E., 1989.** Preservation of organic matter during salinity excursions. *Nature*, 339:271-274.
- Kullenberg, B., 1952.** On the salinity of the water contained in marine sediments. *Göteborgs Kungl. Vetens. Vitter. Handl., Ser. B.*, 6:3-37.
- Le Pichon, X., 1982.** Land-locked oceanic basins and continental collision: The eastern Mediterranean as a case example. In Hsü, K.J. (Ed.), *Mountain Building Processes*: London (Academic Press), 201-211.
- Le Pichon, X., and Angelier, J., 1979.** The Hellenic Arc and Trench system: A key to the neotectonic evolution of the eastern Mediterranean area. *Tectonophysics*, 60:1-42.
- Le Pichon, X., Angelier, J., Aubouin, J., Lyberis, N., Monti, S., Renard, V., Got, H., Mart, Y., Mascle, J., Matthews, D., Mitropoulos, D., Tsoflias, P., and Chronis, G., 1979.** From subduction to transform motion: A SeaBeam survey of the Hellenic Trench system. *Earth Planet. Sci. Lett.*, 44:441-450.
- Le Pichon, X., Lyberis, N., Angelier, J., and Renard, V., 1982.** Strain distribution over the East Mediterranean Ridge: a synthesis incorporating new SeaBeam data. *Tectonophysics*, 86:243-274.
- Lohmann, G.P., and Pride, C.J., 1989.** The eastern Mediterranean estuary: observational evidence favoring estuarine circulation during sapropel formation. *Eos*, 43:1134.

- Lort, J.M., Limond, W.Q., and Gray, F., 1974. Preliminary seismic studies in the eastern Mediterranean. *Earth Planet. Sci. Lett.*, 21:355-366.
- Lyle, M., Murray, D.M., Finney, B.P., Dymond, J., Robbins, J.M., and Brooksforce, K., 1988. The record of Late Pleistocene biogenic sedimentation in the eastern tropical Pacific Ocean. *Paleoceanography*, 3:39-59.
- MacKay, M.E., Moore G.F., Cochrane, G.R., Moore J.C., and Kulm, L.D., 1992. Landward vergence and oblique structural trends in the Oregon margin accretionary prism: Implications and effect on fluid flow. *Earth Planet. Sci. Lett.*, 109:477-493.
- Makris, J., 1977. Geophysical investigations of the Hellenides. *Hamburger Geophys. Einzelschriften, H.*, 27.
- Makris, J., Ben-Avraham, Z., Behle, A., Ginzburg, A., Gieze, P., Steinmetz, L., Whitmarsh, R.B., and Eleftheriou, S., 1983. Seismic refraction profiles between Cyprus and Israel and their interpretation. *Geophys. J. R. Astron. Soc.*, 75:575-591.
- Makris, J., and Stobbe, C., 1984. Physical properties and state of the crust and upper mantle of the eastern Mediterranean Sea as deduced from geophysical data. *Mar. Geol.*, 55:347-363.
- Mart, Y., 1987. Superpositional tectonic patterns along the continental margin of the southeastern Mediterranean: a review. *Tectonophysics*, 140:213-232.
- Masclé, J., Le Cleac'h, A., and Jongsma, D., 1986. The eastern Hellenic margin from Crete to Rhodes: Example of progressive collision. *Mar. Geol.*, 73:145-168.
- McKenzie, D.P., 1978. Active tectonism in the Alpine-Himalayan belt: the Aegean Sea and the surrounding regions (tectonics of the Aegean region). *Geophys. J. R. Astron. Soc.*, 55:217-254.
- McMillen, K.J., and Bachman, S.B., 1981. Bathymetric and tectonic evolution of the Southern Mexico active margin: Deep Sea Drilling Project Leg 66. In Watkins, J.S., Moore, J.C., et al., *Init Repts. DSDP*, 66: Washington (U.S. Govt. Printing Office), 815-822.
- Minagawa, M., and Wada, E., 1984. Stepwise enrichment of  $^{15}\text{N}$  along food chains: further evidence and the relation between  $\delta^{15}\text{N}$  and animal age. *Geochim. Cosmochim. Acta*, 48:1135-1140.
- Mitchell, A.H.G., and Reading, H.G., 1989. Sedimentation and tectonics. In Reading, H.G. (Ed.), *Sedimentary Environments and Facies* (2nd ed.): Oxford (Blackwell Sci.), 471-519.
- Mogi, A., and Mishizawa, K., 1980. Break-down of a seamount in the Trench of Japan. *Proc. Japan Acad. Sci.*, 56(B2):57-259.
- Montadert, L., Letouzey, J., and Mauffret, A., 1978. Messinian event: Seismic evidence. In Hsü, K.J., Montadert, L. et al., *Init. Repts. DSDP*, 42: Washington (U.S. Govt. Printing Office), 1037-1050.
- Moore, J.C., and Byrne, T., 1987. Thichening of fault zones: A mechanism of melange formation in accreting sediments. *Geology*, 15:1040-1043.
- Morris, R.J., McCartney, M.J., and Weaver, P.P.E., 1984. Sapropelic deposits in a sediment from the Guinea Basin, South Atlantic. *Nature*, 309:611-614.
- Müller, C., 1990. Nannoplankton biostratigraphy and paleoenvironmental results from the Tyrrhenian Sea, ODP Leg 107. In Kastens, K.A., Masclé, J., et al., *Proc. ODP, Sci. Results*, 107: College Station, TX (Ocean Drilling Program), 95-512.
- Müller, P.J., and Suess, E., 1979. Productivity, sedimentation rate and sedimentary organic matter in the oceans- organic carbon preservation. *Deep-Sea Res.*, 27A:1347-1362.
- Müller, P.J., Erlenkeuser, H., and von Grafenstein, R., 1983. Glacial-interglacial cycles in ocean productivity inferred from organic carbon contents in eastern North Atlantic sediment cores. In Thiede, J., and Suess, E. (Eds.), *Coastal Upwelling*, Part B: New York (Plenum), 365-398.
- Murdoch, W.W., and Onuf, C.P., 1974. The Mediterranean as a system, part I - large ecosystems. *Intern. J. Environmental Stud.*, 5:275-284.
- Nesteroff, W.D. 1973. Distribution of the fine-grained sediment component in the Mediterranean. In Ryan, W.B.F., Hsü, K.J., et al., *Init. Repts. DSDP*, 13: Washington (U.S. Govt. Printing Office), 666-670.
- Nur, A., and Ben Avraham, Z., 1978. The eastern Mediterranean and the Levant: Tectonics of continental collision. *Tectonophysics*, 46:297-311.
- Olausson, E., 1961. Studies of deep-sea cores. *Rep. Swedish Deep-Sea Expedition*, 8 (6):337-391.

- Parisi, E., Erba, E., and Cita, M.B., 1987. Stratigraphy and sedimentation in the anoxic Bannock Basin (eastern Mediterranean). *Mar. Geol.*, 75:93-117.
- Pedersen, T.F., 1983. Increased productivity in the eastern equatorial Pacific during the last glacial maximum (19000 to 14000 yr B.P.). *Geology*, 11:16-19.
- Pedersen, T.F., and Calvert, S.E., 1990. Anoxia vs. productivity: what controls the formation of organic-carbon-rich sediments and sedimentary rocks? *Am. Ass. Petr. Geol. Bull.*, 74:454-466.
- Prahl, F.G., 1992. Prospective use of molecular paleontology to test for iron limitation on marine primary productivity. *Mar. Chem.*, 39:167-186.
- Prahl, F.G., Muehlhausen, L.A., and Lyle, M., 1989a. An organic geochemical assessment of oceanographic conditions at MANOP Site C over the past 26,000 years. *Paleoceanography*, 5:495-510.
- Prahl, F.G., de Lange, G.J., Lyle, M., and Sarrow, M.A., 1989b. Post-depositional stability of long-chain alkenones under contrasting redox conditions. *Nature*, 341:434-437.
- Rabinowitz, P.D., and Ryan, W.B.F., 1970. Gravity anomalies and crustal shortening in the eastern Mediterranean. *Tectonophysics*, 10:585-608.
- Rau, G.H., Froelich, P.N., Takahashi, T., and DesMarais, D.J., 1991. Does sedimentary organic  $\delta^{13}\text{C}$  record variations in Quaternary ocean  $[\text{CO}_2(\text{aq})]$ ? *Paleoceanography*, 6:335-347.
- Reimers, C.E., and Suess, E., 1983. The partitioning of organic carbon fluxes and sedimentary organic matter decomposition rates in the ocean. *Mar. Chem.*, 13:903-910.
- Rieke, H.H., and Chilingarrian, G.V., 1974. *Compaction in Argillaceous Sediments*: Amsterdam (Elsevier).
- Robertson, A.H.F., 1991. Tectonic evolution of Cyprus. In Moores, E.M., et al. (Eds.), *Ophiolites and Oceanic Lithosphere*, Proc. Int. Symp. Nicosia, 235-250.
- Robertson, A.H.F., Eaton, S., Follows, E.J., and McCallum, J.E., 1991. The role of local tectonics versus global sea-level change in the Neogene evolution of the Cyprus active margin. *Spec. Pub. Int. Ass. Sediment.*, 12:331-369.
- Rohling, E.J., and Gieskes, W.W.C., 1989. Late Quaternary changes in Mediterranean intermediate water density and formation rate. *Paleoceanography*, 4:531-545.
- Rohling, E.J., and Hilgen, F.J., 1991. The eastern Mediterranean climate at times of sapropel formation: a review. *Geol. Mijnbouw*, 70:253-264.
- Rosignol-Strick, M., 1983. African monsoons, an immediate climate response to orbital insolation. *Nature*, 304:46-49.
- Ruddiman, W.F., Raymo, M.E., Martinson, D.G., Clement, B.M., and Backman, J., 1989. Pleistocene evolution: Northern Hemisphere ice sheets and North Atlantic Ocean. *Paleoceanography*, 4:353-412.
- Ryan, W.B.F., Hsü, K.J., et al., 1973. *Init. Repts. DSDP*, 13: Washington (U.S. Govt. Printing Office).
- Sancetta, C., Lyle, M., Heuser, L., Zahn, R., and Bradbury, J.P., 1992. Late-glacial to Holocene changes in winds, upwelling, and seasonal production of the northern California Current system. *Quat. Res.*, 38:359-370.
- Sarmiento, J., Herbert, T., and Toggweiler, J., 1988. Mediterranean nutrient balance and episodes of anoxia. *Global Biogeochem. Cycles*, 2:427-444.
- Sarnthein, M., Winn, K., Duplessy, J.-C., and Fontugne, M.R., 1988. Global variations of surface ocean productivity in low and mid latitudes: influence on  $\text{CO}_2$  reservoirs of the deep ocean and atmosphere during the last 21,000 years. *Paleoceanography*, 3:361-399.
- Schmitz, B., 1987. Barium, equatorial high productivity, and the northward wandering of the Indian continent. *Paleoceanography*, 2:63-78.
- Seely, D.R., 1977. The significance of landward vergence and oblique structural trends on trench inner slopes. In Talwani, M., and Pitmann, S.C. (Eds.), *Island Arcs, Deep Trenches, and Back-Arc Basins*. Am. Geophys. Union, Maurice Ewing Ser., 1:187-198.

- Smith, D.J., Eglinton, G., and Morris, R.J., 1986. The lipid geochemistry of a recent sapropel and associated sediments from the Hellenic Outer Ridge, eastern Mediterranean Sea. *Philos. Trans. R. Soc. London*, A319:375-419.
- Sutherland, H.E., Calvert, S.E., and Morris, J.R., 1984. Geochemical studies of the recent sapropel and associated sediment from the Hellenic Outer Ridge, eastern Mediterranean Sea I. Mineralogy and chemical composition. *Mar. Geol.*, 56:79-92.
- Tada, R., Koizumi, I., Cramp, A., and Rahman, A., 1992. Correlation of dark and light layers, and the origin of the cyclicity in the Quaternary sediments from the Japan Sea. In Tamakai, K., et al. (Eds.), *Proc. ODP, Sci. Results*, 127/128, Pt. 2:577-596.
- Taira, A., Hill, I., and ODP Leg 131 Scientific Party, 1992. Sediment deformation and hydrogeology of the Nankai Through accretionary prism: Synthesis of shipboard results of ODP Leg 131. *Earth Planet. Sci. Lett.*, 109:419-430.
- ten Haven, H.I., Baas, M., Kroot, M., de Leeuw, J.W., Schenck, P.A., and Ebbing, J., 1987. Late Quaternary Mediterranean sapropels. III: assessment of source of input and palaeotemperature as derived from biological markers. *Geochim. Cosmochim. Acta*, 51:803-810.
- Thunell, R.C., and Williams, D.F., 1989. Glacial-Holocene salinity changes in the Mediterranean Sea: hydrographic and depositional effects. *Nature*, 338:493-496.
- Thunell, R.C., Williams, D.F., and Belyea, P.R., 1984. Anoxic events in the Mediterranean Sea in relation to the evolution of late Neogene climates. *Mar. Geol.*, 59:105-134.
- Underhill, J.R., 1989. Late Cenozoic deformation of the Hellenide foreland, western Greece. *Geol. Soc. Am. Bull.*, 101(5):613-634.
- Vergnaud-Grazzini, C., Ryan, B.F.W., and Cita, M.B., 1977. Stable isotopic fractionation, climate change and episodic stagnation in the eastern Mediterranean during the late Quaternary. *Mar. Micropaleontol.*, 2:353-370.
- Vergnaud-Grazzini, C., Devaux, M., and Znaidi, J., 1986. Stable isotope "anomalies" in Mediterranean Pleistocene records. *Mar. Micropaleontol.*, 10:35-69.
- von Huene, R., and Lee, H., 1982. The possible significance of pore fluid pressure in subduction zones. In Watkins, J.S. and Drake, C.L. (Eds.), *The Geology of Continental Margins*, AAPG Memoir, 34:781-791.
- Westbrook, G.K., and Smith, M.J., 1983. Long decollements and mud volcanoes: evidence from the Barbados Ridge Complex for the role of high pore-fluid pressure in the development of an accretionary complex. *Geology*, 11:279-283.
- Williams, D.F., Thunell, R.C., and Kennett, J.P., 1978. Periodic freshwater flooding and stagnation of the eastern Mediterranean Sea during the late Quaternary. *Science*, 201:252-254.
- Woodside, J., and Bowin, C., 1970. Gravity anomalies and inferred crustal structure in the eastern Mediterranean Sea. *Geol. Soc. Am. Bull.*, 81:1107-1122.
- Wortel, M.J.R., Goes, S.D.B., and Spakman, W., 1990. Structure and seismicity of the Aegean subduction zone. *Terra Nova*, 2(6):554-462.
- Wust, G., 1961. On the vertical circulation of the Mediterranean Sea. *J. Geophys. Res.*, 66:3261-3271.
- Yamazaki, T., and Y. Okamura, 1986. Subducting seamounts and deformation of overriding forearc wedges around Japan. *Tectonophysics*, 160:207-230.
- Zahn, R., and Mix, A.C., 1991. Benthic foraminiferal  $\delta^{18}\text{O}$  in the ocean's temperature-salinity-density field: constraints on ice age thermohaline circulation. *Paleoceanography*, 6:1-20.
- Zahn, R., and Pedersen, T.F., 1991. Late Pleistocene evolution of surface and mid-depth hydrography at the Oman Margin: planktonic and benthic isotope records at ODP Site 724. In Prell, W.L., and Niitsuma, N. (Eds.), *Proc. ODP, Sci. Results*, 117: College Station, TX (Ocean Drilling Program), 291-308.
- Zahn, R., Winn, K., and Sarnthein, M., 1986. Benthic foraminiferal  $\delta^{13}\text{C}$  and accumulation rates of organic carbon (*Uvigerina peregrina* group and *Cibicidoides wuellerstorfi*). *Paleoceanography*, 1:27-42.
- Zahn, R., Sarnthein, M., and Erlenkeuser, H., 1987. Benthic isotope evidence for changes of the Mediterranean outflow during the late Quaternary. *Paleoceanography*, 2:543-559.

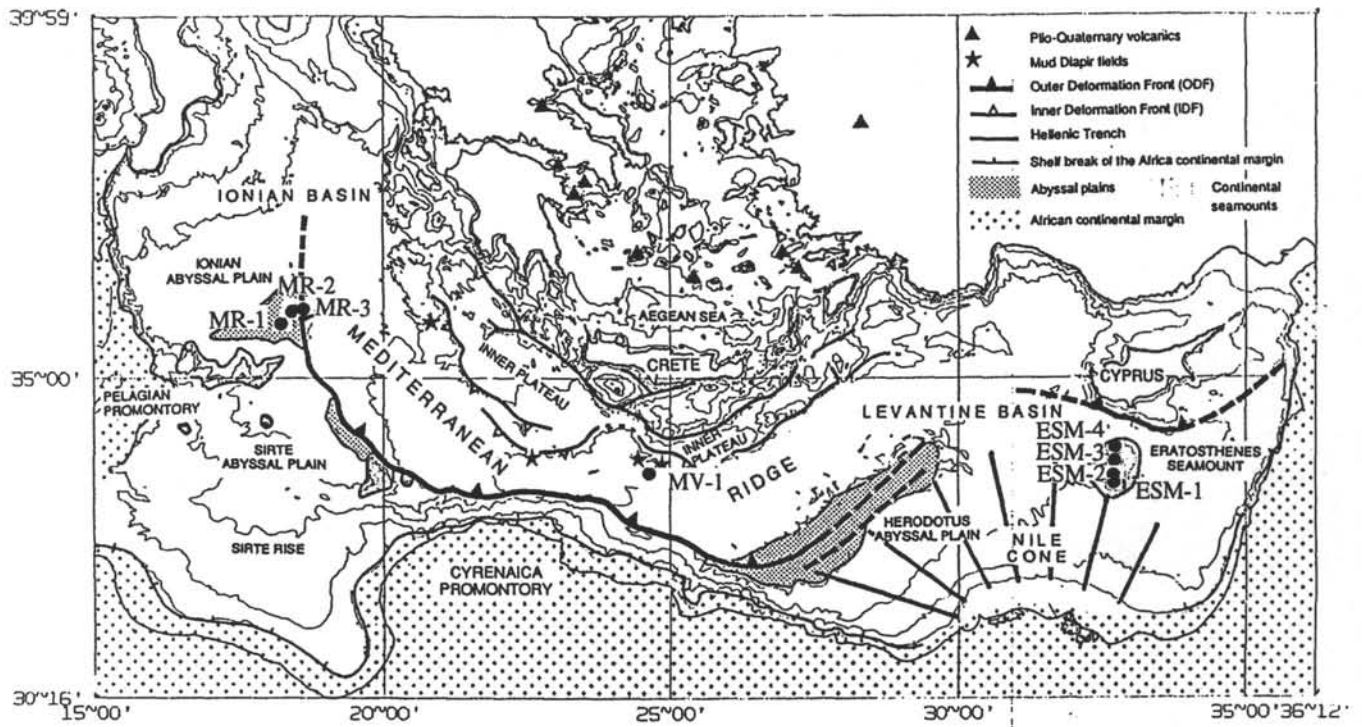


Figure 1A. Tectonic scheme of the eastern Mediterranean collisional margin and location of proposed sites on the Outer Deformation Front of the Mediterranean Ridge, the Eratosthenes Seamount, and the mud volcano.

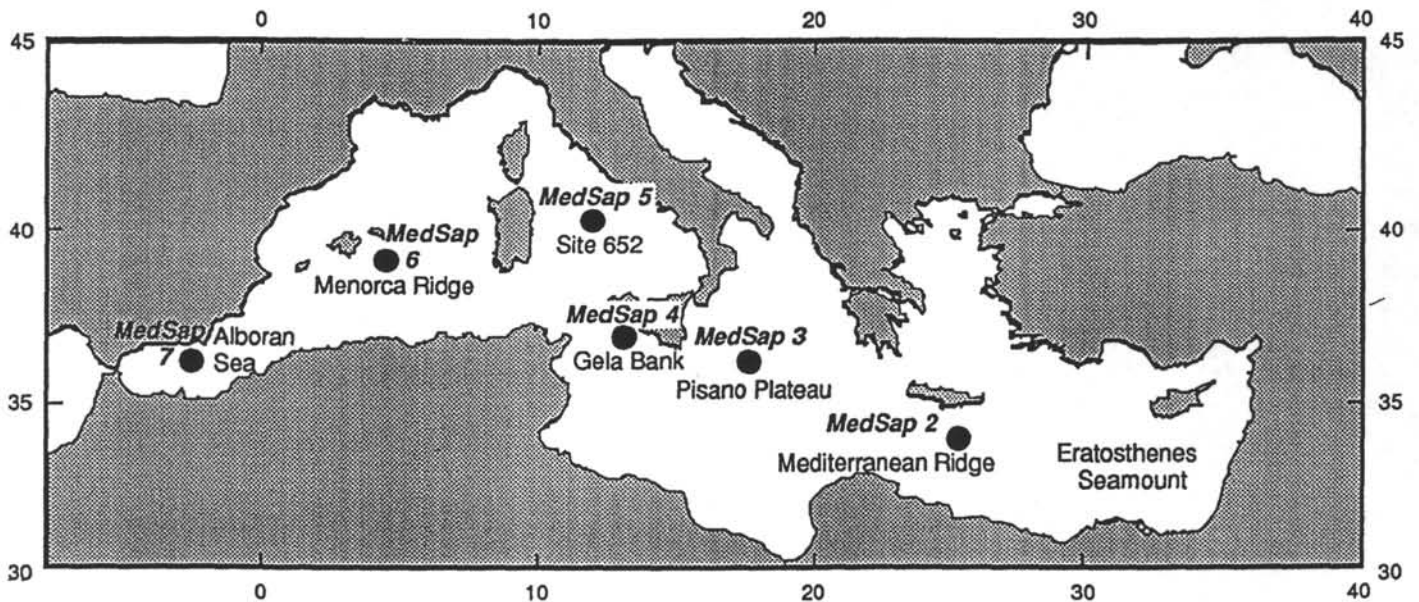


Figure 1B. Proposed site locations to investigate the origin of sapropels in the eastern Mediterranean. Proposed sites in the western Mediterranean (Leg 162), where sapropels did not form, will be used as reference sites.

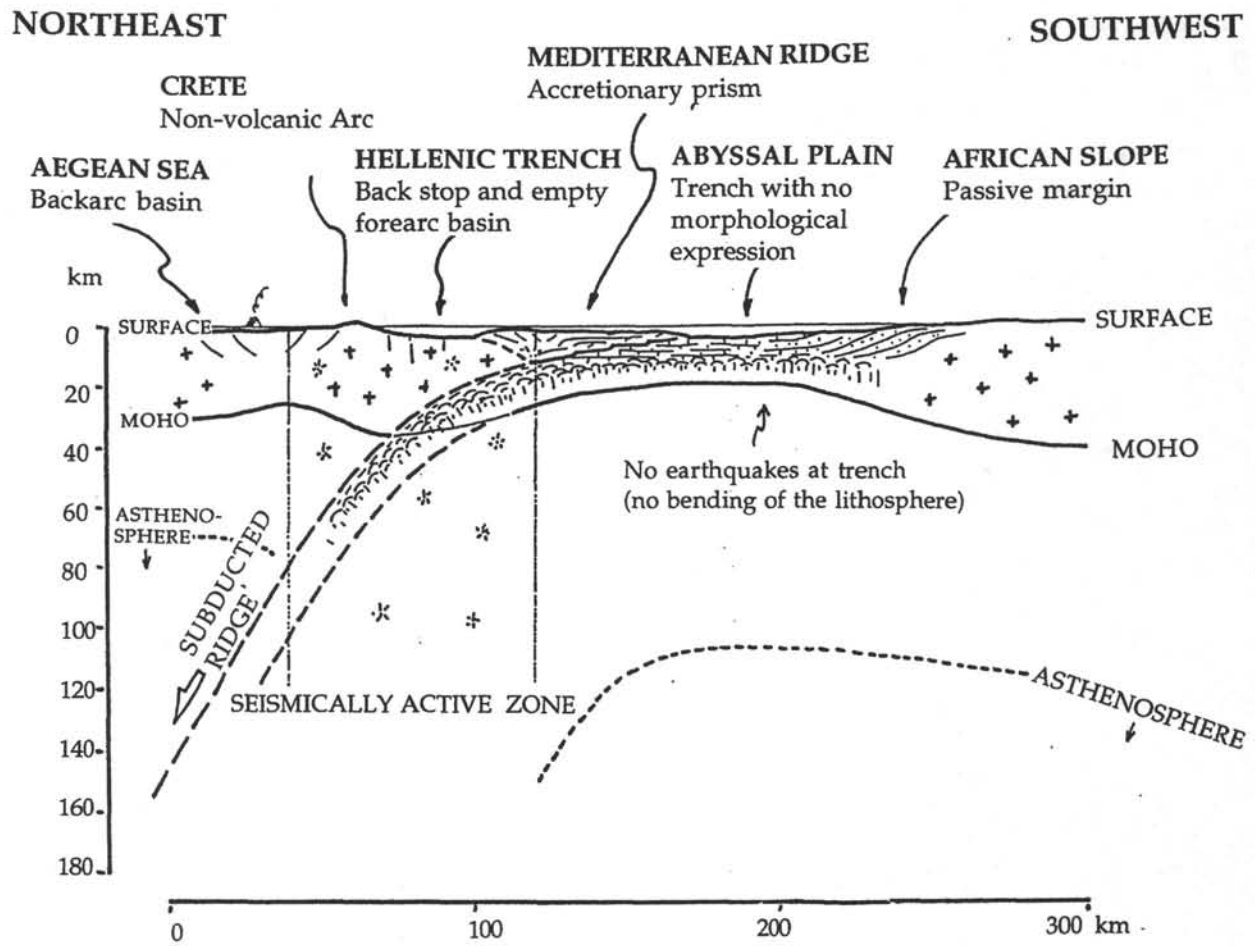


Figure 2. Generalized lithospheric cross section of the western portion of the eastern Mediterranean (Ionian and Sirte).

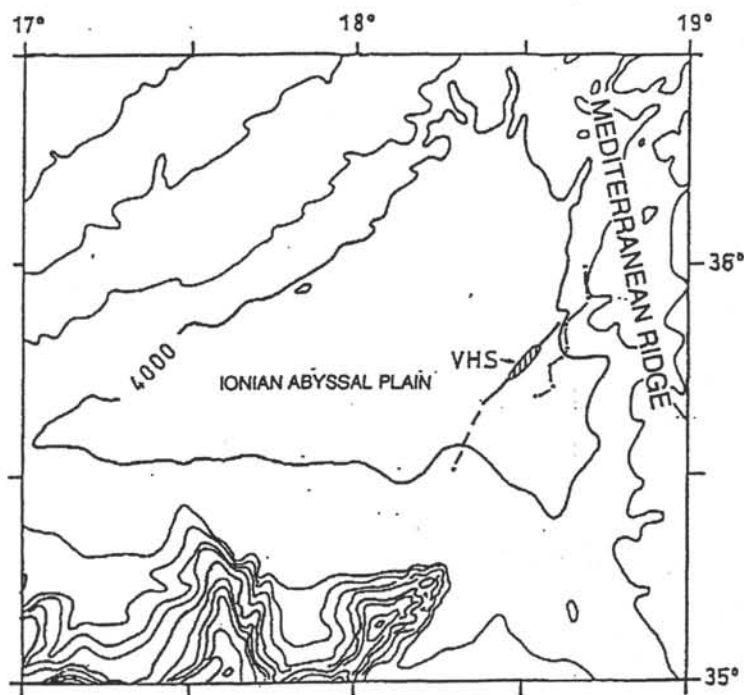
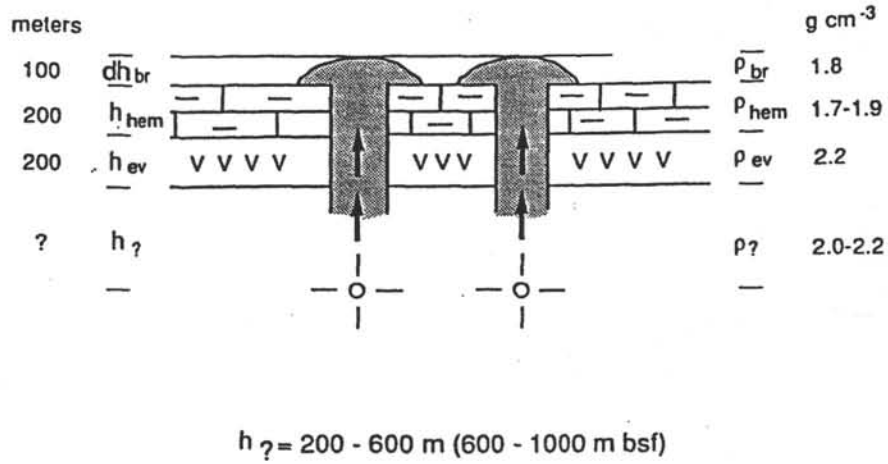
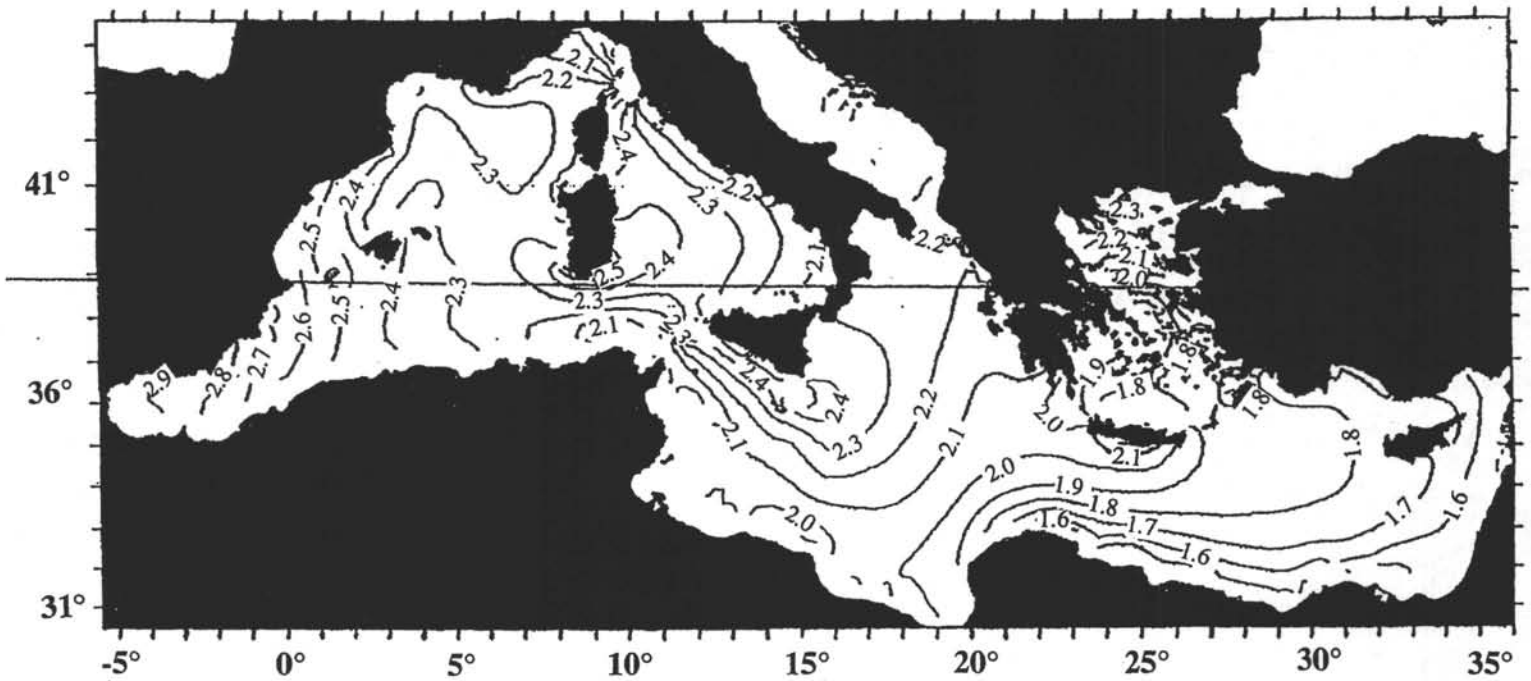


Figure 3. Position of Victor Hensen Structure (dashed line, including the Victor Hensen Seahill (VHS)) and Ionian Deformation Front (dotted line).



**Figure 4.** Simple model of mud diapir intrusion indicating a depth of provenance of at least 600 mbsf, thus from well below the Messinian evaporites. br: diapiric mud breccias; hem: hemipelagic host sediments; ev: Messinian evaporites; ?: source area.



**Figure 5.** Modelled distribution of nutrients (given in units of  $\text{mg atNm}^{-3}$ ) in the Mediterranean. Due to the physical circulation input parameters, nutrient concentrations - and thus, primary productivity - are highest in the western Mediterranean. If sapropel formation was driven by higher rates of primary production in the eastern Mediterranean, what caused the redistribution of nutrients from the western to the eastern basin? Courtesy of Renzo Mosetti, Osservatorio Geofisico Sperimentale Trieste.

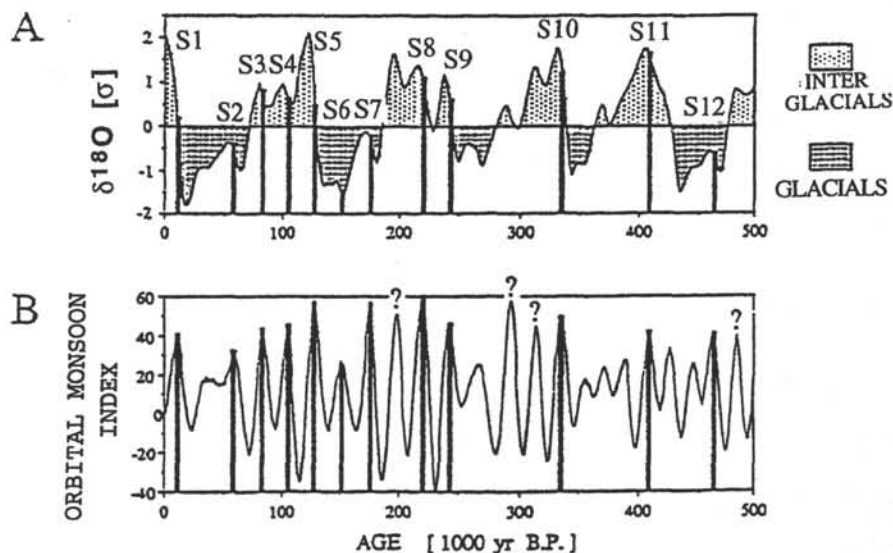


**Figure 6.** Distribution of eastern Mediterranean sapropels as a function of (A) global climate and (B) the orbital monsoon index *sensu* Rossignol-Strick (1983).

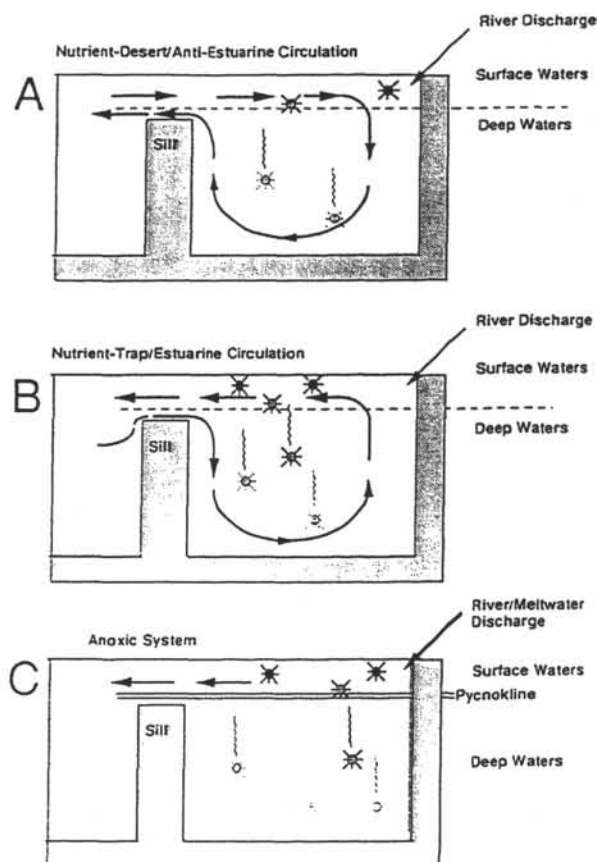


**Figure 7.** Schematic diagrams showing modern and hypothetical past circulation patterns of the Mediterranean Sea. (A) Modern anti-estuarine system. (B) Estuarine system. (C) Stagnant "anoxic" system. Scenarios (B) and (C) would have promoted the formation of sapropels through either enhanced preservation of organic carbon due to bottom water anoxia or through enhanced rates of biological productivity in the surface waters which would have led to increased fluxes of organic carbon to the seafloor.

Core MD 84641, Eastern Mediterranean  
(33°02'N, 32°38'E, 1375 m)

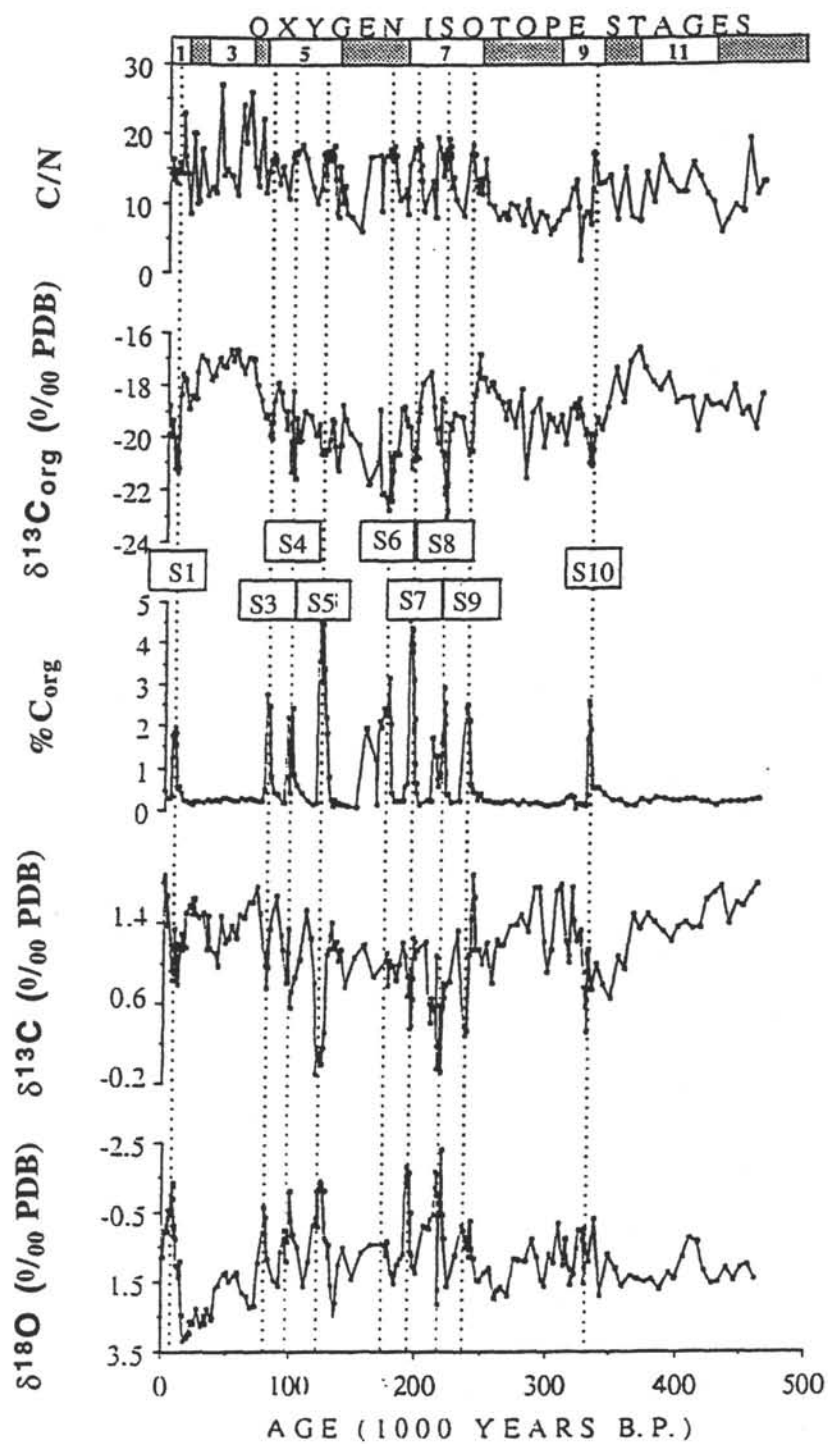


**Figure 8.** Stable isotope records (*G. ruber*,  $\delta^{18}O$ ,  $\delta^{13}C$ ), organic carbon content (percent by weight), carbon isotope composition of the organic fraction ( $\delta^{13}C_{org}$ ), and carbon/nitrogen ratios along Core MD84641 in the eastern Mediterranean. Data from Fontugne and Calvert (1992).

**TABLE 1**  
**PROPOSED SITE INFORMATION**  
**and**  
**DRILLING STRATEGY**

<b>SITE:</b> MR-1	<b>PRIORITY:</b>	<b>POSITION:</b> 35°42.1'N, 18°21.2'E
<b>WATER DEPTH:</b> 4100m	<b>SEDIMENT THICKNESS:</b> 5100m	<b>TOTAL PENETRATION:</b> 300m
<b>SEISMIC COVERAGE:</b> MCS - OGS line MS-21 and MS-112 - Cruise MEDRAC ( <i>Valdivia</i> )		

**Objectives:** Ionian Abyssal Plain. To sample the incoming sediment section. To sample the top of the buried Victor Hensen Structure. To determine the influence of salt on fluid circulation.

**Drilling Program:** APC and XCB coring.

**Logging and Downhole Operations:** Heat flow measurements.

**Nature of Rock Anticipated:** Ooze, clay, sand, and mudstone.

<b>SITE:</b> MR-2	<b>PRIORITY:</b>	<b>POSITION:</b> 35°46.8"N, 18°42.8'E
<b>WATER DEPTH:</b> 3950m	<b>SEDIMENT THICKNESS:</b> 5100m	<b>TOTAL PENETRATION:</b> ~ 200m
<b>SEISMIC COVERAGE:</b> MCS - OGS line MS-21 and MS-112 - Cruise MEDRAC ( <i>Valdivia</i> )		

**Objectives:** Ionian Deformation Front. To sample the uplifted sediments. To calculate deformation rates. To determine the influence of salt on fluid circulation.

**Drilling Program:** APC, XCB, and RCB coring.

**Logging and Downhole Operations:** Heat flow measurements. Standard geophysical tool and geochemical tool with RCB hole.

**Nature of Rock Anticipated:** Ooze, clay, and sand.

<b>SITE:</b> MR-3	<b>PRIORITY:</b>	<b>POSITION:</b> 35°46.8'N, 18°56.0'E
<b>WATER DEPTH:</b> 3700m	<b>SEDIMENT THICKNESS:</b> 5100m	<b>TOTAL PENETRATION:</b> ~ 200m
<b>SEISMIC COVERAGE:</b> MCS - OGS line MS-21 and MS-112 - Cruise MEDRAC ( <i>Valdivia</i> )		

**Objectives:** Ionian Deformation Front. To sample the uplifted sediments. To calculate deformation rates. To determine the influence of salt on fluid circulation.

**Drilling Program:** APC and XCB coring.

**Logging and Downhole Operations:** Heat flow measurements.

**Nature of Rock Anticipated:** Ooze, clay, and sand.

<b>SITE:</b> MV-1	<b>PRIORITY:</b>	<b>POSITION:</b> 33°43.7'N, 24°41.8'E
<b>WATER DEPTH:</b> 1900m	<b>SEDIMENT THICKNESS:</b> kms	<b>TOTAL PENETRATION:</b> 200m
<b>SEISMIC COVERAGE:</b> <i>R/V Geledzhic</i> (Izmir, June 25 - Istanbul July 15 1993) - TBP		

**Objectives:** Olimpi. To date intrusion of the mud volcano. To sample deep-fluid composition. To obtain physical properties of the mud volcano.

**Drilling Program:** XCB and RCB coring.

**Logging and Downhole Operations:** Heat flow measurements. Standard geophysical tool and geochemical tool with RCB hole.

**Nature of Rock Anticipated:** Mud breccia and ooze.

<b>SITE:</b> ESM-1	<b>PRIORITY:</b>	<b>POSITION:</b> 33°38'N, 32°40'E
<b>WATER DEPTH:</b> 750m	<b>SEDIMENT THICKNESS:</b> kms	<b>TOTAL PENETRATION:</b> 250m
<b>SEISMIC COVERAGE:</b> MCS - BEICIP lines B-14 and B-28 and OGS line MS-54.		

**Objectives:** Eratosthenes Seamount. To obtain information regarding the vertical motions and erosional patterns on the highest peak of the seamount and indications for lateral variation in redox potential of sapropels.

**Drilling Program:** APC and XCB coring.

**Logging and Downhole Operations:** Heat flow measurements.

**Nature of Rock Anticipated:** Plio-Pleistocene unconsolidated sediments.

<b>SITE:</b> ESM-2	<b>PRIORITY:</b>	<b>POSITION:</b> 33°52'N, 32°44'E
<b>WATER DEPTH:</b> 1500m	<b>SEDIMENT THICKNESS:</b> kms	<b>TOTAL PENETRATION:</b> 150m
<b>SEISMIC COVERAGE:</b> MCS - BEICIP lines B-14 and B-28 and OGS line MS-54.		

**Objectives:** Eratosthenes Seamount. To evaluate the depositional environment, sediments sources, and vertical motions close to the northern edge of the African Plate during incipient collision with Eurasia (Cyprus).

**Drilling Program:** XCB and RCB coring.

**Logging and Downhole Operations:** Heat flow measurements. Formation microscanner.

**Nature of Rock Anticipated:** Plio-Pleistocene unconsolidated sediments and Miocene rock.

<b>SITE:</b> ESM-3	<b>PRIORITY:</b>	<b>POSITION:</b> 34°05'N, 32°45'E
<b>WATER DEPTH:</b> 2600m	<b>SEDIMENT THICKNESS:</b> kms	<b>TOTAL PENETRATION:</b> 500m
<b>SEISMIC COVERAGE:</b> MCS - BEICIP lines B-14 and B-28 and OGS line MS-54.		

**Objectives:** Eratosthenes Seamount. To trace sediment sources in the collisional trough and to determine the history of the Plio-Pleistocene series, including the sapropels.

**Drilling Program:** APC and XCB coring.

**Logging and Downhole Operations:** Heat flow measurements.

**Nature of Rock Anticipated:** Plio-Pleistocene unconsolidated sediments.

<b>SITE:</b> ESM-4	<b>PRIORITY:</b>	<b>POSITION:</b> 34°11'N, 32°46'E
<b>WATER DEPTH:</b> 2000m	<b>SEDIMENT THICKNESS:</b> kms	<b>TOTAL PENETRATION:</b> 300m
<b>SEISMIC COVERAGE:</b> MCS - BEICIP lines B-14 and B-28 and OGS line MS-54.		

**Objectives:** Eratosthenes Seamount. To penetrate the collisional front and locate the boundary between Africa and Cyprus and to determine the depositional environments and sedimentary events near the collisional front.

**Drilling Program:** APC, XCB, and RCB coring.

**Logging and Downhole Operations:** Heat flow measurements. Standard geophysical tool and geochemical tool with RCB hole.

**Nature of Rock Anticipated:** Plio-Pleistocene unconsolidated sediments.

<b>SITE:</b> MedSap 2B	<b>PRIORITY:</b>	<b>POSITION:</b> 33°45.1'N, 24°42.3'E
<b>WATER DEPTH:</b> 1930m	<b>SEDIMENT THICKNESS:</b> 150m	<b>TOTAL PENETRATION:</b> 150m
<b>SEISMIC COVERAGE:</b> TREDMAR III and BAN-89a Line 0/33 kHz		

**Objectives:** To recover complete sediment sections on a structural high with known occurrences of late Quaternary sapropels. This site represents the central tie-point of the paleoenvironmental transect.

**Drilling Program:** Triple HPC/APC

**Nature of Rock Anticipated:** Calcareous muds and oozes, tephra, and sapropels. Evaporites below 80 m.

<b>SITE:</b> MedSap 3	<b>PRIORITY:</b>	<b>POSITION:</b> 36°15.3'N, 17°44.3'E
<b>WATER DEPTH:</b> 3640m	<b>SEDIMENT THICKNESS:</b> *	<b>TOTAL PENETRATION:</b> *
<b>SEISMIC COVERAGE:</b> N/O URANIA		

\* To be determined.

**Objectives:** This site is located on the Calabrian Ridge on the Pisano Plateau between the Beato Angelico Trough and Raffaello Basin and is a crucial site for establishing land-sea correlations. Deep coring has recovered several old sapropel layers (>S12).

**Drilling Program:** Triple HPC/APC

**Nature of Rock Anticipated:** Calcareous muds and oozes, tephra, and sapropels (in existing Core KC01B).

<b>SITE:</b> MedSap 4A	<b>PRIORITY:</b>	<b>POSITION:</b> 37°01.9'N, 13°10.9'E
<b>WATER DEPTH:</b> 470m	<b>SEDIMENT THICKNESS:</b> 300m	<b>TOTAL PENETRATION:</b> 300m
<b>SEISMIC COVERAGE:</b> Tyro Lines SC4, MT7, and MT9, MCS G82-142 and -121C.		

**Objectives:** To establish current regimes across the Strait of Sicily during sapropel deposition. This site is critical for land-sea correlation of the Pliocene-Quaternary sections.

**Drilling Program:** Triple HPC/APC

**Nature of Rock Anticipated:** Calcareous muds and oozes, turbidites, tephra, and sapropels.

OR

<b>SITE:</b> MedSap 4C	<b>PRIORITY:</b>	<b>POSITION:</b> 37°03.9'N, 13°15.3'E
<b>WATER DEPTH:</b> 502m	<b>SEDIMENT THICKNESS:</b> 450m	<b>TOTAL PENETRATION:</b> 450m
<b>SEISMIC COVERAGE:</b> Tyro Lines SC7, and MT11, and MCS G82-122.		

**Objectives:** To establish current regimes across the Strait of Sicily during sapropel deposition. This site is critical for land-sea correlation of the Pliocene-Quaternary sections.

**Drilling Program:** Triple HPC/APC

**Nature of Rock Anticipated:** Calcareous muds and oozes, turbidites, tephra, and sapropels.

*LEG 162*

*Mediterranean Sea II -  
The Western Mediterranean*

## LEG 162

### MEDITERRANEAN SEA II - THE WESTERN MEDITERRANEAN

---

Modified from Proposals 391-Rev2 and 323-Rev3 Submitted By:

**Rainer Zahn, Maria-Bianca Cita, Gert de Lange, Kay-Christian Emeis, and Adrian Cramp  
and Maria C. Comas, Anthony B. Watts, V. García-Dueñas, Robert B. Kidd, Andres Maldonado,  
Jacki Platt, Randall Stephenson, and John Woodside**

**To Be Named: Co-Chief Scientists and Staff Scientist**

---

#### ABSTRACT

Leg 162 represents the second in a two-leg program to investigate the tectonic and paleoceanographic history of the Mediterranean Sea and focuses upon the evolution of the Alboran Sea, a typical "Mediterranean backarc basin", and the origin of sapropels, laminated organic-rich layers deposited in the eastern Mediterranean Basin. The cause of the extension in basins such as the Alboran Sea Basin, and the rapid evolution of a collisional zone into superimposed regions of extension and adjacent contraction, has not yet been adequately explained and the Alboran Basin presents an ideal situation to investigate the competing hypothesis. The Neogene extensional basin beneath the Alboran Sea developed behind an arc-shaped mountain belt and is located on the site of Late Cretaceous/Paleogene orogen generated from collisional stacking. The region straddles the boundary between the European and African plates which converged during the Neogene; the basin thus formed in an overall environment of plate convergence. During the Miocene, the migration of the arcuate mountain front may have been nearly coeval with extension in the inner part of the arc that resulted in crustal attenuation and basinal spreading on the Alboran Domain. The basin formed from early Miocene onwards, whereas, outside the arc, the thrusting processes continued.

In order to determine the influence of the various factors on sapropel formation, we must obtain multi-proxy records along an east-west transect across the entire Mediterranean and synoptically map the hydrographic and climatic conditions throughout the Mediterranean both at the sites of sapropel formation in the eastern basin and at sites in the western basin where no sapropels formed. During Leg 161, drilling will be conducted at the easternmost sites (proposed sites MedSap 2B, 3, and 4) and Leg 162 will concentrate on sampling the westernmost occurrence of sapropels and areas in the western part of the basin where no sapropels formed (proposed sites MedSap 5, 6, and 7). Only this Mediterranean-wide data base will allow us to determine the driving force behind sapropel formation at different times, and how the Mediterranean's physical circulation and chemical cycling preconditioned the eastern basin towards sapropel formation.

## INTRODUCTION

### **Extensional Basins in Collisional Settings: The Scientific Problem**

Much of the Mediterranean region is underlain by Neogene extensional basins that are located on the sites of Late Cretaceous to Paleogene orogens generated by collisional stacking (Fig. 1A), and surrounded by highly arcuate thrust belts that were active before and during extension in the basins. They are in some ways analogous to the marginal basins of the western Pacific and western Atlantic oceans, which form by extension behind island arc/trench systems, but they differ in several important respects: they are smaller, the basins are largely floored by extended continental crust, and in several cases the surrounding convergent arcs are also largely intra-continental. These attributes characterize the so-called "Mediterranean backarc basins" (Horvath and Berckhemer, 1982). The Aegean and southern Tyrrhenian Basins are most closely comparable to marginal basins in that they lie above clearly defined subduction zones with attendant island arcs (the Aeolian and Hellenic Arcs), and the Tyrrhenian Basin may be locally floored by quasi-oceanic crust (Kastens et al., 1988). The evolution of the North Balearic Basin may also have been analogous to western Pacific backarc basins: it is generally accepted that the Paleogene-Neogene extension of the North Balearic Basin (Ligurian Sea), the anti-clockwise rotation of Sardinia, and the subduction of residual Mesozoic Tethyan oceanic crust beneath the island occurred contemporaneously. In the case of the northern Tyrrhenian Sea, the Pannonian Basin, or the Alboran Sea, however, there is no clear geophysical evidence to support subduction of oceanic lithosphere during the period of extension in the basin. The directions of extension in the basins, and of relative convergence in the surrounding arcs, vary markedly, and show no direct relationship to the overall relative motion of the African and Eurasian plates that bound these systems. There is no general agreement about the causes of extension in the basins, and the rapid evolution of a collision zone into superimposed regions of extension, adjacent contraction and arc migration has not yet been adequately explained.

As far as the origin of the basins is concerned, some authors have emphasized the role of anomalous mantle diapirism, the extensional locus of the basin being static (Van Bemmelen, 1972; Weijermars, 1985; Wezel, 1985; Doblasi and Oyarzun, 1989), whereas others consider that the basinal extension is contemporary with the subduction, similar to the western Pacific backarc model (Biju-Duval et al., 1978; Rehault et al., 1985; Dercourt et al., 1986; Malinverno and Ryan, 1986; Kastens et al., 1988). Removal and detachment of the thickened mantle lithosphere during

the last episode of the convergent process has been invoked to explain the subsequent lithosphere thinning superimposed on the collision zone, either by delamination (Bird, 1979) or by convection (Houseman et al., 1981). To explain extensional basins postdating and superimposed on continental collision sutures, Channel and Mareschal (1989) suggest that the rapid evolution of the collision suture into a zone of rifting, and the development of closely juxtaposed region of compression and extension, can be explained by a mechanism involving collision-induced delamination ("subduction") of continental mantle lithosphere. Their models for the Tyrrhenian Basin-Calabrian Arc show that asymmetric lithospheric thickening generates asymmetrical flow in the underlying mantle, and extension and contraction in contiguous regions.

Several conflicting hypotheses on the origin of the Alboran Sea have been the subject of various papers, however, most of them are poorly supported by data with regard to the extensional mechanism and kinematics causing the crustal attenuation of the Betic-Rif orogen and the formation of the Alboran Basin. Below, we briefly discuss the two, most accepted, hypotheses that best fit the structural organization of the region.

Platt and Vissers (1989) suggest that convective removal of a thickened lithospheric root could explain the formation of the Alboran extensional basin, on the site of a former collisional orogen (Fig. 2). In this hypothesis, the thickened ridge above, with no supporting lithospheric root below, is not supported isostatically, so, the ridge can begin to collapse and force thrust sheets outward, to condition radial emplacement of thrust-nappes around the Alboran Sea Basin. After that, the lithosphere can subside thermally to generate the Alboran Basin. In this model, extension is invoked to drive the peripheral compressive events, and therefore rifting in the Alboran Basin predates peripheral collision.

Garcia-Dueñas et al. (1992) and Comas et al. (1993) envisage a different scenario for the origin of the Alboran Basin-Gibraltar Arc, based on the concept of asymmetric delamination of the lithosphere mantle (Channel and Mareschal, 1989), that produced not radial, but preferential migration of the arcuate mountain front (the Gibraltar Arc) to the west-southwest (Fig. 3). This hypothesis suggests that the westward progression of the mountain front (with thickened crust) obliterated a thinned crust at 30-20 Ma, and that the collision between the mountain front and the adjacent continental margins (Maghrebian and South Iberian) to form the Gibraltar Arc occurred at 21 Ma (Fig. 3 A to B). When asymmetric delamination (because the offset of lithosphere thickness) became active, crustal thinning in the "back-arc" region started. Later (by 16 Ma, Fig.

3C), the extension propagated west-southwest and reached the Gibraltar Arc (extension superimposed on a former contraction) and the contraction propagated outward towards the paleo-margins (Fig. 3B to C). This hypothesis relates the initial crustal thinning in the Alboran Basin and the preferential westward migration of the Gibraltar Arc (between 21 and 16 Ma), with the origin of the South Balearic Basin. From 16 to 7 Ma, preferential westward migration of the locus of extension conditioned additional crustal thinning in the Alboran Sea region (Fig. 3C to D). Therefore, rifting in the Alboran Basin continuously postdated collision.

The processes discussed above operate to some extent independently of plate tectonics, and improved understanding of their nature and causes are vital to the development of a truly global tectonic theory. The Alboran Basin is a clear cut, well-defined, and well-studied example of an extensional basin that developed in a collisional setting, where these competing hypotheses can be fully investigated.

### **The Origin of Sapropels**

The Mediterranean sapropels represent paleoceanographic windows through which we may study, in great detail, key processes which lead to the burial and preservation of carbon at the sea floor in relation to marine chemical cycling and physical water mass circulation. In view of the existence of similar facies in other marginal seas and even the open ocean (Japan Sea, Black Sea, equatorial Pacific; see above), it is evident that gaining knowledge about these processes is crucial to gain a better understanding of how the ocean carbon cycle operates.

The FY95 Leg 161 prospectus (this report) details the rationale, background, objectives, and drilling strategy for the proposed investigation of sapropel formation in the Mediterranean. The reader is referred to this prospectus for in-depth discussion. During Leg 162 (Fig. 1C), we will continue the systematic stable isotope, geochemical, and micro-paleontological survey of the Mediterranean sapropels in a concerted program using stable isotope stratigraphy and paleoceanography (foraminiferal  $\delta^{18}\text{O}$  and  $\delta^{13}\text{C}$ ), geochemical oxygen, nutrient and productivity tracers (Ba, Br, Cd, I, Mn), carbon source biomarkers (long-chain alkenones, dinosterol, plantwax lipids,  $\delta^{13}\text{C}_{\text{org}}$ ,  $\delta^{15}\text{N}_{\text{org}}$ ), and microfaunal assemblage analysis.

## STUDY AREA

### The Alboran Sea

The Alboran Sea forms the westernmost part of the Mediterranean, and is about 400 km long and 200 km wide (Fig. 1B). It is surrounded to the north, west and south by the Betic (Southern Spain) and Rif (Morocco) compressional mountain chains, which connect around the Gibraltar Arc. The system as a whole is bounded to the north and south by the Iberian and African continental forelands, and to the east and west by the oceanic Balearic Basin and the Atlantic Ocean.

Plate-motion studies by Dewey et al. (1989) suggest that this part of the Africa/Europe plate boundary experienced about 200 km of roughly north-south convergence between mid-Oligocene and Late Miocene time, followed by about 50 km of west-northwest-directed oblique convergence in Late-Miocene to Recent time. The Alboran Basin therefore formed in an overall environment of plate convergence. This convergent history is not directly reflected in the kinematics either of the surrounding mountain chains, or of the extension in the Alboran Basin.

The Alboran Crustal Domain (Internal Zones) (Fig. 1B) of the surrounding Betic and Rifian mountain chains represent the disrupted and extended fragments of a convergent orogenic belt (Fig. 3) that evolved from Late Cretaceous to Early Miocene time (Balanyá and García-Dueñas, 1987, 1988; De Jong, 1991; Monié et al., 1991). Pre-Miocene convergence caused substantial crustal thickening, accompanied by high-pressure low-temperature metamorphism (Bakker et al., 1989; Tubia and Gil Ibarra, 1991; Gofé et al., 1989). The remains of this orogen affected by Miocene extension probably also underlie much of the Alboran Sea itself, and sampling of the basement beneath the basin is therefore one of the priorities of our proposed drilling program. Onshore, extensional detachment systems and fault-bounded sedimentary basins of Miocene age are superimposed upon the continental collision structures (Balanyá and García-Dueñas, 1987; Galindo et al., 1989; García-Dueñas and Balanyá, 1991; Platt and Vissers, 1989; García-Dueñas et al., 1992), and this extensional phase was accompanied by a distinctive low-pressure high-temperature metamorphic event (Torres-Roldán, 1979, 1981; Zeck et al., 1992). The crustal thinning over much of the region, both on- and offshore, is likely to be a result of this phase of extension (e.g., Van der Beek and Cloetingh, 1992).

Both the Iberian and Maghrebian continental margins and the Flysch Trough Units (Fig. 1B) (Betic- Rifean External Zones) reflect continued crustal shortening during the Miocene on the Iberian and African continental margins surrounding the Alboran Domain, while crustal extension occurred on the Alboran Domain itself. Shortening began in the basal Aquitanian (Early Miocene), apparently almost coevally with the beginning of extension in the internal parts of the system, and continued into the Late Miocene. Shortening directions vary from northwest in the Betic Cordillera (Banks and Warburton, 1991), to west in the Gibraltar Arc region (Balanyá and García-Dueñas, 1987, 1988) to west-southwest in the Rif (Frizon de Lamotte, 1987).

From the whole region, we can postulate that during the Early to Middle Miocene, the migration of the arcuate mountain front was nearly coeval with the extension in the inner part of the arc that resulted in crustal attenuation and basinal spreading on the Alboran Domain. In such a way, the Alboran Basin formed from Early Miocene onwards, whereas outside the arc thrusting processes continued. Schematic true scale sections across the Alboran Sea and adjacent mountain belts to illustrate the position of the basin in a convergent orogenic setting are in Fig. 4.

The Alboran Sea is underlain by continental crust between 14 and 25 km thick (e.g., Banda et al., 1983). Commercial wells and DSDP Site 121 established that the crust in those locations is made up of metamorphic rock closely related to that exposed in the nearby Betic and Rifean mountain chain. A sample of cordierite-sillimanite schist from DSDP Site 121 gave a K/Ar age of 16 Ma (Kornprobst, 1973; Steiger and Frick, 1973), suggesting rapid exhumation of high-grade metamorphic rocks beneath the Alboran Sea, comparable to that seen onshore (Zeck et al. 1992).

The Alboran Sea has a complex morphology, with several sub-basins, ridges, banks, and platforms (Fig. 5A). A sedimentary cover of Miocene to Recent sediments, 1-7 km thick (Comas et al., 1992; Jurado and Comas, 1992), occupies the various sub-basins. One of the ridges, the Alboran Ridge, is locally emergent, forming the small island of Alborán, with exposures of volcanic rock. The structure of the Alboran Basin (Fig. 5B) results from superimposed tectonic stages in basin evolution (Comas et al., 1992, 1993). Earlier structures correspond to extensional grabens of several rifting episodes (from earliest Burdigalian ? to early Tortonian ?). Magmatic events and mud diapirism were related to rifting. Later structures testify to a post-rift north-south contraction, involving folding and strike-slip faulting (e.g., de Larouzière et al., 1988; Mauffret et al., 1987; Woodside and Maldonado, 1992) which conditioned the present day sea-floor morphology. The last faulting episode took place by the Early Pliocene (?) and is related to basin

subsidence or collapse (?) during the Pliocene-Quaternary. This episode is believed to have influenced the location of the present day coastline. Aeromagnetic anomaly maps (Galdeano et al., 1974) suggest a pattern of volcanic ridges within the basin, and late Serravalian to Pliocene volcanics of various alkaline and calc-alkaline types (Bellon et al., 1983; Hernández et al., 1987) are exposed onshore and have been detected offshore (Comas et al., 1990a, b, 1992). These characteristics are consistent with an origin of the basin by rifting, extension, and subsidence in Neogene times.

The mantle beneath the Alboran Sea shows anomalously low seismic velocities, around 7.6-7.9 km/sec (Banda et al., 1983), at a relatively shallow depth. Two powerful earthquakes at about 600 km depth beneath Granada have been interpreted by Grimison and Chen (1986) as indicating the presence of a detached fragment of sinking lithosphere. Marked positive gravity anomalies along the coast (e.g., Bonini et al., 1973) suggest that mantle material locally approaches the surface. These anomalies are spatially associated with the Ronda and Beni Bousera outcrops of mantle peridotite onshore. The origin and significance of these bodies is the subject of considerable debate. They have been interpreted as a deep-rooted body (Bonini et al., 1973; Weijermars, 1985; Doblas and Oyarzun, 1989), but the field evidence suggests that they form an allochthonous sheet of mantle rock interleaved with crustal rocks (Lundeen, 1978; Dickey et al., 1979; Tubía and Cuevas, 1986; Balanyá and García-Dueñas, 1991). Recent gravity modelling of the Ronda peridotites body (Torné et al., 1992) supports this interpretation. Additional offshore geophysical data and drilling in their vicinity may help to discriminate between these ideas.

### **Circulation and Water Mass Distribution in the Mediterranean Sea**

The Mediterranean's physical circulation is mainly driven by the surface wind field and modulated by its complex bottom topography. Its principal features resemble those of an open-ocean sub-basin (100-km-scale) and mesoscale (10-km-scale) eddy circulation which is driven by seasonal winds and thermohaline gradients. This circulation pattern defines the distribution of nutrients in the Mediterranean, which tend to be highest in the western basin and lowest in the eastern basin thus leading to inter-basin differences in primary production (Fig. 6). Inflowing Atlantic waters influence the Mediterranean's physical circulation and define the biogeochemical and physical inventory of the upper layer (50 m) which drives the primary production in the Mediterranean and controls the flux of biologically-cycled constituents to the seafloor and into the sediments. The close connection between the Mediterranean's general circulation and the asymmetric distribution

of trophic levels between its western and eastern basins points to the importance of understanding the past variability of the Mediterranean's physical oceanography as a whole so as to unravel the origin of sapropel formation in the east. The FY95 Leg 161 prospectus (this report) provides a more detailed coverage of this topic.

### **Formation of Mediterranean Sapropels**

Sapropel formation occurred basin-wide within the eastern Mediterranean throughout Miocene-Pliocene-Pleistocene times. Correlation with standard oxygen isotope stratigraphy provides an excellent framework to evaluate the occurrence of the upper Pleistocene sapropels with respect to the state of global climate (Fig. 7). Apparently, sapropels formed rather unsystematically during full-glacial stages (sapropels S6, S12), full-interglacial stages (sapropels S8, S10, S11), and during interstadial stages (e.g., Vergnaud-Grazzini et al., 1977; Cita et al., 1977). A more systematic correlation has been obtained between the distribution of sapropels and maxima of the so-called orbital insolation monsoon index (Rossignol-Strick, 1983) (Fig. 7). The reader is referred to the FY95 Leg 161 prospectus (this report) for more detailed discussion of the following topics.

#### *The Deep-Water Stagnation Hypothesis*

According to traditional thinking, preservation of organic carbon should be enhanced during oceanic anoxia. The most viable means to deplete oxygen in deep waters is by way of extremely strong gravitational stability of the water column; this would shut off thermohaline overturn and thus terminate deep water ventilation (Fig. 8). Strongest support for this model comes from negative oxygen isotope anomalies recorded in planktonic foraminifera which are associated with the sapropels (e.g., Williams et al., 1978; Vergnaud-Grazzini, 1986). These anomalies imply the existence of a low-salinity and, thus, low-density surface layer in the eastern Mediterranean at times of sapropel deposition.

This stagnation hypothesis has been recently questioned for several reasons. First, the modern Mediterranean receives largely all of its waters from inflowing Atlantic surface-subsurface waters, which are intrinsically nutrient-depleted (Fig. 8). Thus, overall nutrient concentrations are low and the Mediterranean is an oligotrophic system in which no major productive areas exist (e.g., Murdoch and Onuf, 1974). At this low rate of biosynthetic marine organic carbon input,

sedimentary organic carbon concentrations would barely reach the elevated levels observed in the sapropels (Calvert, 1983). Second, areal mapping of the negative oxygen isotope anomalies observed in sediment cores from around the Nile cone suggests that the low-salinity surface layer extant during the formation of sapropel S1 was strongest in the immediate vicinity of the river mouth, presumably because the fresh waters mixed rapidly with the highly saline waters of the easternmost Mediterranean (Jenkins and Williams, 1984). Thus, the potential stabilizing effect of the low-salinity surface layer could have been restricted to the area closest to the Nile cone, whereas thermohaline overturn could have still prevailed in the easternmost Mediterranean. Third, geochemical evidence indicates that the early-Holocene sapropel (containing up to 14% organic carbon) in the Black Sea must have formed under well-ventilated, fully-oxic conditions (Calvert, 1990) and there are no sapropels forming there at present, even though the modern Black Sea is regarded as the type fully-anoxic basin.

#### *The Productivity Hypothesis*

Enhanced rates of biosynthetic carbon fixation are well recognized to be the primary factor controlling elevated levels of carbon in seafloor sediments. Organic carbon variations in sediment cores from high-productivity areas of equatorial divergence and coastal upwelling systems have been attributed to climate-controlled variations of primary productivity (Arrhenius, 1952; Pedersen, 1983; Müller et al., 1983; Morris et al., 1984; Zahn et al., 1986; Lyle et al., 1988; Prahl et al., 1989a, b; Sancetta et al., 1992). Estimates of the production rates needed to produce the carbon concentrations of 5-15% at depth typically found in the eastern Mediterranean sapropels, are similar to low to moderate primary production rates observed in the upwelling system off Northwest Africa. Although new cadmium and barium data (Boyle and Lea, 1989) suggest some possible contribution of riverine carbon input, other isotopic and geochemical tracers point to a predominantly marine origin of the sapropel organic carbon (Sutherland et al., 1984; Smith et al., 1986; ten Haven et al., 1987). Therefore, formation of the Mediterranean sapropels was probably promoted by enhanced rates of marine productivity rather than increased supplies of terrestrial carbon.

Several models have been put forward to explain how higher productivity levels in the otherwise oligotrophic Mediterranean could have been brought about. It has been postulated, for instance, that enhanced volumes of freshwater input during deglacial meltwater surges and/or monsoon-controlled river floodings would have reversed the Mediterranean circulation towards an anti-

estuarine system (Fig. 8) (Sarmiento et al., 1988; Lohmann and Pride, 1989; Thunell and Williams, 1989); however, this circulation reversal is in apparent contradiction with benthic foraminiferal  $\delta^{13}\text{C}$  signatures obtained from sediment cores to the west of the Strait of Gibraltar. Rohling and Gieskes (1989) recently envisioned a causal link between the development of deep chlorophyll maxima at the base of the euphotic zone and the formation of sapropels; however, this model does not provide a unique solution to the problem of sapropel formation but has recently been supported by quantitative analyses of calcareous nannofossil assemblages in eastern Mediterranean sediment cores. Salient maxima of dinosterols and long-chain alkenones (Smith et al., 1986; ten Haven et al., 1987) were used to infer that coccolithophorid and dinoflagellate productivity was high during sapropel formation, thus pointing to the potential importance of primary productivity for the formation of the Mediterranean sapropels.

## SCIENTIFIC OBJECTIVES AND METHODOLOGY

### Summary of Objectives

- 1) To better our understanding of the dynamics, kinematics, and deformation of the lithosphere, particularly in regard to a) the development of extensional basins on collisional orogens, b) the dynamics of the collapse of collisional ridges resulting in extensional basins surrounded by arc-shaped orogenic belts, c) the brittle/ductile deformation of the lithosphere, the role of magmatism, and of the upper mantle in crustal modification and lithosphere evolution, and d) actual or sub-actual collisional processes.
- 2) To investigate the nature of the pre-existing crust, i.e. the Paleozoic to Triassic basement.
- 3) To develop a lithosphere model to accommodate the observed rifting system and establish a) models for Miocene rifting, particularly to constrain the nature of the basement and the geometry of rifting, b) the behavior of the locus of extension, c) the magnitude and timing of extensional faulting, d) the nature of syn-rift versus post-rift subsidence and the pattern of total tectonic subsidence, and e) the timing and role of volcanism during extension.
- 4) To investigate post-rift deformation, i.e. deformation during later subsidence, the Late Miocene to Recent contractive reorganization, the transition to strike-slip recent tectonics, the role of volcanism, and the recent collapse of the basin, i.e. the post-Miocene subsidence.

- 5) To determine the sedimentary sequence and establish the amplification of the Global Isotopic Signal, the Late Miocene desiccation of the Mediterranean basins, and to calibrate the sea-level signal.
- 6) To investigate the long-term history of sapropel formation in relation to the history of atmospheric circulation and water mass variability in the Mediterranean, the inter-sapropel geochemical variability as a function of different environmental boundary conditions, and the water column redox conditions and (paleo-) productivity levels during sapropel formation.

### **Specific Tectonic Objectives and Methodology**

Drilling in the Alboran Sea will shed light on an important current problem in understanding convergent plate boundaries, that is the development of extensional basins on collisional orogens. These basins formed from extreme attenuation of a continental crust, thickened from collisional stacking, and developed from extension and basinal spreading in the inner part of an arcuate and migrating mountain front. Drilling will systematically test the response of the crust to both compressional and extensional forces.

Furthermore, the continental rift system that led to the development of the Alboran Basin provides an opportunity to examine variation in the brittle/ductile deformation of the lithosphere, the variable role of magmatism in rifting processes, and the role of upper mantle in crustal modification and lithospheric evolution. The Alboran Basin, as a part of the Mediterranean Sea, can be considered as a "natural laboratory" where actual or sub-actual collisional processes can be investigated. There is no doubt that these investigations in the Alboran Sea will have immediate implications in establishing models to explain the origin and evolution of the Western Mediterranean as well as other "Mediterranean-type" backarc basins in the world.

Drilling cannot directly resolve arguments about the kinematics of deformation of the lithosphere, or the dynamics of the process by which the Alboran Basin formed, but by providing accurate information on the stratigraphic record, basin geometry, timing and nature of deformation, rates of subsidence, and nature of the basin floor, it can usefully test the predictions of some of the competing genetic hypotheses. To answer some of the questions, it is necessary to integrate geological and geophysical data and results, not only from the Alboran Basin itself, but also from the surrounding orogenic belt. This tectonically-oriented drilling program represents an effort to

integrate detailed site surveys with onshore geological and geophysical data regarding the mountain chains that surround the basin (the Alboran Basin basement outcrops within these chains) in order to maximize the value of the drilling results.

#### *The Nature of the Pre-existing Crust*

Only by sampling the floor of the basin can we establish to what extent its development was controlled by the pre-existence of a collisional orogen. Petro-structural and petrological studies (metamorphic fabrics, PTT (pressure-temperature-time) path, and radiometric ages) of the predicted-metamorphic basement rocks on the graben flank in the Western Alboran Basin (proposed site ALB-1 or ALB-2) will determine the history of convergent tectonism, and their affinity to a particular crustal domain, or units within those domains.

#### *Rifting System and Rifting Processes - Lithosphere Model*

If the continental floor of the basin has been greatly extended, metamorphic rocks may have been exhumed from considerable depth within the crust along normal faults. The pressure-temperature histories of basement rocks at proposed site ALB-1 (or ALB-2) also will reveal the rate and thermal history of the extension (Buck et al., 1988; Ruppel et al., 1988; Voorhoeve and Houseman, 1988) beneath the Alboran Sea. Only sampling by drilling the basement, can we determine if these basement rocks belong to the hanging wall of the detachment systems outcropping on land, or to the exhumed footwall (Fig. 2 or Fig. 3).

What was the geometry of the rifting process? Was extension symmetrical or asymmetrical at the upper crustal level, and can we use the pattern of subsidence to determine the degree of asymmetry in the lithosphere?. Was extension normal, parallel, or oblique to the east-west axis of the basin, or did it vary spatially?. What is the role of multiple rifting events on basin evolution ? What rifting geometry can explain the absence of lower crust in the orogen as suggested from refraction data ? Was the locus of the extension fixed or was migrating during the basin evolution? What was the relationship between extension in the Alboran Sea and in the adjacent South Balearic Basin?. Drilling results on the timing of extensional faulting, combined with seismic data, can resolve these questions, essential to understanding the whole western Mediterranean and other world-wide basins with similar tectonic and geodynamic setting.

What is the magnitude of the extension and how does it vary spatially within the basin ? What were the relative proportions of syn-rift to post-rift subsidence, and can we interpret the subsidence data in terms of finite rifting or other types of thermal models? Back-stripping of biostratigraphic data from wells allows an estimate of the thickness of the crust to be made and compared to present day estimates of the thickness based on seismic and gravity anomaly data. By comparing the calculated and observed thicknesses we should be able to determine the initial thermal structure and elevation and/or processes that modified the crust since rifting. Comparison with back-stripped subsidence curves computed for onshore Betic Neogene basins (Clothing et al., 1992) will quantify the extension for the Miocene Alboran Basin as a whole.

How long did extension last? Drilling the basin-fill sedimentary sequence is essential to provide good stratigraphic control on extensional structures identified on seismic lines. Is the timing of extension strictly coeval with development of compressional structures on surrounding chains? The timing relations between rifting in the basin and convergence in the peripheral thrust belts is essential to understanding the origin of the basin and its relation to the evolution of the orogenic arc.

What was the role of volcanism during extension? There are indication from commercial wells and seismic data that volcanic and volcano-sedimentary rocks intercalate into Middle Miocene to Pliocene sediments in the basin fill. The age and chemistry of those volcano and volcanoclastic levels within the sedimentary sequence will provide direct constraints on the thermal and structural evolution of the underlying mantle (Lachenbruch and Morgan, 1990; Latin and White, 1990; White and McKenzie, 1989).

#### *Post-Rift Deformation*

What was the extent of the continuing deformation in the basin during the post-Messinian subsidence phase? Recent models for the extensional of collapse of collisional orogens (England and Houseman, 1989) suggest that the tectonic style is closely related to the potential energy of the system, and hence to surface elevation. The opportunity of comparative studies between the elevated onshore part of the basin and the offshore part on the Alboran ridge offers unique possibilities in this respect.

What was the nature of the postulated Late Miocene to Recent contractional reorganization that produced folding, strike-slip faulting, and pull-apart type structures in the basin ?

### **Specific Paleoceanographic Objectives and Methodology**

#### *Amplification of the Global Isotopic Signal, Late Miocene Desiccation , and Calibration of the Sea-Level Signal*

In the present day configuration, the Alboran Sea sits within one of the key oceanographic gateways. Over the 132-m-deep Gibraltar sill, a surface water mass inflows from the Atlantic and a deep water mass exits from the Mediterranean as a dense saline flow that is detectable as one of the principal intermediate water masses in much of the North Atlantic. The earlier connections between the Atlantic and Mediterranean and, before that, with Tethys have been controlled by the tectonic evolution of this region and the Alboran Sea may not have been a direct gateway until after the Messinian isolation of the Mediterranean (Adams et al., 1977). Nevertheless, comparative studies of the development of Atlantic and Mediterranean water masses represent one of the prime targets still to be addressed by paleoceanographers (Kennett, 1982). It will be possible to address a number of important paleoceanographic objectives from sedimentary sequences at all the proposed sites.

Apart from the ODP Leg 107 campaign in the Tyrrhenian Sea, no hydraulic piston coring has been carried out in the Mediterranean. All of the sites proposed in the Alboran Sea are in present-day pelagic or hemipelagic settings and will provide an integrated high-resolution stratigraphic record for the Plio-Pleistocene. Bio- and magneto-stratigraphic analyses can be carried out for integration with the oxygen isotope record and then can be refined by the suite of core logging techniques now available to shipboard scientists. Vergnaud Grazzini and Pierre (1991) have drawn attention to the amplification of the isotope record in the enclosed Mediterranean through studies of surface piston cores from the Alboran Sea. The evolution of this amplified signal since the onset of Northern Hemisphere glaciation will be targeted during Alboran drilling.

DSDP Leg 13 and 42A addressed the phenomenon of the Late Miocene desiccation of the Mediterranean basins (Ryan, Hsü et al., 1973; Hsü, Montadert et al., 1978). Key sites in the confirmation of the deep-water desiccation hypothesis were DSDP Sites 372 on the Menorca Rise and DSDP Sites 375 and 376 on the Flores Rise, west of Cyprus, which penetrated the feather

edge of the Messinian evaporite sequence (Hsü et al., 1977). Cover recovery at the onset of evaporite conditions and at the Mio-Pliocene boundary was crucial to the debate. Further recovery of undisturbed material over these intervals at other locations within the Mediterranean is needed to allow more detailed studies of these important paleoceanographic boundaries. The Alboran drill sites will penetrate the Messinian erosional unconformity (M) of the feather edges of the Upper Messinian sequences, ensuring that the upper evaporitic and Main Salt sequences are avoided, offering prime sites for continuation of these paleoceanographic studies.

The extensive suite of MCS and high-resolution SCS profiles that we have available in this area has allowed detailed mapping of reflectors throughout the Alboran sub-basins and onto the thick sequences of the margins. A seismic stratigraphy has been established for the margin sequences (Comas et al., 1992; Jurado and Comas, 1992; Maldonado et al., 1992) that appears linked to Cenozoic sea-level change, despite the changing tectonic picture within this region. The Alboran drill sites allow calibration of this regional data set and potentially can contribute to the debate over tectonic versus sea-level effects on seismic stratigraphy. Detailed sedimentological studies of the reflector transitions are planned as a subsidiary objective of this study.

### *Origin of Sapropels*

In order to determine the influence of the various factors on sapropel formation, we must obtain multi-proxy records along an east-west transect across the entire Mediterranean and synoptically map the hydrographic and climatic conditions throughout the Mediterranean both at the sites of sapropel formation in the eastern basin and at sites in the western basin where no sapropels formed. During Leg 161, drilling will be conducted at the easternmost sites and Leg 162 will concentrate on sampling the westernmost occurrence of sapropels and areas in the western part of the basin where no sapropels formed. Only this Mediterranean-wide data base will allow to determine the driving force behind sapropel formation at different times, and how the Mediterranean's physical circulation and chemical cycling preconditioned the eastern basin towards sapropel formation. The reader is referred to the FY95 Leg 161 prospectus (this report) for a detailed discussion of the approach to be employed in testing the stratigraphic, anoxic, and productivity models for the formation of sapropels and an example of a multi-proxy survey (Fig. 9) that was conducted by Fontugne and Calvert (1992) on sediments from the eastern Mediterranean. The study by Fontugne and Calvert produced a wealth of information on the tracer

distribution within the more recent sapropels and the Leg 161 and 162 program will extend this type of work back to times of changing environmental conditions during the Miocene and Pliocene.

#### Testing the Stratification Model

Foraminiferal oxygen isotope profiles provide the primary evidence for global climatic change. In addition to the climate-controlled "ice-effect", foraminiferal  $\delta^{18}\text{O}$  data combine the signals of regional temperature and salinity effects. Because the Mediterranean acts as a concentration basin in which evaporation exceeds precipitation and riverine freshwater input, salinity effects - in addition to the global ice-effect - may be expected to be the dominant contributors to the glacial-interglacial amplitudes of foraminiferal oxygen isotope records (e.g., Thunell and Williams, 1989). If indeed regional salinity anomalies existed, they could also have been brought about in part by a redistribution of freshwater between the eastern and western Mediterranean due to changes in atmospheric circulation (Rohling and Hilgen, 1991). In both cases - increased river runoff and/or precipitation - we would expect a gradual decrease in magnitude of the associated foraminiferal  $\delta^{18}\text{O}$  anomalies from the eastern to the western basin. This would also mean that thermohaline overturn would have decreased during these periods because of weaker salinity gradients between the western and eastern basins. Whether or not this led to stagnation of the deep waters depends on the resulting density contrasts in the Mediterranean. This would be tested using traditional temperature-salinity-density diagrams in combination with  $\delta^{18}\text{O}$ -equilibrium fractionation scenarios (see Zahn and Mix, 1991). That is, synoptic mapping of contemporaneous planktonic  $\delta^{18}\text{O}$  signals in the eastern and western Mediterranean will be an essential part in detecting possible inter-basin density contrasts and determining their effects as triggers for sapropel formation.

#### Testing the Anoxia Model

The ratio of the two halogens bromine (Br) and iodine (I) in marine sediments is directly controlled by the redox conditions prevailing during sediment deposition and the relative abundances of Br and I in the sediments can be used to determine whether the sediments originally accumulated under oxic or anoxic conditions (e.g., Calvert, 1990). The distribution of solid-phase manganese (Mn) can also be used to decipher the redox conditions at the sediment/water interface. Sub-surface anoxic sediments which have originally accumulated under oxic conditions generally contain high

concentrations of solid-phase Mn whereas sediments accumulating under anoxic conditions tend to have solid-phase Mn concentrations which are close to crustal abundance levels.

#### Testing the Productivity Model

Most organic compounds of marine origin are intrinsically labile and are, as such, removed from the sedimentary record during early diagenesis. Of the few original biomarkers that persist in the sediments, long-chain alkenones and dinosterol are the clearest indicators of marine carbon sources (e.g., Prahl, 1992). Both compounds are biosynthetic products characteristic of coccolithophorid and dinoflagellate productivity, respectively. They appear to be important components of the organic fraction in Mediterranean sapropels S1 and S7 (Smith et al., 1986; Ten Haven et al., 1987) and can be used as paleo-environmental indicators.

Atmospheric and riverine input of continentally-derived particulate carbon represents another potentially important source contributing to the sapropel organic carbon. Plantwax lipids are considered the most powerful indicator of terrestrial carbon and are readily identified by capillary gas chromatography. Stable carbon isotope analysis of the organic sediment fraction also has a great potential for separating organic carbon derived from terrestrial and marine sources.

In addition, analysis of  $\delta^{13}\text{C}_{\text{org}}$  will be most helpful (i) in combination with the analysis of plantwax lipids to separate the contribution of terrestrial versus marine carbon sources to the sapropels and (ii) in determining productivity levels during sapropel formation by way of estimating both the concentration of aqueous  $\text{CO}_2$  and total biomass of the signal carrying primary producers.

The isotopic composition of nitrogen in oceanic particulates provides useful information on the sources of nitrogen in, and export from, the mixed layer and on the recycling of particles throughout the water column and new evidence that the fractionation between  $^{15}\text{N}$  and  $^{14}\text{N}$  is influenced by the availability of nitrate as a nutrient (Altabet and Francois, 1992) allows the use of  $\delta^{15}\text{N}$  values as an indicator of nutrient concentration and thus primary production.

The concentration of barium (Ba) in marine sediments appears to be directly related to the rate of primary production at the sea surface and lattice-bound cadmium (Cd) in the shells of calcareous

foraminifera has been shown to be a sensitive tracer of changes in the nutrient content of ambient water masses (Boyle, 1988 ).

## **DRILLING PLAN/STRATEGY**

A description and location of the proposed Alboran Sea drill sites is given in Table 1 and Fig. 5B, respectively.

Proposed site ALB-2 is located on the graben in the Western Alboran Basin. At this site, a monitoring hole for reentry ( Hole C) will be cored to 200 m (?), using the RCB if necessary for safety. Then, we will offset to begin a second hole (Hole D) for setting a reentry cone and case the hole as necessary. We will then core from 200 m using one or more RCB bits to sample the basement by at least 150 m to total depth. The unlogged part of Hole B will be logged in the reentry hole prior to abandonment. The abandonment procedures may be standard with mud or cement plugging. This site is not considered hazardous and no special precautions are required.

We propose to log these holes using the standard Schlumberger suite of logging tools, WSTP and WL (SEIS, STRAT, GEO-CHEM, MAG) , including the formation microscanner (FMS). The temperature tool will be run to afford extrapolation of equilibrium temperatures. A velocity survey may be done to correlate hole depth to seismic reflection time. In sampling the basement, oriented cores are essential.

One short hole using the APC will be drilled at proposed site ALB-3, situated on the southern flank of the Alboran Ridge where existing MCS and single channel seismic reflection profile data indicate a zone of deformation during and following deposition of the sediments. Standard logging to total depth will be conducted prior to abandonment.

Proposed site ALB-4 is located on a small graben structure to the north of the Yusuf Ridge in the East Alboran Sea Basin and to the east of a northeast-southwest-trending strike-slip fault system. The objective at this site is to use a RCB to penetrate and sample about 650 m on the sedimentary sequence. However, if time permits, we will continue for a further 250 m to sample the underlying sediments. If a bit change is required and time is available, a free-fall funnel may be deployed. The RCB hole will be logged with the standard logging tools. Depending on RCB core recovery and the time remaining, an additional APC hole may be drilled.

To unravel the origin of sapropel formation, it is necessary to establish the paleoceanography of the entire Mediterranean to discover how physical circulation and chemical cycling preconditioned the eastern basin towards sapropel formation. During Leg 161, drilling will be conducted at the easternmost sites of sapropel formation in the Mediterranean Sea (proposed sites MedSap 2, 3, and 4) and Leg 162 will concentrate on sampling the westernmost occurrence of sapropels and areas in the western part of the basin where no sapropels formed (proposed sites MedSap 5, 6, and 7). The drill sites must fulfill the four essential requirements of stratigraphic continuity, high stratigraphic resolution, long stratigraphic range (as sapropels did form under very different global climatic settings), and optimum areal coverage. In order to ensure highest-quality information on the depositional environment during sapropel formation, sampling density of the sapropel layers, as well as the "normal" sediments immediately below and above the sapropels, must be on scales of centimeters to millimeters. Such high sampling resolution is essential for determining the factors that have led to the formation of the sapropels and which have helped in maintaining an environment favorable for the formation of sapropels over time scales of  $10^2$  to  $10^3$  years. Triple HPC/APC coring may be necessary to allow such intense sampling at the proposed eastern Mediterranean sites where sapropels do occur (Leg 161).

## **PROPOSED DRILL SITES**

### **Proposed site ALB-2**

Proposed site ALB-2 is located on the graben in the Western Alboran Basin, at Shot Point 1258 on GSI MCS line Alb-39 (filtered migration). The alternate proposed site ALB-2a is located at Shot Point 1335 on GSI-MCS line 75-234 (filtered stack). These sites are situated over the west flank of a basement high thought to be a Middle Miocene horst of the continental basement of the Alboran Basin. This structural high has an irregular facing to the west - a fault-controlled escarpment roughly parallel to the axis of the main Early-to-Middle Miocene graben in the Western Alboran Sea.

A deep hole at proposed site ALB-2 is expected to sample about 2,250 m of the post-rift and syn-rift sequences, estimated to be as old as late Langhian (Recent to Middle Miocene), that overlies the basement and then, penetrate and sample about 150 m of basement. We propose an alternate

“backup” hole at ALB-2a on the same basement high and in equivalent structural position. Differences between primary and alternative sites are insignificant.

At proposed site ALB-2, we will not penetrate the early and lowermost-Middle Miocene units in the basin. These earliest sediments have already been penetrated in commercial wells in the Spanish and Moroccan margins and these data therefore already contain information on the early subsidence history of the basin. The early subsidence history is reasonably well defined in the Alboran A-1 well. Moreover, since basement was penetrated in two wells, there are indications (depending on paleo-bathymetry estimates) of the early subsidence history at these wells. The subsidence history of the Alboran A-1 well has been interpreted by Watts et al. (in press) in terms of a finite rifting model in which rifting in the Alboran Basin took place over a finite period, perhaps as short as 6 m.y.

The determination of the early subsidence history of a basin such as a Alboran Sea depends critically on our ability to determine the paleo-bathymetry of the earliest sediments. The paleo-bathymetry at the Alboran A-1 well is reasonably well constrained but, it is by no mean clear that it would be well constrained at other sites on the Alboran Sea, especially ones that are presently located in deep water in the basin center. There is therefore a risk introduced by drilling the earliest sequences in the center of the basin that uncertainties in paleo-bathymetry may preclude accurate determination of the subsidence history as they have done, for example, at the El Jebha well.

Although the form of the early subsidence provides information on the rifting times, the most important constraint on geodynamic models is the Total Tectonic Subsidence (TTS). This is because the TTS is determined by the amount of crustal and lithosphere thinning and heating that occurred at the time of rifting. For example, Watts et al. (in press) have show the crustal thickness implied from TTS at the Alboran A-1 well is greater than that implied from gravity and seismic modelling, suggesting that there has been more extension at the well site than is indicated in the subsidence data. One explanation for this discrepancy is that the crust was initially above sea level so that some of the subsidence occurred aerially. This tectonic uplift, could be explained by either crustal thickening or lithosphere thinning. The TTS therefore provides more critical information on the amount of uplift, and hence magnitude, of initial crust and/or thickness at the drilling sites.

In addition to the above mentioned reasons, on land data (Garcia Dueñas et al., 1992) indicate that the more important west-southwest-directed extensional detachment system, which affected

the outcropping metamorphic-basement on Betics and Rift, occurred after 16 Ma, during the Middle Miocene. Drilling results therefore would provide critical information on the TTS from this extensional phase in the Alboran Basin.

The drilling plan at proposed site ALB-2 includes substantial penetration and sampling of the metamorphic basement. This remains as our highest drilling priority and will constrain current geodynamic models for the origin of the basin.

As known from onland data, elements of four pre-Miocene crustal domains are involved in the Gibraltar Arc - 1) the South Iberian continental margin, 2) the Maghrebic continental margin, 3) the Flysh Trough, and 4) the Alboran Crustal Domain. (Fig. 1B). Prevailing hypotheses suggest that the basement of the Alboran Basin is formed by the Alboran Domain, itself composed of a polyphase thrust stack that includes three nappe complexes, labelled (in ascending order) Nevado-Filabrides, Alpujarrides, and Malaguides. The Alpine metamorphic facies in the Alpujarrides and Nevado-Filabrides show evolution from high P-low T to low P-high T conditions, while the Malaguides have undergone very low grade Alpine metamorphism. These metamorphic complexes, affected by Miocene extension, probably also underlie the Alboran Sea itself. Because the nature of these metamorphic complexes is well known, petro-structural and petrological studies (metamorphic fabrics, PTT path and radiometric ages) of the predicted metamorphic basement will establish their affinity to a particular crustal domain, or units within those domains.

By sampling the basement, we will know if these basement rocks belong to the hanging wall of the detachment systems outcropping onland, or to the exhumed footwall. Consequently, drilling results tie to on-land structural data and will help to discriminate between models for lithosphere rifting (Fig. 2 or 3) based on the following reasoning:

- 1) The hypothesis from Fig. 2 implies that the basement of the Alboran Sea Basin will correspond to the footwall of the extensional detachments. If it is the case, the basement sampled at proposed site ALB-2 must correspond to the lower complexes of the metamorphic pile nappe of the Alboran Crustal Domain - i.e. rocks from the lowermost units of the Alpujarride complex either from the Nevado-Filabride complex, or even-lower unknown units.
- 2) Alternatively, and as predicted in Fig. 3, the basement rocks at proposed site ALB-2 will correspond to the middle or upper part of the Alpujarride complex or to the Malaguide complex

- i.e. to the upper tectonic elements of the pre-Miocene stacking of the Alboran Crustal Domain because we will drill, according to this hypothesis, in the hanging wall of the predicted westward-directed main extensional detachment (Fig. 3C and Fig. 4A).

### **Proposed site ALB-3**

Proposed site ALB-3 is located on the *Robert D. Conrad*/LDGO MCS line 825 (filtered migration) at CDP 2122, and is situated on the southern flank of the Alboran ridge where existing MCS and single channel seismic reflection profile data indicate a zone of deformation during and following deposition of the sediments. The deformation is expressed as a series of folds near the base of the ridge. On the southern ridge flank, there is evidence that the deformed zone (5 km wide) extends laterally for up to 50 km. Both deformation and tilting appear to be relatively recent. The southern flank of the ridge aligns with the Jebha fault and, therefore, may form part of a major, late, sinistral strike-slip fault system across the Alboran Sea. About 860 m (0.9 sec twt) of folded and tilted sediment, estimated to be as old as lowermost Pliocene, overlies the probably volcanic basement at the proposed drill site.

The objective at this site is to calibrate the recent stratigraphy of the southern part of the Alboran Basin, and to time the later tilting and uplift of the Alboran ridge and the associated folds, and strike-slip faulting. Comparison between recent folding and strike-slip faulting onland (elevated onshore parts) and the offshore deformation, which occurred contemporaneously with the Pliocene-to-Recent subsidence, will allow to constrain the later stage of contractional reorganization of the basin.

Our main objective is to penetrate the intra-Pliocene unconformity that lies at about 250 mbsf. Basement objectives on this deformed area will be addressed from dive studies and we expect these results will complement drilling.

### **Proposed site ALB-4**

This site is located on LDGO MCS Line 823 (filtered migration) at CDP 2340 and is situated on a small graben structure to the north of the Yusuf ridge in the East Alboran Sea Basin and to the east of a northeast-southwest trending strike-slip fault system. According to our data, the East Alboran Basin does not seem to have the same structural pattern as the West Alboran Basin. This region is

underlain by northwest-southeast or east-west trending basement ridges and basins with a thin and probably younger sedimentary fill (West Alboran) and relative lack of extensional structures.

Platt and Visers (1989) and Watts et al. (in press) suggest that "much of the active extension occurred when the region was still above sea level and the syn-rift fill may have been thin and mainly continental". According to this hypothesis, the present basin fill is interpreted as "passive fill that was deposited during a pot-rift subsidence phase". Other working hypotheses interpret the different structural character between the West and East Alboran Sea Basins in terms of strike-slip tectonics, considering that an Early-to-Middle Miocene major structure controlled the origin of the Alboran Basin and separates crustal blocks with different lithosphere behavior (the controversial "trans -Alboran Shear Zone", as defined in de Larouzier et al., 1988 ). In this scenario, the small basins beneath the eastern Alboran Sea, as well as the bigger Western Alboran Basin are considered as "pull-apart" basins.

The tectonic objective at proposed site ALB-4 is to sample the "syn-rift" and "post-rift" sediments to understand the subsidence history of the East Alboran Basin as compared to that of the West Alboran Basin, testing the above-mentioned hypotheses. Comparing the subsidence history from both regions will have strong implications on constraining the tectonic model and structural evolution for the whole Alboran Basin. Additionally, it is important to calibrate the sediment fill stratigraphy and seismic units in this region where there are no prior sampling references from drilling. Because the West and the East Alboran Basins are separated by residual structural highs, an accurate correlation between the sedimentary fill in both basins is not possible from seismic data.

This site was selected because it shows a clearly developed lower sequence of tilted, hummocky, reflectors. This sequence may represent the earliest sediments that infilled the graben and therefore may be of "syn-rift" type. The tilted sequence is overlain by "passive" ( post-rift ?) Plio-Quaternary(?) sediments. Our main objective is to penetrate and sample the unconformity which lies at about 650 mbsf and that separates syn- and post-rift sequences. The proposed sediment penetration is a minimum estimate . If time allows we should continue for a further 250 m to sample "syn-rift" sediments to obtain data on the relative proportions of syn-rift to post-rift subsidence. In addition, drilling result from proposed site ALB-4, placed as it is in the eastern end of the Alboran Sea, will permit more accurate correlation through seismic profiling with the South Balearic Basin.

New migrated reflection profiles indicate that the basement cannot be clearly identified. It appears that, at this site, there could be a substantial sedimentary section beneath the upper syn-rift units. Therefore, basement sampling is not feasible in time allowed. However, basement objectives, at least regarding basement highs around this site, will be accomplished by dive studies.

#### **Proposed site MedSap 5**

Proposed site MedSap 5 reoccupies ODP Leg 107 Site 652 in the Tyrrhenian Sea. The primary goal of Leg 107 drilling was to determine the tectonic history of the area and to obtain Pliocene-Pleistocene sedimentary sequences. Site 652 has penetrated 684 m of Messinian through Pleistocene sediments and has retrieved 8 sapropels. This makes the site the westernmost location of documented occurrence of sapropels. Discontinuous recovery and rotary drilling of Site 652 requires a reoccupation and deployment of the HPC/APC-technology to retrieve continuous and undisturbed cores for our sapropel program. We propose to drill the upper 200 m of sediments. Beyond this depth, evaporitic sequences are likely to hamper drilling for safety reasons.

#### **Proposed site MedSap 6A**

Proposed site MedSap 6A is located on the Menorca Ridge. This site is at the location of core MT 15 which retrieved 9.5 m of pelagic sediments. Initial inspection of the sediments revealed warm interglacial faunas at 900 cm which possibly coincide with the last interglacial stage 5e (~ 125 ka), implying average sedimentation rates of 7 cm.k.y.<sup>-1</sup>.

#### **Proposed site MedSap 7B**

Proposed site MedSap 7B is the westernmost site of our drilling transect. Its purpose is to document the Atlantic-Mediterranean exchange of water masses. Proposed site MedSap 7B is at the location of DSDP Site 121 in the western Alboran Sea. Drilling at Site 121 penetrated through 690 m of Plio-Pleistocene sediments with a fairly rich and diverse foraminiferal fauna. A major hiatus was mapped at this site between the Lower Pliocene and the late Miocene. Thus, at this site, we would obtain a complete Plio-Pleistocene sequence with no major disturbances in the Pleistocene section and some intercalated turbidites in the Pliocene section. Apparently, at any site in the

Alboran Sea, there would always be a Plio-Miocene unconformity due to salt tectonics related to the Messinian salt diapirs. Thus, in the Alboran Sea, we would not be able to obtain a complete Pleistocene through Miocene sequence. Nevertheless, an Alboran Sea site would make this program a well-rounded survey and reoccupation of Site 121 will at least allow to get a complete picture of the Mediterranean Sea paleoceanography during the Plio-Pleistocene.

## REFERENCES

- Adams, C.G., Benson, R.H., Kidd, R.B., Ryan, W.B.F., and Wright, R.C., 1977. The Messinian salinity crisis and the evidence of late Miocene eustatic changes in the world ocean. *Nature*, 269 (5627):383-386.
- Altabet, M.A., and Francois, R., 1992. Sedimentary nitrogen isotopic ratio records surface ocean nitrate utilization. Submitted.
- Arrhenius, G. O., 1952. Sediment cores from the East Pacific. In Petterson, H. (Ed.), *Reports of the Swedish Deep-Sea Expedition*, 5(1).
- Banda, E., and Ansoorge, J., 1980. Crustal structure under the central and eastern part of the Betic Cordillera. *Geophys. J. R. Astron. Soc.*, 63:515-532.
- Banda, E., Udias, A., Mueller, S., Mezcuca, J., Boloix, M., Qallart, J., and Aparicio, A., 1983. Crustal structure beneath Spain from deep seismic sounding experiments: *Phys. Earth Planet. Inter.*, 31:277-280.
- Balanyá, J.C., and García-Dueñas, V., 1987. Les directions structurales dans le Domaine d'Alboran de part et d'outre du Détroit de Gibraltar. *C. R. Acad. Sci. Paris*, 304, Ser. II:929-933.
- Balanyá, J.C., and García-Dueñas, V., 1988. El cabalgamiento cortical de Gibraltar y la tectónica de Béticas y Rif. *II Congreso Geol. España (Simposios)*:35-44.
- Bakker, H.E., De Jong, K., Helmers, H., and Biermann, C., 1989. The geodynamic evolution of the internal zone of the Betic Cordilleras (south-east Spain): A model based on structural analysis and geothermobarometry. *J. Metamorph. Geol.*, 7:359-381.
- Banks, C.J., and Warburton, J., 1991. Mid-crustal detachment in the Betic system of southern Spain. *Tectonophysics*, 191:275-289.
- Bellon, H., Bordet, P., and Montecat, C., 1983. Le magmatisme néogène des Cordillères bétiques (Espagne): Cronologie et principaux caractères géochimiques. *Bull. Soc. Géol. Fr.*, (7), 25 (2): 205-218.
- Biju-Duval, B., Letouzey, J., and Montadert, L., 1978. Structure and evolution of the Mediterranean basins. In Hsü, K.J., et al., *Init. Repts. DSDP*, 42A:Washington (U.S. Govt. Printing Office), 951-984.
- Bird, P., 1979. Continental delamination and the Colorado Plateau. *J. Geophys. Res.*, 84:7561-7571.
- Bonini, W.E., Loomis, T.P., and Robertson, J.D., 1973. Gravity anomalies, ultramafic intrusions, and the tectonic of the region around the Straits of Gibraltar. *J. Geophys. Res.*, 78:1372-1382.
- Boyle, E.A., 1988. Cadmium: chemical tracer of deep water paleoceanography. *Paleoceanography*, 4:471-489.
- Boyle, E.A., and Lea, D.W., 1989. Cd and Ba in planktonic foraminifera from the eastern Mediterranean: evidence for river outflow and enriched nutrients during sapropel formation. *Eos*, 43: 1134.
- Buck, R., Martinez, F., Steckler, M.S., and Cochran, J.R., 1988. Thermal consequences of lithospheric extension: Pure and simple. *Tectonics*, 7:213-234.
- Calvert, S.E., 1983. Geochemistry of Pleistocene sapropels and associated sediments from the eastern Mediterranean. *Oceanol. Acta*, 6:255-267.
- Calvert, S.E., 1990. Geochemistry and origin of the Holocene sapropel in the Black Sea. In Ittekkot, V., Kempe, S., Michaelis, W., and Spitzky, A. (Eds.), *Facets of Modern Biogeochemistry*: Berlin (Springer-Verlag), 328-353.
- Channel, J.E.T., and Mareschal, J.C., 1989. Delamination and asymmetric lithospheric thickening in the development of the Tyrrhenian Rift. In Coward, M.P., et al. (Eds.), *Alpine Tectonics*:Spec. Publ. - Geol. Soc. London, 45:285-300.
- Cita, M.B., Vergnaud-Grazzini, C., Robert, C., Chamley, H., Ciaranfi, N., and D'Onofrio, S., 1977. Paleoclimatic record of a long deep sea core from the eastern Mediterranean. *Quat. Res.*, 8: 205-235.
- Clothing, S., van der Beek, P.A., van Rees, D., Roep, Th.B., Biermann, C., and Stephenson, R.A., 1992. Flexural interaction and the dynamics of Neogene extensional basin formation in the Alboran-Betic region. *Geo-Mar. Lett.*, 12:66-67.

- Comas, M.C., García-Dueñas, V., and Jurado, M.J., 1990a. Sedimentation and structure of the Northern Alboran Basin: extensional steps in basin evolution. *Geology of the Ocean Intern. Conf.* : Palermo, Italy, 33 (Abstracts).
- Comas, M.C., García-Dueñas, V., Maldonado, A., and Megias, A.G., 1990b. The Alboran Basin: Tectonic regime and evolution of the Northern Alboran Sea. In Global events and Neogene evolution of the Mediterranean. *IX Congress R.C.M.N.S.*, 107-108 (Abstracts).
- Comas, M.C., García-Dueñas, V., and Jurado, M.J., 1992. Neogene tectonic evolution of the Alboran Basin from MCS data. *Geo-Mar. Lett.*, 12:157-164.
- Comas, M.C., García-Dueñas, V., Soto, J.E., and Campos, J., 1993. An extensional basin developed on a collisional orogen: the Alboran Sea, In Seranne, M., and Malavielle J. (Eds.), *Late Orogenic Extension in Mountain Belts*. Doc BRGM Fr., 219n°, 44-45.
- De Jong, K., 1991. Tectono-metamorphic studies and radiometric dating in the Betic Cordilleras (SE Spain) [Thesis]. Vrije Universiteit, Amsterdam.
- de Larouzière, F.D., Bolze, J., Bordet, P., Hernandez, J., Montenat, C., and Ott d'Estevou, P., 1988. The Betic segment of the lithospheric trans-Alboran shear zone during the Late Miocene. *Tectonophysics*, 152:41-52.
- Dercourt, J., Zonenshain, L.P., Ricou, L.E., Kazmin, V.G., Le Pichon, X., Knipper, A.L., Grandjacquet, C., Shotshikov, I.M., Geysant, J., Lepvrier, C., Perchersky, D.H., Boulin, J., Sibuet, J.C., Savostin, L.A., Srokhitin, Westphal, M., Bazhenov, M.L., Lauer, J.P., and Bijou-Duval, B., 1986. Geological evolution of the Tethys belt from the Atlantic to the Pamirs since the Lias. *Tectonophysics*, 123: 241-315.
- Dewey, J.F., Helman, M.L., Turco, E., Hutton, D.H.W., and Knott, S.D., 1989. Kinematics of the western Mediterranean. In Coward, M.P., et al. (Eds.), *Alpine Tectonics*. Spec. Publ. - Geol. Soc., 45:265- 283.
- Dickey, J.S., Jr., Lundeen, M.T., and Obata, M., 1979. Geologic map of the Ronda ultramafic complex. *Geol. Soc. Am., Chart Series*, 29:1-4.
- Doblas, M., and Oyarzun, 1989. Mantle core complexes Neogene extensional detachment tectonics in the western Betic Cordilleras, Spain: An alternative model for the emplacement of the Ronda peridotite. *Earth Planet. Sci. Lett.*, 93:76-84.
- Emeis, K.C., et al., 1991. The occurrence and significance of Pleistocene and upper Pliocene sapropels in the Tyrrhenian Sea. *Mar. Geol.*, 100:155-182.
- England, P. C., and Houseman, G.A., 1989. Extension during continental convergence, with application to the Tibetan plateau. *J. Geophys. Res.*, 94:17,561-17,579.
- Fontugne, M.R., and Calvert, S.E., 1992. Late Pleistocene variability of the carbon isotopic composition of organic matter in the eastern Mediterranean: monitor of changes in carbon sources and atmospheric CO<sub>2</sub> concentrations. *Paleoceanography*, 7:1-20.
- Frizon de Lamotte, D., 1987. Un exemple de collage synmétamorphe: la déformation miocène des Tamsamane (Rif externe, Maroc). *Bull. Soc. Géol. Fr.*, 3:337-344.
- Galdeano, A., Courtillot, V., Le Borgne, E., Le Mouel, J.-L., Rossignol, J.-C., 1974. An aeromagnetic survey of the southwest of the western Mediterranean: Description and tectonic implications. *Earth Planet. Sci. Lett.*, 23:323-336.
- Galindo, J., Gonzalez Lodeiro, F., and Jabaloy, A., 1989. Progressive extensional shear structures in a detachment contact in the Western Sierra Nevada (Betic Cordilleras, Spain). *Geodinam. Acta*, 3:73-85.
- García-Dueñas, V., and Balanyá, J.C., 1991. Fallas normales de bajo ángulo a gran escala en las Béticas occidentales. *Geogaceta*, 9:29-33.
- García-Dueñas, V., Balanyá, J.C., and Martínez-Martínez, J.M., 1992. Miocene extensional detachments in the outcropping basement of the northern Alboran basin (Betics) and their tectonic implications. *Geo-Mar. Lett.*, 12:88-95.
- Grimison, N.L., and Chen, W.P., 1986. The Azores-Gibraltar plate boundary: focal mechanisms, depths of earthquakes, and their tectonic implications. *J. Geophys. Res.*, 91:2029-2047.

- Hernandez, J., de Larouzière, F.D., Bolze, J., and Bordet, P., 1987.** Le magmatisme néogène bético-rifain et le couloir de décrochement trans-Alboran: *Bull. Soc. Géol. Fr.*, 3:257-267.
- Horvarth, F., and Berckhemer, H., 1982.** Mediterranean backarc basins. In Berckhemer, H., and Hsü, K. (Eds.), *Alpine Mediterranean Geodynamics*: Washington, D.C.(American Geophysical Union), 141-173.
- Houseman, G.A., MacKenzie, D.P., and Molnar, P., 1981.** Convective instability of a thickened boundary layer and its relevance for the thermal evolution of continental convergence belts. *J. Geophys. Res.*, 86:6115-6132.
- Hsü, K.J., et al., 1977.** History of the Mediterranean salinity crisis. *Nature*, 267:399-403.
- Hsü, K.J., Montadert, L., et al., 1978.** *Init. Repts. DSDP*, 42, Part 1:Washington (U.S. Govt. Printing Office).
- Jenkins, P., and Williams, D.F., 1984.** Nile water as a cause of eastern Mediterranean sapropel formation: Evidence for and against. *Mar. Micropaleontol.*, 8:521-534.
- Jurado, M.J., and Comas, M.C., 1992.** Well log interpretation and seismic character of the Cenozoic sequence in the Northern Alboran Sea. *Geo-Mar. Lett.*, 12:129-136.
- Kastens, K., Mascle, J., et al., 1988.** ODP Leg 107 in the Tyrrhenian Sea: Insights into passive margin and back-arc basin evolution. *Geol. Soc. Am. Bull.*, 100:1140-1156.
- Kennett, J.P., 1982.** *Marine Geology*: Englewood Cliffs, N.J. (Prentice-Hall).
- Kidd, R.B., Cita, M.B., and Ryan, W.B.F., 1978.** Stratigraphy of eastern Mediterranean sapropel sequences recovered during DSDP Leg 42A and their paleoenvironmental significance. In Hsü, K.J., Montadert, L., et al., *Init. Repts. DSDP*, 42, Part 1:Washington (U.S. Govt. Printing Office), 421-443.
- Kornprobst, J., 1973.** Petrographical study of "acoustic basement" and associated breccia at Site 121 - Western Alboran basin: a comparison with the Bético-Rifean basement. In Ryan, W.B.F., Hsü, K.J., et al., *Init. Repts. DSDP*, 13, Part 2:Washington (U.S. Govt. Printing Office), 759-761.
- Lachenbruch, A.H., and Morgan, P., 1990.** Continental extension, magmatism, and elevation; formal relations and rules of thumb. *Tectonophysics*, 174:39-62.
- Latin, D., and White, R.S., 1990.** Generating melt during lithospheric extension: Pure shear versus simple shear. *Geology*, 18:327-331.
- Lohmann, G.P., and Pride, C.J., 1989.** The eastern Mediterranean estuary: observational evidence favoring estuarine circulation during sapropel formation. *Eos*, 43:1134.
- Lundeen, M., 1978.** Emplacement of the Ronda peridotite, Sierra Bermeja, Spain. *Geol. Soc. Am. Bull.*, 89:172-180.
- Lyle, M., Murray, D.M., Finney, B.P., Dymond, J., Robbins, J.M., and Brooksforce, K., 1988.** The record of Late Pleistocene biogenic sedimentation in the Eastern Tropical Pacific Ocean. *Paleoceanography*, 3:39-59.
- Maldonado, A., Campillo, A.C., Mauffret, A., Alonso, B., Woodside, J., and Campos, J., 1992.** Alboran Sea late Cenozoic tectonic and Stratigraphic evolution. *Geo-Mar. Lett.*, 12:179-186.
- Malinverno, A., and Ryan, B., 1986.** Extension in the Tyrrhenian Sea and shortening in the Apennines as a result of arc migration driven by sinking of the lithosphere: *Tectonics*, 5:227-245.
- Mauffret, A., El-Robrini, M., and Gennesseaux, M., 1987.** Indice de la compression récente en mer Méditerranée: un bassin losangique sur la marge nor-algérienne. *Bull. Soc. Géol. Fr.*, 8:1195-1206
- Monié, P., Galindo-Zaldivar, J., Gonzalez Lodeiro, F., Goffé, B., and Jabaloy, A., 1991.** <sup>40</sup>Ar/<sup>39</sup>Ar geochronology of Alpine tectonism in the Betic Cordilleras (southern Spain). *J. Geol. Soc. London*, 148:289-297.
- Morris, R.J., McCartney, M.J., and Weaver, P.P.E., 1984.** Sapropelic deposits in a sediment from the Guinea Basin, South Atlantic. *Nature*, 309:611-614.
- Müller, P.J., Erlenkeuser, H., and von Grafenstein, R., 1983.** Glacial-interglacial cycles in ocean productivity inferred from organic carbon contents in eastern North Atlantic sediment cores. In Thiede, J., and Suess, E. (Eds.), *Coastal Upwelling*, Part B:New York (Plenum), 365-398.
- Murdoch, W.W., and Onuf, C.P., 1974.** The Mediterranean as a system, part I - large ecosystems. *Intern. J. Environmental Stud.*, 5:275-284.

- Pedersen, T.F., 1983. Increased productivity in the eastern equatorial Pacific during the last glacial maximum (19000 to 14000 yr B.P.). *Geology*, 11:16-19.
- Platt, J.P., and Vissers, R.L.M., 1989. Extensional collapse of thickened continental lithosphere: a working hypothesis for the Alboran Sea and Gibraltar Arc. *Geology*, 17:540-543.
- Prahl, F.G., 1992. Prospective use of molecular paleontology to test for iron limitation on marine primary productivity. *Mar. Chem.*, 39:167-186.
- Prahl, F.G., Muehlhausen, L.A., and Lyle, M., 1989a. An organic geochemical assessment of oceanographic conditions at MANOP Site C over the past 26,000 years. *Paleoceanography*, 5:495-510.
- Prahl, F.G., de Lange, G.J., Lyle, M., and Sarrow, M.A., 1989b. Post-depositional stability of long-chain alkenones under contrasting redox conditions. *Nature*, 341:434-437.
- Rehault, J.P., Boillot, G., and Mauffret, A., 1985. The western Mediterranean basin. In Stanley, D.J., and Wezel, F.C. (Eds.), *Geological Evolution of the Mediterranean Basin*: New York (Springer - Verlag), 101-130.
- Rohling, E.J., and Gieskes, W.W.C., 1989. Late Quaternary changes in Mediterranean intermediate water density and formation rate. *Paleoceanography*, 4:531-545.
- Rohling, E.J., and Hilgen, F.J., 1991. The eastern Mediterranean climate at times of sapropel formation: a review. *Geol. Mijnbouw*, 70:253-264.
- Rosignol-Strick, M., 1983. African monsoons, an immediate climate response to orbital insolation. *Nature*, 304:46-49.
- Ruppel, C., Royden, L., and Hodges, K.V., 1988. Thermal modelling of extensional tectonics: application to pressure-temperature-time histories of metamorphic rocks. *Tectonics*, 7:947-957.
- Ryan, W.B.F., Hsü, K.J., et al., 1973. *Init. Repts. DSDP*, 13: Washington (U.S. Govt. Printing Office).
- Sancetta, C., Lyle, M., Heuser, L., Zahn, R., and Bradbury, J.P., 1992. Late-glacial to Holocene changes in winds, upwelling, and seasonal production of the northern California Current system. *Quat. Res.*, 38:359-370.
- Sarmiento, J., Herbert, T., and Toggweiler, J., 1988. Mediterranean nutrient balance and episodes of anoxia. *Global Biogeochem. Cycles*, 2:427-444.
- Smith, D.J., Eglinton, G., and Morris, R.J., 1986. The lipid geochemistry of a recent sapropel and associated sediments from the Hellenic Outer Ridge, eastern Mediterranean Sea. *Philos. Trans. R. Soc. London*, A319:375-419.
- Steiger, R.H., and Frick, V., 1973. Isotopic dating of Alboran basement. In Ryan, W.B.F., Hsü, K.J., et al., *Init. Repts. DSDP*, 13, Part 2: Washington (U.S. Government Printing Office), 762.
- Sutherland, H.E., Calvert, S.E., and Morris, J.R., 1984. Geochemical studies of the recent sapropel and associated sediment from the Hellenic Outer Ridge, eastern Mediterranean Sea I. Mineralogy and chemical composition. *Mar. Geol.*, 56:79-92.
- ten Haven, H.I., Baas, M., Kroot, M., de Leeuw, J.W., Schenck, P.A., and Ebbing, J., 1987. Late Quaternary Mediterranean sapropels. III: assessment of source of input and palaeotemperature as derived from biological markers. *Geochim. Cosmochim. Acta*, 51:803-810.
- Thunell, R.C., and Williams, D.F., 1989. Glacial-Holocene salinity changes in the Mediterranean Sea: hydrographic and depositional effects. *Nature*, 338:493-496.
- Torné, M., and Banda, E., 1992. Crustal thinning from the Betic Cordillera to the Alboran Sea. *Geo-Mar. Lett.*, 12:76-81.
- Torné, M., Banda, E., García-Dueñas, V., and Balanyá, J.C., 1992. Mantle-lithosphere bodies in the Alboran crustal domain (Ronda Peridotites, Betic-Rifean orogenic belt). *Earth Planet. Sci. Lett.*, 110:163-171.
- Torres-Roldán, R., 1979. The tectonic subdivision of the Betic Zone (Betic Cordilleras, Southern Spain): Its significance and one possible geotectonic scenario for the westernmost Alpine belt. *Am. J. Sci.*, 279:19-51.
- Torres-Roldán, R.L., 1981. Plurifacial metamorphic evolution of the Sierra Bermeja peridotite aureole (Southern Spain). *Estudios Geol.*, 37:115-133.

- Tubía, J.M., and Cuevas, J., 1986.** High-temperature emplacement of the Los Reales peridotite nappe (Betic Cordillera, Spain). *J. Struct. Geol.*, 8:473-482.
- Tubia, J.M., and Gil Iburguchi, J.L., 1991.** Eclogites of the Ojen nappe: a record of subduction in the Alpujárride complex (Betic Cordilleras, southern Spain). *J. Geol. Soc. London*, 148:801-805.
- Van Bemmelen, R.W., 1972.** Driving forces of Mediterranean orogeny (Tyrrhenian test-case). *Geologie en Mijnbouw*, 51:548-573.
- van der Beek, P.A., and Cloething, S., 1992.** Lithosphere flexure and the tectonic evolution of the Betic Cordilleras (SE Spain). *Tectonophysics*, 203:325-344.
- Vergnaud-Grazzini, C., Devaux, M., and Znaidi, J., 1986.** Stable isotope "anomalies" in Mediterranean Pleistocene records. *Mar. Micropaleontol.*, 10:35-69.
- Vergnaud-Grazzini, C., and Pierre, C. 1991.** High Fertility in the Alboran Sea since the Last Glacial Maximum. *Paleoceanography*, 6:519.
- Vergnaud-Grazzini, C., Ryan, B.F.W., and Cita, M.B., 1977.** Stable isotopic fractionation, climate change and episodic stagnation in the eastern Mediterranean during the late Quaternary. *Mar. Micropaleontol.*, 2:353-370.
- Voorhoeve, H., and Houseman, G., 1988.** The thermal evolution of lithosphere extending on a low-angle detachment zone. *Basin Research*, 1:1-9.
- Watts, A.B., Platt, J.P., and Bulh, P., in press.** Tectonic evolution of the Alboran Sea Basin. *Basin Research*.
- Weijermars, R., 1985.** Uplift and subsidence history of the Alboran Basin and a profile of the Alboran Diapir (W-Mediterranean). *Geologie en Mijnbouw*, 64:349-356.
- Wezel, F.C., 1985.** Structural features and basins tectonics of the Tyrrhenian Sea. In Stanley, D.J., and Wezel, F.C. (Eds.), *Geological Evolution of the Mediterranean Basin*:Berlin (Springer-Verlag), 153-194.
- White, R., and McKenzie, D., 1989.** Magmatism at rift zones: the generation of volcanic continental margins and flood basalts. *J. Geophys. Res.*, 94:7685-7729.
- Williams, D.F., Thunell, R.C., and Kennett, J.P., 1978.** Periodic freshwater flooding and stagnation of the eastern Mediterranean Sea during the late Quaternary. *Science*, 201:252-254.
- Woodside, J.M., and Maldonado, A., 1992.** Styles of compressional neotectonics in the Eastern Alboran Sea. *Geo-Mar. Lett.*, 12:111-116.
- Zahn, R., and Mix, A.C., 1991.** Benthic foraminiferal  $\delta^{18}\text{O}$  in the ocean's temperature-salinity-density field: constraints on ice age thermohaline circulation. *Paleoceanography*, 6:1-20.
- Zahn, R., Winn, K., and Sarnthein, M., 1986.** Benthic foraminiferal  $\delta^{13}\text{C}$  and accumulation rates of organic carbon (*Uvigerina peregrina* group and *Cibicidoides wuellerstorfi*). *Paleoceanography*, 1:27-42.
- Zeck, H.P., Monié, P., Villa, I.M., and Hansen, B.T., 1992.** Very high rates of cooling and uplift in the Alpine belt of the Betic Cordilleras, southern Spain. *Geology*, 20:79-82.

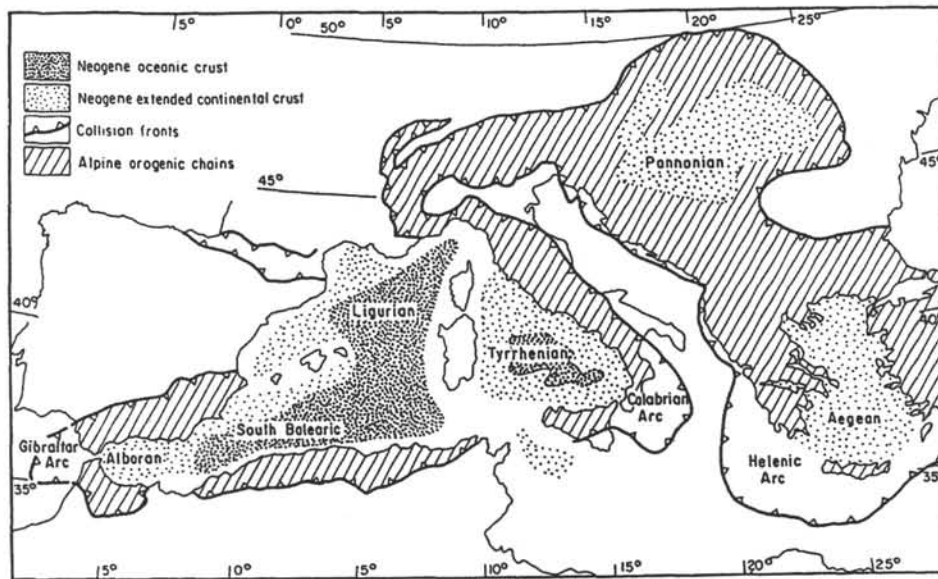


Figure 1A. Tectonic map of Mediterranean basins and mountains belts (based on data from various sources).

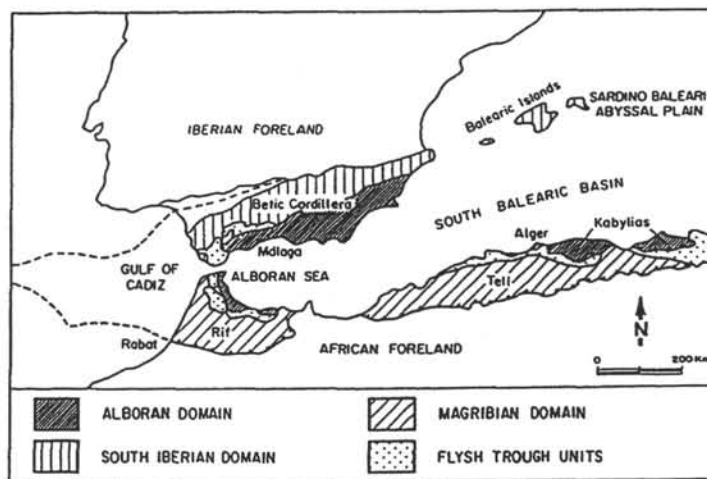


Figure 1B. The Alpine chains surrounding the Alboran Sea, general tectonic subdivision of crustal domains (from Balanyá and Garcia-Dueñas, 1987). Onshore distribution of this domains indicates that the continental basement beneath the Alboran Sea belongs to the Alboran Crustal Domain.

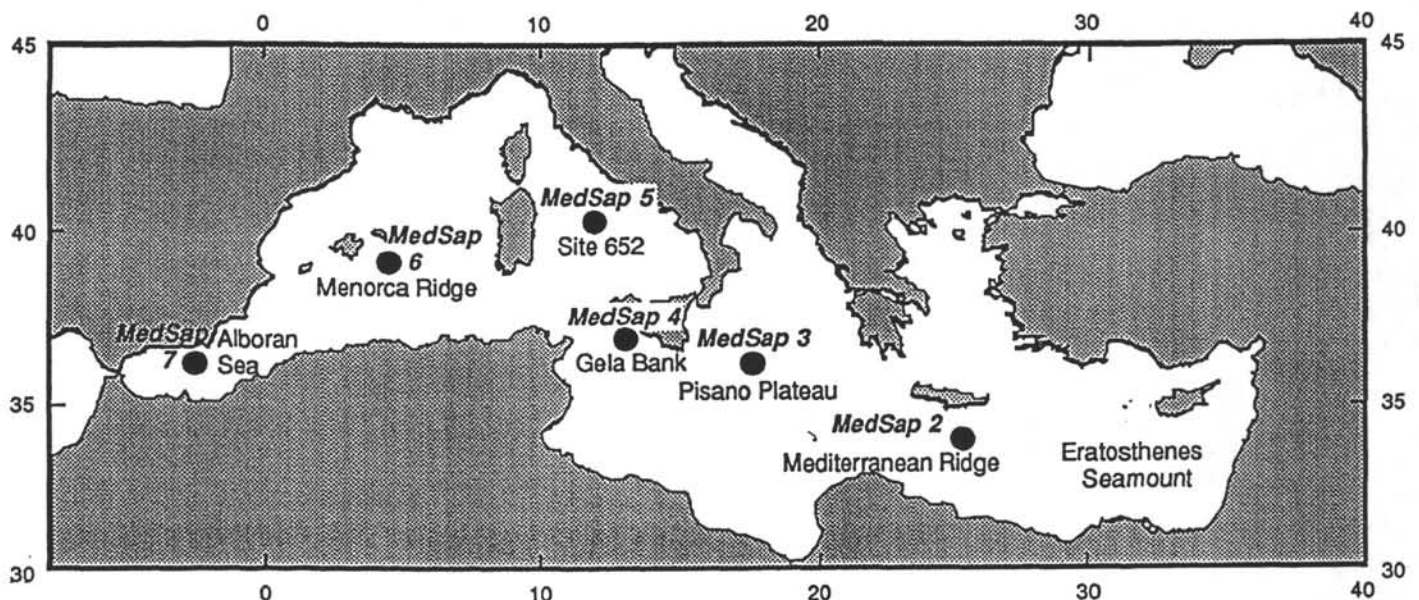
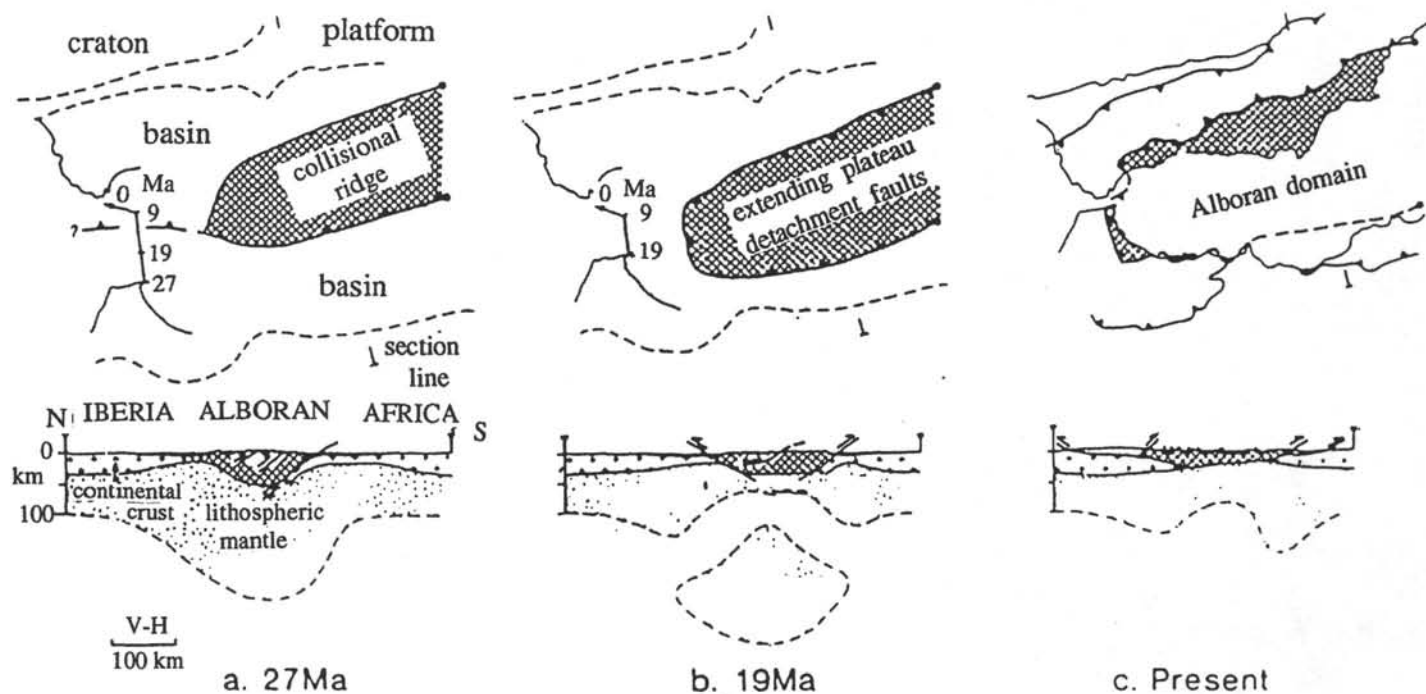


Figure 1C. Proposed site locations to investigate the origin of sapropels in the eastern Mediterranean. Proposed sites in the western Mediterranean (Leg 162), where sapropels did not form, will be used as reference sites.



**Figure 2.** Tectonic evolution of Alboran region, as hypothesized by Platt and Vissers (1989).

a) Mid-Oligocene - Collisional ridge with thickened lithospheric root formed by Late Cretaceous-Paleogene convergence. Map (above) shows coastlines around Gibraltar and Tangiers for reference, and plate motion vectors for Africa relative to Europe from 27 Ma to present after Dewey et al. (1989). Basins were probably underlain by thin continental crust.

b) Burdigalian - Convective removal of lithospheric root has caused uplift, increase in potential energy of collisional ridge, and extension. Extension is accommodated by crustal shortening around margins, producing the external Betic-Rif thrust belts. High-T peridotite emplaced at the base of the crust.

c) Extending Alboran Domain has been emplaced onto surrounding continental margins; center subsides as lithosphere thickens by cooling and continued slow convergence.

Note: Crustal volume is conserved in these figures, but cross-sectional area is not, because of radial pattern of motion.

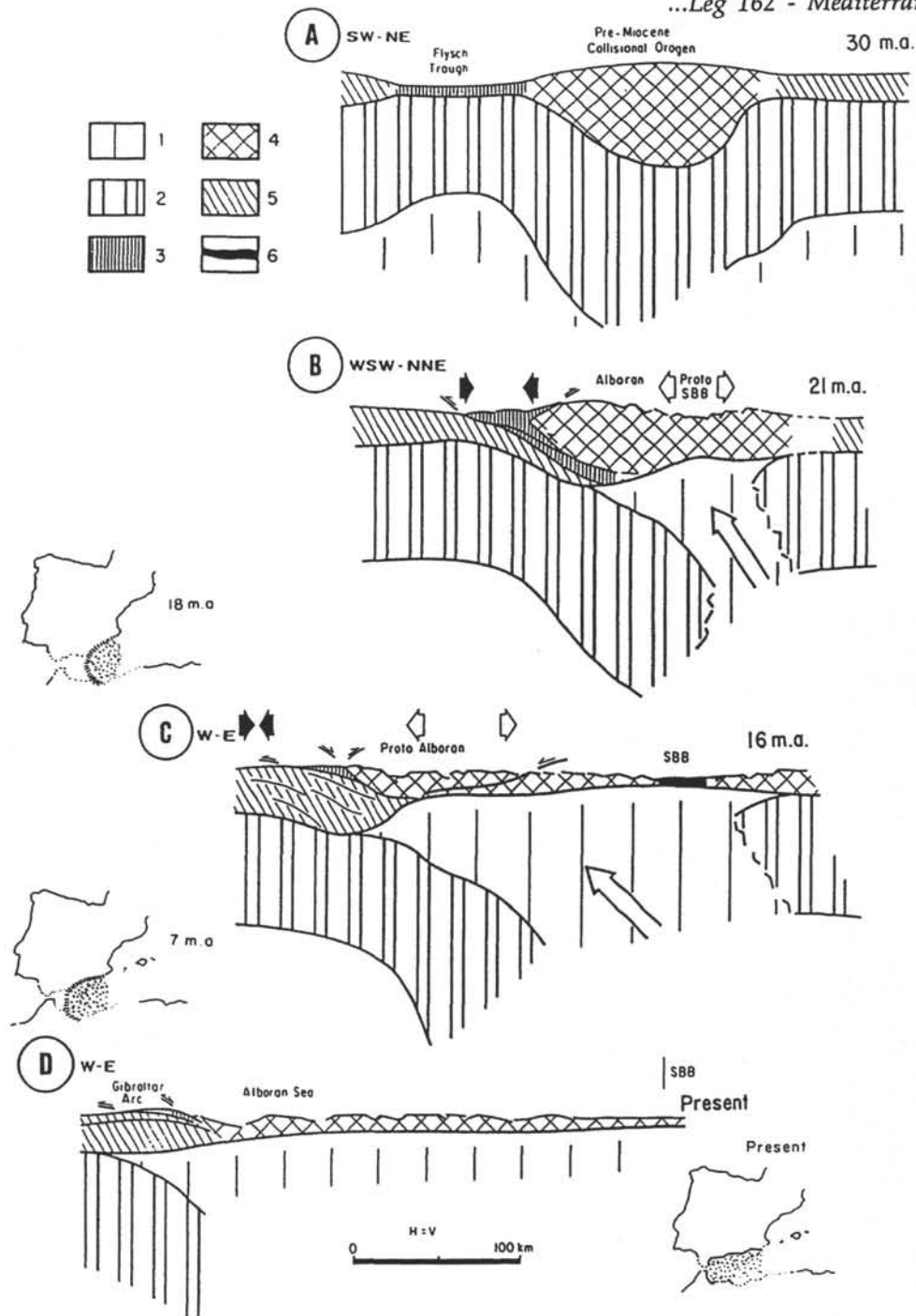


**Figure 3.** Hypothesis for the origin of the Alboran Basin considering the case of initial asymmetric lithosphere thickness (offset) in the collisional orogen, and then subsequent "delamination" of the lithosphere. Note that this model implies that the onset of extension on the Alboran Basin itself (B) postdates the Miocene continental collision which conditioned the Gibraltar Arc (B), and that the locus of the extension migrated (from the South Balearic to the "proto"-Alboran basin) contemporaneously with outwardly vergent thrust belt development (B to C).

1: Low density mantle. 2: Lithosphere mantle. 3: Flysch Trough. 4: Alboran Crustal Domain. 5: South Iberian / Magrebian continental margins. 6: Oceanic or very thin anomalous crust.

SBB: South Balearic Basin. Proposed position for the Gibraltar Arc front at 18 and 7 Ma. is shown. Note change of orientation from section A to D (from Comas and García-Dueñas, in press.)

Schematic true-scale sections across the Gibraltar Arc and the Alboran Sea basin to illustrate the large-scale E-W structure of the basin and its location on a convergent orogenic setting. Crustal thickness from Banda and Ansoerge (1980) and supposed position of ductile extensional detachments (7) within the CAD. CAD: Crustal Alboran Domain. D: Mud diapirs. FT: Flysch Trough units. LM: Lithosphere Mantle. LMD: Low-density mantle. M: Moho. Pt: Ronda peridotites. SIC: South-Iberian paleomargin cover. SIB: South-Iberian paleomargin basement. V: volcanics superimposed to the CAD. SBB: South Balearic Basin. WAB: Western Alboran Basin. Proposed drill site location (ALB-1 and ALB-4) is shown in Section II.

**Inset Map:** Structural map of chains surrounding the Alboran Sea. 1: Miocene to Recent sediments. 2: South-Iberian and Maghrebic paleomargin basements. 3: South-Iberian paleomargin cover. 4: Maghrebic paleomargin cover. 5: Flysch Trough Units. 6: Crustal Alboran Domain. 7: Ductile extensional detachments. 8: Strike-slip faults. According to this section, the basement beneath the Alboran Sea would correspond to the hanging wall of a major crustal extensional detachment. Note that the slab of Ronda peridotites are also placed on the hanging-wall of the extensional detachment (García-Dueñas et al., 1992; Comas et al., 1993). Note that this cross-section is the same as cross-section D in Fig. 3.

Bouguer anomaly and schematic true-scale section across the Alboran Sea Basin and adjacent mountains belts.

Upper profile: Bouguer anomaly, the calculated anomaly based on the density model shown, and the calculated anomaly assuming the basin is in Air-type isostatic equilibrium.

Middle profile: density model with the assumed densities in  $\text{kg m}^{-3}$ .

Lower profile : Geological cross section to illustrate the large-scale N-S structure of the basin and its position in a convergent orogenic setting. Deep reflectors (ICR: intra crustal reflector and, TRLC: top of reflective lower crust) recognized on seismic line Conrad 827 (arrowed segment) are interpreted as a continuation of the detachments faults onshore (from Watts et al., in press).

Note that, as known from onshore data, the movement directions on thrusts and extensional detachments have a strong westerly component, oblique to the line of section.

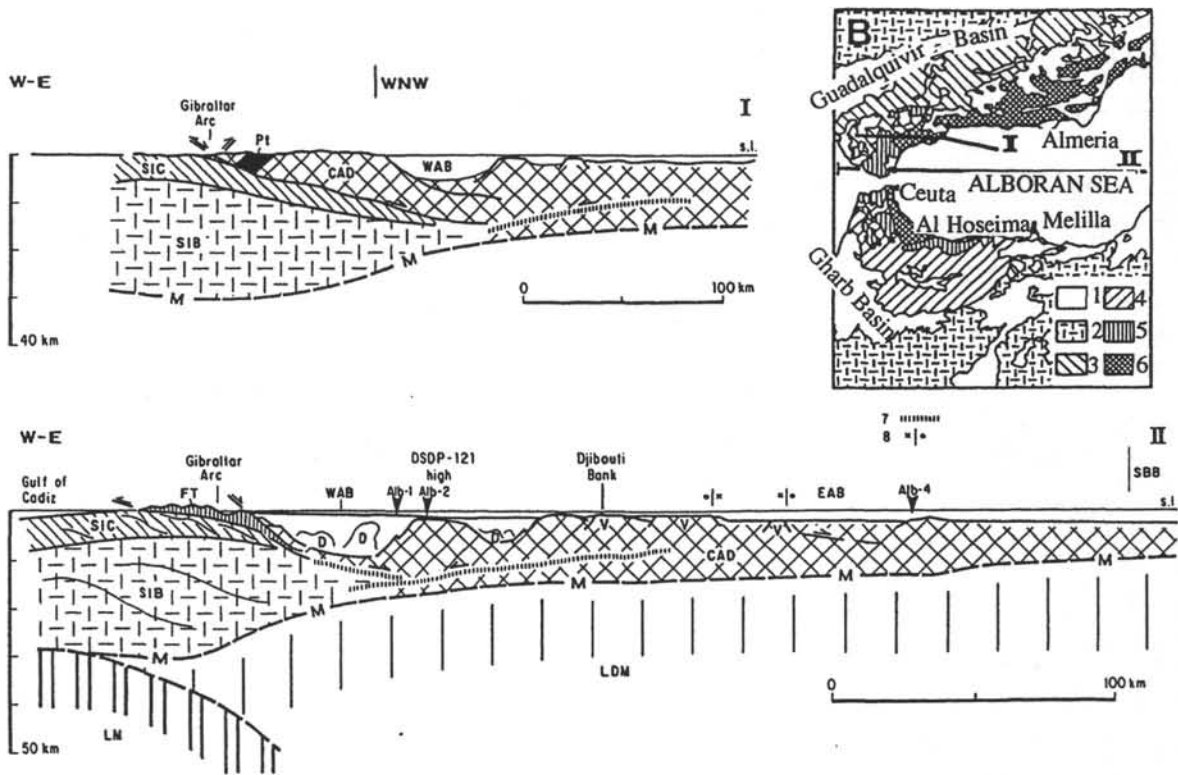


Figure 4A.

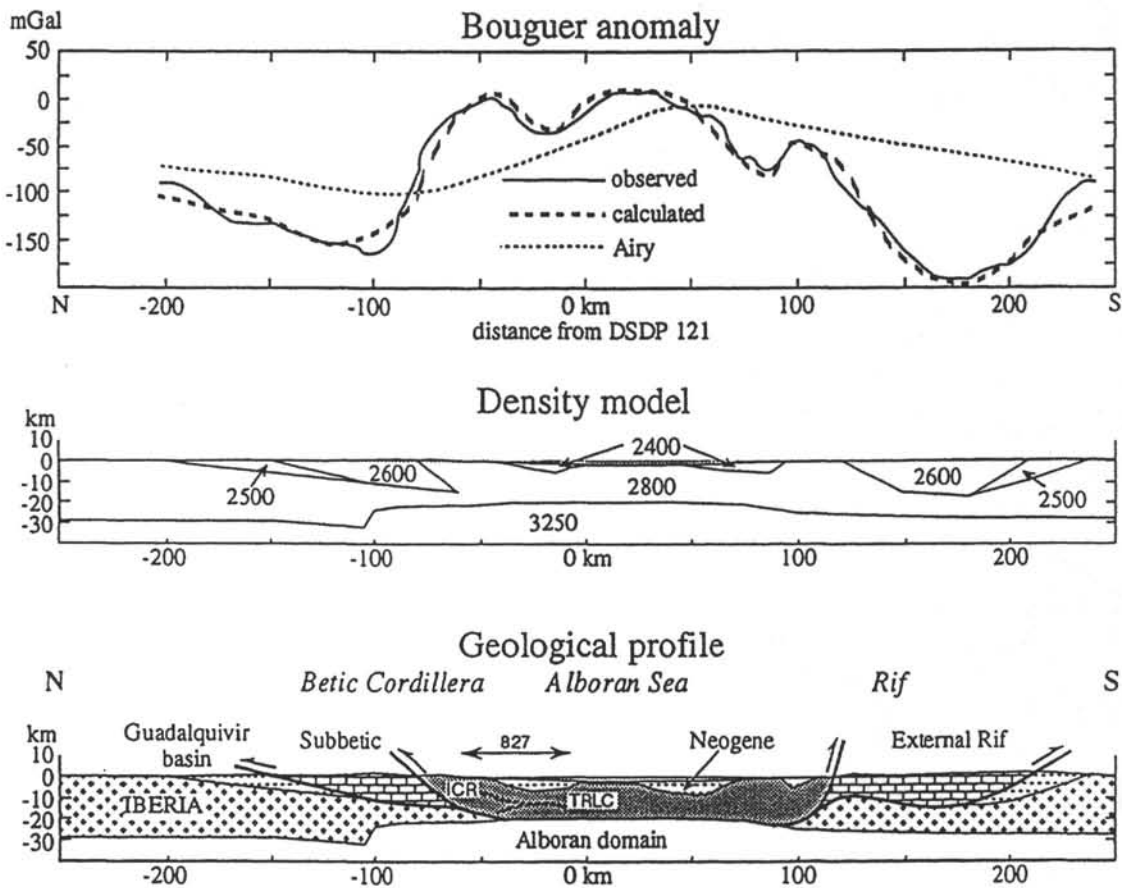
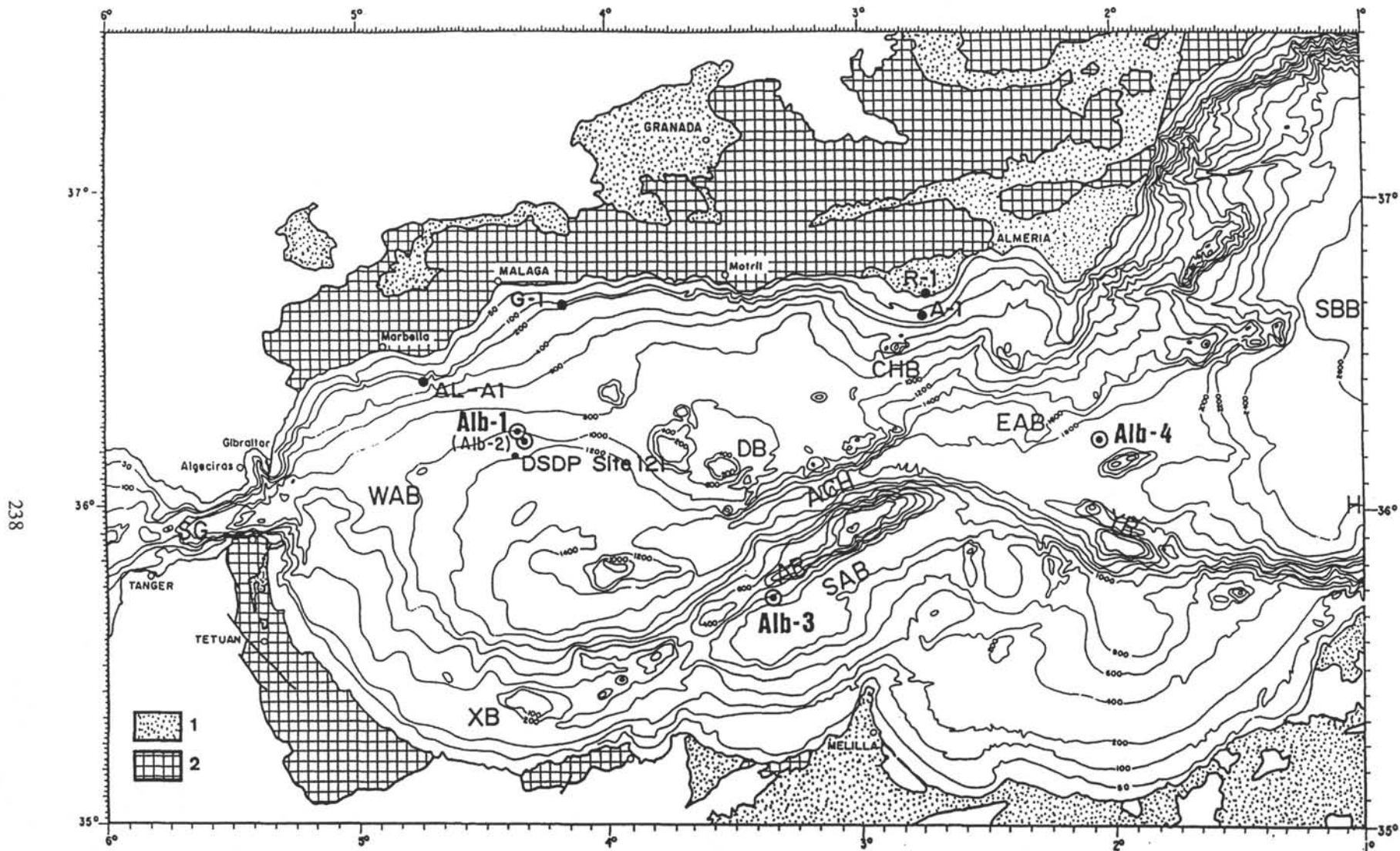


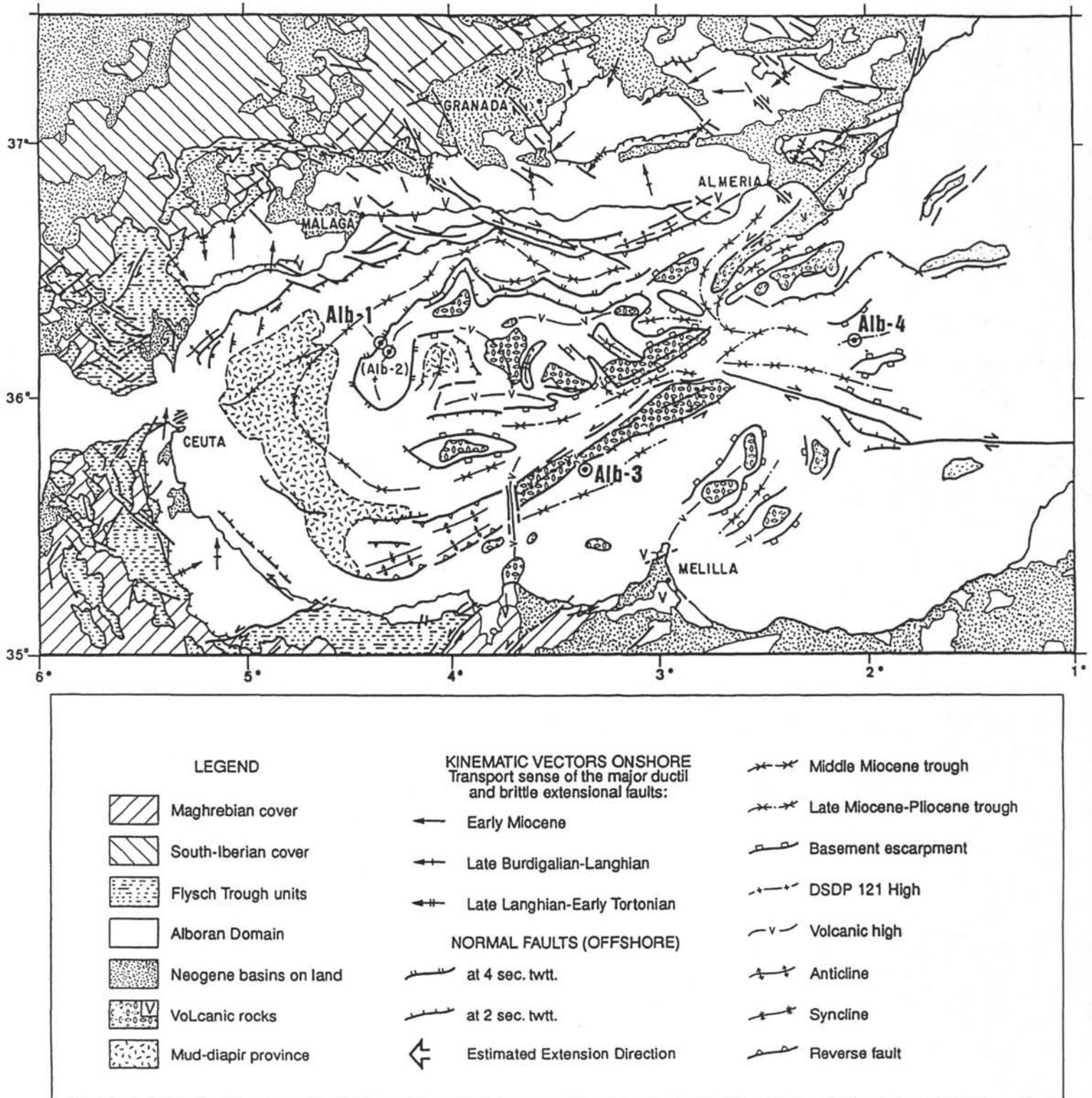
Figure 4B.



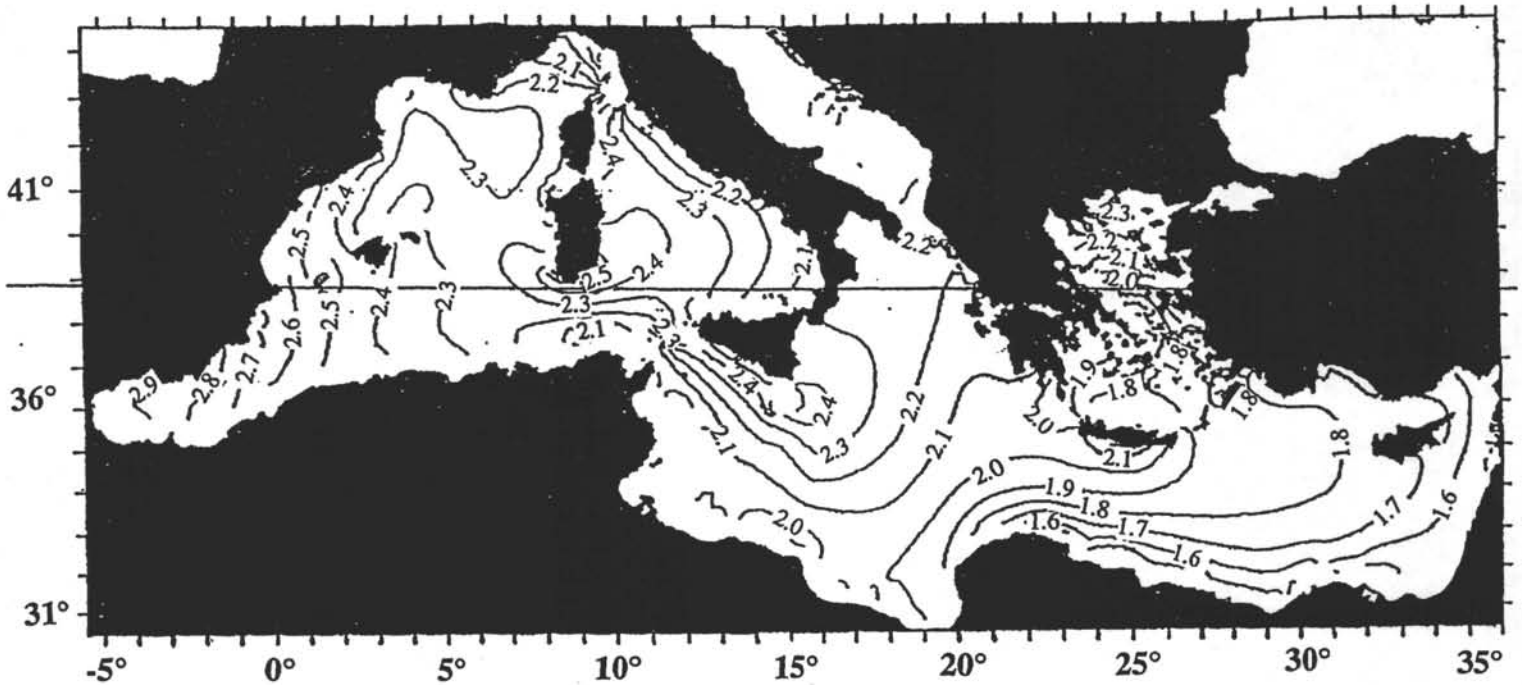
238

Figure 5A. Bathymetric map of the Alboran Sea.

Map onshore: 1: Miocene marine sediments and 2: Alboran Domain. ACH: Alboran Channel. AR: Alboran Ridge. CHB: Chella Bank. DB: Djibuti Bank. EAB: Eastern Alboran Basin. SAB: South Alboran Basin. SBB: South Balearic Basin. SG: Strait of Gibraltar. WAB: West Alboran Basin. XB: Xauen Bank. YR: Yusuf Ridge. Black dots: commercial wells on the Spanish margin. Encircled points: proposed drill sites. Contour lines in meters.



**Figure 5B.** Updated structural map of the Alboran Sea based on interpretation of MCS profiles. Main extensional stage which conditioned the origin of the Alboran Sea Basin is thought to be related to the late-Langhian/early Tortonian extensional system recognized onshore (Note "late Langhian-early Tortonian" onshore kinematic vectors and extensional transport sense in the Alboran Crustal Domain) (from Comas et al. 1993 ) Position of the proposed drill sites within the structural setting is shown.



**Figure 6.** Modelled distribution of nutrients (given in units of  $\text{mg at Nm}^{-3}$ ) in the Mediterranean. Due to the physical circulation input parameters, nutrient concentrations - and thus, primary productivity - are highest in the western Mediterranean. If sapropel formation was driven by higher rates of primary production in the eastern Mediterranean, what caused the redistribution of nutrients from the western to the eastern basin? Courtesy of Renzo Mosetti, Osservatorio Geofisico Sperimentale Trieste.

**Figure 7.** Distribution of eastern Mediterranean sapropels as a function of (A) global climate and (B) the orbital monsoon index *sensu* Rossignol-Strick (1983).

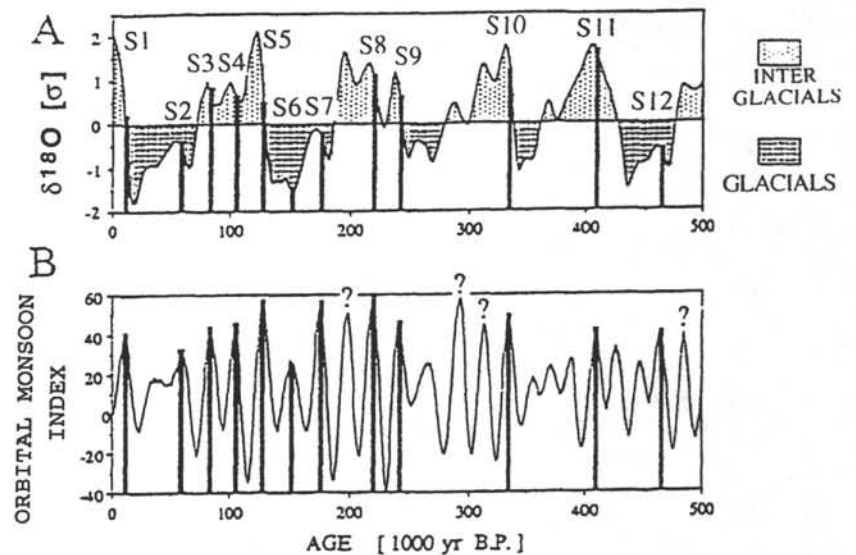
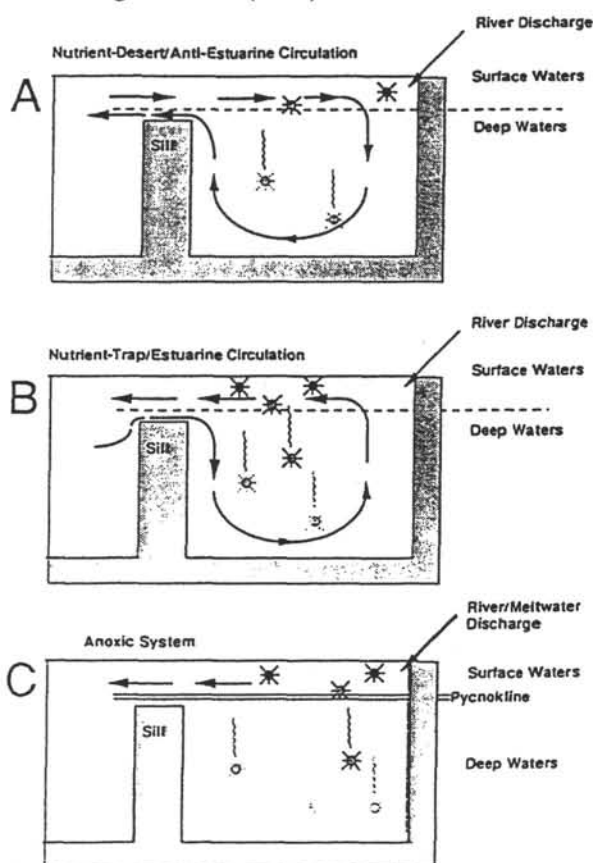


**Figure 8.** Schematic diagrams showing modern and hypothetical past circulation patterns of the Mediterranean Sea. (A) Modern anti-estuarine system. (B) Estuarine system. (C) Stagnant "anoxic" system. Scenarios (B) and (C) would have promoted the formation of sapropels through either enhanced preservation of organic carbon due to bottom water anoxia or through enhanced rates of biological productivity in the surface waters which would have led to increased fluxes of organic carbon to the seafloor.

Core MD 84641, Eastern Mediterranean  
(33°02'N, 32°38'E, 1375 m)

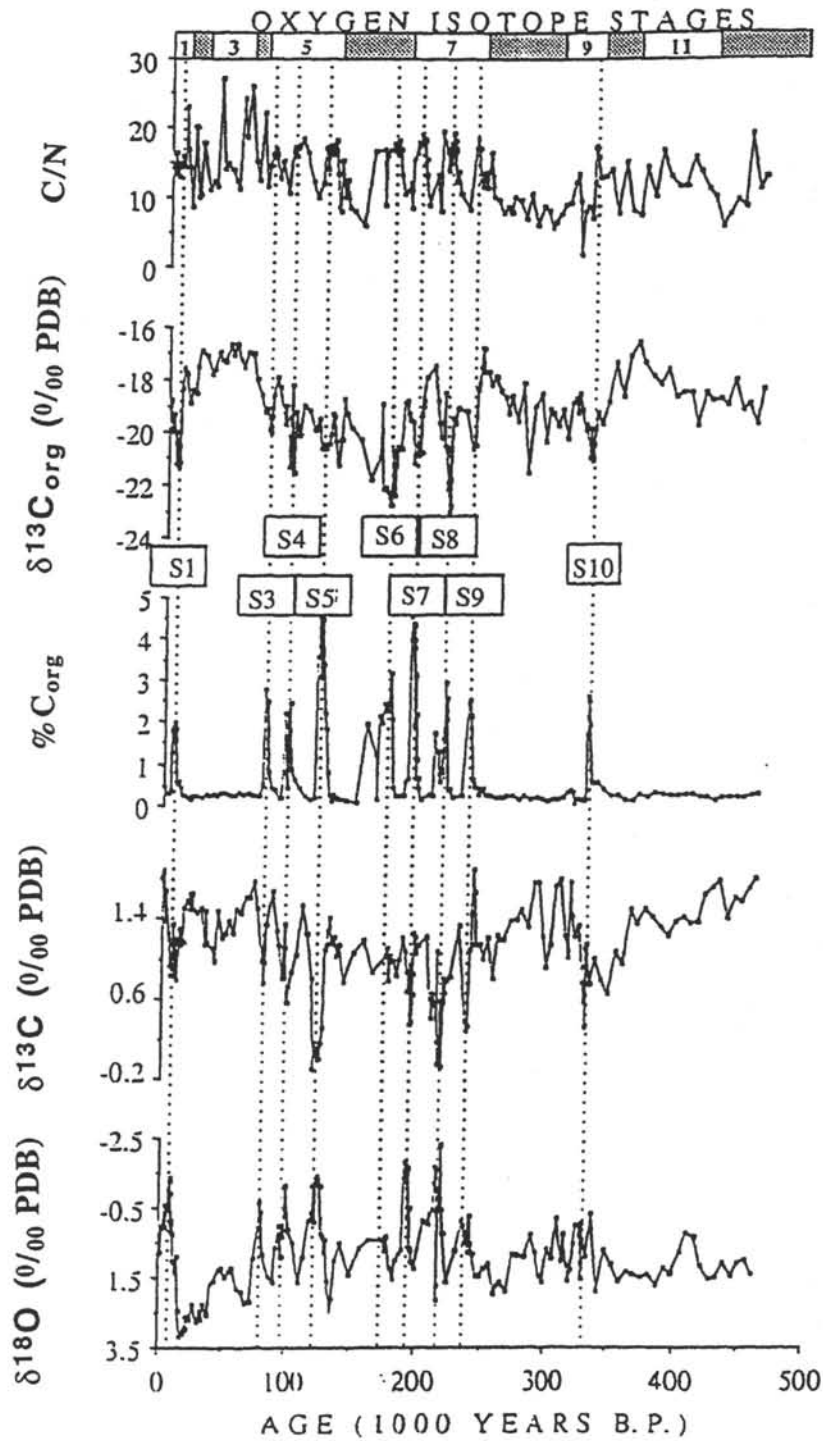


**Figure 9.** Stable isotope records (*G. ruber*,  $\delta^{18}\text{O}$ ,  $\delta^{13}\text{C}$ ), organic carbon content (percent by weight), carbon isotope composition of the organic fraction ( $\delta^{13}\text{C}_{\text{org}}$ ), and carbon/nitrogen ratios along Core MD84641 in the eastern Mediterranean. Data from Fontugne and Calvert (1992).

**TABLE 1**  
**PROPOSED SITE INFORMATION**  
**and**  
**DRILLING STRATEGY**

<b>SITE:</b> ALB-2	<b>PRIORITY:</b> 1	<b>POSITION:</b> 36°12'36.6"N, 4°18'57"W
<b>WATER DEPTH:</b> 1080m	<b>SEDIMENT THICKNESS:</b> 540m	<b>TOTAL PENETRATION:</b> 690m *
<b>SEISMIC COVERAGE:</b> MCS line Alb-39 (SP 1258).		

\* 540 m of sediments and minimum 150 m basement

**Objectives:** To penetrate and sample the basement at DSDP Site 121 high. To conduct petrologic studies on basement rocks (PTT path, radiometric ages on metamorphic rocks) to reveal the rate and thermal history of extension. To determine rifting geometry. To discriminate between proposed models for the origin of the Alboran Sea.

**Drilling Program:** RCB coring and reentry. Basement sampling.

**Logging and Downhole Operations:** Standard runs (geophysical, geochemical, and FMS), magnetic susceptibility, in situ stress measurements, temperature tool, and oriented cores.

**Nature of Rock Anticipated:** Poorly cemented TB turbidites, marly oozes, pelagic marls, basal conglomerate or minor carbonates (?).

OR

<b>SITE:</b> ALB-2a	<b>PRIORITY:</b> 1	<b>POSITION:</b> 36°10'54"N, 4°20'07.9"W
<b>WATER DEPTH:</b> 1095m	<b>SEDIMENT THICKNESS:</b> 620m	<b>TOTAL PENETRATION:</b> 770m *
<b>SEISMIC COVERAGE:</b> MCS line 75-234 (SP 1335).		

\* 620 m of sediments and minimum 150 m basement

**Objectives:** To penetrate and sample the basement at DSDP Site 121 high. To conduct petrologic studies on basement rocks (PTT path, radiometric ages on metamorphic rocks) to reveal the rate and thermal history of extension. To determine rifting geometry. To discriminate between proposed models for the origin of the Alboran Sea.

**Drilling Program:** RCB coring and reentry. Basement sampling.

**Logging and Downhole Operations:** Standard runs (geophysical, geochemical, and FMS), magnetic susceptibility, in situ stress measurements, temperature tool, and oriented cores.

**Nature of Rock Anticipated:** Poorly cemented TB turbidites, marly oozes, pelagic marls, basal conglomerate or minor carbonates (?).

<b>SITE:</b> ALB-3 3°21'21.6"W	<b>PRIORITY:</b> 3	<b>POSITION:</b> 35°41'42.4"N,
<b>WATER DEPTH:</b> 967m	<b>SEDIMENT THICKNESS:</b> 860m	<b>TOTAL PENETRATION:</b> 250m
<b>SEISMIC COVERAGE:</b> Robert D. Conrad LDGO MCS line 825 (CDP 2122).		

**Objectives:** To penetrate the major intra-Pliocene unconformity on a zone of compressional deformation on the south flank of the Alboran Ridge. To constrain the timing of latest uplift of the Alboran Ridge and associated folding.

**Drilling Program:** APC coring.

**Logging and Downhole Operations:** Standard runs (geophysical, geochemical, and FMS), magnetic susceptibility, in situ stress measurements, and temperature tool.

**Nature of Rock Anticipated:** Oozes, clay, silt, marl, TB turbidites, pelagic facies.

<b>SITE:</b> ALB-4	<b>PRIORITY:</b> 2	<b>POSITION:</b> 36°13'58"N, 2°3'28"W
<b>WATER DEPTH:</b> 1900m	<b>SEDIMENT THICKNESS:</b> 1775-1800m	<b>TOTAL PENETRATION:</b> >650m *
<b>SEISMIC COVERAGE:</b> LDGO MCS line 823 (CDP 2340).		

\* sediment penetration is a minimum estimate. If time permits, we will continue to drill for a further 250 m to sample the "syn-rift" sediments.

**Objectives:** To penetrate the sedimentary sequence in a graben structure in the East Alboran Basin. To determine the post-rift subsidence in the East Alboran Sea. To determine the age of the "syn-rift" sequence and determine syn-rift subsidence as near as possible from the achieved penetration.

**Drilling Program:** RCB coring. FFF?

**Logging and Downhole Operations:** Standard runs (geophysical, geochemical, and FMS), magnetic susceptibility, in situ stress measurements, and temperature tool.

**Nature of Rock Anticipated:** Oozes, clay, sand, silt, marl, TB turbidites, pelagic facies.

<b>SITE:</b> MedSap 5 *	<b>PRIORITY:</b>	<b>POSITION:</b> 40°21.3'N, 12°08.6'E
<b>WATER DEPTH:</b> 3466m	<b>SEDIMENT THICKNESS:</b> 188m	<b>TOTAL PENETRATION:</b> 200m
<b>SEISMIC COVERAGE:</b> MCS Line ST01 SP 4250		

\* Reoccupation of ODP Leg 107 Site 652

**Objectives:** This site represents the westernmost documented occurrence of sapropels and represents a tie-point for the east-west correlation.

**Drilling Program:** Triple HPC/APC

**Nature of Rock Anticipated:** Calcareous muds and oozes, and sapropels.

<b>SITE:</b> MedSap 6A	<b>PRIORITY:</b>	<b>POSITION:</b> 38°53.9'N, 04°30.5'E
<b>WATER DEPTH:</b> 2369m	<b>SEDIMENT THICKNESS:</b> 350m	<b>TOTAL PENETRATION:</b> 350m
<b>SEISMIC COVERAGE:</b> Tyro MR1/MR6 and SCS Bannock BAL09/BAL15		

**Objectives:** To study the evolution of surface and intermediate water masses in the western Mediterranean at times of sapropel deposition in the eastern Mediterranean. This site represents the central tie-point in the western Mediterranean

**Drilling Program:** Triple HPC/APC

**Nature of Rock Anticipated:** Calcareous muds and oozes.

<b>SITE:</b> MedSap 7B *	<b>PRIORITY:</b>	<b>POSITION:</b> 36°09.7'N, 04°22.4'W
<b>WATER DEPTH:</b> 1163m	<b>SEDIMENT THICKNESS:</b> 860m	<b>TOTAL PENETRATION:</b> 690m
<b>SEISMIC COVERAGE:</b> DSDP Site 121 site survey package		

\* DSDP Leg 13 Site 121

**Objectives:** To study gateway circulation between the Atlantic and the Mediterranean. To reconstruct the paleoceanographic exchange and monitor the effects of tectonic/sea level changes since the Pliocene.

**Drilling Program:** Triple HPC/APC

**Nature of Rock Anticipated:** Calcareous muds and oozes and turbiditic interlayers (?).

*LEG 163*

*North Atlantic -  
Arctic Gateways II*

# LEG 163

## NORTH ATLANTIC - ARCTIC GATEWAYS II (NAAG)

---

Modified From NAAG-DPG Report (Proposals 305, 320, and 336)  
and 6-8 October 1993 OHP Meeting

To Be Named: Co-Chief Scientists and Staff Scientist

---

### ABSTRACT

The Arctic and sub-Arctic areas exert major influences on global climate and ocean systems. Understanding the causes and consequences of global climatic and environmental change is an important challenge for humanity. The high northern latitude oceans are of great relevance for this task since they directly influence the global environment through the formation of permanent and seasonal ice-cover, transfer of sensible and latent heat to the atmosphere, deep-water formation and deep-ocean ventilation which control or influence both oceanic and atmospheric chemistry. Thus, any serious attempt to model and understand the Cenozoic variability of global climate must take into account these paleoenvironmentally oriented topics.

Leg 163 represents the second in a two-leg program to investigate four major geographic locations (the Northern Gateway Region, the East Greenland Margin, the Greenland-Norway Transect (Iceland Plateau), and the Southern Gateway Region) with the aim of reconstructing the temporal and spatial variability of the oceanic heat budget and the record of variability in the chemical composition of the ocean. ODP Leg 151, the first leg in this program, successfully completed operations at five sites within the Northern Gateway region, one site in the East Greenland Margin region, and one site within the Greenland-Norway Transect. Together, the Leg 151 and Leg 163 program undertakes a study of circulation patterns in a warm ocean, and the mechanisms of climatic change in a predominantly ice-free climatic system and will provide a collection of sequences containing records of biogenic fluxes ( $\text{CaCO}_3$ , opal, and organic carbon) and stable-isotopic carbon and oxygen records which will address aspects of facies evolution and depositional environments and the carbon cycle and productivity. The drilling approach focuses on high-resolution, Milankovitch-scale paleoclimatic analysis of rapidly-deposited sediment sequences. The proposed sites are either 1) arrayed as broad north-south and east-west transects to monitor spatial paleoclimatic variability or closely spaced suites of cores across depth ranges to monitor vertical variability, 2) deep drilling targets to constrain the time of opening of Fram Strait, or 3) placed to monitor downstream sedimentological effects of deep flow through narrow gateway constrictions.

## INTRODUCTION

During the last decade it has been realized that much of the natural variance in the Earth's environment on time scales less than 1 m.y. originates from changes in the geometry of the Earth-Sun orbital system. The sensitivity of the Earth system to orbital forcing has been especially high over the last one million years. Both for understanding how this high sensitivity to external forcing has evolved from periods of less sensitivity and lower amplitude variation, and for understanding the way environmental change is forced both by this and other forcing mechanisms which operate on longer time scales (such as: plate reorganizations, orogeny, carbon cycle variations), it is necessary to obtain records that document how the climatically-sensitive, high-latitude regions have developed.

It follows that this focus on high northern latitude paleoenvironmental questions require deep-sea drilling in the areas north of the Greenland-Scotland Ridge. From south to north these seas consist of the Norwegian and Iceland Seas, the Greenland Sea and the Arctic Ocean, which together commonly are referred to as the Arctic Mediterranean (Sverdrup et al., 1942) or the Nordic Seas (Hurdle, 1986).

The deep-water areas of the Nordic Seas have previously been drilled during DSDP Leg 38 which occupied 17 sites spread out over some of the major basins (Talwani, Udintsev et al., 1976), and ODP Leg 104 which occupied three sites on a transect across the Vøring Plateau in the eastern Norwegian Sea (Eldholm, Thiede, Taylor et al., 1987) and recently by ODP Leg 151. The sites from Leg 38 were almost exclusively chosen to meet structural and geophysical objectives. They did not retrieve the complete stratigraphical sequences essential to establish chronologic resolution and precision, the requirements of modern paleoceanography. The Leg 104 sites were drilled with the Advanced Piston Corer (APC) with high recovery and very good sample quality. The sequences from Leg 104 document portions of the Neogene fairly well despite a number of hiatuses (Goll, 1989). The Paleogene intervals of these sites are either missing or seriously altered by diagenesis and thus no sequences are available to document the whole Cenozoic history of these oceans. Although especially the upper Neogene is rather complete on the Vøring Plateau, the location of the sites basically implies that they must be considered as a single sample point along the meridional and latitudinal transects herein advocated. During Leg 151, three sites were drilled on the Yermak Plateau, two sites were drilled in the Fram Strait, one site was drilled along the East Greenland Margin, and one site was drilled on the Iceland Plateau.

The Arctic/Nordic Seas region contains a large number of paleoclimatic objectives of first-order scientific importance which can only be addressed by a large array of sites and Leg 163 will further investigations that were initiated during Leg 151.

## STUDY AREA

### Oceanographic Setting

The series of interconnected basins comprising the Nordic Seas contain a total volume of roughly  $10 \times 10^6 \text{ km}^3$ , if excluding the Amerasian Basin of the Arctic Ocean, or about 0.7% of the volume of the world ocean. The Eurasian basin of the Arctic Ocean makes up nearly 60% of this volume. Despite the small volume of these areas, they nevertheless act as a primary source of a large portion of deep, ventilated waters in the world ocean. The idea that deep waters are formed in the Norwegian-Greenland Seas (Helland-Hansen and Nansen, 1909), and that some of this newly formed water flows into the deep Atlantic across saddles on the Greenland-Scotland Ridge (see Warren, 1981; Mantyla and Reid, 1983 for reviews) was suggested a long time ago. Previous notions about the Arctic Ocean indicated that it has been a passive recipient of ventilated water from the south. In recent years, however, it has been demonstrated that the Arctic Ocean itself is an important contributor of deep waters which flow southward through the Fram Strait, and, after mixing with deep waters formed in the Greenland/Iceland Seas, pass further on into the world ocean (Aagaard, 1981; Aagaard et al., 1985). The processes leading to the formation of dense deep waters in the Arctic Ocean are thought to involve either intense cooling of Atlantic waters on the Barents Sea Shelf (Swift et al., 1983), or an increase in salinity through salt release during sea-ice formation on the large Arctic shelves (Aagaard et al., 1985). Smethie et al. (1988) suggest that both processes are in operation.

The chief components of the surface water systems of the Nordic Seas involve the influx of warm and relatively high-salinity waters via the North Atlantic Current, which continues its northward flow as the Norwegian Current, and outflow via the cold and low-salinity East Greenland Current. The Norwegian Current is sufficiently cooled to allow deep water formation within the cyclonic gyre of the Greenland Sea. Another branch of this current continues along the western margin of Svalbard as the West Spitsbergen Current, before entering the Arctic Ocean. Within the Arctic this relatively warm water mass mixes with low-salinity surface waters, sinks and flows as an

intermediate water mass counterclockwise before being exported out of the Arctic via the Fram Strait along the Greenland Margin. The surface outflow from the Arctic Ocean sweeps the east margin of Greenland before entering the Irminger Sea of the North Atlantic via the Denmark Strait.

Aagaard et al. (1985) concluded that nearly 50% of the water volume in the Nordic Seas, including the Amerasian Basin, is potentially in communication with the world ocean (Fig. 1). The Nordic Seas might hence be characterized as the "lungs" of the present world ocean, implying that it is of fundamental importance to derive a detailed understanding of the timing and history of deep and shallow water exchange between the Nordic Seas and the remainder of the world ocean. The unique topographic constraints provided by a single deep, narrow passageway to the North (the Fram Strait), and a major submarine ridge system to the south (Greenland-Scotland Ridge) make it pertinent to address the question of the Cenozoic paleoceanography of the Nordic Seas as a gateway problem.

### **The Gateways and Paleoceanography**

The tectonic development and the opening of the Fram Strait has determined the history of water mass exchange between the Arctic Ocean and the Greenland-Norwegian-Iceland Seas. Submergence below sea level of the southern gateway, or parts of it, has determined the possibilities for water mass exchange between the Nordic Seas and the Atlantic Ocean, and thus the world ocean.

The Fram Strait, with a present critical sill depth of 2600 m, represents the only deep connection between the Arctic Ocean and the global ocean. The initiation of this connection may have taken place as early as Anomaly 13 time, close to the Eocene/Oligocene boundary (Crane et al., 1982; Eldholm et al., 1987; see also reviews by Vogt, 1986a, b). The tectonic history of the Fram Strait area, however, is characterized by complex and, at present, vaguely understood processes, which might include stretching of the Svalbard continental crust and hotspot activity. When taking into account the strongly oblique opening of the Fram Strait and the nearness to surrounding land areas (Greenland and Svalbard), it seems possible that a truly deep Arctic Ocean/Greenland-Norwegian Sea connection became established considerably later than Anomaly 13 time, perhaps as late as Anomaly 6 time. The history of water mass exchange between the Arctic Ocean and the world ocean via the Greenland-Norwegian-Iceland Seas is a key element in any large scale model of

post-Eocene paleoceanography. However, the documentation of this history will depend on new drilling efforts to make available material from within and from both sides of the gateway.

There are few oceanic gateways that can compete with the Greenland-Scotland Ridge in having such a profound influence on the present world hydrography (Bott et al., 1983). Overflow from northern sources occurs in the Faeroe-Shetland Channel, across the Iceland-Faeroe Ridge and in the Denmark Strait. Tracer studies indicate that the overflow waters originate from waters shallower than 1000-1200 m, probably to a large extent formed by deep convection in the Iceland Sea (Peterson and Rooth, 1976; Warren, 1981; Aagaard et al., 1985). Reconstructions of the subsidence history of the ridge system, suggest that its eastern parts sank beneath sea level probably sometime during middle Eocene times, and during early to middle Miocene times in the Denmark Strait area. The distribution of shallow water benthic foraminifera, however, indicates that the Nordic Seas were effectively isolated from any "deep" Atlantic influence until middle Miocene times (Berggren and Schnitker, 1983; Thiede, 1983; Thiede and Eldholm, 1983). The overflows have both influenced the Atlantic and global deep water masses through their contribution to North Atlantic Deep Water (NADW) production and to the formation of North Atlantic sedimentary records. Basic questions as to why and when NADW production was initiated, and how and why the chemical and physical signature of this major water mass has varied, remain to a large degree unanswered. Quite obviously the physical and chemical characterization of surface and deep waters through time directly in the main source regions, i.e. north of the Greenland-Scotland Ridge, will greatly improve the understanding of world ocean hydrography, global energy budgets and North Atlantic patterns of sedimentation and erosion.

The Nordic Seas are characterized by strong latitudinal gradients in the sea surface environment, but also by unusually strong meridional gradients due to the warm Atlantic influence in the east and the cold polar influence in the west. Strong seasonal variability is also a prominent feature of the surface environments, resulting in strong and rapidly migrating ocean fronts. The onset and subsequent variability of these fronts are almost totally unknown. Apart from the data obtained from the Norwegian Margin by ODP Leg 104, no high quality material exists which is older than a few hundred thousand years. Thus, to derive a comprehensive understanding of the whole ocean-climate system of the Nordic Seas, and the *modus operandi* of this, in a global perspective critical, system, it is necessary to obtain material that can document how sea-surface environments have changed and the underlying causes for these changes through late Paleogene and Neogene times.

## **Climate Evolution of High Northern Latitudes**

A major element in the evolution of Cenozoic environments has been the transformation from warm Eocene oceans with low latitudinal and bathymetric thermal gradients into the later type of oceans characterized by strong thermal gradients, oceanic fronts, cold deep oceans and cold high latitude surface water masses (Shackleton and Boersma, 1981). This transformation is linked with the climatic transition into cold high latitude climates and the connection of both surface and deep-ocean circulation between high latitude regions and the lower latitude oceans. It is still not known what role the Arctic and sub-Arctic regions played in this transformation, or how and when climatic, tectonic and oceanographic changes in the Arctic contributed to the global ocean cooling and increased thermal gradients.

At present it is uncertain when cold climates evolved in the Arctic and surrounding regions. In order to understand the evolution of the global climate system it is necessary to clarify when the Arctic Ocean became ice-covered, and document the variability of ice cover in the Arctic. It has been proposed that the Arctic Ocean has been permanently ice covered since the late Miocene (Clark, 1982). Other studies conclude that this event happened in the Matuyama or at the Brunhes/Matuyama boundary (Herman and Hopkins, 1980; Carter et al., 1986; Repenning et al., 1987). This discrepancy in timing cannot be verified by the available material.

A major threshold of the climate system was passed with the inception of glaciers and ice sheets in the northern hemisphere. Data from ODP Leg 104 document minor input of ice-rafted debris (IRD) into the Nordic Seas in the late Miocene and through the Pliocene, pointing to the existence of periods when large glaciers were able to form and reach coastal areas in some of the areas surrounding the Nordic Seas (Jansen and Sjøholm, 1991). The major shift to a mode of variation characterized by repeated large glacials in Scandinavia probably occurred at about 2.5 Ma and was further amplified at about 1 Ma (Jansen et al., 1988; Jansen and Sjøholm, 1991). With the presently available material it is impossible to document clearly when glaciers started to evolve in the Arctic and high sub-arctic, and it is impossible to describe the glaciation history of the different individual areas, i.e. when was Greenland glaciated? What distinguished the climatic responses in the Arctic parts of this area (Greenland, Svalbard, and Arctic Ocean fringes) from those of the sub-arctic North European areas? Did the cooling and glacial inception of the high Arctic and Greenland take place at an earlier stage than in the sub-arctic? Terrestrial data indicate significant cooling on Iceland at about 10 Ma (Mudie and Helgason, 1983) and glaciation in elevated areas of Iceland in

the latest Miocene and the Pliocene (Einarsson and Albertsson, 1988). Terrestrial evidence also indicates forested areas in the Arctic fringes, which are far north of the present forest-tundra boundary, until about 2 Ma (Carter et al., 1986; Nelson and Carter, 1985; Funder et al., 1985; Repenning et al., 1987). The chronology from these land sites is, however, poorly constrained, and since this is only scattered evidence, there are no continuous records from land sites that document the climatic transition into a cold arctic climate. Both a clear documentation and a proper timing of the climatic evolution will therefore depend on the availability of new, continuous, deep-sea material.

Since the glacial and climatic history of the high northern latitudes are so poorly known, the ability to model and understand linkages between low and high latitude climates and between southern and northern hemisphere climates is limited.

The Norwegian-Greenland Seas and the Arctic Ocean are surrounded by landmasses that acted as loci for the late Cenozoic Northern Hemisphere ice sheets. Therefore these areas are key areas where northern hemisphere glacials can be documented in the form of input of IRD into the ocean. The history of large glaciations in the high northern latitudes has only been firmly documented back to approximately 2.5 m.y. (Shackleton et al., 1984; Ruddiman and Raymo, 1988; Jansen et al., 1988), although glaciation in some areas must have started earlier in the Neogene. This contrasts with the history of glaciation in the Antarctic which probably dates back at least to the early Oligocene, some 36 million years ago (Barron, Larsen, Baldauf, and Leg 119 Scientific Party, 1988). The apparent interhemispheric asynchronicity in the climatic evolution of high latitude regions on the southern and northern hemispheres is a major unresolved question for understanding Cenozoic paleoenvironments.

In addition to the above questions that address the magnitude of glaciations and the passing of certain climatic thresholds in the Earth's history, are the frequency components of the climatic, oceanographic, and glacial evolution of the Arctic and Sub-arctic which are of importance for assessing the climate system's response to external forcing. Results from DSDP Leg 94 sites in the North Atlantic have shown that sea-surface temperatures and ice volumes have a strong response to orbital forcing over the last 3 m.y. However, the amplitudes of climatic variation and the dominant frequencies have varied strongly, indicating variations in the way the climate system responds to external forcing (Ruddiman et al., 1986; Ruddiman and Raymo, 1988; Raymo et al., in press). Work is underway, based on Leg 104 material, to study the cyclicity of IRD input into the sub-

arctic Norwegian Sea. This can aid in understanding the controlling factors for sub-polar ice-sheet variations. However, presently available data does not permit extending this type of high-resolution study on orbital time scales to other parts of the Arctic Ocean and Nordic Seas.

Some models constructed to investigate and explain the evolution and operation of the global climate system include variations in the magnitude and mode of thermohaline ocean circulation, (e.g., Barron and Washington, 1984; Broecker et al., 1985; Mix and Pisias, 1988; Boyle, 1988). Further improvements of such models will thereby partly depend on records that can assess the actual climatic and oceanographic evolution of this particular region.

### **Sediment Budgets**

The rates at which the various deep-sea sediment types accumulate are essential to the global geochemical balances, because mass accumulation rates of biogenic carbonate, opaline silica, organic matter, and non-biogenic sediment components determine the internal cycling of matter in the oceans and are therefore linked to the chemical state of both the oceans and the atmosphere (Broecker and Peng, 1982). Accumulation of biogenic matter and carbonate are, for example, closely linked with atmospheric CO<sub>2</sub> levels. Biogenic sediment components, which account for more than 50% of the deep-sea sediments, accumulate at rates which are determined by the productivity rates in the surface waters and the dissolution of these components at depth.

The availability of nutrients determines the productivity rates which, therefore, also are dependent on the ocean circulation (e.g., vertical mixing, upwelling), and on climate as a driving force for the circulation. Dissolution of biogenic carbonate is basically a function of the degree of calcite saturation in seawater at the sediment/water interface. Averaged globally, the degree of calcite saturation varies in order to balance the total carbonate budget. The ocean circulation, and the underlying causes for its development and change, is thus a key factor among the dissolution-related parameters.

ODP Leg 104 documented a major deepening of the calcite lysocline at about 10 Ma in the Norwegian Sea. This was followed by a series of low frequency variations in carbonate deposition/dissolution and opaline silica preservation. This 10 Ma-event presumably reflects the cumulative effect of a large set of changes occurring in the global sediment budgets and

paleoenvironment at around the middle/late Miocene transition, such as an increase from 5 to 10% in the recycling rate of the total sediment mass on earth (Hay, 1985), the beginning of a remarkable decrease in the global organic carbon reservoir (Shackleton, 1987), or the substantial increase in latitudinal temperature gradients (Shackleton and Kennett, 1975; Thierstein and Berger, 1978). Concomitant changes induced by tectonic forcing also belong in this picture, where the activation of new ocean circulation patterns through newly formed gateways must be an important factor contributing to the large scale changes in the global climate-ocean-sediment system. It follows that many possible cause and effect relationships can be inferred to explain, for example, the deepening of the Norwegian Sea lysocline at 10 Ma. Yet, this shows that global patterns are preserved in the sediments of the Nordic Seas.

### **Biological Evolution**

The coring program envisaged herein will recover high quality APC/XCB sediment material reflecting a wide variety of paleoenvironmental conditions in the Nordic Seas, and it is anticipated that the material also will be used to address a wide array of significant scientific questions which have not been specifically mentioned in the three main themes.

Studying biological evolution is one such additional scientific problem. Such studies will allow the assessment of the response of oceanic biota to changes in climate, ocean circulation, and ocean chemistry. Cores from high northern latitudes, and particularly the Arctic Ocean, will provide the northern hemisphere end-member for examining topics such as patterns and modes of speciation, bipolar evolution, Arctic fauna and flora, and Arctic/sub-Arctic environmental influence on intra- and inter-specific morphological variation.

### **Preliminary Results from Leg 151**

During the Arctic summer of 1993, *JOIDES Resolution*, accompanied by the Finnish icebreaker *MSV Fennica*, recovered the first scientific drill cores from the eastern Arctic Ocean, including material which records the earliest history of the connection between the North Atlantic and Arctic oceans, the onset of glacial climate in the Arctic and the inception of abundant sea-ice formation and sediment ice rafting, and evidence for massive ice caps on the Arctic Ocean margin during certain glaciations.

During ODP Leg 151, drilling operations recovered over 3 km of core, which ranges in age from middle Eocene to Quaternary. Site 907 on the Iceland Plateau recovered a middle Miocene to Quaternary sequence overlying basement basalts with calcareous microfossils only in the upper Pliocene to Quaternary, but with a middle to upper Miocene biosiliceous-rich interval indicating high-productivity conditions. Site 908 in the Fram Strait documents a late Oligocene age for the biosiliceous-rich pre-rifted strata on the Hovgård Ridge microcontinent. Nearby Site 909 penetrated 1061.8 m into the Fram Strait basin, which acts as the corridor for deep-water flow between the Arctic Ocean and Norwegian-Greenland Sea, and recovered an upper Oligocene?/lower Miocene to Quaternary sequence high in organic matter and hydrocarbons but virtually absent of calcareous and siliceous microfossils. Sites 910, 911, and 912 on the Yermak Plateau consist of Pliocene to Quaternary glacio-marine sediments with abundant dropstones and high organic carbon content. Site 913 on the East Greenland Margin drilled a thick section of Pliocene to Quaternary glacio-marine sediments with abundant dropstones, overlying a middle Eocene to lower Oligocene and middle Miocene sequence of clays and silty clays. A biosiliceous-rich interval occurs in the upper Eocene to lower Oligocene.

The oldest sediments recovered, middle Eocene at Site 913, contain the highest abundances of terrigenous organic matter recovered during Leg 151 and indicate the close proximity of a continental source during this initial phase of seafloor spreading in the Greenland Basin. Episodes of laminated sediment deposition suggest a lack of infaunal activity and bioturbation during the middle Eocene. The dissolved-silica level is extremely low, suggesting an absence of biosiliceous deposition and hence indicates a restricted basin or basins receiving nutrient-depleted surface water over shallow sills, well above the mid-water nutrient maxima common in modern oceans. During this time, Fram Strait remained closed to deep-water flow. Productivity increased throughout the middle Eocene, and Site 913 remained below the CCD.

At Site 913, there was a renewed influx of terrigenous organic carbon in the late Eocene, coinciding with the first appearance of preserved biogenic silica. Upsection, the sediments display vivid shades of blue, purple, and green and the preservation and abundance of siliceous microfossils increases. The siliceous intervals were formed during times of high productivity, resulting in high sedimentation rates and high abundances of marine organic carbon. Nevertheless, ventilation of the deep waters was poor, resulting in lamination and probably causing the accumulation of CO<sub>2</sub> in deep water, which dissolved carbonate.

The late Oligocene to earliest Miocene interval from Site 908 on the Hovgård Ridge suggests moderately well-mixed oceanic conditions in the Norwegian-Greenland Sea. The sediments record relatively high but variable surface-water productivity, well demonstrated by the most highly variable organic carbon of any Leg 151 site (0.75% to 2.0%). High productivity is also indicated by the abundance of siliceous microfossils. This site was below the CCD during this time, and the intermediate waters were poorly ventilated. Extensive bioturbation suggests at least intermediate bottom-water oxygen levels, but thin, poorly bioturbated and laminated intervals suggest episodes of very low oxygen content. Laminated-sediment intervals continued until about the middle/late Miocene boundary (Site 907, Site 909, Site 913) and provide evidence for restricted circulation in the early Miocene Greenland-Norwegian Sea. Deep-water flow from the Arctic or production in the Nordic Seas did not occur before this time.

The late Miocene time interval is represented only at two sites. Site 909 is characterized by a paucity of microfossils, while Site 907 is rich in siliceous microfossils, which began prior to the middle/late Miocene boundary but ended by about 7 Ma, suggesting that deep-water formation began to better mix the Nordic Seas, but that true North Atlantic Deep Water (NADW) was not formed until the latest part of the Miocene. The disappearance of anoxic indicators marks the start of deep mixing in the Greenland Basin, while the presence of siliceous production on the Iceland Plateau shows that the southern part of the Nordic Seas still had net upward transfers of nutrients from deeper waters to the surface, unlike modern conditions. The gradient from north to south reflects either the beginning of inflow of Arctic deep waters into the Nordic Seas or the development of a strong temperature gradient in surface waters and the beginning of basinal deep-water formation in the north.

At all sites, the Pliocene and Quaternary interval is marked by evidence of ice, with significant quantities of dropstones appearing near the late Miocene/Pliocene boundary, with a marked increase at about 2.5 Ma.

Pliocene and Quaternary sediments on the Yermak Plateau at the southern edge of the Arctic Ocean are extremely thick, deposited either by the melting of a sediment-laden pack ice transported to the region by Arctic surface circulation or during interglacials as ice melted from a massive Barents Sea ice sheet or an ice cap centered on Svalbard. The former scenario seems more likely, because the melting ice edge now supports high productivity, which could cause the observed high levels of

marine organic carbon deposition. The summer edge of Arctic pack ice must then have been near the Yermak Plateau for most of the Plio-Pleistocene interval.

Site 910 was marked by a highly overconsolidated interval, beginning at about 25 m depth in the sediment column. No such interval was found at the deeper water Site 912 (south) or Site 911 (north). At Site 912, sedimentary evidence of the ice sheet was recorded for the same time interval. The consolidated interval was traced along the Yermak Plateau with seismic reflection profiles. This consolidation possibly indicates that an ice lobe of the Barents ice sheet reached well out to sea in the late Pleistocene and was grounded on the top of the Yermak Plateau. These event(s) may have occurred prior to the last glacial maximum at 18 ka. Evidence for the extension of the Barents ice sheet westward will provide important constraints for Pleistocene ice models.

## SCIENTIFIC OBJECTIVES AND METHODOLOGY

### Summary of Objectives

#### *Cenozoic Paleoceanography of the Nordic Seas*

- 1) To study the timing and history of deep and shallow water exchange between the Arctic Ocean and the Norwegian-Greenland Sea via the Fram Strait (Northern Gateway).
- 2) To study the timing and history of deep and shallow water inflow and outflow between the Norwegian-Greenland Sea and the North Atlantic across the Greenland-Scotland Ridge (Southern Gateway).
- 3) To investigate water mass evolution, particularly addressing the initiation and variability of east-west and north-south oceanic fronts in surface waters, the initiation and variability of northern source deep-water formation, and the history of vertical physical and chemical gradients.

#### *Cenozoic Evolution of Climate in High Northern Latitudes: Cenozoic Cooling, Sea-Ice and Continental Ice-Sheet Formation, and Deposition of IRD*

- 1) To investigate the timing and development of polar cooling and the evolution of low to high latitude thermal gradients in the northern hemisphere.

- 2) To establish the temporal and spatial variation of sea-ice distribution, the glacial history of the circum-Arctic, Greenland and Northern Europe, and the history of IRD sedimentation in the Arctic.
- 3) To investigate variations in climatic zonality and meridionality through time as response to tectonic forcing.
- 4) To establish the history of the higher frequency components of the climatic and glacial evolution of the Arctic and sub-Arctic areas.
- 5) To identify ocean-atmosphere interactions associated with northern Hemisphere deep-water formation and the interhemispheric couplings and contrasts in climatic evolution.

#### *Sediment Budgets*

- 1) To investigate fluxes of biogenic carbonate, opaline silica, organic matter, and non-biogenic sediment components through time.
- 2) To study bathymetric variability through time of the CCD and lysocline.
- 3) To establish the spatial and temporal history of silica preservation.
- 4) To investigate Arctic and sub-arctic oceanic influence on global biogeochemical cycles.

#### **Specific Objectives and Methodology**

##### *Surface Water Mass Evolution*

The Norwegian-Greenland Sea links the cold Arctic Ocean with the warm-temperate North Atlantic Ocean via northern and southern “gateways” (Fig. 1). Fram Strait in the north is the single passage to the Arctic Ocean through which surface and deep waters are exchanged. Similar exchanges occur farther south at both the Denmark Strait, Faeroe-Shetland Channel, and Iceland-Faeroe Ridge.

The Nordic Seas are characterized by strong oceanographic gradients not just latitudinally but also meridionally, due to the northward flow of warm Atlantic water in the east and southward flow of cold polar water and ice in the west. Strong seasonal variability also results in rapid migrations of sharply defined fronts. Apart from material obtained from the Norwegian margin by ODP Leg 104, the history of these surface-ocean gradients is almost totally unknown prior to the last few hundred thousands years. ODP drilling will provide material from the colder western regions for tracing the spatial evolution of surface-water environments and thus enhancing the understanding of climatic change.

#### *Temporal and Spatial Variation of Sea-Ice Distribution*

The present Arctic climate is strongly influenced by its sea ice cover, which greatly increases the regional albedo and reduces heat and gas exchange with the atmosphere. Very little is known about how this ice cover first developed and subsequently varied. Although prevented from drilling within the permanent pack ice in the Central Arctic, *JOIDES Resolution* drilling along the present ice margins will provide better constraints on the history of sea-ice extent just north of a key Arctic gateway and southward into Nordic Seas.

#### *The Gateway Problem*

The gateways in the north (Fram Strait) and south (Greenland-Scotland Ridge) are among the most important submarine topographic constrictions to global oceanic circulation. Opening of Fram Strait and subsidence of the Greenland-Scotland Ridge below critical levels are necessary conditions for deep water exchange between the Nordic Seas and Atlantic Ocean, although other tectonic changes may also play a role in determining the subsequent long-term evolution of meridional exchanges across these former barriers. The history of these gateways is thus a key component in understanding the long-term evolution of both Northern Hemisphere and global climate.

Leg 151 focused on two key objectives not addressed in previous drilling: 1) constraining the tectonic history of opening of these barriers, primarily by drilling to obtain basement ages; and (2) defining the subsequent history of surface and deep-water exchange across these barriers, based both on proxy water mass indicators and on current-sculpted features on the sea floor. Leg 163 will further these objectives.

### *Deep Water-Mass Evolution*

At present, deep waters of the sub-Arctic North Atlantic form partly from dense saline waters cooled in the Greenland and Iceland Seas, and partly from deep waters flowing out of the Arctic Ocean. Because of their rapid formation and short residence times, these deep waters are rich in O<sub>2</sub> but poor in CO<sub>2</sub> and nutrients. The deep water spills over the Greenland-Scotland Ridge and mixes with warmer North Atlantic waters to form southward-flowing North Atlantic Deep Water (NADW). NADW helps to oxygenate the deep ocean and transfers heat and salt to the Antarctic. Glacial/interglacial changes in deep-water formation in the Nordic Seas are implicated in conceptual models of atmospheric CO<sub>2</sub> variations.

ODP drilling in the Nordic Seas will improve the understanding of deep-water evolution by providing: spatial/vertical transects that constrain the development of physical/chemical gradients in deep waters; sites located in regions where vigorous deep-water outflow has altered normal pelagic sedimentation; and evidence of surface ocean climate changes in regions of deep-water formation.

### *History of Mountain Glaciers and Ice Sheets around the Nordic Seas*

Results from ODP Leg 104 trace the glacial history of the Fennoscandian Ice Sheet back to 2.57 Ma. Sporadic earlier occurrences of minor quantities of ice-rafter debris in various North Atlantic drill sites indicate a still earlier onset of limited glaciation around the Nordic Seas. Both the location and kind of ice remain uncertain. Were there mountain glaciers that reached the sea, or small ice sheets? Were they located on Greenland, on Svalbard, or over the Barents Sea? It is thus a primary drilling objective to obtain sediments from sites adjoining these regions to assess their glacial histories individually.

### *Sediment Budgets*

In order to derive a broad understanding of global sediment budgets, it is necessary to integrate biogenic (and lithogenic) flux data from all ocean basins. The present coverage of high-quality material from the Nordic Seas is insufficient both regionally (no sites in the central, western, or northern parts) and vertically (lack of deeper sites). The proposed drill sites cover the major water

masses and depth gradients and will permit calculation of burial fluxes of opal,  $\text{CaCO}_3$ , and organic carbon, as well as deductions about the intensity of  $\text{CaCO}_3$  dissolution through time.

## DRILLING PLAN/STRATEGY

Most of the NAAG objectives require drilling long sequences of rapidly deposited (>20 m/m.y.) sequences, with double APC coring to refusal (or occasional triple HPC coring as necessary). This approach permits retrieval of continuous sections for high resolution analysis of the higher frequency (orbital-scale or higher) variations of the climate system. At the same time, it also provides sequences spanning millions of years, during which the long-term baseline climatic state may evolve toward generally colder conditions, as may the spectral character of orbital-scale variations. In the following discussion of objectives, references to the history, evolution, or development of key components of the Arctic/Nordic climate system should thus be understood to include both orbital-scale and tectonic-scale changes.

Sites drilled during Leg 151 and sites proposed for Leg 163 are either 1) arrayed as broad north-south and east-west transects to monitor spatial paleoclimatic variability or closely spaced suites of cores across a range of depths to monitor vertical variability, 2) deep drilling targets that will better constrain the time of opening of Fram Strait, or 3) placed to monitor downstream sedimentological effects of deep flow through narrow gateway constrictions.

The north-south transect extends from the Arctic Ocean (the Yermak Plateau) via the Fram Strait, the Greenland and Iceland Seas into the north-western North Atlantic. It thereby ties into existing North Atlantic (DSDP Leg 81, 94), and Labrador Sea (ODP Leg 105) high resolution stratigraphies. This transect covers the major ocean basins of the region and provide sites on both sides of the two important gateways (the Fram Strait) and the Greenland-Scotland Ridge, and it will address the evolution of north-south environmental gradients from the Arctic to the temperate North Atlantic.

The east-west transect will use the Leg 104 sites on the Vøring Plateau as its eastern tie-point and will extend across to the areas immediately off east Greenland. The main intention of this transect is to sample the strong environmental gradient between the polar regions off east Greenland and the temperate Atlantic waters off Norway, in order to study the inception and evolution of the strong mid to high latitude east-west gradients and oceanic fronts, and to investigate differences in the

oceanic and glacial evolution between Greenland and Northern Europe. Additionally it is necessary to include a central sample point along this transect in order to obtain clean pelagic records from the central portions of the basin.

Two bathymetric transects are also proposed in order to study sediment budgets, lysocline/CCD-variability, and bathymetric gradients in ocean chemistry: one on the Yermak Plateau in the Arctic and the other on the slope between the Iceland Plateau and the Aegir Ridge (extinct axis) in the Norwegian Basin. This area is located centrally in the Norwegian Sea and will not be influenced by continental margin effects.

## PROPOSED SITES

### **The Yermak Plateau**

The Yermak Plateau is a topographic high due north of Svalbard. The Morris Jesup and northeastern Yermak Rises are a pair of plateaus rising to crestral depths of 0.5 to 1 km, which apparently were formed in Paleocene-Oligocene time by excess, Iceland-like volcanism along the southwestern Nansen ridge. The southern part of the Yermak Plateau may be thinned continental crust (Jackson et al., 1984). There is thick sediment draping on both the western and eastern flanks. Gravity and piston cores show that the present sediment cover contains some biogenic calcareous components and document normal pelagic sedimentation rates.

Drilling in this area will enable a study of environmental responses pre- and postdating the opening of the deep gateway into the Arctic. It will document the timing of this event, the physical and chemical nature of the water masses associated with the gateway opening and its influence on ocean circulation and climate. It will furthermore provide a check for the theory linking this event with changes in the relative plate motion starting at about Anomaly 13 time, and the possible global impacts of the establishment of a deep connection between the Arctic Ocean and the World Ocean. The other main achievement from drilling this area is that it should provide a continuous late Neogene record from the Arctic Ocean of the same quality as is available from lower latitude areas. This will make it possible to identify the onset of permanent ice cover in the Arctic, test models of the pre-glacial ice-free Arctic, and the magnitude of glaciation and ice sheets in the Arctic areas by identifying the onset and variation of IRD input into the Arctic Ocean. It should further enable

studies of Milankovitch cyclicity in Arctic Ocean climates and circulation and how this cyclicity has evolved with time.

The area forms the most northernmost end member of a north-south transect of drill sites that ties into the other oceans. It will be the northernmost control point for stratigraphic/chronostratigraphic studies, a reference area for Arctic studies, and a northern tie point for studies of the evolution of global thermal gradients. It is necessary to drill a series of sites in this region to recover a complete stratigraphic section from the time period of interest and, since the area lies in the marginal ice zone, and especially the northern and western sites are only accessible during favorable ice years, it is essential to have a choice of proposed sites, should one of them not be accessible. It is also desirable to obtain a bathymetric transect of sites in the Arctic to monitor depth gradients in sediment accumulation and water mass properties.

#### *Leg 151 Sites*

Leg 151 represented the first scientific drilling in any part of the Arctic, conducting operations at three sites on the Yermak Plateau (Fig. 2) - Site 910 (proposed site YERM-4), Site 911 (proposed site YERM-3) and Site 912 (proposed site YERM-2A) and two sites in the Fram Strait (Site 908 and Site 909).

Site 912 was designed to study the Neogene glacial history of the Arctic, the history of North Atlantic surface water influx to the Arctic, and to be an intermediate member of a bathymetric transect. Sites 911 and 910 are located on a thick sequence of draping sediment cover on the eastern flank and western flank, respectively, of the plateau and were designed to study Neogene variations in climate and oceanography, specifically address the Neogene Arctic glacial history, the Neogene variations in Atlantic water influx to the Arctic and also represent the shallow-water members of the bathymetric transect.

#### *Proposed Sites*

Proposed site YERM-1 (Fig. 2, Table 1) is located on the eastern flank of the plateau and is designed as a deep water target to document the subsidence history of the Yermak Plateau and its effects on water mass exchange through the Arctic gateway, and to determine the age and nature of basement. It will also provide records of surface and deep-water communication between the Arctic

and Norwegian Sea, and the IRD-sedimentation history of the Arctic. YERM-1 was originally scheduled to be drilled during Leg 151 with proposed site YERM-2A (Leg 151 Site 912) proposed as an alternate. Proposed site YERM-2A is located deeper than proposed site YERM-1 on the southwest slope of the plateau. It will, however, not be drilled to basement. Besides being an alternate site for YERM-1, this site is designed to study the Neogene glacial history of the Arctic, the history of North Atlantic surface water influx to the Arctic, and to be an intermediate member of a bathymetric transect. Basement is considered to be oceanic crust.

Proposed site YERM-5 (Fig. 2, Table 1) is located at 2850 m on a conformable draping sediment sequence on the lower western slope of the Plateau). The site will be used to document the glacial history of the Arctic Ocean for the Neogene, the history of sea-ice cover, the history of Atlantic water influx, deep water variations and will serve as the deep end member of the bathymetric gradient.

## **The Fram Strait**

### *Leg 151 Sites*

Leg 151 conducted operations at sites in the Fram Strait (Fig. 2), Site 908 (proposed site FRAM-2) and Site 909 (proposed site FRAM-1A).

Site 909 is located in the Fram Strait on a gentle elevated area northeast of the Hovgaard Ridge and was designed to document the timing of the opening of a deep passageway through the Fram Strait, the history of deep and shallow water exchange between the Arctic and the world ocean, and to provide records of Arctic glacial history and the climatic evolution of the Arctic region.

Site 908 is situated on the crest of the Hovgaard Ridge and was proposed in order to determine the age and lithology of the sedimentary processes immediately postdating the opening of the Fram Strait, and investigate the water mass exchange in and out of the Arctic Ocean.

### *Proposed Sites*

Proposed site SVAL-1 is located in the eastern part of Fram Strait (Fig. 2, Table 1). This site is to be drilled on the Svalbard margin to examine the onset of glaciation in the European Arctic and

establish the history of the Barents ice shelf, including dating the transition from a terrestrial- to marine-based ice sheet. Svalbard is believed to be the likely location for the initiation of Pliocene glaciation in the European Arctic. This site will also address questions related to glacial fan development and will serve as a counterpoint to proposed site EGM-4. This site is closely related to the European research program PONAM (Late Cenozoic Evolution of the Polar North Atlantic Margins).

### **The East Greenland Margin**

The proposed sites on the East Greenland Margin (Fig. 2, Table 1) are located on a north-south transect paralleling the path of the East Greenland Current (EGC). The objectives are to date the onset of the EGC, monitor deep-water formation and surface-water paleoenvironments in the Greenland Sea, determine their influence on the variability of the polar front and on the northern hemisphere paleoclimate, decipher the evolution of the Greenland Ice Sheet, monitor contour current activity and sediment drift deposition in the Greenland Basin, and study Paleogene paleoceanography.

#### *Leg 151 Sites*

Leg 151 conducted operations at one site on the East Greenland Margin (Fig. 2) - Site 913 (proposed site EGM-2). Site 913 is located on the lower slope of the east Greenland continental margin and is the northern end of a north-south transect along the margin and was proposed in order to document the history of the EGC and of deep water flow out of the Arctic downstream from Fram Strait. Difficulties were encountered coring the uppermost 400 m of sediment and, the lack of carbonate at this site precludes many of the planned paleo-circulation studies.

#### *Proposed Sites*

Proposed site EGM-4 is situated on the lower slope of the Trough Mouth Fan at Scoresby Sund (Fig. 2, Table 1). It is intended for high-resolution studies of the late Neogene history of IRD input and evolution of the Greenland Ice Sheet. It is also located where intermediate and deep waters from the Greenland Sea flow towards Denmark Strait. Proposed site EGM-3 is a low priority alternate.

## **The Iceland Plateau**

The sites proposed for this area (Fig. 2, Table 1) comprise a bathymetric transect of three sites as well as a site in the central Iceland Sea designated to be a part of the east-west transect.

### *Leg 151 Sites*

Leg 151 conducted operations at one site on the Iceland Plateau (Fig. 2) - Site 907 (proposed site ICEP-1). Site 907 represents the mid-point in the east-west transect located in the southern Nordic Seas, and was proposed in order to monitor the history of oceanic and climatic fronts moving east and west across the Iceland Plateau, derive an open ocean record of IRD and carbonate, and determine the history of the formation of northern source deep waters.

### *Proposed Sites*

During Leg 151, only one hole could be drilled at Site 907. While this hole did not have abundant carbonate, an excellent record of siliceous microfossils extending back to the middle Miocene and physical property time series from this hole record impressive Milankovitch-scale cyclicity. Given that this site is likely to become a type section for this region, additional offset holes are desirable. Proposed site ICEP-1 is located on top of the plateau and is an open-ocean site isolated from continental marine influence on IRD records. Site 907 will be completed with two more holes.

Due to an expected poor carbonate record, only the central site of the bathymetric transect, proposed site ICEP-3, will be drilled. This site will enable a study of oceanic response to different stages of opening of the Greenland-Scotland Gateway north of the ridge. It will also provide a record of pelagic IRD input well away from the ice sheets, thereby avoiding strong continental influence. This, combined with a location further east, will improve the chance for recovery of a carbonate biogenic record.

## **Northern and Southern Iceland-Faeroe Ridge**

The two sites north and south of the Iceland-Faeroe Ridge (Fig. 2, Table 1) were expected to provide information on the early spreading stages of the southern Norwegian Sea and the subsidence history of the Iceland-Faeroe Ridge. The location of the proposed sites provide the

opportunity of determining the age and nature of the Iceland-Faeroe Ridge and of the overlying sediments, which could provide information about the early history of the ridge. Drilling in this area could also determine if a step-wise or more sudden exchange of surface and bottom water occurred across the Iceland-Faeroe Ridge during the early Neogene. However, given the lack of carbonate records recovered north of the ridge, the potential to recover high quality geochemical records of overflow history from sites south of the ridge, and the results from surrounding ice core records and Heinrich layers, proposed site NIFR is consider a second priority site only and proposed site SIFR a third priority site.

### **Northern North Atlantic**

The major objectives of these site (Fig. 2, Table 1) will address water mass evolution and the role of thermohaline circulation on controlling the exchange of carbon between the ocean and atmosphere. In particular, these sites will address the character, causes, and consequences of sub-Milankovitch climate variability with the goal of correlation to the ice core records for the Quaternary and the establishment of when these high frequency variations were established. The ice core record of stage 5e seems to suggest that ice sheets are not necessarily a prerequisite for rapid oscillations in ocean-atmosphere circulation. With these sites we should be able to establish whether this type of climate “instability” was present during the early Pleistocene or prior to major northern hemisphere glaciation. One of the lower sedimentation rate sites is expected to extend into the Oligocene.

Proposed site NAMD-1 represents a re-occupation of DSDP Leg 12 Site 116 on top of the Rockall Plateau. Information from this site will help reconstruct the water mass behavior in the North Atlantic on glacial-interglacial time scales of the Plio-Pleistocene with special emphasis on the formation of Glacial North Atlantic Intermediate Water (GNAIW). In addition, we will be able to document the water mass structure in the North Atlantic during the late middle Miocene when the Iceland-Faeroe Ridge subsided to depths that finally allowed deep water exchange between the Nordic Seas and the North Atlantic to evolve. The recovery of a pre-middle Miocene section should document North Atlantic water mass circulation at times when no NADW existed; obtaining Oligocene sediment sections will allow us to study how the high-latitude North Atlantic responded to early intervals of apparent Antarctic glaciation as implied by the existence of glacially-derived sediments in the Southern Ocean area. Site 116 seems to be well suited for the proposed program in that a discontinuously drilled carbonate record back to the Oligocene has been recovered at this

location. Its position on a structural high protects this site from turbidites and its shallow depth greatly diminishes the risk of carbonate dissolution due to vertical fluctuations of the carbonate compensation depth. Furthermore, this site is in the flow path of the Iceland-Faeroe Ridge overflow waters which comprise a major constituent of NADW and it is in the area of potential GNAIW formation. As such, the site is at a key location for documentation of NADW/GNAIW variability and it will allow us to study in detail the initiation of water mass convection in the North Atlantic which has much importance for the long-term evolution of the world ocean's thermohaline circulation.

Proposed site GARDAR-1 is located on the Gardar Drift in 1980 m of water on the eastern flank of the Reykjanes Ridge. It is located at the depth of Glacial North Atlantic Intermediate Water during the last glaciation. Site survey results suggest that sedimentation rates as high as 20 cm/k.y. will be found here, providing an unprecedented record of both glacial-interglacial and millennial scale variations in thermohaline circulation, surface water temperatures, and ice-rafting history.

Proposed site FENI-1 is located on the Feni Drift and will recover an approximately 100 m record of the Brunhes chron at sedimentation rates of better than 100 cm/k.y. This site will be used to study mid-depth nutrient variability (2157 m), deep water circulation, and the surface-deep water links on both Milankovitch and millennial time scales.

Proposed site FENI-2 is situated at the same depth as FENI-1 and should recover a late Pliocene to Pleistocene record of sediment, also at greater than 10 cm/k.y. This site is essentially an extension of proposed site FENI-1 at a nearby location on the drift and would address many similar scientific objectives.

Proposed site BJORN-1 is located in the same region as GARDAR-1 at a shallower depth. Sedimentation rates are lower (5-9 cm/k.y.), although still high by open-ocean pelagic standards. This site has the ability to provide a high-resolution record of intermediate water circulation extending back to the Miocene. This site is a first priority alternate.

## REFERENCES

- Aagaard, K., 1981. On the deep circulation in the Arctic ocean. *Deep-Sea Res.*, 15:281-296.
- Aagaard, K., Swift, J.H., and Carmack, E.C., 1985. Thermohaline circulation in the Arctic Mediterranean Seas. *J. Geophys. Res.* C3, 90: 4833-4846.
- Barron, J., Larsen B., Baldauf, J., and Leg 119 Shipboard Party, 1988. Early glaciation of Antarctica. *Nature*, 333:303-304.
- Barron, A.J., and Washington, W.M., 1984. The role of geographical variables in explaining paleoclimates: results from Cretaceous climate model sensitivity studies. *J. Geophys. Res.* 89:1267-1279.
- Berggren W.A., and Schnitker, D., 1983. Cenozoic marine environments in the North Atlantic and Norwegian-Greenland Sea. In Bott, M.H.P., et al. (Eds.), Structure and Development of the Greenland-Scotland Ridge. *NATO Conf. Ser. IV: New York (Plenum Press)*, 495-548.
- Bott, M.H.P., Saxov, S., Talwani, M., and Thiede, J., (eds), 1983. In Bott, M.H.P., et al. (Eds.), Structure and Development of the Greenland-Scotland Ridge. *NATO Conf. Ser. IV: New York (Plenum Press)*, 1-685.
- Boyle, E.A., 1988. Vertical ocean nutrient fractionation and glacial/interglacial CO<sub>2</sub> cycles. *Nature*, 331:55-56.
- Broecker, W.S., and Peng, T.-H., 1982. Tracers in the Sea: Palisades, New York (Eldigio Press).
- Broecker, W.S., Peteet, D.M., and Rind, D., 1985. Does the ocean-atmosphere system have more than one stable mode of operation? *Nature*, 315:21-26.
- Carter, L.D., Brigham-Grette, J., Marinkovich, L., Pease, V.L., and Hillhouse, J.W., 1986. Late Cenozoic Arctic Ocean sea-ice and terrestrial paleoclimate. *Geology*, 14:675-678.
- Clark, D.L., 1982. Origin, nature and world climate effect of Arctic Ocean ice-cover. *Nature*, 300:321-325.
- Crane, K., Eldholm, O., Myhre, A.M., and Sundvor, E., 1982. Thermal implications for the evolution of the Spitsbergen transform fault. *Tectonophysics*, 89:1-32.
- Einarsson, T., and Albertsson, K.J., 1988. The glacial history of Iceland during the past three million years. *Philos. Trans. R. Soc. London*, B 318:637-644.
- Eldholm, O., Faleide, J.I., and Myhre, A.M., 1987. Continent-ocean transition at the western Barents Sea/Svalbard continental margin. *Geology*, 15:1118-1122.
- Eldholm, O., Thiede, J., Taylor, E., et al., 1987. *Proc. ODP, Init. Repts.*, 104: College Station, TX (Ocean Drilling Program).
- Funder, S., Abrahamsen, N., Bennike, O., and Feyling-Hanssen, R.W., 1985. Forested Arctic: evidence from North Greenland. *Geology*, 13:542-546.
- Goll, R.M., 1989. A synthesis of Norwegian Sea biostratigraphies: ODP Leg 104 on the Vøring Plateau. *Proc. ODP, Sci. Results*, 104: College Station, TX (Ocean Drilling Program), 777-826.
- Helland-Hansen, B., and Nansen, F., 1909. The Norwegian Sea: Its physical oceanography based upon the Norwegian researches 1900-1904. *Rep. Norw. Fish. Mar. Invest.*, 2:1-390.
- Herman, Y., and Hopkins, D.M., 1980. Arctic Ocean climate in late Cenozoic times. *Science*, 209:557-562.
- Hurdle, B.G., (Ed.), 1986. *The Nordic Seas*: New York (Springer-Verlag).
- Hay, W.W., 1985. *Impact of Ocean Drilling on the Earth Sciences*. JOI pamphlet.
- Jackson, H.R., et al., 1984. The Yermak Plateau; formed at a triple junction. *J. Geophys. Res.*, B89:3223-3232.
- Jansen, E., Bleil, U., Henrich, R., Kringstad, L., and Slettemark, B., 1988. Paleoenvironmental changes in the Norwegian Sea and the Northeast Atlantic during the last 2.8 Ma.: DSDP/ODP Sites 610, 642, 643 and 644. *Paleoceanography*, 3:563-581.
- Jansen, E., and Sjöholm, J., 1991. Reconstruction of glaciation over the past 6 Myr from ice-borne deposits in the Norwegian Sea. *Nature*, 349:600-603.
- Kristofferson, Y., 1982. United States ice drift station FRAM IV: Report on the Norwegian field program. Norsk Polarinstitutt Rapportserie, 11.

- Mantyla, A.W., and Reid, J.L., 1983. On the abyssal circulation of the world ocean. *Deep-Sea Res.*, 30: 805-833.
- Mix, A.C., and Pisias, N.G., 1988. Oxygen isotope analyses and deep sea temperature changes: implications for rates of oceanic mixing. *Nature*, 331:249-251.
- Mudie, P.J., and Helgason, J., 1983. Palynological evidence for Miocene climatic cooling in eastern Iceland about 9,8 Myr ago. *Nature*, 303:689-692.
- Nelson, R.E., and Carter, L.D., 1985. Pollen analysis of a late Pliocene and early Pleistocene section from the Gubik Formation of Arctic Alaska. *Quat. Res.*, 24:295-306.
- Peterson, W.H., and Rooth, C.G.H., 1976. Formation and exchange of deep water in the Greenland and Norwegian seas. *Deep-Sea Res.*, 23:273-283.
- Raymo, M.E., Ruddiman, W.F., Backman, J., Clement, B.M., and Martinson, D.G., in press. Late Pliocene variation in Northern Hemisphere ice sheets and North Atlantic Deep Water circulation. *Paleoceanography*.
- Repenning, C.A., Brouwers, E.M., Carter, L.D., Marincovitch, L., Jr., and Ager, T.A., 1987. The Beringian ancestry of *Phenacomys* (Rodentia: Cricetidae) and the beginning of the modern Arctic Ocean borderland biota. *U.S. Geol. Survey Bull.*, 1687:1-28.
- Ruddiman, W.F., Raymo, M., and McIntyre, A., 1986. Matuyama 41,000-year cycles: North Atlantic Ocean and northern hemisphere ice sheets. *Earth Planet. Sci. Lett.*, 80:17-129.
- Ruddiman, W.F., and Raymo, M.E., 1988. Northern hemisphere climate regimes during the last 3 Ma: Possible tectonic connections. *Philos. Trans. R. Soc. London*, B 318:411-430.
- Shackleton, N.J., 1987. The carbon isotope record of the Cenozoic: History of carbon burial and of oxygen in the ocean and atmosphere. In Brooks, J., and Fleet, A.J. (Eds.), *Marine Petroleum Source Rocks*. Spec. Publ. - Geol. Soc., 26:423-434.
- Shackleton, N.J., Backman, J., Zimmerman, H., Kent, D.V., Hall, M.A., Roberts, D.G., et al., 1984. Oxygen isotope calibration of the onset of ice-rafting and history of glaciation in the North Atlantic region. *Nature*, 307:620-623.
- Shackleton, N.J., and Boersma, A., 1981. The climate of the Eocene ocean. *J. Geol. Soc. London*, 138: 153-157.
- Shackleton, N.J., and Kennett, J.P., 1975. Late Cenozoic oxygen and carbon isotopic changes at DSDP Site 284: Implications for glacial history of the Northern Hemisphere and Antarctic. In Kennett, J.P., Houtz, R.E., et al., *Init. Repts. DSDP*, 29: Washington (U.S. Govt. Printing Office), 801-807.
- Smethie, W.M., Chipman, D.W., Swift, J.H., and Kolterman, K.P., 1988. Chlorofluoromethanes in the Arctic Mediterranean Sea: Evidence for formation of bottom water in the Eurasian Basin and deep-water exchange through Fram Strait. *Deep-Sea Res.*, 35:347-370.
- Sundvor, E., et al., 1982. Marine geophysical survey on the Yermak Plateau. The Norwegian Petroleum Directorate Geological/Geophysical Investigations Scientific Report, 7.
- Sverdrup, H.U., Johnson, M.W., and Fleming, R.H., 1942. *The Oceans: Their Physics, Chemistry, and General Biology*: New Jersey (Prentice-Hall), 1-1087.
- Swift, J.H., Takahashi, T., and Livingston, H.D., 1983. The contribution of the Greenland and Barents Seas to the deep water of the Arctic Ocean. *J. Geophys. Res.*, 88:5981-5986.
- Talwani, M., Udintsev, G., et al., 1976. *Init. Repts. DSDP*, 38: Washington (U.S. Govt. Printing Office), 1-1256.
- Thiede, J., 1983. Outstanding geological problems of the Greenland-Scotland Ridge: An introduction. In Bott, M.H.P., et al. (Eds.), *Structure and Development of the Greenland-Scotland Ridge*. *NATO Conf. Ser. IV*: New York (Plenum Press), 313-318.
- Thiede, J., 1988. Scientific cruise report of Arctic expedition ARK IV/3. *Ber. Polarforschung*, 43.
- Thiede, J., and Eldholm, O., 1983. Speculations about the paleo-depth of the Greenland-Scotland Ridge during Late Mesozoic and Cenozoic times. In Bott, M.H.P., et al., (Eds.), *Structure and Development of the Greenland-Scotland Ridge*. *NATO Conf. Ser. IV*: New York (Plenum Press), 445-456.
- Thierstein, H.R., and Berger, W.H., 1978. Injection events in ocean history. *Nature*, 268:461-466.

...Leg 163 - North Atlantic Arctic Gateways II...

- Vogt, P.R., 1986a.** Seafloor topography, sediments, and paleoenvironments. *In* Hurdle, B.G. (Ed.), *The Nordic Seas*: New York (Springer Verlag), 237-412.
- Vogt, P.R., 1986b.** Geophysical and geochemical signatures and plate tectonics. *In* Hurdle, B.G. (Ed.), *The Nordic Seas*: New York (Springer Verlag), 413-662.
- Warren, B.A., 1981.** Deep circulation of the world ocean. *In* Warren, B.A. and Wunsch, C., (Eds.), *Evolution of Physical Oceanography*: Cambridge, Mass.(MIT Press), 6-41.

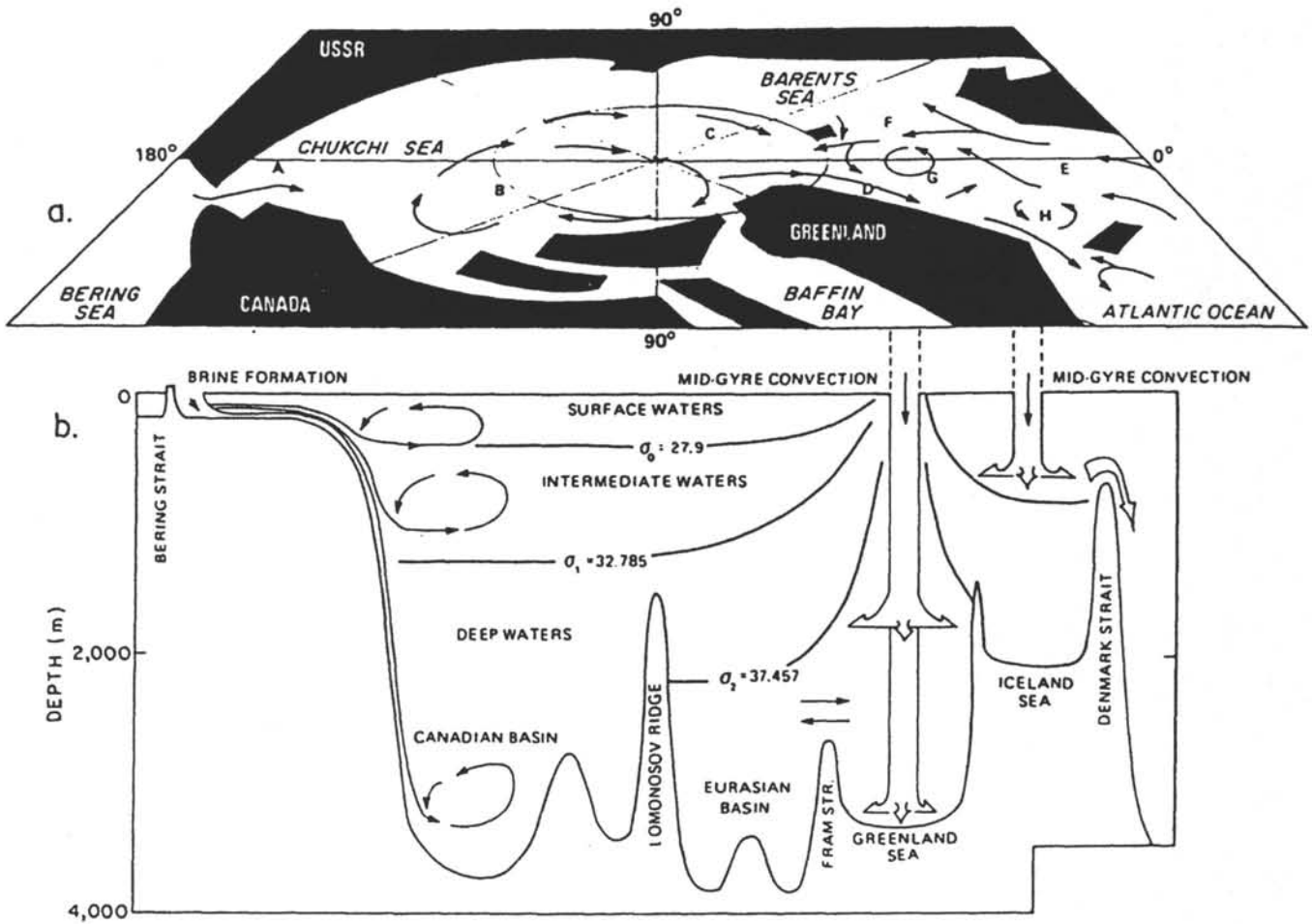


**Figure 1.** Schematic illustration of ocean circulation in the Arctic Ocean and Nordic seas (from Aagaard et al., 1985).

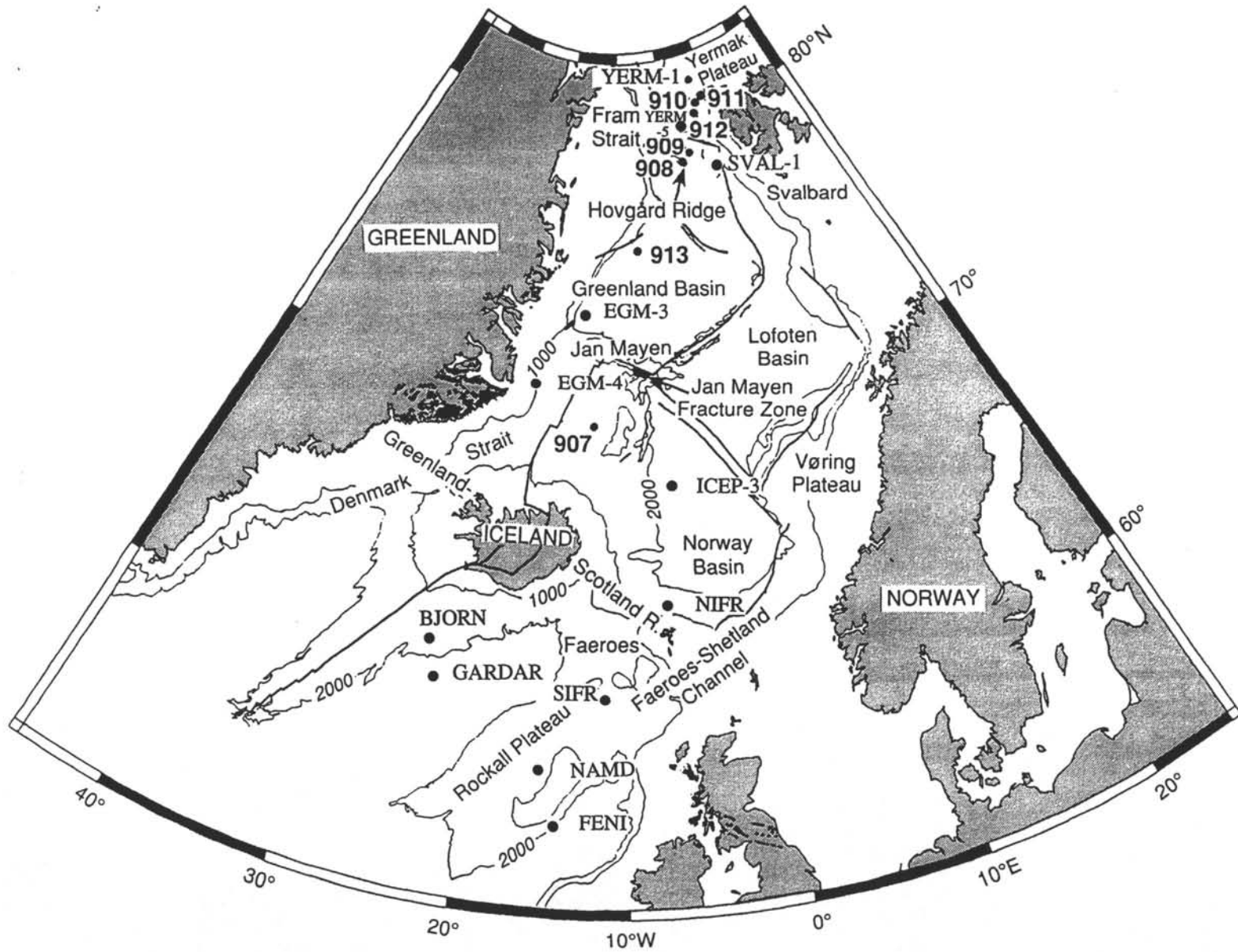


Figure 2. Location of Leg 151 sites and Leg 163 proposed sites.

**TABLE 1**  
**PROPOSED SITE INFORMATION**  
**and**  
**DRILLING STRATEGY**

<b>SITE:</b> YERM-1	<b>PRIORITY:</b> 1	<b>POSITION:</b> 81°06'N, 7°E
<b>WATER DEPTH:</b> 900m	<b>SEDIMENT THICKNESS:</b> 680m	<b>TOTAL PENETRATION:</b> 750m
<b>SEISMIC COVERAGE:</b> BU 79-7 SP 400. BU 79-2 crossing		

**Objectives:** To study the subsidence history of the Yermak Plateau and its control on water mass exchange through the Arctic Gateway. To identify the nature of the basement. To study the history of surface and deep-water communication between the Arctic and the Norwegian-Greenland Sea. To study the history of IRD sedimentation in the Arctic.

**Drilling Program:** APC, and RCB or XCB coring.

**Logging and Downhole Operations:** Standard logging.

**Nature of Rock Anticipated:** Glacio-marine muds, mudstones, and sands and basalts.

<b>SITE:</b> SVAL-1	<b>PRIORITY:</b> 1	<b>POSITION:</b> 77°15.57'N, 9°05.5'E
<b>WATER DEPTH:</b> 2120m	<b>SEDIMENT THICKNESS:</b> TBP <sup>1</sup>	<b>TOTAL PENETRATION:</b> 800m
<b>SEISMIC COVERAGE:</b> TBP		

**Objectives:** To examine the onset of glaciation in the European Arctic and establish the history of the Barents ice shelf, including dating the transition from a terrestrial to marine based ice sheet. To address questions concerning glacial fan development and to serve as a counterpoint to proposed site EGM-4.

**Drilling Program:** APC/XCB coring.

**Logging and Downhole Operations:** Standard logging.

**Nature of Rock Anticipated:** TBP

OR

<b>SITE:</b> YERM-5	<b>PRIORITY:</b> 2	<b>POSITION:</b> 79°58.5'N, 1°42'E
<b>WATER DEPTH:</b> 2850m	<b>SEDIMENT THICKNESS:</b> >2000m	<b>TOTAL PENETRATION:</b> 600m
<b>SEISMIC COVERAGE:</b> BU 79-18 SP 80.		

**Objectives:** To study the glacial history of the Arctic for the Neogene. To investigate the history of the influx of North Atlantic water into the Arctic Ocean. To form the deep end-member of a bathymetric transect to study depth gradients in sediment accumulation.

**Drilling Program:** Triple APC and XCB coring

**Logging and Downhole Operations:** Standard logging.

**Nature of Rock Anticipated:** Glacio-marine sediments.

<sup>1</sup> TBP = To be provided

<b>SITE:</b> EGM-4	<b>PRIORITY:</b> 1	<b>POSITION:</b> 70°30'N, 18°20'W
<b>WATER DEPTH:</b> 1670m	<b>SEDIMENT THICKNESS:</b> 1000m	<b>TOTAL PENETRATION:</b> 800m
<b>SEISMIC COVERAGE:</b> GGU 82-12 SP 2270		

**Objectives:** To monitor the history of the Greenland ice sheet and study the latitudinal development of the EGC.

**Drilling Program:** APC, and XCB or RCB coring.

**Logging and Downhole Operations:** Seismic stratigraphy and geochemistry.

**Nature of Rock Anticipated:** Glacial marine sediments.

OR

<b>SITE:</b> EGM-3	<b>PRIORITY:</b> 2	<b>POSITION:</b> 73°28.5'N, 13°9'W
<b>WATER DEPTH:</b> 2650 m	<b>SEDIMENT THICKNESS:</b> ~1000m	<b>TOTAL PENETRATION:</b> 900m
<b>SEISMIC COVERAGE:</b> MCS NGT 46 SP 804		

**Objectives:** To date the onset of the East Greenland Current, monitor the development of deep-water formation in the Greenland Sea, and document the history of IRD inputs.

**Drilling Program:** APC, and XCB or RCB coring.

**Logging and Downhole Operations:** Seismic stratigraphy and geochemistry.

**Nature of Rock Anticipated:** Glacial marine and biogenic sediments, terrigenous mud.

<b>SITE:</b> ICEP-1 (Site 907B, C)	<b>PRIORITY:</b> 1	<b>POSITION:</b> 69°15'N, 12°42'W
<b>WATER DEPTH:</b> 1812m	<b>SEDIMENT THICKNESS:</b> TBP	<b>TOTAL PENETRATION:</b> 230m
<b>SEISMIC COVERAGE:</b> Leg 151		

**Objectives:** To monitor the history of oceanic and climatic fronts moving east and west across the Iceland Plateau. To derive an open-ocean record of IRD and carbonate. To determine the history of formation of northern-source deep waters.

**Drilling Program:** APC/XCB coring. Holes 907B and 907C.

**Logging and Downhole Operations:** Standard logging.

**Nature of Rock Anticipated:** TBP

<b>SITE:</b> ICEP-3	<b>PRIORITY:</b> 1	<b>POSITION:</b> 66°56'N, 6°27'W
<b>WATER DEPTH:</b> 2807m	<b>SEDIMENT THICKNESS:</b> 800m	<b>TOTAL PENETRATION:</b> 500m
<b>SEISMIC COVERAGE:</b> UB-ICEP-2 Segment D SP 4700, Segment B (crossing)		

**Objectives:** To document the oceanic response to different stages of the opening of the Greenland-Scotland Gateway. To form an intermediate-member of a bathymetric transect of sites for monitoring the history of CCD, carbonate preservation, and biogenic silica sedimentation/accumulation as a response to changing climatic and oceanographic conditions.

**Drilling Program:** Triple APC and XCB coring.

**Logging and Downhole Operations:** Standard logging.

**Nature of Rock Anticipated:** Glacial marine sediments, calcareous and siliceous muds and oozes.

<b>SITE:</b> NAMD-1 (DSDP Site 116)	<b>PRIORITY:</b> 1	<b>POSITION:</b> 57°29.8'N, 15°55.5'W
<b>WATER DEPTH:</b> 1150m	<b>SEDIMENT THICKNESS:</b> TBP	<b>TOTAL PENETRATION:</b> 820m
<b>SEISMIC COVERAGE:</b> DSDP Leg 12		

**Objectives:** To reconstruct water mass behavior in the North Atlantic on glacial-interglacial time scales of the Plio-Pleistocene, particularly the formation of GNAIW. To document water mass structure in the North Atlantic during the late middle Miocene and to obtain a pre-middle Miocene section to document North Atlantic water mass circulation at times when no NADW existed. To study NADW/GNAIW variability and the initiation of water mass convection in the North Atlantic.

**Drilling Program:** APC/XCB coring.

**Logging and Downhole Operations:** Standard logging.

**Nature of Rock Anticipated:** TBP

<b>SITE:</b> GARDAR	<b>PRIORITY:</b> 1	<b>POSITION:</b> 60°25.30' N, 23°23.23'W
<b>WATER DEPTH:</b> 1980m	<b>SEDIMENT THICKNESS:</b> TBP	<b>TOTAL PENETRATION:</b> 400m
<b>SEISMIC COVERAGE:</b> TBP		

**Objectives:** To obtain a record of glacial-interglacial and millennial scale variations in thermohaline circulation, surface water temperatures, and ice-rafting history.

**Drilling Program:** APC/XCB coring.

**Logging and Downhole Operations:** Standard logging.

**Nature of Rock Anticipated:** TBP

<b>SITE:</b> FENI-1	<b>PRIORITY:</b> 1	<b>POSITION:</b> 55°30'N, 14°42'W
<b>WATER DEPTH:</b> 2157m	<b>SEDIMENT THICKNESS:</b> TBP	<b>TOTAL PENETRATION:</b> 100m
<b>SEISMIC COVERAGE:</b> TBP		

**Objectives:** To study mid-depth nutrient variability, deep water circulation, and the surface-deep water links on both Milankovitch and millennial time scales.

**Drilling Program:** APC/XCB coring.

**Logging and Downhole Operations:** Standard logging.

**Nature of Rock Anticipated:** TBP

<b>SITE:</b> FENI-2	<b>PRIORITY:</b> 1	<b>POSITION:</b> 55°30'N, 14°42'W
<b>WATER DEPTH:</b> 2157m	<b>SEDIMENT THICKNESS:</b> TBP	<b>TOTAL PENETRATION:</b> 300m
<b>SEISMIC COVERAGE:</b> TBP		

**Objectives:** To study mid-depth nutrient variability, deep water circulation, and the surface-deep water links on both Milankovitch and millennial time scales.

**Drilling Program:** APC/XCB coring.

**Logging and Downhole Operations:** Standard logging.

**Nature of Rock Anticipated:** TBP

OR

<b>SITE:</b> BJORN	<b>PRIORITY:</b> 2	<b>POSITION:</b> 61°25.17'N, 24°06.33'W
<b>WATER DEPTH:</b> 1653m	<b>SEDIMENT THICKNESS:</b> TBP	<b>TOTAL PENETRATION:</b> 700m
<b>SEISMIC COVERAGE:</b> TBP		

**Objectives:** To obtain a high-resolution record of intermediate water circulation extending back to the Miocene.

**Drilling Program:** APC/XCB coring.

**Logging and Downhole Operations:** Standard logging.

**Nature of Rock Anticipated:** TBP

OR

<b>SITE:</b> NIFR-1	<b>PRIORITY:</b> 2	<b>POSITION:</b> 63°26.55'N, 7°14.51'W
<b>WATER DEPTH:</b> 1240m	<b>SEDIMENT THICKNESS:</b> >1200m	<b>TOTAL PENETRATION:</b> 1000m
<b>SEISMIC COVERAGE:</b> IF30, IF52 crossing.		

**Objectives:** To determine the age and nature of the Iceland-Faeroe Ridge. To document the Paleogene environmental situations in the southern Norwegian Sea, and monitor the early phases of warm water inflow into the Norwegian Sea.

**Drilling Program:** APC and XCB coring.

**Logging and Downhole Operations:** Standard logging.

**Nature of Rock Anticipated:** Hemipelagic biogenic muds.

OR

<b>SITE:</b> SIFR-1	<b>PRIORITY:</b> 3	<b>POSITION:</b> 60°33.30'N, 11°29.0'W
<b>WATER DEPTH:</b> 1215m	<b>SEDIMENT THICKNESS:</b> >1200m	<b>TOTAL PENETRATION:</b> 500m
<b>SEISMIC COVERAGE:</b> IF02, IF06 crossing.		

**Objectives:** To reconstruct the early subsidence history of the Iceland-Faeroe Ridge. To document the onset of Neogene surface-water exchange over the Iceland-Faeroe Ridge. To compare faunal assemblages north and south of the Iceland-Faeroe Ridge.

**Drilling Program:** APC and XCB coring.

**Logging and Downhole Operations:** Standard logging.

**Nature of Rock Anticipated:** Hemipelagic/pelagic biogenic muds.

*LEG 164*

*Gas Hydrate Sampling*

# LEG 164

## GAS HYDRATE SAMPLING ON THE BLAKE RIDGE AND CAROLINA RISE

---

Modified From Proposal 423 Submitted By

Charles K. Paull, William P. Dillon, Timothy Collett, Steve Holbrook,  
Keith A. Kvenvolden, Richard P. von Herzen, and William Ussler

To Be Named: Co-Chief Scientists and Staff Scientist

---

### ABSTRACT

Gas hydrates are a solid phase composed of water and low molecular weight gases (predominantly methane) which form under conditions of low temperature, high pressure, and gas saturation; conditions that are common in the upper few hundred meters of rapidly accumulated marine sediments (Claypool and Kaplan, 1974; Sloan, 1989). Although gas hydrates may be a common phase in the shallow geobiosphere, they are unstable under normal surface conditions, and thus surprisingly little is known about them.

The in situ characteristics of gas-hydrated sediments can best be studied by drilling where gas hydrates are as extensive as possible and their influence on sediment properties are largest. The Blake Ridge - Carolina Rise gas hydrate field is an excellent area for a gas hydrate drilling program because it is associated with sediments that have especially high interval velocities and distinct reflection characteristics, is well surveyed, contains one of the worlds most laterally extensive gas hydrate fields including a well developed BSR (bottom-simulating-reflector), and lacks tectonic influences that complicate hydrate distribution and fluid circulation in accretionary prisms.

Drilling in the Blake Ridge - Carolina Rise area will 1) determine the amounts of gas trapped in extensively hydrated sediments, 2) contribute to an understanding of the lateral variability in the extent of gas hydrate development, 3) investigate the distribution and fabric of gas hydrates within sediments, 4) establish the physical property changes associated with gas hydrate formation and decomposition in continental margin sediments, 5) assess whether the gas captured in gas hydrates is produced locally or has migrated in from elsewhere, 6) measure changes in the porosity (and permeability?) structure associated with gas hydrate cemented sediments, and 7) determine the role of gas hydrates in stimulating or modifying fluid circulation.

## INTRODUCTION

Enormous volumes of natural gas may be associated with gas hydrated sediments (Kvenvolden and Barnard, 1983; Kvenvolden, 1988a). Large quantities of gas may be stored in the gas hydrate cemented sediments because up to 164 times the saturation concentration of gas at STP condition exists in these solid phases per unit volume (Sloan, 1989). It is estimated that there are about  $10^4$  Gt ( $Gt = 10^{15}$  gm) of carbon stored in gas hydrates, which is about two times the estimate for the carbon in all other fossil fuel deposits (Kvenvolden 1988b). Moreover, there may be considerable volumes of free gas trapped beneath the overlying solid gas hydrate-cemented zones that are associated with the BSR. However, we know too little about hydrates at present to be confident about these estimates (Kvenvolden, 1988b).

### **Sedimentary and Geochemical Importance of Gas Hydrates**

One explanation for some of the major slumps on continental rises relates to instability of the sediments from the break down of gas hydrates (Summerhayes et al., 1979; Embley, 1980; Carpenter, 1981; Cashman and Popenoe, 1985; Prior et al., 1989). Seismic data near some slump areas show that there are numerous normal faults that sole out at or near the BSR (Paull et al., 1989). If gas hydrates comprise a significant portion of the volume of rise prism sediments above the BSR (Heling, 1970; Harrison and Curiale, 1982), the physical properties of sediments will change dramatically when gas hydrates decompose. Solid gas hydrates decompose to water plus (over-pressured?) gas (Kayen, 1988). Sediment instability and failure are likely to be concentrated along this lubricated horizon. The gas hydrates may play an important role in sediment tectonics, strengthening the sediments above and weakening the sediments at and below the BSR. Thus, the potential for physical property changes that significantly alter the mechanical strength of the margin will best be understood by establishing the extent of the gas hydrate formation in the overlying sediments and the physical characteristics of the sediments both at and beneath the BSR.

### *Effects on Fluid Circulation*

At present our collective knowledge about the processes, rates, and plumbing involved in fluid exchange between the porous sedimentary flanks of continents and the adjacent ocean water is rudimentary. Considerable interest has been generated by the patterns of fluid circulation and the

associated seawater-rock exchange at ocean ridges. However, the importance of fluid exchange between the ocean and its edges is unknown and cannot be resolved without additional knowledge of fluid circulation systems in a variety of settings (National Research Council, 1989). Extensively hydrated rise prism sediments are one of the sediment types that need to be understood.

#### *Modification of Fluids*

Methane and saline fluids may be expelled from abyssal sediments as a consequence of gas hydrate formation and deterioration. In the process of gas hydrate formation, water and low molecular weight gases (i.e., methane) form a crystalline solid which cements the sediment, leaving the remaining pore fluids enriched in salts (Hesse and Harrison, 1981; Harrison and Curiale, 1982). At greater depths gas hydrates break down and add methane and fresh water back into the pore waters, decreasing the salinity and increasing the methane concentration. Gas hydrate decomposition leaves a porous zone that is charged with methane beneath the stable gas hydrate zone. If gas hydrate formation is extensive, it may be exerting a strong influence on the composition of continental margin pore fluids.

#### *Drilling Hazard*

Due to safety reasons the various academic drilling projects have generally avoided drilling in areas where well-developed BSR's are known to occur. Safety panels are concerned with gas blowouts related to the decomposition of gas hydrates or the release of free gas from beneath the gas hydrates. Thus, most gas hydrate samples have come from the edges of the hydrated areas where it can be assumed that hydration is not as extensive (Jenden and Gieskes, 1983). Whether these safety concerns are realistic or not is simply unknown; however, academic drilling in hydrated areas will be impeded until more is known about gas hydrate structure and until techniques are established that can assess the potential risk of blowouts in particular areas. Unfortunately, the drilling of many other scientific targets are being stymied because they occur beneath hydrated sediments.

#### *Future Resource?*

The resource potential of marine gas hydrates is currently unknown, but considering the possibility of enormous gas reservoirs, gas hydrates will continue to attract attention until they are development targets or it is demonstrated that they do not have resource value.

## **Paleoceanographic Importance of Gas Hydrates**

### *Storage of a Greenhouse Gas*

The stability of continental rise gas hydrates will be affected by the change in pressure that is associated with substantial sea level changes. During the Pleistocene glaciations sea level was more than 100 meters lower than it is today and the associated pressure change would cause the lower limit of gas hydrate stability to rise about 20 meters. This may have created a weak "lubricated" zone along the rise at the base of the BSR that could have resulted in frequent sediment failures. Thus, when sea level drops, large volumes of methane (a greenhouse gas) may be released. Conversely, when sea level rises, the lower limit of gas hydrate stability will migrate downward and may trap more gas. These changes in the stability field will change the size of the marine gas hydrate reservoir by a few percent. Given that there are about 3.6 Gt of methane carbon in the modern atmosphere, a release of one tenth of one percent of the carbon from the gas hydrate reservoir would be equivalent to the anthropogenic inputs of the last century! Scenarios can be constructed that suggest the exchange between the gas hydrate reservoir and the atmosphere may determine the limits of glaciation (Nisbet, 1990; MacDonald, 1990; Paull et al., 1991). Unfortunately, neither the volumes of gas that are involved, nor their dynamics are well enough understood to assess whether or to what degree marine gas hydrates act as a buffer or accentuator to climatic change.

## **THE STUDY AREA**

### **Nature and Detection of Gas Hydrates**

#### *Seismic Detection of Marine Gas Hydrates*

Gas hydrates are usually detected in marine sediments with seismic reflection data because they produce a bottom simulating reflector. The BSR often cuts across normal sediment bedding planes, thus clearly distinguishing itself as an acoustic response to a diagenetic change rather than a depositional horizon. The BSR is believed to represent the base of the gas hydrate stability zone which occurs between about 200 and 600 meter depths below sea floor on continental rises. The pores of sediments above the BSR are partly filled with gas hydrates, which may increase the sediment density, while deeper sediments may contain free gas. The Carolina Rise, particularly

along the Blake Ridge, was the area where marine gas hydrates were first identified on the basis of a BSR and is an area where gas hydrates appear to be especially extensive (Fig. 1) (Markl et al., 1970; Tucholke et al., 1977; Shipley et al., 1979; Paull and Dillon, 1981; Dillon and Paull, 1983; Markl and Bryan, 1983) and might be considered the "type section" for marine gas hydrates.

Where gas hydrates have been detected in seismic reflection data, the BSR is a very high amplitude reflector that is associated with a phase reversal (Shipley, et al., 1979; White, 1979). Phase reversals are diagnostic of a change from high acoustic impedance (density x velocity) above to lower impedance below. This phase reversal may indicate that the upper sediments are extensively cemented with gas hydrates while another zone exists at or beneath the BSR where the gas hydrates have decomposed (or trapped gas from below) and released free gas back into the sediment pores. The published velocity measurements in sediments from the Carolina Rise indicate very high velocities above the BSR and very low velocities just below the BSR (Fig. 2). These low velocities have been attributed to gas-charged sediments and it has been hypothesized that the gas hydrates may be a seal for a significant natural gas reservoir (Dillon et al., 1980). While similar velocity structures have been found elsewhere (Andreassen et al., 1990), lesser velocity contrasts occur at the BSR at some other sites (Miller et al., 1991; Hyndman and Spence, 1992).

### *Sampling of Marine Gas Hydrates*

Gas hydrates are believed to be common in continental margin sediments because seismic reflection data have indicated their presence in every ocean basin (Kvenvolden and Barnard, 1983; Kvenvolden, 1988a, b). Gas hydrates are well known from permafrost drilling (Makogon, 1981; Collett and Kvenvolden, 1987; Kvenvolden and Grantz, 1991) and have been recovered from piston cores (Yefremova and Zizhchenko, 1975; Brooks et al., 1984; Brooks et al., 1991); they have also been sampled in DSDP and ODP holes (i.e. Legs 67, 68, 76, 84, 96, & 112).

An attempt to drill a strong BSR was made on DSDP Leg 11 on the Blake Ridge. At the time the origin of the BSR was a mystery. Very gassy sediments that self-extruded from their core liners were recovered at Sites 102, 103, and 104. Although the conclusion at the time was that the level of the BSR had been penetrated and it corresponded with a hard layer at the base of the hole (Hollister et al., 1972), this interpretation was based on estimates of sediment velocity that are lower than subsequent work has indicated occur at this site. Therefore, we question whether DSDP Leg 11 actually penetrated to the level of the BSR.

DSDP Site 533 was successfully drilled on the flanks of the Blake Ridge to sample hydrated sediments. Site 533 was intentionally located on the periphery of the major gas hydrate field, and did not penetrate into sediments associated with significant seismic blanking that is indicative of extensive hydrate formation. Nevertheless significant amounts of hydrate were encountered (Kvenvolden et al., 1983). Seismic reflection profiles only identify well developed gas hydrates, while the smaller patches of gas hydrate remain undetected. Thus inventories of the extent of gas hydrates based on seismic reflection data should be treated as minimum estimates.

## **SCIENTIFIC OBJECTIVES AND METHODOLOGY**

### **Summary of Objectives**

- 1) To determine the amounts of gas trapped in extensively hydrated sediments.
- 2) To understand the lateral variability in the extent of gas hydrate development.
- 3) To investigate the distribution and fabric of gas hydrates within sediments.
- 4) To establish the physical property changes associated with gas hydrate formation and decomposition in continental margin sediments.
- 5) To assess whether the gas captured in gas hydrates is produced locally or has migrated in from elsewhere.
- 6) To measure changes in the porosity (and permeability?) structure associated with gas hydrate cemented sediments.
- 7) To determine the role of gas hydrates in stimulating or modifying fluid circulation.

### **Specific Objectives and Methodology**

#### *Quantity of Gas Hydrates*

The amount of methane that may be stored as gas hydrate within marine sediments is at present poorly known. One large step toward assessing the size of this inventory is to establish the amount

of methane that exists in the most extensively hydrated areas. Unambiguous estimates of in situ gas hydrate volumes can best be determined by pressure core sampling (PCS). Multiple runs of the PCS tool will be required to adequately characterize the extent of variation, especially with stratigraphic and lithologic changes. However, other types of detailed subsurface information and geophysical techniques can be calibrated here to estimate the amounts of gas hydrate in other areas.

#### *Spatial Variation of Gas Hydrate Development.*

To date, most studies on the distribution and occurrence of gas hydrates have been directed at regional distribution patterns that are inferred from BSR characteristics. However, seismic reflection profiles also show that there is an enormous amount of local lateral variability in the strength of the BSR and extent of the acoustically blank zone above the BSR within individual gas hydrate containing regions. The causes of these variations are not understood and merit further study via the drilling of closely-spaced holes.

The subsurface depth of the BSR in multichannel seismic reflection profiles from the Carolina Rise - Blake Ridge gas hydrate field shows the predicted linear increase with increasing water depth (Fig. 3). However, there are considerable variations on this trend, which should not occur in a homogeneous system. Thus, there are either errors of  $\pm 25\%$  in the velocities that are used to calculate the depth to the BSR (perhaps related to lateral variabilities in the extent of hydration), local changes in the composition of the subsurface gases and fluids, local changes in the thermal structure of the sediment column, or zones where gas hydrates have not reached equilibrium with local conditions. The relative importance of these parameters in causing BSR depth variations needs to be examined.

#### *Fabric and In Situ Distribution of Gas Hydrates*

The physical characteristics of the gas hydrates that have been sampled from marine sediments also suggest that gas hydrate distribution is quite patchy in a vertical sense. At present, little is known about the effects of either grain size or lithology on gas hydrate formation. Hydrates may form as either veins or lenses that have some horizontal continuity, or as isolated gas hydrate nodules within the sediment matrix. If they are in fact laterally continuous layers, they may control the local permeability and velocity structure. In some hydrate-containing cores, the gas hydrates form layers up to several cm in thickness, particularly in coarser grained sediments, suggesting an association

with more permeable conduits. The relative importance of finely disseminated gas hydrates in terms of the size of the hydrate pool is difficult to assess. Finely disseminated gas hydrates may be under-sampled because they are not visually detected and leave only slight chemical signatures in normal core samples. More and better fabric data on gas hydrate occurrences are needed to improve the quality of gas hydrate volume estimates and to understand the effects of the gas hydrates on the structure of the sediments, which will require detailed sampling and in situ experiments in different settings.

### *Seismic Velocity Estimates*

By measuring the acoustic velocities of hydrated sediments it may be possible to assess the amounts of gas hydrate that exists in the subsurface. The inferred occurrence of gas hydrate in the sediment is adequate to increase the sediment interval velocities by ~25% in some places, which suggests the amount of gas hydrate must be extensive. However, the consequences of adding high velocity material to the sediment column are difficult to predict, especially without knowing whether the gas hydrates can be best thought of as a pervasive cement or discrete nodules in otherwise unaltered sediments (Toksoz et al., 1976).

Various elastic wave velocities have been reported for experimentally grown gas hydrates that range from 2.4 to 3.8 km/sec (Stoll, Ewing, and Bryan, 1971; Stoll and Bryan, 1979; Davidson et al., 1983; Pandit and King, 1982). However, these measurements have all been made on systems containing pure propane and ethane gas hydrates (type II) which may not be representative of the methane gas hydrates (type I). Thus, the relationship between gas hydrate amounts and sediment velocities needs to be calibrated in situ.

The addition of gas hydrates to sediments may be analogous to cementation of the sediments and is believed to decrease the impedance contrast between the sediment layers above the BSR and produce the amplitude blanking zone that is observed above the BSR. These changes in the acoustic impedance have been used to model the amount of gas hydrates that are in the sediments (Dillon et al., 1991; Miller et al., 1991; Lee, in prep.). Modeling estimates indicate large amounts of gas hydrate are required to produce the observed acoustic blanking in the sediment, especially in the Carolina Rise Blake-Ridge area (Dillon et al., 1991).

Determining the in situ sediment velocities in areas of extensive gas hydrates will require special care to collect and integrate data from the different techniques for velocity measurement. Well log data provide accurate information on the velocity structure that occurs within a few meters of the hole. Vertical seismic profiles (VSP) can provide data on the interval velocities (Hardage, 1985; Shipboard Scientific Party, 1990). Thus, differences between the averaged values (VSP) and the well log velocities will indicate how typical the core site is of the surrounding sediments. Shipboard physical property measurements are frequently done after the gas hydrates have started to or are completely decomposed. Comparisons with velocity log data and velocimeter measurements may provide insight into the velocity change associated with gas hydrate decomposition.

*Sources of the Gas (in situ Production or Upwards Migration?)*

We are interested in assessing whether the gas hydrate system is sustained by in situ production or requires gas to migrate from elsewhere. In order to have gas hydrate formation, saturation of methane or another hydrate-forming gas is required. Because the existing isotopic and compositional data on the Blake Ridge suggest that this gas is biogenic methane (Brooks et al., 1983; Galimov and Kvenvolden, 1983), it is frequently assumed that the gas is produced locally beneath surficial, sulfate-reducing sediments. Thus, between the zone of sulfate depletion and the BSR, the onset of gas hydrate formation (~100 mM CH<sub>4</sub> concentrations under in situ P/T conditions) must occur. Depth-concentration profiles of microbial byproducts will indicate whether there has been adequate amount of local microbial gas production (Claypool and Kaplan, 1974) to account for the observed methane concentrations.

Conversely, if the in situ production of methane and other gases is not adequate to generate saturation at shallow depths, then there must be addition of gas from below (Hyndman and Davis, 1992). Biogenic gas may accumulate as a result of recycling of gas at the base of the gas hydrate stability zone. As continental rise sediments are progressively buried, they experience an increase in temperature associated with the geothermal gradient. At some point the sediments will leave the gas-hydrate stability field. Gas bubbles produced by gas hydrate decomposition would be expected to move upward and reenter the gas-hydrate field above. If the recapture of the gas that is mobilized into the sediments above by the gas hydrates is perfectly efficient, the gas will never get out of the system. Thus, the gas that is above the BSR may have been produced at any time in the history of

the rise. The gas hydrates which form the ~3 m thick layer in the Middle America Trench (Kvenvolden and McDonald, 1985) almost certainly formed in a flow conduit.

Another approach to discriminate between locally produced gas and migrated gas may come from the depth distribution of gas hydrates. If the gas hydrates are produced locally in favorable lithologies, there should be a gradual increase in the amount of gas-hydrate with depth. However, if the gas is advected up from below gas-hydrate amounts will increase dramatically near the base of their stability field (i.e., near the BSR).

#### *Physical Property Changes in the Sediments*

The formation of gas hydrates within sediment pores may significantly alter the mechanical properties of the sediment in a number of ways: 1) the pore volume will be decreased by authigenic mineral (hydrate and carbonate) formation and will lead to a reduction in the porosity and presumably the permeability structure of the sediments; 2) the authigenic addition of the gas hydrate will also change the mechanical properties and consolidation pathways of the sediments; and 3) the low thermal conductivity of gas hydrates will alter the thermal structure of hydrated sediments.

Very little data are available on the porosity structure of hydrated sediments. Shipboard physical property data suggest that the normal porosity reduction may have taken place by gas hydrate infilling. For example, data collected by DSDP at Site 533 indicate the porosity remains near 57% right to the base of the hole (399 m), which is surprisingly high for silty-claystones (Gregory, 1977).

Changes in the velocity structure of hydrated sediments suggest that either the volumes of gas hydrate are very high or the gas hydrates are very efficient at binding the sediments together to produce a high velocity medium. At present we do not know whether the gas hydrates preferentially grow in the voids or at grain contacts or how effective they are at binding sediment together. However, the growth of gas hydrates in the sediment pores will inevitably affect the sediment's compaction history. Thus samples that were extensively hydrated, but have passed out of the gas-hydrate stability realm, should be under-consolidated and mechanically weak, especially if the pore spaces are now gas charged. The potential change in physical properties related to dehydration needs to be assessed as a mechanism for causing slope failure (Kayen, 1988; Paull et al., 1991).

The thermal conductivity of gas hydrates is lower than that of the pore waters they replace (Stoll and Bryan, 1979; Sloan, 1989) and the thermal conductivity of free gas layers is very low. Thus areas where there is any appreciable volume of gas-hydrate (above the BSR) and gas (at or beneath the BSR), may act as a thermal insulator within continental margin sediments. Lateral variations in the thermal characteristics of sediment may occur because zones of extensively hydrated sediment will be better insulated than less hydrated areas. Heat may be refracted toward less extensively hydrated sediments. If lateral thermal gradients exist, then they may stimulate fluid circulation.

Some heat flow measurements from the Carolina Rise were made in 1991. Additional measurements will be made at the drill sites in September 1992 by von Herzen et al. The existing data show that the gradients are between 20° and 40°C/km. While adjacent measurements tend to be similar, there are larger than expected variations along transects which may be related to lateral variations in hydrate development.

#### *Hydrologic Circulation within Gas Hydrated Sediment Sections*

Sediments associated with extensive gas hydrate formation may have undergone a significant porosity reduction. As a consequence, the gas hydrate cemented sediments in the Blake Ridge - Carolina Rise gas hydrate field may act as a barrier for pore water exchange between the continental margin sediments and the adjacent ocean waters. Any fluid flow which is in response to regional gradients (Manheim and Horn, 1968; Manheim and Paull, 1981) will be concentrated into breaks in the gas hydrate seal. Moreover, local circulation systems might be stimulated as a consequence of hydration processes because 1) saline fluids in the hydrated zone will be heavy and will tend to sink, or conversely, waters associated with the natural breakdown of gas hydrates in the subsurface will be buoyant with respect to seawater and thus will rise, 2) the lower thermal conductivity of the free gas beneath the gas hydrates will refract heat away from areas that are extensively hydrated toward areas that are less hydrated (thermal differences may stimulate small circulation systems, Kohout, 1967), and 3) compactive expulsion of pore waters from sediments (Shi and Wang, 1986) may occur either above or below the gas hydrates. Compactive expulsion may be particularly active underneath the gas hydrates as the sediments undergo a porosity and pore fluid pressure increase as a consequence of dehydration and the release of gas (Kayen, 1988). Fluids may migrate laterally to escape upward at breaks in the overlying seal.

If there are circulation cells within the hydrated sediments, their internal characteristic may be indicated by patterns of velocity variations in the sediment, pore waters and heat flow gradients that overlie these cells. A close relationship between sediment physical properties and pore water advection may exist in hydrated regions of continental margins which will require closely spaced holes that are carefully sited with respect to known lateral changes in reflection characteristics.

### *Chemical Changes Associated with Gas Hydrated Sediment Sections*

#### Effects of Ion Exclusion During Gas Hydrate Formation on Continental Rise Pore Waters

The ionic concentration of pore fluids increases as gas hydrate formation proceeds because the gas hydrates remove water and gas (e.g., methane) and leave behind the residual salts. Thus, the composition of continental rise pore waters (especially Cl<sup>-</sup> concentration) may be used as a predictor of gas hydrate presence and extent (Fig. 4). Moreover, if no anomalies exist, then either there is no appreciable amount of gas hydrate formation, or fluid circulation has wiped out the anomalies.

#### Isotopic Fractionation and Signature of the Pore Water Sources

During the formation of gas hydrates, there is a tendency for the heavy molecules of water (H<sub>2</sub><sup>18</sup>O or DH<sup>16</sup>O) to become preferentially concentrated in the gas hydrate lattice, while the isotopically lighter molecules of water (H<sub>2</sub><sup>16</sup>O) are left in the residual water (Davidson et al., 1983). This phenomenon has been employed to explain deep-sea sediment cores that contain water with higher δ<sup>18</sup>O content and lower salinities than seawater as having been generated by the recent breakdown of gas hydrates (Hesse and Harrison, 1981; Harrison and Curiale, 1982), and other pore waters from deeper cores that are isotopically light and saline as resulting from the expulsion of fluids during gas hydrate formation (Kvenvolden and Kastner, 1989).

#### Solid Phase Records

At present we do not have techniques to indicate whether gas hydrates were once developed in ancient sediments. However, there is a largely unassessed potential for significant diagenetic changes (e.g., Wada et al., 1981) to occur as a consequence of gas hydrate formation and

decomposition. For example, the oxygen isotope ratios in diagenetic siderite found on the Blake Ridge are believed to be related to gas hydrate decomposition (Matsumoto, 1989). Thus, these materials may contain a record of paleo-BSR positions. To evaluate these materials, we need more sampling from sedimentary units that have experienced the diagenetic changes associated with extensive gas hydrate formation.

#### Calibrating the BSR as a Temperature-Pressure-Composition Indicator

The BSR pins the boundary at which three phases (hydrate-gases-water) co-exist. Thus, in theory, if one knows the chemical composition and the depth at the BSR one can calculate the temperature from gas hydrate phase data (Fig. 5) and use the BSR as a tracer of sediment temperatures. Unfortunately the gas hydrate phase equilibria is very sensitive to the composition of the pore fluids and gases and trace levels of various microbial or thermogenic gases (e.g., H<sub>2</sub>S, CO<sub>2</sub>, CH<sub>4</sub>, C<sub>2</sub>H<sub>6</sub>) and ions (e.g., Cl<sup>-</sup>) which shift the phase boundaries (Deaton and Frost, 1946; Kobayashi et al., 1951; de Roo et al., 1983).

Because the ionic concentration of pore fluids increases as gas hydrate formation proceeds, the hydrate-gases-water phase boundary will shift toward higher pressure and lower temperature.

In situ data on the characteristics of gas hydrates are needed. While a considerable research effort is being directed toward hydrate research using surface techniques, ultimately the only way to unequivocally establish the in situ characteristics of the gas hydrated sediments is by drilling in areas that are well surveyed and where the influence of hydrates is most dramatic (Max et al., 1991).

### **DRILLING PLAN/STRATEGY**

Two different types of drilling strategies can be envisioned to investigate the properties of extensive gas hydrates; 1) holes could be drilled through the entire hydrated section and well into the sediments below, or 2) drilling can be targeted to sample extensively hydrated sediments above the BSR, but stop before the base of the gas hydrate zone (as indicated by the BSR) is penetrated. Proposals to drill through the entire hydrate zone in areas that may be associated with extensive gas hydrates may be stymied by safety concerns. Thus, a program that pursues option 2 and poses

minimal safety concerns is outlined here. However, this program can be easily expanded to include drilling through the BSR's. The proposed drilling strategy stresses closely spaced holes, pressure core sampling, downhole fluid sampling, and borehole geophysical experiments.

Drilling is proposed along transects in three areas in the Blake Ridge - Carolina Rise gas hydrate field where the geology and topography are relatively simple, so that the basic properties of the hydrated sediments and their spatial variation can be addressed (Table 1). These areas have been selected for detailed gas hydrate studies from the extensive regional seismic survey data because they are areas where the patterns around the BSR and of the seismic blanking are especially clear. However, rapid lateral changes occur along the proposed transects from areas where the BSR's are extremely well-developed to areas where the influence from gas hydrates are minimal or undetectable in seismic data.

The three areas have been selected to contrast the influences of gas-hydrate properties under different continental rise settings. These include an area where the gas for the hydrates may have been produced in situ, an area where the gas for hydrate formation may have migrated from below, and an area where the hydrates have been disturbed and may have decomposed within the sediment column.

Special efforts will be devoted to in situ sampling using the PCS and WSTP tools during the drilling of these hole. A high priority will given to running a full suite of logs and to conducting VSP before leaving these holes. Exact site selection should include input from the safety panel.

Area I is on the crest of the Blake Ridge (Fig. 1), a major sediment drift (Tucholke et al., 1977). This area has been selected because 1) it is a topographically simple area, 2) it is expected to have very extensive gas hydrates because it is associated with the highest interval velocities that have been reported for a gas hydrate-cemented area, 3) the crest of the ridge provides structural closure on the BSR surface which should make an effective seal that prevents gas escape so that extensive free gas could be trapped beneath the BSR, 4) it lies on old oceanic crust (Klitgord and Behrendt, 1979) so that heat flow should be uniform, and 5) the sources of gas are more limited than in Areas II and III because the sedimentary section is thin and there is no obvious source of migrated gas. Moreover piston core data indicate that sulfate depletion and the advent of microbial methane production occurs at shallow depths (~10 m) on the Blake Ridge, which suggests that gas-hydrates may have been produced by in situ methane production at this site.

The strategy in Area I is to drill holes at three closely spaced sites down the northern flank of the Blake Ridge (proposed sites BRH-1a, BRH-2a, and BRH-3a) in an area where the sedimentary units dip upward toward the sea floor. Here the same sedimentary units can be sampled and compared over short lateral distances, but where they apparently contain varying amounts of hydrate. Also this transect will enable the assessment of the lateral hydrate variations due to local lithologic, chemical, and hydrologic factors.

Area II is on the upper Carolina Rise (Fig. 1). This area has been selected because 1) it is on a normal section of the rise rather than a sediment drift, 2) it corresponds with an extremely well-developed BSR that is crossed by stratal reflectors making the lithologic control identifiable, 3) it is about the topographically smoothest area on the rise and is not associated with diapirs or slump scarps, and 4) at these sites, the potential for migration of gas through various layers will be examined. This area overlies the thickest section of the Carolina Trough which is composed of rift-stage crust overlain with ~8 km of continental shelf strata before being capped by the modern rise sediments (Hutchinson et al., 1982). As a consequence, Area II will have different sources of fluids than Area I. Existing piston core data indicate that the pore fluid sulfate concentration gradients are much more gentle in Area II than in Area I, which suggests, that the potential for microbial methane production is much less at this site. In Area II, the sedimentary layers slope upward toward the sea floor through the hydrate stability field. Beneath the BSR an appreciable thickness of very reflective layers are observed on seismic reflection profiles. These reflective layers apparently are sediment beds of variable porosity and grain size. Where these beds cross the BSR they lose their reflectivity in the blank zone, but they again become clearly traceable in the section a few hundred meters above the blank zone. Here the same layers can be penetrated and cored over a short lateral distance. Thus the physical properties of individual sediment layers can be compared between closely spaced sites where geophysical data indicate a lateral transition from non-hydrated to hydrated sediment.

Area III is on the upper rise around 33°00'N, 75°55'W in ~2500 m of water (Fig. 1). Area III is in the same geologic setting as Area II, but is associated with the sole of a major slump scar and the crest of an exhumed diapir. Piston core and dredge samples from the top of the diapir contain hemipelagic materials of diverse Tertiary ages. The continuity of the BSR is lost near the diapir. Thus, the diapir apparently produced a "hole" in the regional gas hydrate field. In contrast to Areas I and II, this "hole" in the gas hydrate field has a tectonic origin that is associated with slumping

and/or the emplacement of a diapir. Area II will serve as a “background” control of what Area III samples were like before the tectonic disturbance to the hydrate system.

## PROPOSED SITES

### Area I

Proposed site BRH-1a is located on the crest of the Blake Ridge (CH-06-92, line 31 - 31°50.59'N, 75°28.12'W) in 2722 m of water. Here, a well developed BSR is at 0.54 sec subbottom. DSDP Site 102 was drilled to a total depth of 661 m nearby, where the BSR occurs at 0.62 sec.

Experience from DSDP Site 102 indicates that bore holes can approach, and perhaps penetrate, the BSR in this area without problems. At 1850 m/sec (a low velocity which minimizes the chances of encountering the level of the BSR unintentionally) the BSR originates from at least 499 m sub-bottom. We are proposing that one hole be drilled at proposed site BRH-1 into the thick section of acoustically “transparent” sediments to 480 m. If gas has slowly infused into the overlying sediments from below the BSR, hydrate development may be at an extreme in this hole. At the highest velocities that have been suggested (2500 m/sec), the BSR would be penetrated by 675 m. Thus, it is proposed that this hole be extended to 750 m (BRH-1a ext.) .

Proposed site BRH-2a is located on the upper flank of the Blake Ridge (on CH-06-92, line 31 - 31°49.85'N, 75°25.11'W) in 2825 m of water. The BSR is not evident at this site although strong BSR's exist at the up- and down-slope proposed sites, BRH-1a and BRH-3a. Thus, a “hole” in the BSR's surface exists at this site. However, a series of strong reflections that are apparently related to stratigraphic horizons beneath the predicted level of the BSR (~0.55 sec sub-bottom as projected up and down slope) occur here. The hole drilled at proposed site BRH-2a should penetrate well below the level of hydrate stability, into these reflective sediments. With a range of sediment velocities between 1850 and 2500 m/sec, the inferred base of the hydrate stability zone would lie between 509 and 688 m, respectively. To be sure that this level is penetrated, the proposed depth of the hole is 800 m.

Proposed site BRH-3a is located on the upper flank of the Blake Ridge (on CH-06-92 line 31 - 31°54.40'N, 75°23.02'W) in 2965 m water. Here, a BSR is at 0.57 sec subsurface. Assuming a velocity of 1850 m/sec, the BSR is at 527 m sub-bottom depth. We are proposing to drill through the upper 500 m at this site into a thick section of acoustically “transparent” sediments. This bore

hole is intended to obtain a direct comparison of the same stratigraphic horizons above the BSR that were sampled below the projected level of the BSR at proposed site BRH-2a. The horizons which extend to the shallower depths from proposed sites BRH-2a to BRH-3a are acoustically transparent at the latter, but reflective at the former. From the discontinuous nature of the BSR, this site is inferred to have the least amount of free gas near the BSR. Now assuming a high velocity of 2500 m/sec, the BSR is at 684 m sub-bottom. This hole would need to be extended from 500 m (as proposed for the hole at proposed site BRH-3a) to 750 m (BRH-3a.ext).

If these extended holes are approved for drilling, it is suggested that the drilling order be changed so that the BSRs of increasing strength are drilled sequentially. Thus, the reference holes at proposed sites BRH-2a and CRH-1 should be drilled first followed by extended holes at proposed sites BRH-3a (BRH-3a ext.), CRH-2 (CRH-2 ext) and finally BRH-1a (BRH-1a ext).

## **Area II**

In Area II, holes are proposed at two sites (proposed sites CRH-1 and CRH-2). Proposed site CRH-1 is at SP 100653 on CH-06-92 line 41 (32°46.88'N, 75°57.4'W) in 2647 m water. No BSR exists here. However, there are a series of reflective horizons at 0.6 to 0.8 sec that are below the inferred level of hydrate stability. This hole at this site is planned to penetrate 800 m into these sediments.

Proposed site CRH-2 is at SP 100539 on CH-06-92 line 41 (32°46.76'N, 75°55.20'W) in 2732 m water. The BSR is at 0.55 sec. The proposed depth of the hole at this site is 540 m. This hole is intended to obtain a direct comparison of the same stratigraphic horizons above and below the projected level of the BSR. The units in proposed site CRH-1 project to the shallower depths and can be sampled in proposed site CRH-2 above the level of the BSR. However, these units are acoustically transparent at the latter, but reflective at the former. The strategy at proposed sites CRH-1 and CRH-2 is similar to that at proposed sites BRH-2 and BRH-3, but the inferred source of the gas in area I and II may be substantially different. The hole at proposed site CRH-2 may be deepened from 540 m to 750 m (CRH-2 ext). Thus, even at the higher range of proposed sediment velocities, the hole would penetrate well into the section beneath the BSR.

### **Area III**

A transect of shallow drill holes (50 m deep) through the sole of a major slump on the flank of the Cape Fear Diapir are proposed (proposed sites CFD-1, CFD-2, CFD-3, and CFD-4) in Area III. One of the objectives of drilling this transect is to establish the tectonic, thermal, and hydrologic influence of the diapir on gas hydrates. In addition, samples will be obtained from a structural transect from sediments that are beneath the sole of a major slump, crossing upturned strata and to the crest of the diapir. These sample should have been exposed to differing degrees of hydrate formation and decomposition. The zone of deformed sediments that rims this diapir may provide a conduit for fluid flow from deeper zones including the fluids from beneath the zone of hydrate stability. Shallow samples from the crest of this diapir will provide information on the conditions deeper in the rise. We will also examine the nature of fluid and gas transport through the sole of this major sediment scar. These strata were buried to more than 140 m depths before being exhumed by slumping and the process of re-equilibration to new shallower conditions may provide great insight into the sensitivity of hydrated sediment to changes in the physical conditions and to the dynamics of gas-hydrate venting. Although this and other Atlantic diapirs are believed to be salt structures, the existence of salt has not been documented and the previous sampling on top of these structures has not produced data to confirm this assumption. Drilling in Area III should establish the nature of these diapirs.

Proposed site CFD-1 is at SP 1873 on CH-15-91 line 10 (33°00.95'N, 75°56.75'W) in 2690 m of water and the hole at this site will penetrate into Plio-Pleistocene sediments that are not directly affected by diapirism. Proposed site CFD-2 is at SP 1808 on CH-15-91 line 10 (33°00.3'N, 75°55.8'W) in 2700 m of water at the edge of the diapir. Proposed site CFD-3 is at SP 1765 on CH-15-91 line 10 (32°59.9'N, 75°55.18'W) in 2650 m of water on the middle of the diapir's flank. Proposed site CFD-4 is at SP 1708 on CH-15-91 line 10 (32°59.3'N, 75°54.25'W) in 2590 m of water, near the crest of the diapir where a melange of materials are expected.

This transect covers a horizontal distance of only 3600 m and may not require that the drill string be pulled between holes. Although these holes are being proposed to only 50 m sub-bottom because of safety concerns, these sections will be adequate to develop meaningful two dimensional picture of the compositional and chemical gradients associated with gas hydrate cemented sediments that have been deformed by slumping and diapir emplacement. Experience with surface ship piston coring has shown that the diapiric material is too firm for wire-line coring techniques. A Deep-

Tow survey of the crest of this diapir will be conducted in October 1993 which may result in modification of the individual hole locations.

## **ADDITIONAL CONSIDERATIONS**

### **Drilling Safety**

The potential existence of free gas beneath the BSR represents a significant drilling safety concern. Whether these concerns are realistic or not can only be assessed on a site-specific basis. However, uncertainty about hydrate properties will remain if drilling is limited to marginal sites and areas where the geophysical anomalies do not suggest the presence of gas. Thus, to understand the full significance of hydrated sediments, we need to cautiously approach sites of major hydrate formation.

Site-specific information suggests that appreciable amounts of free gas do not exist beneath the BSR in the areas that were approved for drilling. Over-pressured gas pockets, which cause blow-outs, are unlikely near the BSR, because an increase in the gas pressure would extend the range of the hydrate stability, causing the boundary between gas and hydrate to migrate downward until a new equilibrium is re-established.

## REFERENCES

- Abbott, D.H., Hobart, M.A., and Embley, R.M., 1986.** Heat flow and mass wasting in the Wilmington canyon region: U.S. continental margin. *Geo-Mar. Lett.*, 6:131-138.
- Andreassen, K., Hogstad, K., and Berteussen, K.A., 1990.** Gas hydrates in the Barent Sea, indicated by a shallow seismic anomaly. *First Break*, 8:235-245.
- Bernard, B.B., Brooks, J.M., and Sackett, W.M., 1977.** A geochemical model for characterization of hydrocarbon gas sources in marine sediments. *Proceeding of the Ninth Annual Offshore Technology Conference*, OTC 2934, Houston, Texas:435-438.
- Brooks, J.M., Bernard, L.A., Weisenburg, D.A., Kennicutt, M.C., and Kvenvolden, K.A., 1983.** Molecular and isotopic compositions of hydrocarbons at Site 533, Deep Sea Drilling Project Leg 76. In Sheridan R.E., Gradstein, F.M., et al., *Init. Repts. DSDP*, 76:Washington (U.S. Government Printing Office), 377-390.
- Brooks, J. M., and Bryant, W.R., 1985.** *Geological and Geochemical Implications of Gas Hydrates in the Gulf of Mexico*. U.S. Department of Energy, DOE, MC, 21088-1964.
- Brooks, J.M., Field, M.E., and Kennicutt, M.C., 1991.** Observations of gas hydrates offshore Northern California. *Mar. Geol.*, 96:103-109.
- Brooks, J.M., Kennicutt, M.C., Bidigare, R.R., and Fay, R.A., 1985.** Hydrates, oil seepage, and chemosynthetic ecosystems on the Gulf of Mexico slope. *Eos*, 66(10):106.
- Brooks, J.M., Kennicutt, M.C., Fay, R.A. McDonald, T.C., and Sassen, R., 1984.** Thermogenic gas hydrates in the Gulf of Mexico. *Science*, 225:409-411.
- Carpenter, G., 1981.** Coincident sediment slump/clathrate complexes on the U.S. Atlantic continental slope. *Geo-Mar. Lett.*, 1:29-32.
- Cashman, K.V., and Popenoe, P., 1985.** Slumping and shallow faulting related to the presence of salt on the Continental Slope and Rise off North Carolina. *Mar. Pet. Geol.*, 2: 260-272.
- Claypool, G.E., and Kaplan, I.R., 1974.** Methane in marine sediments. In Kaplan, I.R. (Ed.), *Natural Gases in Marine Sediments*: New York (Plenum Press), 99-139.
- Claypool, G.E., and Threlkeld, C.N., 1983.** Anoxic diagenesis and methane generation in sediments of the Blake Outer Ridge, Deep Sea Drilling Project Site 533, Leg 76. In Sheridan R.E., Gradstein, F.M., et al., *Init. Repts DSDP*, 76: Washington (U.S. Government Printing Office), 591-594.
- Collett, T.S., and Kvenvolden, K.A., 1987.** Evidence for naturally occurring gas hydrates on the North Slope of Alaska. *U.S. Geol. Surv.*, Open File Report, 87-225:8.
- Davidson, D.W., Leaist, D.G., and Hesse, R., 1983.** Oxygen-18 enrichment in the water of a hydrate. *Geochim. Cosmochim. Acta*, 47:2293-2295.
- Deaton, W.M., and Frost, E.M., 1946.** Gas hydrates and their relation to the operation of natural gas pipe lines. *U.S. Bur. Mines Monograph*, 8.
- de Roo, J.L., Peters, C.J., Lichtenthaler, R.N., and Diepen, G.A.M., 1983.** Occurrence of methane in hydrated sediments and undersaturated solutions of sodium chloride and water in dependence of temperature and pressure. *American Institute of Chemical Engineers Journal*, 29:651-657.
- Dillon, W.P., Fehlhaber, K.L., Lee, M.W., Booth, J.M., and Paull, C.K., 1991.** Methane hydrate in sea floor sediments off of the Southeastern U.S.; amounts and implication for climate change. *Geol. Soc. Am. Abstr. Progr.*, 23:23.
- Dillon, W.P., Grow, J.A., and Paull, C.K., 1980.** Unconventional gas hydrate seals may trap gas off the Southeastern U.S. *Oil & Gas J.*, January 7:124-130.
- Dillon, W.P., and Paull, C.K., 1983.** Marine gas hydrates: II Geophysical Evidence. In Cox, J.L. (Ed.), *Natural Gas Hydrates, Properties, Occurrence and Recovery*: Woburn, Mass. (Butterworth), 73-90.
- Dillon, W.P., Popenoe, P., Grow, J.A., Klitgord, K.D., Swift, B.A., Paull, C.K., and Cashman, K.V., 1982.** Growth faulting and salt diapirism: Their relationship and control in the Carolina Trough, Eastern North America. In Watkins, J. S., and Drake, C. L. (Eds.), *Studies of Continental Margin Geology*, AAPG Mem., 34:21-46.

- Embly, R.W., 1980.** The role of mass transport in the distribution and character of deep-ocean sediments with special reference to the North Atlantic. *Mar. Geol.*, 38:28-50.
- Galimov, E.M., and Kvenvolden, K.A., 1983.** Concentrations of carbon isotopic compositions of CH<sub>4</sub> and CO<sub>2</sub> in gas from sediments of the Blake Outer Ridge, Deep Sea Drilling Project Site 533, Leg 76. In Sheridan R.E., Gradstein, F.M., et al., *Init. Repts. DSDP*, 76:Washington (U. S. Government Printing Office), 403-410.
- Gregory, A.R., 1977.** Aspects of rock physics from laboratory and log data that are important to seismic interpretation. In Payton, C.E. (Ed.), *Seismic Stratigraphy - Applications to Hydrocarbon Exploration*, AAPG Mem., 26:15-46.
- Hand, J.H., Katz, D.L., and Verma, V.K., 1974.** Review of gas hydrates with implication for oceanic sediments. In Kaplan, I.R. (Ed.), *Natural gases in marine sediments*: New York (Plenum Press), 179-194.
- Hardage, B.A., 1985.** Vertical Seismic Profiling- A measurement that transfers Geology to Geophysics. In Berg, O.R., and Woolverton, D.G. (Eds.), *Seismic Stratigraphy II, An Integrated Approach*, AAPG Mem., 26:13-36.
- Harrison, W.E., and Curiale, J.A., 1982.** Gas hydrates in sediments of Holes 497 and 498A, Deep Sea Drilling Leg 67. In Aubouin, J., and von Huene, R., et al., *Init. Repts. DSDP*, 67:Washington (U. S. Government Printing Office), 591-595.
- Heling, D., 1970.** Microfabrics of shales and their rearrangement by compaction. *Sedimentology*, 15:247-260.
- Helmberger, D.V., 1968.** The crust-mantle transition in the Bering sea. *Bull. Seis. Soc. Am.*, 58: 179-214.
- Hesse, R., and Harrison, W.E., 1981.** Gas hydrates(Clathrates) causing pore-water freshening and oxygen isotope fractionation in deep-water sedimentary sections of terrigenous continental margins. *Earth Planet. Sci. Lett.*, 55:453-462.
- Hollister, C.D., et al., 1972.** Sites, 102, 103, 104, Blake-Bahama Outer Ridge (Northern End). In Hollister, C.D., Ewing, J.I., et al., *Init. Repts.DSDP*, 11:Washington (U.S. Government Printing Office), 135-218.
- Hovland, M., and Judd, A.G., 1988.** *Seabed Pockmarks and Seepages: Impact on Geology, Biology and the Marine Environment*: London (Graham and Trotman).
- Hutchinson, D.R., Grow, J.A., Kiltgord, K.D., and Swift, B.A., 1982.** Deep structure and evolution of the Carolina Trough. In Watkins, J.S., and Drake, C.L. (Eds.), *Studies of Continental Margin Geology*, AAPG Mem., 34:129-152.
- Hyndman, R.D., and Davis, E.E., 1992.** A mechanism for formation of methane and seafloor bottom-simulating reflectors by vertical fluid expulsion. *J. Geophys. Res.*, 97, B5:7025-7041.
- Hyndman, R.D., and Spence, G.D., 1992.** A seismic study of methane hydrate marine bottom simulating reflectors. *J. Geophys. Res.*, 97, B5:6683-6698.
- Jenden, P.D., and Gieskes, J.M., 1983.** Chemical and isotopic composition of interstitial water from Deep Sea Drilling Project Sites 533 and 534. In Sheridan R.E., Gradstein, F.M., et al., *Init. Repts. DSDP*, 76:Washington (U. S. Government Printing Office), 453-461.
- Katzman, R., Holbrook, W.S., Purdy, G.M., and Paull, C.K., 1992.** A combined vertical-incidence and wide-angle seismic study of a gas hydrate zone Blake Outer Ridge. *Eos*, 73:356.
- Kayen, R.E., 1988.** The mobilization of Arctic Ocean landslides by sea level fall induced gas hydrate decomposition [MS thesis]. Stanford University.
- Klitgord, K.D., and Behrendt, J.C., 1979.** Basin structure in the U. S. Atlantic margin. In Watkins, J.S., Montadert, L., and Dickerson, P. W., *Geological and Geophysical Investigations of Continental Margins*, AAPG Mem., 29:85-112.
- Kobayashi, R., et al., 1951.** Gas Hydrate formation with brine and ethanol solutions. *Proc. 30<sup>th</sup> Annual Conference Natural Gasoline Association of America*, 27-31.
- Kohout, F.A., 1967.** Ground-water flow and the geothermal regime of the Floridian Plateau. *Transactions of the Gulf Coast Association of Geological Societies*, 17:339-343.
- Kvenvolden, K., 1988a.** Methane hydrates and Global Climate. *Global Biochemical Cycles*, 2:221-229.

- Kvenvolden, K., 1988b.** Methane hydrate - A major reservoir of carbon in the shallow geosphere? *Chem. Geol.*, 71: 41-51.
- Kvenvolden, K., and Barnard, L.A., 1983.** Hydrates of natural gas in continental margins. In Watkins, J.S., and Drake, C.L. (Eds.), *Studies in Continental Margin Geology*, AAPG Mem., 34:631-640.
- Kvenvolden, K., Barnard, L.A., and Cameron, D.H., 1983.** Pressure core barrel: Application to the study of gas hydrates, Deep-Sea Drilling Project Site 533, Leg 76. In Sheridan R.E., Gradstein, F.M., et al., *Init. Repts. DSDP*, 76: Washington (U.S. Government Printing Office), 367-375.
- Kvenvolden, K.A., and Grantz, A., 1991.** Gas hydrates of the Arctic Ocean region. In Grantz, A., Johnson, L., and Sweeney (Eds.), *The Arctic Ocean Region, The Geology of North America*, v. L., Geological Society of America, Washington, D.C., 539-549.
- Kvenvolden K.A., and Kastner, M., 1989.** Gas hydrates of the Peruvian outer continental margin. In Suess, E., and von Huene, R., et al., *Proc. ODP, Sci. Results*, 112:College Station, TX (Ocean Drilling Program), 517-526.
- Kvenvolden, K.A., and McDonald, T.J., 1985.** Gas hydrates in the Middle America Trench. In von Huene, R., Aubouin, J., et al., *Init. Repts. DSDP*, 84:Washington (U.S. Government Printing Office), 667-682.
- MacDonald, G.J., 1990.** Role of methane clathrates in past and future climates. *Clim. Change*, 16:247-281.
- Makogon, Y.F., 1981.** *Hydrates of Natural Gas*: Tulsa, Oklahoma (Penn Well Books).
- Manheim, F.T., and Horn, M.K., 1968.** Composition of deeper subsurface waters along the Atlantic continental margin. *Southeastern Geology*, 9:215-236.
- Manheim, F.T., and Paull, C.K., 1981.** Patterns of groundwater salinity changes in a deep continental - oceanic transect off the southeastern Atlantic coast of the U. S. A. *J. Hydrology*, 54:95-105.
- Markl, R.G., and Bryan, G.M., 1983.** Stratigraphic evolution of the Blake Outer Ridge. *AAPG Bull.*, 67: 663-683.
- Markl, R.G., Bryan, G.M., and Ewing, J.I., 1970.** Structure of the Blake-Bahama Outer Ridge. *J. Geophys. Res.*, 75:4539-4555.
- Martens, C.S., and Berner, R.A., 1974.** Methane production in the interstitial waters of sulfate-depleted sediments. *Science*, 185:1167-1169.
- Matsumoto, R., 1989.** Isotopically heavy oxygen-containing siderite derived from the decomposition of methane hydrate. *Geology*, 17:707-710.
- Max, M.D., Dillon, W.P., Malone, R.D., and Kvenvolden, K.A., 1991.** National workshop on gas hydrates. *Eos*, 72 (44):476-479.
- Miller, J.J., Lee, M.W., and von Heune, R., 1991.** A quantitative analysis of gas hydrate phase boundary reflection (BSR), offshore Peru. *AAPG Bull.*, 75:910-924.
- National Research Council, 1989.** *The Margin Initiative: Interdisciplinary Studies of Processes Attending Lithospheric Extension and Convergence*, Proceedings of a Workshop Sponsored by the National Research Council, Irvine, California, November 20-23, 1988.
- Nisbet, E.G., 1990.** The end of the ice age. *Can. J. Earth Sci.*, 27:148-1157.
- Pandit, B.I., and King, M.S., 1982.** Elastic wave velocities of propane gas hydrates. In French, H.M. (Ed.), *Proceedings of the Canadian Permafrost Conference: the Roger J.E. Brown Memorial Volume*: Ottawa, Canada (Canadian National Research Council), 335-352.
- Paull, C.K., and Dillon, W.P., 1981.** Appearance and distribution of the gas hydrate reflector in the Blake Ridge Region, Offshore southeastern United States. *USGS Miscellaneous Field Studies Map*, 1252.
- Paull, C.K., Schmuck, E.A., Chanton, J., Manheim, F.T., and Bralower, T.J., 1989.** Carolina Trough Diapirs: Salt or Shale? *Eos*, 70:370 (Abstract).
- Paull, C.K., Ussler, W., and Dillon, W.P., 1991.** Is the extent of glaciation limited by marine gas-hydrates? *Geophys. Res. Lett.*, 18:432-434.
- Prior, D.B., Doyle, E.H., and Kaluza, M.J., 1989.** Evidence for sediment eruption on deep sea floor, Gulf of Mexico. *Science*, 243:517-519.
- Sayles, F.L., Manheim, F.T., and Waterman, L.S., 1972.** Interstitial water studies on small core samples, Leg 11. In Hollister, C.D., Ewing, J.I., et al., *Init. Repts. DSDP*, 11:Washington (U.S. Government Printing Office), 997-1008.

- Shi, Y., and Wang, C., 1986. Pore pressure generation in sedimentary basins: Overloading versus aquathermal. *J. Geophys. Res.*, 91, B2:2153-2162.
- Shipboard Scientific Party, 1990. Site 794. In Ingel, J.C., Jr., Suyehiro, K., von Breymann, M.T., et al., *Proc. ODP, Init. Repts.*, 128:College Station, TX (Ocean Drilling Program), 67-120.
- Shipley, T.H., Houston, M.H., Buffler, R.T., et al., 1979. Seismic reflection evidence for widespread occurrence of possible gas-hydrate horizons on continental slopes and rises. *AAPG Bull.*, 63:2204-2213.
- Sloan, E.D., 1989. *Clathrate Hydrates of Natural Gases*: New York (Marcel Decker, Inc.).
- Sloan, E.D., and Parrish, W.R., 1983. Gas hydrate phase equilibrium. In Cox, J.L. (Ed.), *Natural Gas Hydrates, Properties, Occurrence and Recovery*, Butterworth, Woburn, Mass., 17-34.
- Stoll, R.D., and Bryan, G.M., 1979. Physical properties of sediments containing gas hydrates. *J. Geophys. Res.*, 84:1629-1634.
- Stoll, R.D., Ewing, J., and Bryan, G.M., 1971. Anomalous wave velocities in sediments containing gas hydrates. *J. Geophys. Res.*, 76:2090-2094.
- Summerhayes, C.P., Bornhold, B.D., and Embley, R.W., 1979. Surficial slides and slumps on the continental slope and rise of South West Africa: A reconnaissance study. *Mar. Geol.*, 31:265-277.
- Toksoz, N., Cheng, C.H., and Timur, A., 1976. Velocities of seismic waves in porous rocks. *Geophysics*, 41:621-645.
- Tucholke, B.E., Bryan, G.M., and Ewing, J. I., 1977. Gas hydrate horizon detected in seismic reflection-profiler data from the western North Atlantic. *AAPG Bull.*, 61:698-707.
- Wada, H, Niitsuma, N., Nagasawa, K., and Okada, H., 1981. Deep sea carbonate nodules from the America Trench Area off Mexico, Deep Sea Drilling project Leg 66. In Watkins, J.S., Moore, J.C., et al., *Init. Repts. DSDP*, 66:Washington (U.S. Government Printing Office),453-464.
- White, R.S., 1979. Gas hydrate layers trapping free gas in the Gulf of Oman. *Earth Planet. Sci. Lett.*, 42:114-120.
- Whiticar, M.J., and Faber, E., 1986. Methane oxidation in sediment and water column environments - Isotopic evidence. *Org. Geochem.*, 10:759-768.
- Yefremova, A.G., and Zhizhchenko, B.P. 1975. Occurrence of crystal hydrates of gases in sediments of modern marine basins. *Dokl. Acad. Sci. USSR, Earth Sci. Section* (English Translation), 214:219-220.

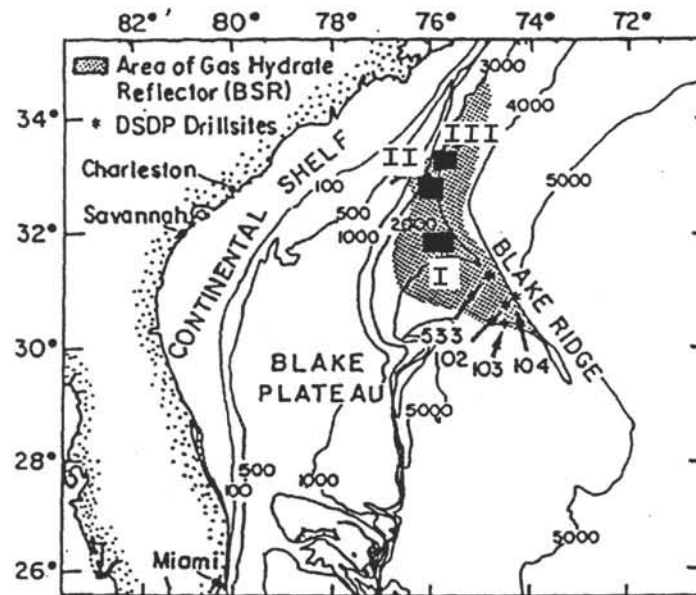


**Figure 1.** Distribution of bottom-simulating reflectors (BSRs) off the southeastern United States. Bathymetric contours are in meters. The areas proposed for drilling are indicated by boxes. From Dillon and Paull, 1983

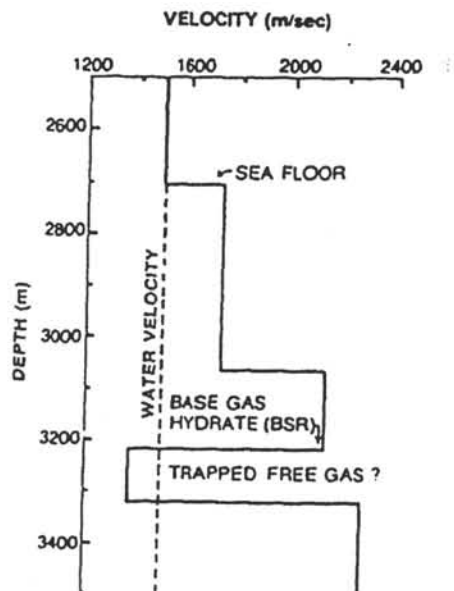


**Figure 2.** Velocity analysis of CDP data across the BSR. High velocities are indicated above the BSR and average velocities less than seawater occur in the interval beneath the BSR. Resolution of the velocities is at best limited to zones that are about 100 m thick (from Dillon and Paull, 1983).

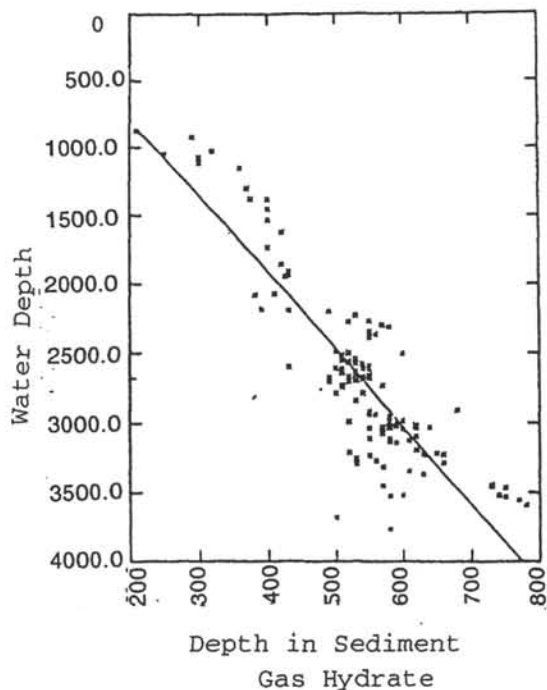


**Figure 3.** The sub-bottom depth to the base of the gas hydrate layer (BSR) compared with the water depth in meters for the Carolina Rise gas hydrate field (Fig. 1). The velocity of the sediments above the BSR is assumed to be 2000 m/s. The scatter from the best fit line indicates variations in the extent of hydration, variations in the sediment lithologies, fluid circulation patterns, differing pore water gas and fluid compositions, or variations in subsurface temperature.

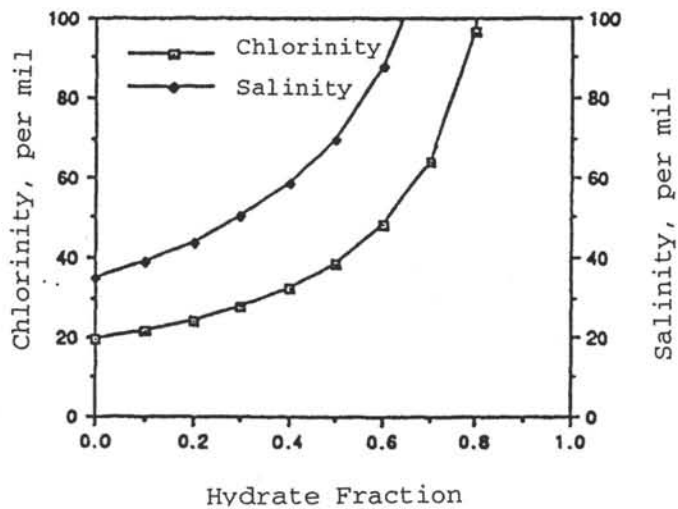


**Figure 4.** Theoretical relationship between pore water salinity and chlorinity with the amount of gas hydrate formation, assuming the sediment pore spaces are a closed system. Note that the seismic velocity estimates (Dillon et al., 1991; Miller et al., 1991) suggest that more than 50% (0.5 hydrate fraction) of the pore spaces are commonly filled with hydrate. Thus elevated sediment salinities should occur in extensively hydrated sediments.

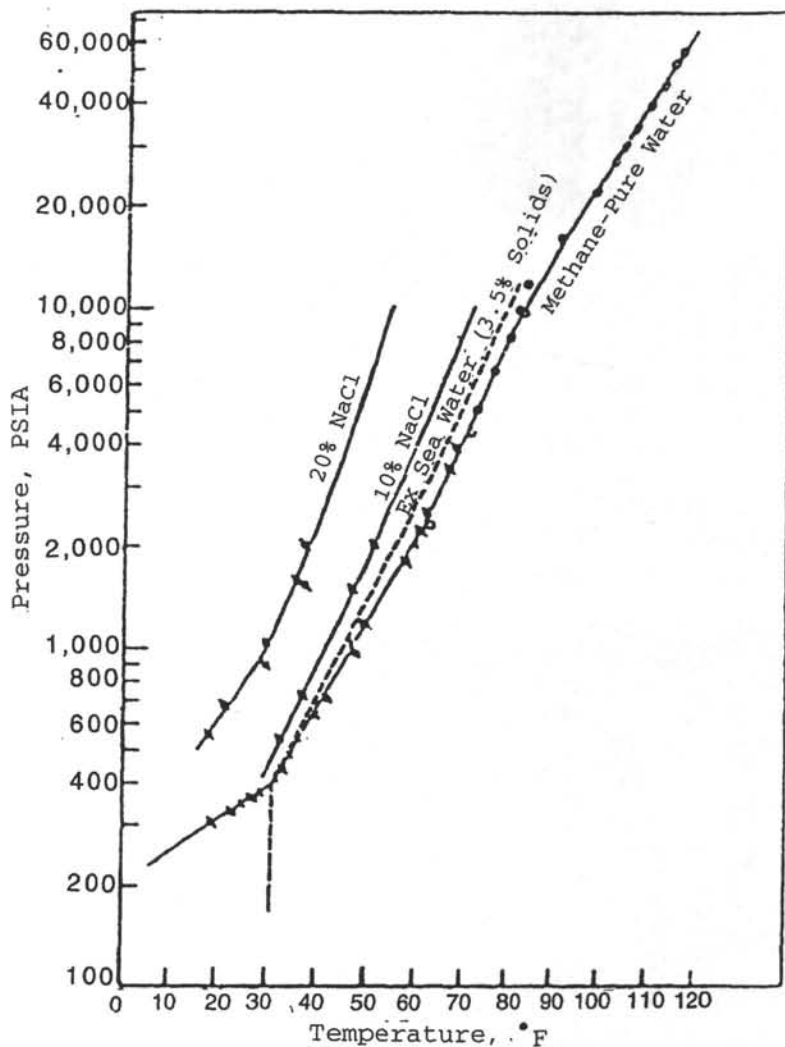


**Figure 5.** The stability field of hydrate-gases-water system is shown as a function of temperature and pressure. The effect of NaCl on the methane gas hydrate phase boundary is also given in this plot (data from Kobayashi et al., 1951; figure from Hand et al., 1974). The salinity of the pore waters exerts a significant effect on the location of the BSR.

**TABLE 1**  
**PROPOSED SITE INFORMATION**  
**and**  
**DRILLING STRATEGY**

<b>SITE:</b> BRH-1a	<b>PRIORITY:</b>	<b>POSITION:</b> 31°50.59'N, 75°28.12'W
<b>WATER DEPTH:</b> 2722m	<b>SEDIMENT THICKNESS:</b> ~2km	<b>TOTAL PENETRATION:</b> 480m
<b>SEISMIC COVERAGE:</b> CH-06-92 line 31		

**Objectives:** To sample a thick section of acoustically "transparent" sediments on the crest of Blake Ridge where gas hydrates may be extensive.

**Drilling Program:** XCB, PCS and RCB coring.

**Logging and Downhole Operations:** Logging and VSP.

**Nature of Rock Anticipated:** Hemipelagic silt and clay.

<b>SITE:</b> BRH-1a ext.	<b>PRIORITY:</b>	<b>POSITION:</b> 31°50.59'N, 75°28.12'W
<b>WATER DEPTH:</b> 2722m	<b>SEDIMENT THICKNESS:</b> ~2km	<b>TOTAL PENETRATION:</b> 750m
<b>SEISMIC COVERAGE:</b> CH-06-92 line 31		

**Objectives:** To sample the sediments and gases that are associated with a string BSR.

**Drilling Program:** XCB, PCS and RCB coring.

**Logging and Downhole Operations:** Logging and VSP.

**Nature of Rock Anticipated:** Hemipelagic silt and clay.

<b>SITE:</b> BRH-2a	<b>PRIORITY:</b>	<b>POSITION:</b> 31°52.84'N, 75°25.11'W
<b>WATER DEPTH:</b> 2828m	<b>SEDIMENT THICKNESS:</b> ~2km	<b>TOTAL PENETRATION:</b> 800m
<b>SEISMIC COVERAGE:</b> CH-06-92 line 31		

**Objectives:** To drill through the base of the hydrate stability field and into the sediments below which are in an area associated with a "hole" in the BSR.

**Drilling Program:** APC, XCB, and RCB coring

**Logging and Downhole Operations:** Logging and VSP.

**Nature of Rock Anticipated:** Hemipelagic silt and clay.

<b>SITE:</b> BRH-3a	<b>PRIORITY:</b>	<b>POSITION:</b> 31°54.40'N, 75°23.02'W
<b>WATER DEPTH:</b> 2965m	<b>SEDIMENT THICKNESS:</b> 2km	<b>TOTAL PENETRATION:</b> 500m
<b>SEISMIC COVERAGE:</b> CH-06-92 line 31		

**Objectives:** To sample the same stratigraphic units as proposed sites BRH-2a, but where they are believed to contain gas hydrates because they are acoustically "transparent".

**Drilling Program:** APC, XCB, PCS, and RCB coring.

**Logging and Downhole Operations:** Logging and VSP.

**Nature of Rock Anticipated:** Hemipelagic silt and clay.

<b>SITE:</b> BRH-3a ext.	<b>PRIORITY:</b>	<b>POSITION:</b> 31°54.40'N, 75°23.02'W
<b>WATER DEPTH:</b> 2965m	<b>SEDIMENT THICKNESS:</b> 2km	<b>TOTAL PENETRATION:</b> 750m
<b>SEISMIC COVERAGE:</b> CH-06-92 line 31		

**Objectives:** To sample the sediments and gases that surround a weak BSR.

**Drilling Program:** APC, XCB, PCS, and RCB coring.

**Logging and Downhole Operations:** Logging and VSP.

**Nature of Rock Anticipated:** Hemipelagic silt and clay.

<b>SITE:</b> CRH-1	<b>PRIORITY:</b>	<b>POSITION:</b> 32°46.88'N, 75°57.4'W
<b>WATER DEPTH:</b> 2647m	<b>SEDIMENT THICKNESS:</b> ~8km	<b>TOTAL PENETRATION:</b> 800m
<b>SEISMIC COVERAGE:</b> CH-06-92 line 41		

**Objectives:** To drill into sediments beneath the projected level of gas hydrate stability in an area that is not associated with a BSR.

**Drilling Program:** APC, XCB, PCS, and RCB coring.

**Logging and Downhole Operations:** Logging and VSP.

**Nature of Rock Anticipated:** Hemipelagic silt and clay.

<b>SITE:</b> CRH-2	<b>PRIORITY:</b>	<b>POSITION:</b> 32°46.74'N, 75°55.20'W
<b>WATER DEPTH:</b> 2732m	<b>SEDIMENT THICKNESS:</b> ~8km	<b>TOTAL PENETRATION:</b> 540m
<b>SEISMIC COVERAGE:</b> CH-06-92 line 41		

**Objectives:** To sample the same stratigraphic units as at proposed site CRH-1 but where they are believed to contain less gas hydrates because they are acoustically "transparent".

**Drilling Program:** APC, XCB, PCS, and RCB coring.

**Logging and Downhole Operations:** Logging and VSP.

**Nature of Rock Anticipated:** Hemipelagic silt and clay.

...Leg 164 - Gas Hydrate Sampling...

<b>SITE:</b> CRH-2 ext.	<b>PRIORITY:</b>	<b>POSITION:</b> 32°46.74'N, 75°55.20'W
<b>WATER DEPTH:</b> 2732m	<b>SEDIMENT THICKNESS:</b> ~8km	<b>TOTAL PENETRATION:</b> 750m
<b>SEISMIC COVERAGE:</b> CH-06-92 line 41		

**Objectives:** To sample the sediments and gases that are associated with a moderately strong BSR.

**Drilling Program:** APC, XCB, PCS, and RCB coring.

**Logging and Downhole Operations:** Logging and VSP.

**Nature of Rock Anticipated:** Hemipelagic silt and clay.

<b>SITE:</b> CFD-1	<b>PRIORITY:</b>	<b>POSITION:</b> 33°00.95'N, 75°56.75'W
<b>WATER DEPTH:</b> 2690m	<b>SEDIMENT THICKNESS:</b> ~8km	<b>TOTAL PENETRATION:</b> 50m
<b>SEISMIC COVERAGE:</b> CH-15-91 line 10		

**Objectives:** To carry out background sampling along a transect into the diapir. The hole will penetrate the sole of a major slide.

**Drilling Program:** RCB coring.

**Logging and Downhole Operations:**

**Nature of Rock Anticipated:** Hemipelagic silt and clay.

<b>SITE:</b> CFD-2	<b>PRIORITY:</b>	<b>POSITION:</b> 33°00.3'N, 75°55.8'W
<b>WATER DEPTH:</b> 2700m	<b>SEDIMENT THICKNESS:</b> ~8km	<b>TOTAL PENETRATION:</b> 50m
<b>SEISMIC COVERAGE:</b> CH-15-91 line 10		

**Objectives:** To sample beds at the edge of the diapir where the disturbance associated with the diapir is at an extreme.

**Drilling Program:** RCB coring.

**Logging and Downhole Operations:**

**Nature of Rock Anticipated:** Hemipelagic silt and clay.

<b>SITE:</b> CFD-3	<b>PRIORITY:</b>	<b>POSITION:</b> 32°59.5'N, 75°55.18'W
<b>WATER DEPTH:</b> 2650m	<b>SEDIMENT THICKNESS:</b> ~8km	<b>TOTAL PENETRATION:</b> 50m
<b>SEISMIC COVERAGE:</b> CH-15-91 line 10		

**Objectives:** To sample beds at the edge of the diapir where the disturbance associated with the diapir is at an extreme.

**Drilling Program:** RCB coring.

**Logging and Downhole Operations:**

**Nature of Rock Anticipated:** Hemipelagic silt and clay.

<b>SITE:</b> CFD-4	<b>PRIORITY:</b>	<b>POSITION:</b> 32°59.3'N, 75°54.25'W
<b>WATER DEPTH:</b> 2590m	<b>SEDIMENT THICKNESS:</b> ~8km	<b>TOTAL PENETRATION:</b> 50m
<b>SEISMIC COVERAGE:</b> CH-15-91 line 10		

**Objectives:** To sample surface sediments on the crest of an exhumed diapir.

**Drilling Program:** RCB coring.

**Logging and Downhole Operations:**

**Nature of Rock Anticipated:** Salt? Hemipelagic silt and clay.

*LEG 165*

*Diamond Coring System -  
Engineering Tests*

## **LEG 165**

### **DIAMOND CORING SYSTEM: VEMA FRACTURE ZONE A BRIEF ENGINEERING AND OPERATIONS PROSPECTUS**

---

**Modified From The August 1992 Report to the JOIDES Planning Committee  
and Material Prepared and Supplied By Dan Reudelhuber, ODP Engineer**

**To Be Named: Co-Chief Scientist and Staff Scientist**

---

#### **ABSTRACT**

The Vema Fracture Zone has been proposed as the next engineering test site for the Diamond Coring System (Phase II), scheduled for Leg 165 in January - February, 1996. The area is characterized by relatively thin sediments overlying limestone formations, deposited on upthrust blocks of crust. The limestone is anticipated to be on the order of 400-m thick in some areas. Water depths range from a few hundred meters to over 2,000 m.

Only two out of the three previous deployments of the Diamond Coring System can be considered successful. A failure of the secondary heave compensation system during Leg 142 precluded successful coring with the system.

Changes made to the Phase II system during 1992-1993 will be tested at sea for the first time during Leg 165, the most significant of these changes being the modifications made to the secondary heave compensation system. The development, testing, and proving of the secondary heave compensation is critical to the future of the Diamond Coring System, as it is impossible to slimhole core offshore without effectively removing heave motion at the core bit.

A secondary objective of the Leg 165 engineering test will be an assessment of new hardware, in particular the diamond retractable bit which has the potential to significantly improve the operational efficiency of the Diamond Coring System by greatly decreasing the time required for coring bit trips.

## INTRODUCTION

Although the Diamond Coring System (DCS) (Fig. 1) has been deployed three times since its inception in 1988, only two deployments can be considered successful.

The DCS-Phase I system was tested in 1989 during Leg 124E. The concept was to core using a narrow kerf diamond core bit rotated at high speeds with light bit weights and precise heave compensation, all in deep water. Based on the test, the concept appeared feasible and the decision was made to design and develop an operational prototype. The Phase II version of the DCS was designed, built, deployed, and tested during a one-year period between August 1989 and August 1990. A 79-m hole was drilled/cored on Leg 132 at the Bonin Ridge with respectable recovery through the fractured zone. Good quality cores of the elusive, highly fractured basalts were finally, successfully recovered. In 1992, the Phase II version was deployed for the second time on Leg 142 (January-March, 1992). A failure of the secondary heave compensation system precluded successful coring with the system. Based on documented visual observations, there were problems associated with computer control of weight on bit. A bent cylinder and erratic load cell readings were, at that time, felt to be major contributors to the system's failure to compensate.

The Vema Fracture Zone has been proposed as the next engineering test site for the DCS, scheduled for Leg 165 in January-February, 1996. Changes made to the DCS system during 1992-1993 will be tested at sea for the first time during Leg 165. The most significant of these changes has been made to the secondary heave compensation system. A much more robust compensation controller has been designed, and it will be built and tested extensively on land during 1993.

## TEST AREA

Formations expected at the Vema Fracture Zone are characterized by relatively thin sediments overlying limestone formations, deposited on upthrust blocks of crust. The limestone is anticipated to be quite thick in some areas, on the order of 400 m. Water depths range from a few hundred meters to over 2,000 m.

In August, 1992, a multichannel seismic reflection survey was conducted at the Vema Fracture Zone with the ship *OGS Explora* (Fig. 2). The preliminary shipboard analysis of the data, as summarized below, was carried out by E. Vera, M. Ligi, and E. Bonatti.

The transverse ridge, located on the southern side of the Vema Fracture Zone, is an east-west elongated feature that reaches exceptionally shallow bathymetry (up to <600 mbsl) about 80 km west of the intersection of the fracture zone with the Mid-Atlantic Ridge (Fig. 2)

Limestones and other rocks dredged from this segment of the ridge indicate that the transverse ridge is an uplifted sliver of oceanic crust capped by shallow-water reef limestones (Bonatti et al., 1983). From the study of paleofacies and ages of these limestones, Bonatti et al. (1983) concluded that the crustal block was exposed subaerially in middle Pliocene time (about 3 m.y. ago) and subsequently sank to its present depth at an average rate of 0.3 mm/yr, i.e. at a rate one order of magnitude faster than the predicted thermal contraction subsidence.

Vera, Ligi, and Bonatti have tentatively reached the following conclusions, illustrated in Fig. 3:

1. A ~ 400-m thick layer of material with average 2 km/s velocity caps the summit of the transverse ridge. Based on studies of bottom samples, this layer represents a shallow water carbonate platform that emerged as an island up to about 3 Ma.
2. The carbonate cap lies on a horizontal surface, i.e. the top of an uplifted block of igneous rock. The horizontal boundary suggests erosion at sea level during subsidence.
3. The seismic velocity of the top of the basement is ~ 4 km/s, grading up to ~ 5.4 km/s about 200 m below the top of the basement. A possible interpretation calls for basalt grading down into a dike complex, consistent with the transverse ridge being an uplifted block of oceanic crust that is undergoing subsidence since about 3 Ma.
4. The average ~ 2 km/s velocity of the ~ 400-m-thick limestone cap, and the <2 km/s inferred for the top ~ 100 m suggest that unconsolidated sediments prevail near the top of the section.

## **ENGINEERING OBJECTIVES**

### **Summary of Objectives**

- 1) To maximize coring time and recovery time with the DCS.
- 2) To test additional new hardware, such as the DCS retractable bit (DRB) and, if required, a 6-3/4" Drill-In Bottom Hole Assembly (DI-BHA).

## OPERATIONS PLAN

Upon arrival at the Vema Fracture Zone, a bottom TV survey will be conducted in order to locate a possible area for HRB emplacement. Since some limited sediment cover is expected, it is likely that a test hole will be drilled to assess near-surface lithology and to help determine setting depths for the DI-BHA.

The ideal location for the HRB would have less than 1-m sediment cover. A HRB will be assembled and run to bottom once a suitable location is chosen. The 10-3/4" DI-BHA will then be deployed in order to set the stage for coring with the DCS.

The DCS will then be picked up and coring will proceed.

Significant changes will have been made to the secondary heave compensation system prior to Leg 165. Specifically, a completely new compensation system controller will be tested and tuned at the initiation of DCS coring. New bit designs will also be tested when the 10-3/4" DI-BHA is drilled in. Two different diamond bit/center bit designs will be available. These are expected to be much more efficient in the limestone formation than the 12-1/2" roller cone bits used on Leg 142 at the East Pacific Rise (EPR). New bits for the 6-3/4" DI-BHA system may also be tested if hole conditions dictate that a second string of casing be set. The 6-3/4" DI-BHA hardware has also been modified to include a loss of pressure indicator for when back-off occurs.

If initial coring is successful with conventional diamond bits, a segmented DRB system may be tested. The DRB allows the 3.96" diamond core bit to be changed without tripping the DCS tubing out of the hole. This retractable bit hardware will ride on the inner core barrel and can be viewed after each core run. Successful deployment of this hardware will potentially save a significant amount of time that would have been used for tripping the DCS tubing in place of coring.

## REFERENCES

Bonatti et al., 1983. *Tectonophysics*, 91:213-232.

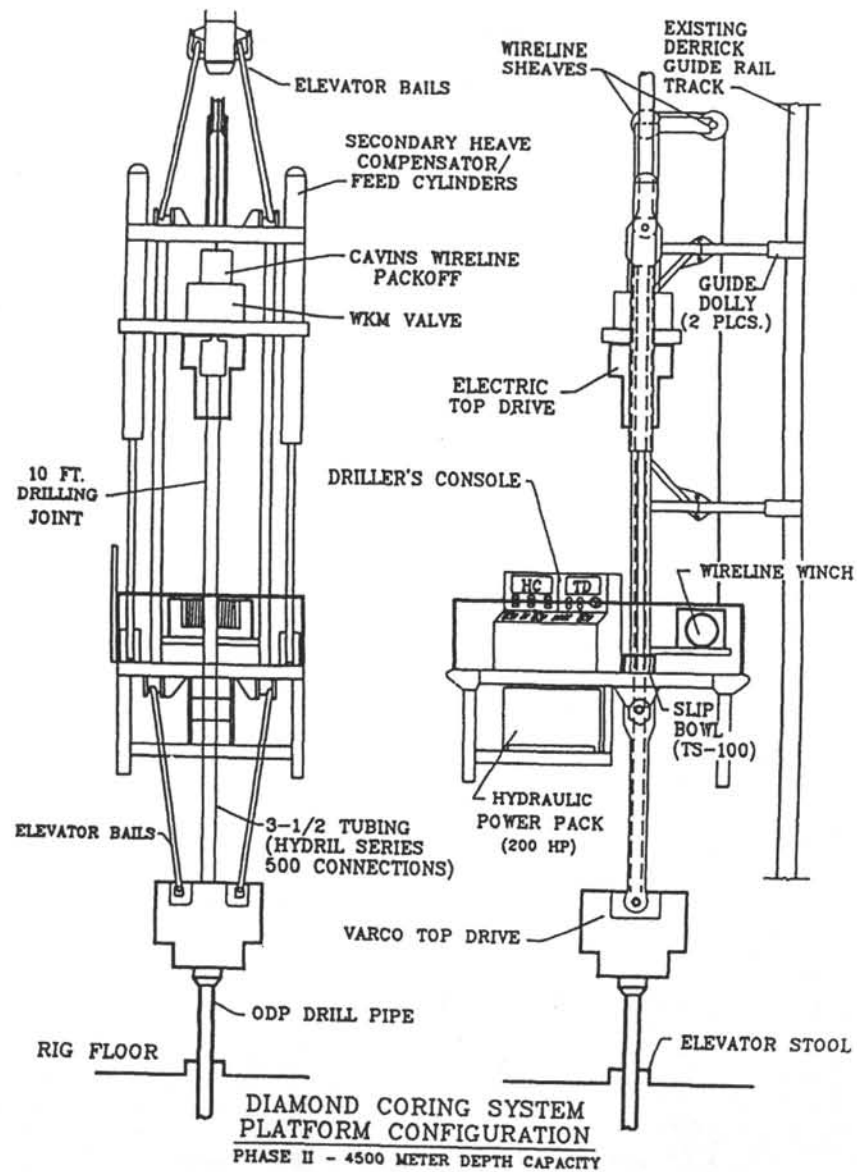
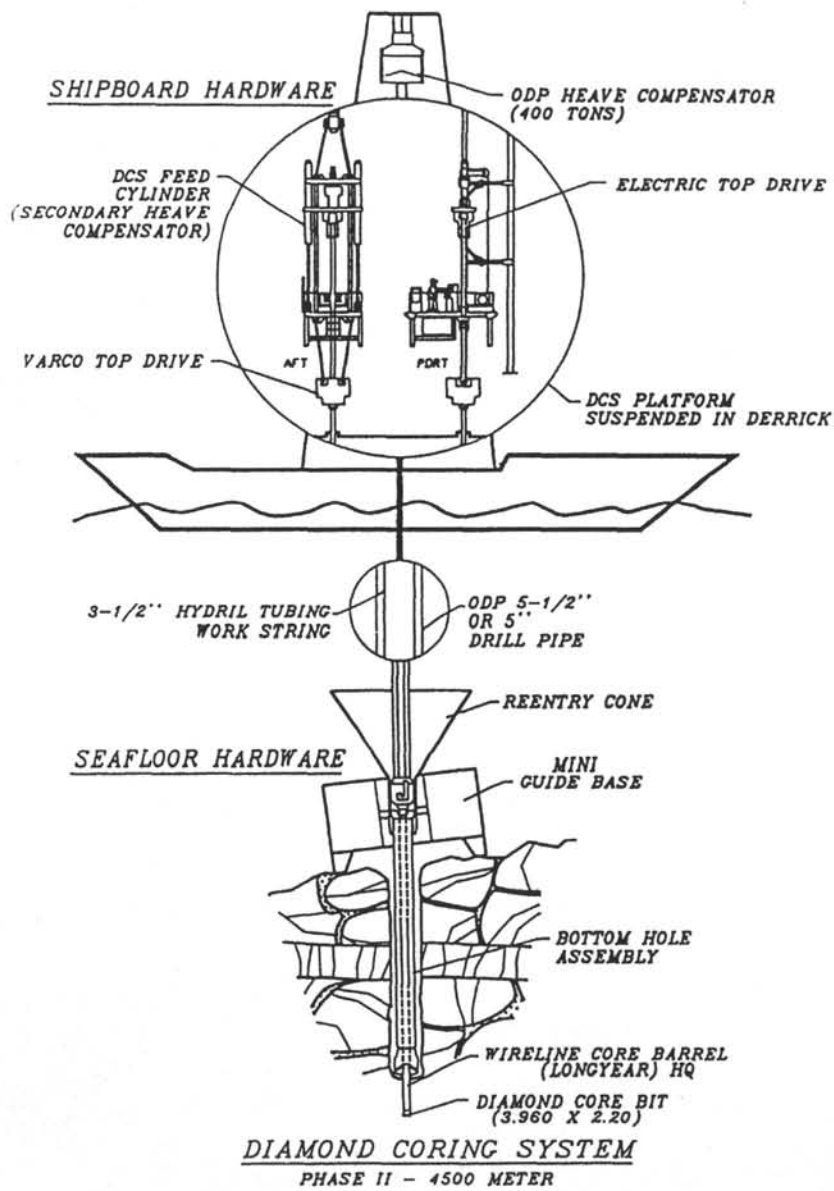


Figure 1. DCS-Phase II configuration during Leg 132 engineering tests.

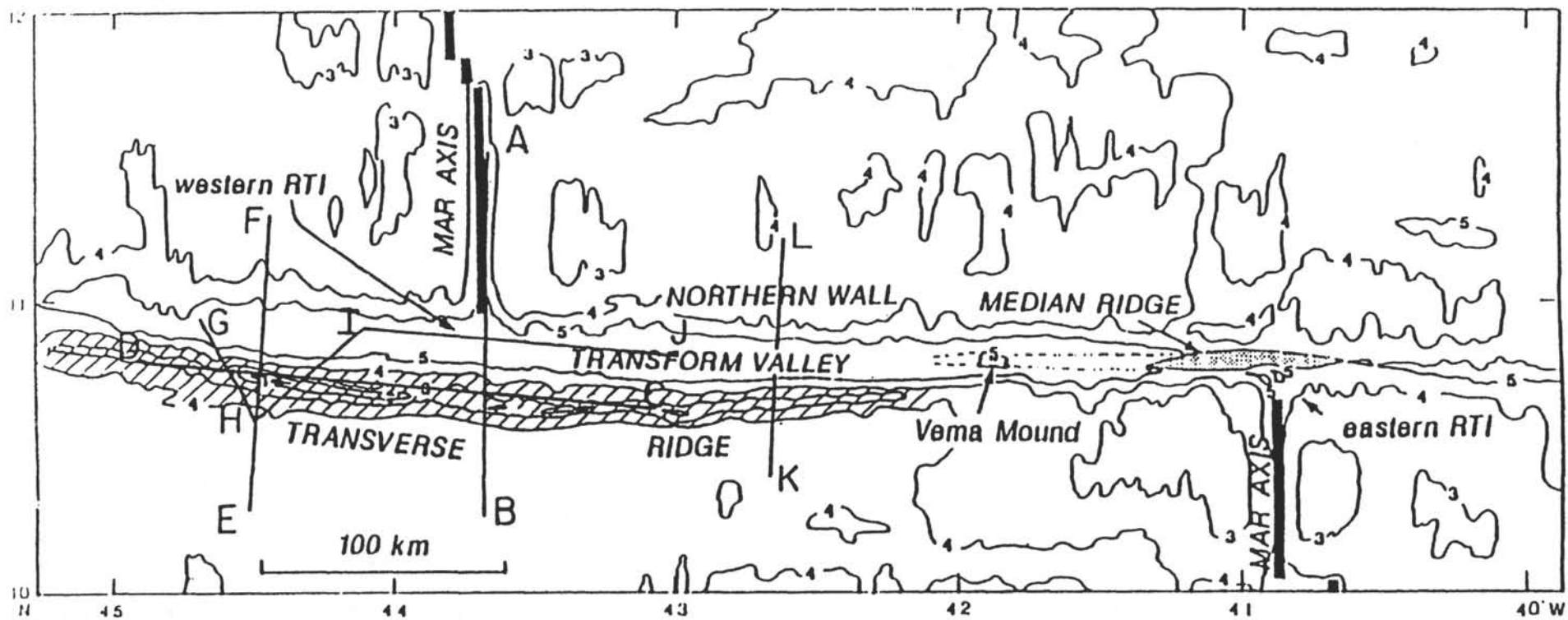


Figure 2. Tracks of the seismic reflection profiles carried out in August 1992 at the Vema Fracture Zone by Vera, Ligi, and Bonatti.

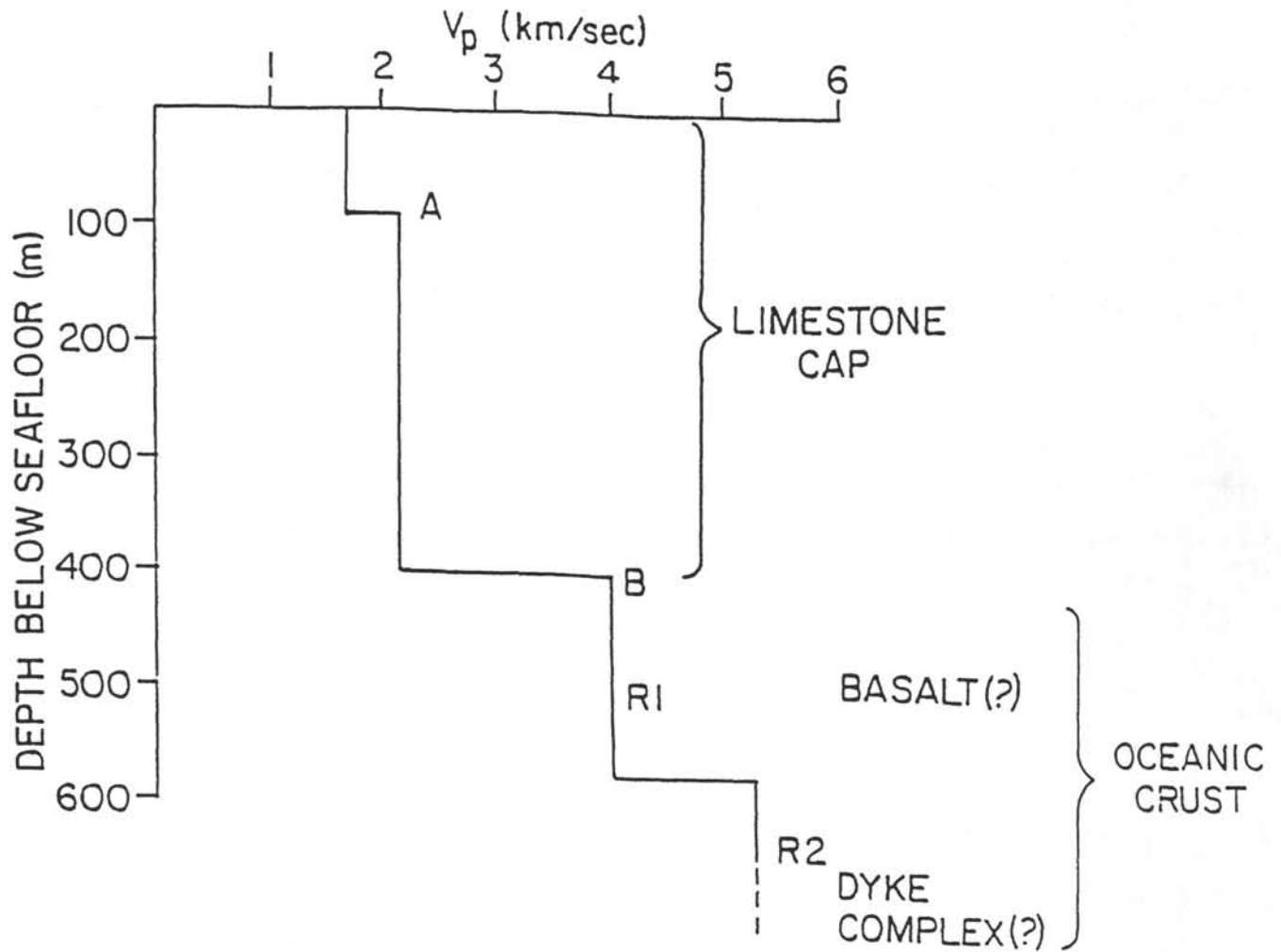


Figure 3. Velocity/depth function for SP 1964 (VEMA-02, August 1992 survey) on the crest of the Vema Transverse Ridge. Water depth is 595 m and  $V_w = 1.475$  km/s.